

Analysis of gene expression, regulation and function of three symbiotic ABC subfamily-B transporters in *Medicago truncatula*

Sonali Roy

A thesis submitted to the University of East Anglia for the degree of Doctor of Philosophy

**John Innes Centre
Norwich
September 2014**

© This copy of the thesis has been supplied on condition that anyone who consults it is understood to recognise that its copyright rests with the author and that use of any information derived there-from must be in accordance with current UK Copyright Law. In addition, any quotation or extract must include full attribution.

Dissertation supervised by

1. Primary supervisor: **Dr. Jeremy Murray**
2. Secondary-supervisor: **Professor Giles Oldroyd**

ABSTRACT

The legume *M. truncatula* overcomes low soil nutrient conditions by forming symbiotic associations with nitrogen-fixing soil bacteria called rhizobia (Root Nodule Symbiosis) and fungi which assist in the acquisition of phosphate, collectively called arbuscular mycorrhizae (Arbuscular Mycorrhizal Symbiosis). Establishment of functional beneficial symbioses requires successful microbial infection. An initial exchange of signalling molecules between the host and the microbe sets off extensive transcriptional reprogramming of the host developmental programme to accommodate the incoming microbe. Microbial lipochitooligosaccharide molecules trigger a signalling pathway comprising a core set of around seven genes common to both symbioses, central to which is the calcium calmodulin kinase, CCaMK. Here I describe the identification and characterization of three novel *M. truncatula* ATP-Binding cassette containing sub-family B transporters, transcriptionally induced upon infection by both rhizobia and mycorrhizae; therefore named AMN for ABC transporters in Mycorrhization and Nodulation. Promoter-GUS expression reveals that these genes are exclusive to infection structure containing root hair cells and arbuscule containing root cortical cells. I use different SYM pathway mutants to show that the induction of these transporters is dependent on CCaMK and other members of the symbiotic pathway. Conservation of these transporters across mycorrhizing angiosperms suggested an important evolutionary function therefore I identified and characterized single and double mutants. In the absence of any aberrant symbiotic phenotype a triple mutant was also generated but remains to be characterized.

Since ABC sub-family B transporters in *Arabidopsis* are known to efflux auxin I also undertook a multipronged approach to identify a role for auxin in rhizobial infection. Using pharmacological and physiological assays I describe results that indicate a positive role for auxin in infection. Lastly I describe the nodulation phenotype of *mtlax2* and *mtiaa8*; a homologue of the *Arabidopsis* AtAUX1 auxin influx carrier and an infection induced AUX/IAA repressor respectively. A lower nodule number in both mutants provide the first genetic evidence for auxin's role in nodule development.

TABLE OF CONTENTS

Abstract	3
Table of Contents	4
Acknowledgements.....	9
List of figures	11
List of tables	14
Abbreviations.....	15
Chapter One: Introduction	17
1.1 A Brief overview of the Root nodule and Arbuscular mycorrhizal Symbioses 17	
1.1.1 A common signalling pathway regulates both rhizobial and mycorrhizal symbioses	18
1.2 A role for auxin in nodulation	21
1.2.1 Auxin and rhizobial infection	24
1.3.1 Section I: Secondary metabolites and transport processes in plant-microbe interactions.....	25
1.3.1.1 Secondary metabolites and transport processes are crucial to symbiosis	25
1.3.1.2 Plant-parasite lifestyles	26
1.4 Section II: ABC transporters and metabolite transport	27
1.4.1 A large complement of plant ABC transporters enables trafficking of diverse metabolites.....	27
1.4.2 Analysis of the <i>Medicago</i> ABC transporter family reveals an expansion of all sub-families.....	28
1.5 Section III: ABC transporters involved in different stages of plant microbe interactions.....	31
1.5.1 Plant signalling to microbes	31
1.5.2 Cellular accommodation of microbes	35
1.5.3 Nutrient exchange and additional processes.....	37
1. 6 Conclusion and future challenges.....	38
1.7 Summary.....	39
Aims and Objectives	40
Chapter Two: Materials and Methods	41
2.1 Plant Methods	41

2.1.1.1 <i>Medicago truncatula</i> lines and growth conditions	41
2.1.1.2 Seed sterilization, scarification and vernalisation	43
2.1.1.3. Cross fertilizations.....	43
2.1.1.4 Generation of stably transformed hairy roots of <i>M. truncatula</i>	44
2.2. Microbiological methods	44
2.2.1 Bacterial methods	44
2.2.1.1 Bacterial strains and growth conditions	44
2.2.1.2 Bacterial plasmid preparation and transformation by heat-shock or electroporation.....	45
2.2.1.3 Plasmid mobilization by Tri-parental mating	47
2.2.1.4 Blue White Screening	47
2.2.2 <i>Saccharomyces cerevisiae</i> transformation and culture.....	48
2.2.2.1 Yeast strains and growth conditions.....	48
2.2.2.2 Yeast competent cell preparation and transformation	48
2.2.2.3 Yeast drop test.....	48
2.3 Molecular Biological methods.....	51
2.3.1 DNA Methods	51
2.3.1.1 Agarose gel electrophoresis.....	51
2.3.1.2 PCR cycling conditions	51
2.3.1.3 Restriction digestion.....	51
2.3.1.4 DNA gel extraction	52
2.3.1.5 Sequencing using BigDye V3.1	52
2.3.1.6 Gateway Cloning: BP reaction and LR reaction	52
2.3.1.7 Golden gate assembly: Level 1 and Level 2 (Binary) vector assembly	53
2.3.2 RNA methods.....	53
2.3.2.1 General sample collection and RNA isolation.....	53
2.3.2.3 Complimentary DNA (cDNA) synthesis	54
2.3.2.4 Primer efficiency calculations and quantitative PCR.....	54
2.4 Assays used in this study	55
2.4.1 Bacterial growth curve assay	55
2.4.2 Root hair length measurement.....	55
2.4.3 Histochemical localization of GUS	56
2.4.4 Infection assay and β -Galactosidase staining	56
2.4.5 SYTO13 Green-Fluorescent staining to visualize rhizobia.....	56
2.4.6 Nodulation assay	57
2.4.7 Mycorrhization assay and Ink staining.....	57

2.4.8 Wheat germ agglutinin (WGA) staining of fungus.....	58
2.5 Bioinformatics Analyses	58
2.5.1 Defining the <i>M. truncatula</i> ABC transporter family.....	58
2.5.2 Retrieving orthologues of candidate genes from different species.....	58
2.5.3 Co-regulation Analysis	59
2.6 Microscopy Techniques.....	59
2.6.1 Light Microscopy	59
2.6.2 Confocal Laser Scanning Microscopy	59
Chapter Three: Analysing the phylogeny and expression of <i>M. truncatula</i> ABC subfamily B transporters during root nodule symbiosis (RNS) and arbuscular mycorrhizal symbiosis (AMS)	61
3. 1 Introduction	61
3. 2 Results and discussion.....	63
3.2.1 The complete <i>M. truncatula</i> ABC transporter family comprises of 167 putative members.....	63
3.2.2 Three ABC sub-family B members are induced specifically in response to symbiosis.....	65
3.2.3 <i>AMN1</i> , <i>AMN2</i> , and <i>AMN3</i> are not present in <i>Arabidopsis</i> but are evolutionarily conserved across all mycorrhizal angiosperms	74
3.2.4 <i>AMNs</i> are expressed in <i>M. truncatula</i> upon infection with symbionts	77
3.2.5 Promoters of <i>AMN1</i> , <i>AMN2</i> , and <i>AMN3</i> are associated with rhizobial infection	78
3.2.6 Promoters of <i>AMN1</i> , <i>AMN2</i> , and <i>AMN3</i> are associated with mycorrhizal infection	81
3.3 Conclusion	86
Chapter Four: Genetic analyses of function and regulation of three ABC sub-family B transporters in mycorrhization and nodulation (<i>AMNs</i>)	88
4.1 Introduction	88
4.2 Results and Discussion	90
4.2.1 The intron-exon structure of <i>AMN1</i> and <i>AMN2</i> is conserved.....	90
4.2.2 Two mutant alleles each of <i>AMN1</i> and <i>AMN3</i> and one for <i>AMN2</i> were identified	91
.....	95
4.2.3 Single mutants of <i>AMN1</i> , <i>AMN2</i> and <i>AMN3</i> are unaffected in their ability to form symbiotic associations with both rhizobia and arbuscular mycorrhizae	96
4.2.4 RNAi knockdown of <i>AMN1</i> and <i>AMN2</i> has a negative effect on nodule number and mycorrhizal percentage colonization	97
4.2.5 Double mutants of <i>AMN1</i> and <i>AMN2</i> do not show any change in nodule number and mycorrhizal colonization.....	102

4.2.6 Constitutive root hair expression of <i>AMN2</i> blocks cortical penetration of Infection threads	104
4.2.7 <i>AMN1</i> , <i>AMN2</i> , and <i>AMN3</i> co-regulation analyses	107
4.2.8 Promoter analyses of 2kb upstream region of the <i>AMNs</i> reveals putative hormone regulatory sites	110
4.2.9 Expression of <i>AMN1</i> , <i>AMN2</i> , and <i>AMN3</i> is not affected by Indole acetic Acid	111
.....	112
.....	113
4.2.10 <i>AMN1</i> , <i>AMN2</i> , and <i>AMN3</i> are <i>DMI3</i> dependent	113
4.3 Conclusions.....	114
Chapter Five: A role for auxin transport in rhizobial Infection	118
5.1 Introduction	118
5.2 Results and Discussion	122
5.2.1 Treatments with auxin efflux and influx inhibitors decrease the frequency of rhizobial infection but do not affect early symbiotic signalling.....	122
.....	124
5.2.2 <i>MtLAX2</i> expression is not associated with infection threads	124
5.2.3 The <i>mtlax2</i> mutant has reduced nodule numbers	127
5.2.4 Mutation in an AUX/IAA gene <i>MtIAA8</i> reduces nodule number.....	127
.....	131
.....	131
5.2.5 Decapitation of the shoot apical meristem (SAM) reduces rhizobial infection frequency and this phenotype can be rescued by IAA	132
5.2.6 Introduction of a dominant negative copy of the <i>Arabidopsis</i> IAA17 does not affect infection structures or nodule number	133
5.3 Conclusion	137
Chapter Six: General Discussion	140
6.1 <i>AMNs</i> are novel ABC transporters with conserved roles in rhizobial and mycorrhizal infection	140
6.2 <i>AMNs</i> are dependent on the Common Symbiosis Signalling pathway for correct expression during either symbiosis.....	143
6.3 Auxin transport plays an important role in root nodule symbiosis.....	146
6.5 Conclusions.....	149
Appendices.....	151
Appendix 1.1 <i>AMN1</i> sequence (As obtained from cDNA sequencing).....	151
Appendix 1.2 <i>AMN2</i> sequence (As obtained from cDNA sequencing).....	152
Appendix 1.3 ABC Domain containing genes encoded in <i>M. truncatula</i>	154

Appendix 1.4: Accession numbers of ABC transporters homologous to <i>AMN1</i> , <i>AMN2</i> , and <i>AMN3</i> across dicots which can either nodulate or mycorrhize	159
Appendix 1.5: Putative Transcription factor binding sites common to 2 kb Upstream region of <i>AMN1</i> , <i>AMN2</i> , and <i>AMN3</i>	161
Appendix 1.6: Infection structures in <i>AMN1/AMN2</i> RNAi lines upon nodulation and mycorrhization.....	163
Appendix 1.7 Infection structures on <i>lax2</i> mutants and promoter-GUS analyses of auxin markers in <i>M. truncatula</i>	164
Appendix 1.8 Quantitative RT PCR showing auxin responsiveness of infection induced genes.....	165
Appendix 1.9 Quantitative RT PCR showing expression of <i>AMN</i> transcripts in their respective mutant backgrounds.....	166
Appendix 1.10 Sensitivity of <i>lax2-1</i> and <i>lax2-1</i> mutants to IAA compared to WT R108 Control.....	167
References	169

ACKNOWLEDGEMENTS

The one person I have interacted with the most over the past three years and who I am deeply indebted to is easily my supervisor, **Jeremy Murray**. For all the time you invested in me, be it personal or professional, influenced my thoughts, for being an authority on symbiosis and therefore being a great guide, Thank-you! A big thank-you also to my co-supervisor **Giles Oldroyd** for constant encouragement, brilliant ideas, a wealth of resources, and excellent guidance! And finally to my teacher and my friend, **Allan Downie** for listening to my ideas, for critically evaluating my hypotheses and experiments, for an inspiring enthusiasm towards science, Thank-you!!

I would also like to thank the people who influenced me in the lab and were my teachers in their own right, starting with my present lab-mate **Chengwu Liu**. Thanks for all the perceptive suggestions on the presentations, interpretation of results and extensive technical know-how because it truly enriched our Friday lab meetings and all of our other interactions. Thank-you **Kirsty Jackson** for having the answers to all my questions and unfailingly finding time to show me things in the lab and **Donna Cousins** not only for the ever popular mycorrhizal inoculum but also for being a great lab-mate! **Andy Breakspear, Anne Edwards, Dian Guan, Tatiana Vernie, Sarah Shailes, Sylvia Singh, and Caitlin Bone** thank-you for being the super smart individuals you are. Our interactions have only enriched my PhD experience and helped me find ways around many scientific hurdles. I am grateful to everyone else in the three research groups, who I interacted with over the past three years and who helped me on the way to my PhD.

My happiest memories in Norwich include **Azahara Martin** and **Paula Garcia**. Thanks for being a part of every high and every low I experienced over the past three years and being my 'home' in England. Thanks also to **Antonio Serrano-Mislata** and members of my street dance gang, **Tobin Florio, Albor Dobon, Stefanie Rosa, Souha Berriri, Livia Scheunemann, Paloma Menguer** for all the amazing late nights and fun weekends, great company and awesome conversations! You guys are the best thing that happened to me in Norwich!

I consider myself very lucky to be one of the few individuals who have had the freedom to pursue what they want in life. I understand now, that this privilege is largely due to my parents and my freedom is the end result of their struggles and persistence. I could neither have started not completed my PhD without my mother **Keka Roy**, who has always supported my decisions and my father **Ashok Roy**, who shares my enthusiasm for my research work. My sister, **Devaki Roy**, provided the emotional safety-net that my PhD required and my little brother, **Varun Roy**, taught me to laugh at my problems when they seemed unsurmountable.

I am also indebted to my teacher **Pallob Kundu** for being very supportive, **Lars Oestergaard** and **Veronica Grieneisen** for never failing to attend my annual meeting, **Anuradha Bansal** for being my statistics guru, **Tilly Eldridge** and other rotation students for their company during the last four years.

Special thanks again to everyone who edited a chapter in my thesis Sylvia, Allan, Chengwu, and Kirsty and of course Jeremy!

Sonali Roy
John Innes Centre
30th September 2014

LIST OF FIGURES

Figure 1.1: Overview of the common symbiotic signalling pathway.	20
Figure 1.2: Overview of early auxin signalling and response.	23
Figure 1.3: Phylogenetic tree showing interrelations between Sub-family G members of <i>M. truncatula</i> and <i>A. thaliana</i> .	30
Figure 1.4: Summary diagram showing ABC transporters associated with Root nodule symbiosis and Arbuscular mycorrhizal symbiosis studied to date.	39
Figure 3.1: An unrooted cladogram showing phylogenetic relationships between members of full-molecule ABC transporter sub-families of <i>M. truncatula</i> .	64
Figure 3.2: Expression of <i>M. truncatula</i> <i>AMN1</i> , <i>AMN2</i> , and <i>AMN3</i> in different tissues.	67
Figure 3.3: Expression of <i>M. truncatula</i> <i>AMN1</i> , <i>AMN2</i> , and <i>AMN3</i> in different tissues upon infection by either mycorrhiza or rhizobia.	68
Figure 3.4: Amino acid sequence alignment of <i>AMN1</i> , <i>AMN2</i> , and <i>AMN3</i> showing characteristic domains of a Full ABC transporter	71
Figure 3.5: Hydrophobicity plots showing predicted transmembrane regions for <i>AMN1</i> , <i>AMN2</i> , and <i>AMN3</i>	72
Figure 3.6: Phylogenetic relationships between sub-family B full-molecule ABC transporters of <i>Arabidopsis</i> , <i>Medicago</i> and <i>Oryza</i> .	75
Figure 3.7: <i>Medicago truncatula</i> <i>AMN1</i> , <i>AMN2</i> , and <i>AMN3</i> orthologues are conserved in dicots which can nodulate or mycorrhize.	76
Figure 3.8: Spatial expression pattern of <i>AMN1</i> , <i>AMN2</i> , and <i>AMN3</i> promoter ten days post inoculation with <i>S. meliloti</i>	79
Figure 3.9: Non-symbiotic expression pattern of <i>AMN1</i> , <i>AMN2</i> , and <i>AMN3</i>	80
Figure 3.10: Spatial expression pattern of the <i>AMN1</i> promoter four weeks post inoculation with <i>R. irregularis</i>	82

Figure 3.11: Spatial expression pattern of the <i>AMN2</i> promoter two weeks post inoculation with <i>R. irregularis</i>	83
Figure 3.12: Spatial expression pattern of the <i>AMN3</i> promoter two weeks post inoculation with <i>R. irregularis</i>	84
Figure 3.13: Staining pattern of vector control hairy root lines	85
Figure 4.1: Identification of <i>amn1</i> , <i>amn2</i> , and <i>amn3</i> mutant alleles of <i>M. truncatula</i>	93
Figure 4.2: DNA Polymerase Chain Reaction confirmation of <i>Tnt1</i> insertion mutant lines	94
Figure 4.3: Semi quantitative RT-PCR confirmation of <i>Tnt1</i> insertion mutant lines	95
Figure 4.4: Symbiotic phenotypes of single mutant alleles of <i>AMN1</i> , <i>AMN2</i> , and <i>AMN3</i>	99
Figure 4.5: Double knockdown of <i>AMN1</i> and <i>AMN2</i> negatively affects both rhizobial and mycorrhizal associations	100
Figure 4.6: Relative expression of <i>AMN1</i> , <i>AMN2</i> , and <i>AMN3</i> in RNAi expressing lines	101
Figure 4.7: Symbiotic phenotypes of <i>AMN</i> double mutant combinations	105
Figure 4.8: <i>EXPANSIN A7</i> driven constitutive expression of <i>AMN2</i> affects nodule number and Infection thread structure.	106
Figure 4.9: Candidate substrates for <i>AMN1</i> , <i>AMN2</i> , and <i>AMN3</i>	114
Figure 4.10: Expression of <i>AMN1</i> , <i>AMN2</i> , and <i>AMN3</i> in different symbiotic pathway mutants.	116
Figure 5.1: Pharmacological dissection of auxin's role in rhizobial infection of <i>M. truncatula</i>	124
Figure 5.2: Phylogenetic and Expression studies of <i>M. truncatula</i> <i>MtLAX2</i>	126
Figure 5.3: Characterization of <i>lax2</i> mutants	129
Figure 5.4: Characterization of <i>iaa8-1</i> mutant	130

Figure 5.5: Confirmation of <i>tnt1</i> mutants described in this chapter	131
Figure 5.6: Effects of decapitation of the shoot apical meristem (SAM) on <i>S. meliloti</i> – <i>M. truncatula</i> interaction	132
Figure 5.7: Effects of Infection induced repression and activation of Auxin signalling on <i>S. meliloti</i> - <i>M. Medicago</i> interaction	134
Figure 5.8: Effects of rhizobially produced auxin on infection	136
Figure 6.1: A schematic representation of the common symbiosis signalling pathways showing the position of the AMNs	145
Figure 6.2: Hypothetical model of Auxin transport and its role in symbiotic nodule organogenesis	148
Supplementary Figure 4.1: Infection associated structures in RNAi Knockdown roots	163
Supplementary Figure 5.2: <i>M. truncatula</i> roots showing expression of different marker genes	164
Supplementary Figure 5.3: Quantitative RT-PCR validation of auxin responsiveness of infection induced genes	165
Supplementary Figure 4.4: Quantitative RT-PCR determination of <i>AMN</i> transcript abundance in their respective mutant backgrounds	166
Supplementary Figure 5.5: <i>lax2-1</i> and <i>lax2-1</i> mutant seedlings are sensitive to IAA compared to WT R108 Control	167
Supplementary Figure 5.6: Graph comparing average ratio of pink/white nodules per mutant genotype	168

LIST OF TABLES

Table 2.1: List of <i>M. truncatula</i> lines used in this study	42
Table 2.2: List of bacterial strains used in this study	45
Table 2.3: Table of vectors, plasmids and constructs used in the study	47
Table 2.4: Yeast strains used in the present study	49
Table 2.5: Recipe for preparation of media used in this study	50
Table 2.6: Antibiotics used in this study	50
Table 2.7: Standard PCR cycling Parameters	51
Table 2.8: List of primers used in this study	60
Table 3.1: A comparison of ABC transporters in <i>Arabidopsis</i> and <i>Medicago</i>	65
Table 3.2: <i>Medicago</i> ABC transporters induced either during Root Nodule Symbiosis (RNS) or Arbuscular Mycorrhizal Symbiosis (AMS)	74
Table 4.1: Genotypic ratios of the crosses tested and described in this thesis.	103
Table 4.2: List of genes co-regulated with <i>AMN1</i> , <i>AMN2</i> , and <i>AMN3</i>	109
Appendix Table S.1: <i>M. truncatula</i> ABC transporters and their closest <i>Arabidopsis</i> homologue, identified in this study	154
Appendix Table S.2: Accession numbers of all <i>AMN1</i> , <i>AMN2</i> and <i>AMN3</i> homologues used to prepare the phylogenetic tree in Figure 3.3	159
Appendix Table S.3: List of Transcription factor binding sites common to the 2 Kb region upstream of <i>AMN1</i> , <i>AMN2</i> and <i>AMN3</i>	161

ABBREVIATIONS

	Full form
5-FI	5-Fluoroindole
ABC	ATP Binding Cassette
AMS	Arbuscular mycorrhizal symbiosis
ARF	Auxin response factor
ATI	Auxin transport inhibitor
ATP	Adenosine triphosphate
AUX/LAX	Auxin1/Like Aux1
BLAST	Basic local alignment search tool
CCaMK	Calcium Calmodulin dependent Kinase
CHPAA	3-chloro-4-hydroxyphenoxyacetic acid
dpi	days post inoculation
DR5	Direct Repeat 5
DWA	Distilled water agar
ENOD	Early nodulin
GA	Gibberellic acid
GUS	β -Glucuronidase
IAA	Indole-3-acetic acid
IMGAG	International <i>Medicago</i> Genome Annotation Group
IT	Infection thread
JA	Jasmonic acid
MDR	Multidrug resistant
MEP	Methylerythritol pathway
MtGEA	<i>Medicago truncatula</i> Gene expression atlas
MtPT4	<i>Medicago truncatula</i> phosphate transporter
Myc	Mycorrhiza
NAA	1-Naphthaleneacetic acid
NCBI	National Centre for Biotechnology Information
NBD	Nucleotide binding domain
Nf	Nod-factor
NFP	Nod factor perception
NIN	Nodule inception
NPA	N-1-Naphthylthalamic acid
NOA	1-naphthoxyacetic acid
ORF	Open reading frame
PCR	polymerase chain reaction
PPA	Pre penetration apparatus
RNAi	RNA interference

RNS	Root nodule symbiosis
SA	Salicylic acid
TIBA	Triiodobenzoic acid
TMD	Transmembrane domain
WGA	Wheat germ agglutinin
wpi	weeks post infection
WT	Wild type

CHAPTER ONE:

Introduction

1.1 A Brief overview of the Root nodule and Arbuscular mycorrhizal Symbioses

Under nitrogen limiting conditions, legumes secrete flavonoids into the rhizosphere and induce symbiotic rhizobia to start producing Nodulation (Nod) factors (NFs). Nod factors are rhizobially produced lipochitooligosaccharide (LCO) molecules that consist of a chitin backbone with an N-linked fatty acid moiety attached to the non-reducing terminal sugar and they confer specificity to host plants (Denarie, Debelle, & Prome, 1996). Two simultaneous but genetically separable processes – infection and nodule organogenesis occur downstream of Nod-factor perception. Nod-factor recognition is followed by plasma membrane depolarization and oscillations in calcium (calcium spiking) in and near the nucleus and the induction of early nodulation genes (*ENODs*) at the epidermal surface. The bacteria then attach to the root hair after which localized production of NFs by the attached rhizobia leads to root hair curling and entrapment of the bacterial micro-colonies in a so-called 'infection pocket' (Murray, 2011). Along with epidermal responses, cortical cells activate mitosis to form a nodule primordium. The infection threads grow towards the developing primordia and rhizobia are released into the inner cells in the nodule via an endocytotic-type mechanism that encapsulates the bacteria within the plant membrane. Nodules with a persistent meristem are called indeterminate such as seen in *Medicago truncatula*. Determinate nodules such as those of *Lotus japonicus* lose their meristematic activity soon after they form.

Low phosphate conditions, trigger an exchange of signals between the plant host and members of phylum Glomeromycota, arbuscular mycorrhizae. More than 80% of land plants can form associations with these arbuscular mycorrhizal (AM) fungi. Plant secreted strigolactones stimulate fungal spore germination and hyphal

branching (Akiyama, Matsuzaki, & Hayashi, 2005; Besserer et al., 2006). Like the bacterial symbionts, AM fungi then produce LCOs which trigger perinuclear calcium oscillations in the host which initiates downstream developmental pathways including root growth (Maillet et al., 2011). Once the AM fungal hypha reaches the root surface it penetrates a hypodermal passage cell and branches extensively to form the arbuscule, which is the primary nutrient exchange site. As the arbuscule develops the host plant generates plasma membrane that extends around the arbuscules across which phosphorus and other nutrients are then exchanged (Bonfante & Genre, 2010). The identity of this peri-arbuscular membrane (PAM) is unique and differs from the cell membrane. Evidence for this is provided by the observation that the symbiotic phosphate transporter MtPT4 is localized specifically to the PAM and is absent from the surrounding cell membrane (Pumplin, Zhang, Noar, & Harrison, 2012).

Concomitant to the plasma membrane synthesis, new cell wall material is also deposited around the infection structures. According to Gage, a central unanswered question to the understanding of infection thread growth pertains to the reorientation of cell wall deposition from the tip of growing root hair cells to the centre of the infection pocket surrounding the bacteria (Gage, 2004). The remodelling of the cell wall to initiate the infection thread is a host-mediated process that requires a pectate lyase (Xie et al., 2012). New cell wall is deposited inside the lumen of the advancing infection thread membrane providing rigidity to the structure. AM fungal entry is also dependent on the plant host for entry, as cell wall degrading enzymes appear to be limited (Garcia-Romera, Garcia-Garrido, & Ocampo, 1992), and unlike the case with pathogenic appressoria, entry does not depend on mechanical pressure from the hyphopodium. Cellular reorganization around the arbuscule includes deposition of β -1,4 glucans, polygalactourans and xyloglucans which are the primary constituents of the peri-arbuscular matrix (Brewin, 2004)(Bonfante and Perroto 1995)

1.1.1 A common signalling pathway regulates both rhizobial and mycorrhizal symbioses

Recognition of Nod-factors and Myc factors (Denarie et al., 1996; Maillet et al., 2011), by LysM domain-containing cell surface receptors are the first step in activating this pathway. Rhizobial Nod-factors are perceived by the signalling receptor MtNFP (NOD FACTOR PERCEPTION) /LjNFR5 (NOD FACTOR RECEPTOR 5) but bacterial admission is allowed only following recognition by the entry receptor MtLYK3 (LysM DOMAIN RECEPTOR KINASE 3) /LjNFR1 (NOD-

FACTOR RECEPTOR 1) (Limpens et al., 2003; Madsen et al., 2003; Radutoiu et al., 2003; Smit et al., 2007). Mutations in these genes block rhizobial entry and nodule formation. Interestingly, these nod-factor receptor mutants are unaffected in their ability to be colonized by mycorrhizal fungi indicating that a separate recognition receptor must exist for Myc-factor perception. Rhizobia and mycorrhiza form endosymbiotic associations which appear vastly different; however the legume host employs a core set of genes which comprise a signalling pathway common to both symbioses. DOES NOT MAKE INFECTION 2 (MtDMI2)/ SYMBIOSIS RECEPTOR KINASE (LjSYMRK) putatively acts as a co-receptor for the other LysM domain containing receptors and is required for both rhizobial and mycorrhizal signalling (Gherbi et al., 2008). Downstream of these recognition events, the cation channels CASTOR and POLLUX in *Lotus* and the POLLUX orthologue DOES NOT MAKE INFECTION 1 (DMI1) in *Medicago* are required for nuclear calcium oscillations serve as signatures that help distinguish the incoming microbe (Charpentier et al., 2008; Riely, Loughon, Ane, & Cook, 2007), Mutations in these genes affect both rhizobial and mycorrhizal colonization of the plant (C. Chen, Fan, Gao, & Zhu, 2009). These calcium signatures are interpreted by the central regulator of symbiosis signalling CALCIUM CALMODULIN KINASE (CCaMK) or DOES NOT MAKE INFECTION 3 (DMI3). Activation of this regulatory kinase is sufficient to initiate nodule organogenesis and initiate formation of the pre-penetration apparatus which develops during mycorrhizal colonization (Gleason et al., 2006; Takeda, Maekawa, & Hayashi, 2012). CCaMK phosphorylates CYCLOPS (*L. japonicus*)/IPD3 (INTERACTING PROTEIN DMI3) a transcriptional activator the absence of which blocks rhizobial infection and impairs mycorrhizal colonization (Horvath et al., 2011; Singh, Katzer, Lambert, Cerri, & Parniske, 2014; Yano et al., 2008). A suite of GRAS domain containing transcription factors act downstream of CCaMK and control nodule formation (S. Hirsch et al., 2009). NSP2 plays an essential role in both nodulation and mycorrhization. NSP1 is solely root nodule symbiosis specific (S. Hirsch et al., 2009; Smit et al., 2005). Mutation in *RAM1* (*REQUIRED FOR ARBUSCULAR MYCORRHIZATION 1*) another GRAS domain containing transcription factor was recently shown to specifically and strongly inhibit mycorrhizal colonization without affecting nodulation (Gobbato et al., 2012). *NODULATION INCEPTION* (*NIN*) encodes another transcription factor that is required for nodule organogenesis. Some epidermal responses to rhizobia occur even in the absence of this gene but the mutant shows hyper curling of infected root hairs and a wider expression zone for the infection marker *ENOD11* (Schauser, Roussis, Stiller, & Stougaard, 1999). The expression of *NIN* itself is higher in the

mutant background indicating that *NIN* must control its own expression in a positive feedback regulatory loop (Marsh et al., 2007). The only other common symbiotic gene known encodes the major sperm domain containing protein, *VAPYRIN*, which is involved in infection thread progression and mycorrhizal colonization. (Murray et al., 2011; Pumplin et al., 2010). *VAPYRIN* is evidence that structural genes that are common to both symbioses exist downstream of the signalling pathway and forms a basis for future research towards discovering the identity and function of such genes (G. E. D. Oldroyd, 2013).

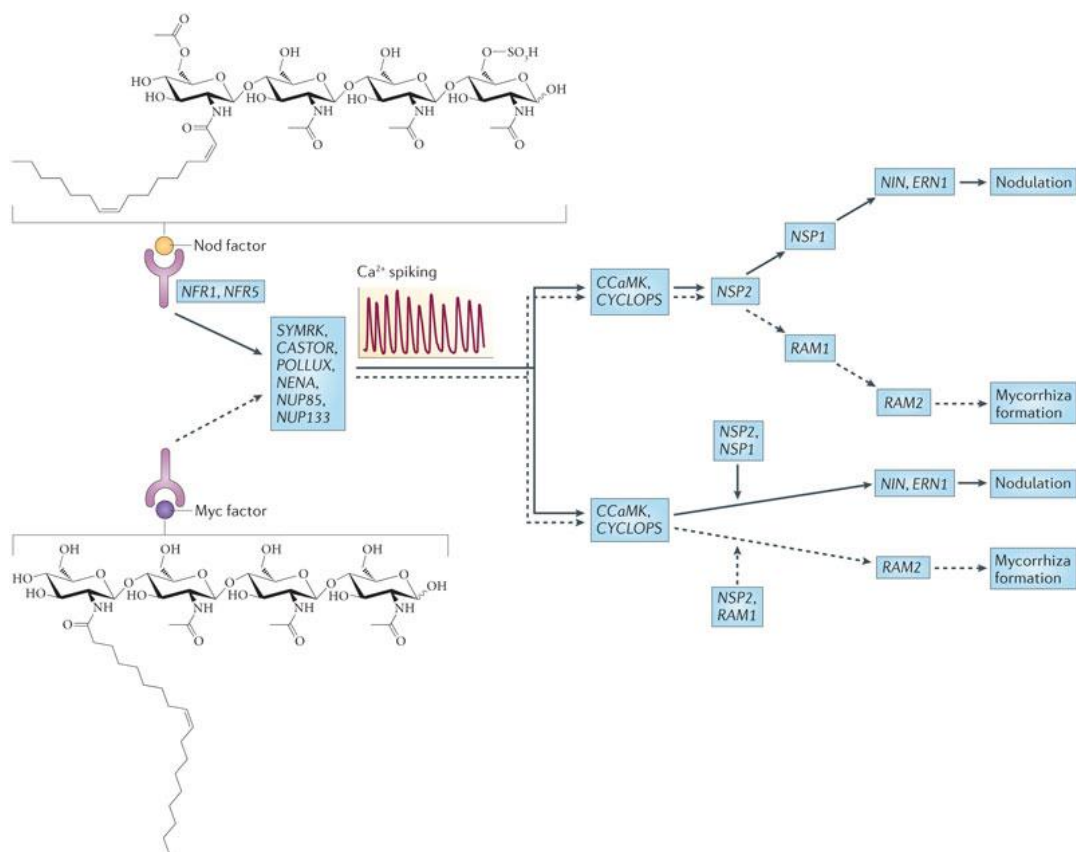


Figure 1. 1: Overview of the common symbiotic signalling pathway

Pathway shows key molecular players downstream of Nod-factor and Myc-factor perception by LysM domain receptors. Perinuclear calcium oscillations decoded by the central regulator of symbiotic signalling CCaMK are relayed to downstream components. Notably the GRAS domain containing TFs NSP1, RAM1 and another TF NIN are not shared by both pathways in establishment of symbioses. Taken from (G. E. D. Oldroyd, 2013)

1.2 A role for auxin in nodulation

Plant development and environment signals are integrated by various plant growth regulators. Plant growth substances namely, auxin, cytokinin, ethylene, abscisic acid as well as jasmonic acid and salicylic acid are noted regulators of plant microbe interactions (Murray et al., 2011). Together with cytokinins, auxins affect almost every aspect of development and therefore can be expected to play important roles in infection and nodule organogenesis.

Went (1926) originally showed that asymmetric application of the plant hormone auxin, on decapitated *Avena* coleoptile, causes it to bend in proportion to the amount of auxin applied. Using this principle, Thimann in 1936 showed that sections of young pea nodules, both, from the base and the meristematic apex, cause significant bending of the *avena* coleoptile. Since the activity was not only ascribed to the nodule meristem but to the entire nodule cortex, he hypothesized that auxin in nodules was perhaps related to tissue infected with rhizobia (Thimann, 1936). Auxin was thus established to play a role in symbiosis. However, it was not until 1989 that Hirsch et al. showed that nodule-like structures could be initiated in the absence of bacterial symbionts using auxin transport inhibitors (ATIs) (A. M. Hirsch, Bhuvanewari, Torrey, & Bisseling, 1989). Further evidence that changes in auxin transport were important for nodulation was provided by studies using the promoter of soybean *GH3*, an early auxin responsive gene, fused to a GUS reporter. Using this tool, Mathesius et al. noted a striking but transient arrest in auxin transport at the site of infection as early as 24 hours post infection followed by a strong increase at the same position where the nodule later initiated (Mathesius et al., 1998). Remarkably, purified Nod-factors were shown to disrupt auxin transport in a similar manner to naphthylphthalamic acid (NPA) (Boot, van Brussel, Tak, Spaink, & Kijne, 1999; Pacios-Bras et al., 2002).

Directional or 'polar auxin transport' (PAT) refers to the cell-to-cell movement of auxin mediated by members of the AUX-LAX family of influx carriers and efflux transporters like the PIN-FORMED (PIN) (Friml, 2003). P-GLYCOPROTEIN (PGP) family proteins also contribute to auxin transport by mediating an apolar efflux of auxin that helps maintain auxin flow to the root meristem (Band et al., 2014). The PGPs are members of the B subfamily of the ABC transporters. To date, four members of the family in *Arabidopsis*, namely *AtABCB1*, *AtABCB4*, *AtABCB19*, *AtABCB21* have been implicated in transport of auxin (Geisler et al., 2005; Kamimoto et al., 2012; Noh, Bandyopadhyay, Peer, Spalding, & Murphy, 2003; Noh,

Murphy, & Spalding, 2001; Terasaka et al., 2005). Although ABCB14 is known to transport malate, the *abcb14* mutant also had reduced auxin transport activity (Kaneda et al., 2011; Lee et al., 2008). This suggests that ABCBs are multi affinity transporters which have inherent auxin transport ability. In *M. truncatula*, there are ten *MtPIN* genes, five AUX-LAX genes (Schnabel & Frugoli, 2004) and based on the latest release of the *Medicago* genome Mt4.0, we have found at least 33 genes encoding full ABC subfamily B type transporters (this study). ABC transporters in nodule organogenesis and microbial infection have been described in detail in the following section.

Auxin acts as a developmental trigger primarily by creating local cellular gradients in the existing auxin stream using this PAT machinery. Both in *Medicago* and *Lotus*, within the first 50 hours post infection the expression of the soybean auxin response marker *GH3* expression accumulates at the site of inoculation (Mathesius et al., 1998; Pacios-Bras et al., 2003). The synthetic auxin marker DR5 which consists of 5 tandem repeats of the auxin response element TGTCTC is widely used as an auxin response marker (Ulmasov, Hagen, & Guilfoyle, 1999). A recently developed marker for auxin activity utilizes the domain II (DII) of the *Arabidopsis* Aux/IAA28 gene which is degraded rapidly upon perception of auxin (Brunoud et al., 2012). The DII domain fused with a fluorescent marker shows high activity in regions with low auxin and absence in high auxin containing tissues, at a cellular resolution. The use of such markers in *Medicago* might provide a better understanding of auxins role in infection and organogenesis but these tools remains to be developed. Upon infection, both the stably transformed GH3 marker and the synthetic auxin marker *DR5-GUS* in *Medicago* hairy roots show an arrest in auxin transport at the inoculation site (Huo, Schnabel, Hughes, & Frugoli, 2006). In determinate nodules of stably transformed *DR5-NLS-GFP* lines of *Lotus*, 72 hrs post infection, marker activity is observed in a few outer cortical cells just below the infected root hair cell. As nodule development progresses, the actively dividing cortical cells of the nodule maintain this *DR5* expression until the rhizobia enter the cortex (Suzaki et al., 2012). By six days post infection, *DR5* marker expression is restricted to the outer cortex of the nodule (Takanashi, Sugiyama, & Yazaki, 2011). The authors suggest that since the *DR5* expression pattern seems to mimic meristem activity within the nodule, restriction of the marker expression to the periphery of a determinate nodule occurs because the parenchymatic cells in this region retain meristematic activity. In *Medicago*, *DR5* expression in mature nodules is especially strong in the vascular

bundles (Guan et al., 2013). In another study, overexpression of miRNA160 in soybean, which silences repressor auxin-response factors (ARFs), resulted in a decrease in nodule number (Turner et al., 2013). However, no effect on infection thread frequency was noted for these lines. ARFs act downstream of AUX/IAA repressor proteins to mediate auxin response.

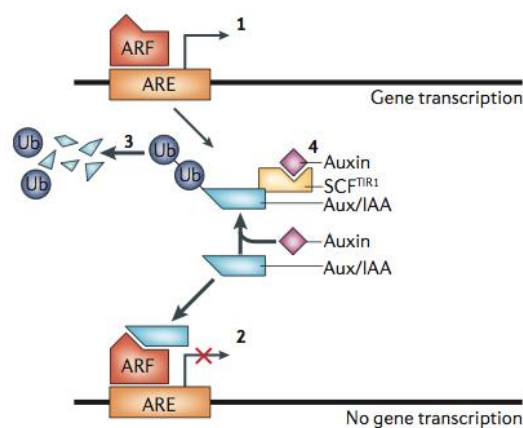


Figure 1. 2: Overview of early auxin signalling and response.

AUX/IAAs form inactive dimers with ARFs and prevent transcription of target genes in the absence of auxin. In the presence of auxin, AUX/IAAs are target for degradation via the 26 S proteasome which results in depression of ARF activity and activation of auxin signalling responses. From (Teale, Paponov, & Palme, 2006)

Since these RNAi lines are hypersensitive to auxin the authors speculate whether auxin might in-fact have a negative role in nodule primordia formation while not affecting rhizobial infection *per se*. However, these studies are difficult to interpret due to the miRNA having been expressed ectopically and having multiple targets which could have unforeseen consequences. Moreover, observations that in the *M. truncatula* hypernodulating mutants *sickle* and *sun*, auxin transport is enhanced, points at a specific role for auxin transport in nodule organogenesis (Prayitno, Rolfe, & Mathesius, 2006; van Noorden, Ross, Reid, Rolfe, & Mathesius, 2006). However, no functional genetic evidence exists to date showing the involvement of auxin in nodule development (Mathesius, 2008).

Plant flavonoids act as natural auxin transport inhibitors by competing with NPA binding sites (Jacobs & Rubery, 1988). Since the inhibition of auxin transport by NPA was shown to initiate nodule like organs (A. M. Hirsch et al., 1989) it follows that endogenous auxin transport inhibitors (ATIs), i.e flavonoids also play a role in nodule organogenesis. Wasson et al. showed that in *M. truncatula*, by silencing the enzyme chalcone synthase which catalyses the first step of the flavonoid biosynthesis pathway nodulation can be eliminated (Wasson, Pellerone, & Mathesius, 2006). Conversely, in the hyper-nodulating mutant of *L. japonicus har1*, a stronger *DR5* expression was associated with a wider cortical area of expression and excessive cell division in comparison to the wild type (Suzaki et al., 2012).

Auxin is thus thought to have a positive role in nodule organogenesis with flavonoids having a potential role in its regulation.

1.2.1 Auxin and rhizobial infection

Most of the research in the nodulation field so far has focused on the involvement of auxin transport in nodule organogenesis rather than its role in infection (Mathesius, 2008). Recently, transcripts of *LjABCB1*, a *L. japonicus* homologue of the auxin transporting *Arabidopsis ABCB4* gene, were found to be nodule-specific. The promoter-GUS fusion further showed its expression was limited to the uninfected cells of the nodule (Takanashi, Sugiyama, Sato, Tabata, & Yazaki, 2012). *S. cerevisiae* expressing *LjABCB1* accumulated less IAA than a control strain transformed with the empty vector control, suggesting that *LjABCB1* functions as an auxin exporter. In another model symbiosis – between the actinomycete *Frankia* and the actinorhizal plant *Casuarina glauca*, the gene encoding the *Casuarina* homologue of the *Arabidopsis* AUX1 permease *CgAux1* was found to be expressed only in infected cells of the nodule (Peret et al., 2007). Moreover, the authors showed that *CgAUX1* is specifically induced in infected root hairs. Using antibodies it was further shown that auxin accumulates in infected cells of the nodule (Perrine-Walker et al., 2010). What role might auxin play in infected cells? Auxin has a well-established role in cell wall expansion/loosening and it can be expected that it may be important for expansion of infection containing cells of the nodule. Although a general expression pattern of members of the *MtLAX* family was studied by *in situ* hybridization in *Medicago* (de Billy, Grosjean, May, Bennett, & Cullimore, 2001), it is not clear whether infection by rhizobia is similarly associated with *AUX1* expression, and studies in model legumes would provide insight into whether this feature is evolutionarily conserved with actinorhizal plants.

1.3 ABC Transporters in Plant-Microbe interactions

1.3.1 Section I: Secondary metabolites and transport processes in plant-microbe interactions

1.3.1.1 Secondary metabolites and transport processes are crucial to symbiosis

Functional, beneficial symbioses culminate in the acquisition of the two mineral nutrients which can be most limiting to plant growth, namely nitrogen and phosphorous. It follows therefore that symbiotic membrane transporters are important targets for crop improvement (Schroeder et al., 2013). The symbiotic phosphate transporter *MtPT4* mediates the uptake of phosphates provided by arbuscular mycorrhizal fungal symbionts, (Harrison, Dewbre, & Liu, 2002). A mutation in this gene disrupts the interaction between the plant host and the microbe and consequently arbuscules degenerate prematurely and symbiosis fails to be established (Javot, Penmetsa, Terzaghi, Cook, & Harrison, 2007; Veereshlingam et al., 2004). However, transporter functions are not restricted to nutrient exchange only. Symbiosis requires a constant communication between two organisms and transport of signals and metabolites is fundamental to every stage of symbiosis (Bapaume & Reinhardt, 2012; Udvardi & Poole, 2013).

Many secondary metabolites provide adaptive advantage to sessile plants, which are subject to the mercy of an ever changing environment. Under low nutrient conditions in the soil, members of the family leguminosae and their compatible bacterial symbionts seek each other out and then establish a mutualistic relation by using a range of metabolites and signals, the transport of which is spatially and temporally fine-tuned. Phenolics such as flavonoids and iso-flavonoids produced as a result of nitrogen deficiency stimulate soil bacteria called rhizobia to produce lipochitooligosaccharides called Nod-factors. Nod-factors in turn trigger nodulation which is accompanied by the production of a variety of host metabolites. Perception of Nod-factors by the host causes increased production of specific (iso) flavonoids, creating a positive feedback loop based on microbial and host secretion of signalling molecules (Hassan & Mathesius, 2012). Some of these metabolic changes have been shown to occur in root hairs upon infection including increases in Nod gene inducing flavonoids (Brechenmacher et al., 2010). Legumes such as the model plant *M. truncatula* also synthesize phytoalexins such as medicarpin which may serve to

ward off both opportunistic soil pathogens and incompatible rhizobia (Dakora & Phillips, 1996).

Under phosphate limitation, specific compounds are produced by plants that can increase mycorrhizal colonization including flavonoids and strigolactones (Akiyama, Matsuoka, & Hayashi, 2002). Strigolactones are sesquiterpene lactones that guide the mutualistic fungi to its host. Secreted strigolactones stimulate fungal spore germination followed by hyphal branching before penetrating the host root (Akiyama et al., 2005; Besserer et al., 2006). Infection by mycorrhiza in turn activates the methylerythritol 4-phosphate pathway (MEP) or non-mevalonate pathway for biosynthesis of terpenoids which includes production of various other apocarotenoids such as mycorradicin whose role in the symbiosis is not yet understood (Walter, Floss, Hans, Fester, & Strack, 2007). At later stages of infection, as a common feature to both rhizobial and mycorrhizal interactions, the host must continually provide food in the form of simple carboxylic acids and various nutrients to maintain the endosymbionts (Pfeffer, Douds, Bécard, & Shachar-Hill, 1999; Poole & Allaway, 2000). Reportedly, the plant allocates 5-21% of photosynthetically fixed carbon to rhizosphere secretions (Walker, Bais, Grotewold, & Vivanco, 2003). Movement of all these substances must occur across intact membranes and energy-dependent transfer of substrates against a concentration gradient must be facilitated by transporters.

1.3.1.2 Plant-parasite lifestyles

In its broadest and most widely accepted definition, symbiosis refers to the close and often long term relation between two species. Thus interactions between pathogens and resistant or susceptible hosts can be included in the umbrella term 'symbioses. However, in this thesis symbiosis is used to refer specifically to the mutually beneficial symbioses, nodulation and mycorrhization. Instead of trying to attract these microbes, the host plant attempts to mount a successful defence reaction by secreting phytoanticipins and phytoalexins to inhibit the entry and proliferation of the pathogen. Pathogens include biotrophs which derive their nutrition from living host tissue while microbes that derive their nutrition from dead infected cells are called necrotrophs. Hemibiotrophs include pathogens who follow an initial biotrophic lifestyle followed by a necrotrophic stage (Oliver & Ipcho, 2004). Hormone signalling networks are wired to mount an attuned defence response based on these pathogenic lifestyles. Salicylic acid, jasmonic acid and ethylene

have been implicated in plant immunity and disease resistance involving extensive inter-communication between their respective signalling pathways (Pieterse, Van der Does, Zamioudis, Leon-Reyes, & Van Wees, 2012).

1.4 Section II: ABC transporters and metabolite transport

1.4.1 A large complement of plant ABC transporters enables trafficking of diverse metabolites

The transport of metabolites can be passive or active. Active or ATP-dependent transport of metabolites has the advantage of being highly regulated in terms of when and where it is activated in a tissue, allowing such transporters to play extremely specialized roles in physiological processes. According to the Transporter Classification Database, transporters can be grouped into 5 well defined classes and further into sub-classes and then again into more than 750 families, based on a functional/phylogenetic five tier system (Saier, Reddy, Tamang, & Vastermark, 2014). The class of 'primary active transporters' further consists of five sub-classes from A to E depending on the energy source which drives the solute transport. ATP Binding cassette containing family of transporters along with 24 other families belong to the subclass A that derives its energy from hydrolysis of diphosphate bonds of inorganic pyrophosphate such as ATP. The ATP binding cassette (ABC) transporter family utilizes the energy derived from magnesium bound ATP (MgATP) hydrolysis to shuttle a diverse array of metabolites across membranes. Efflux transporters move the substrate away from the cytosol while influx transporters move them into the cytosol. Full-molecule functional transporters comprise of two modularly organized segments, each containing a multi-pass transmembrane domain (TMD) and the ATP binding or Nucleotide binding domain (NDB). Genes encoding only a single TMD and NBD are termed half transporters which must homo or hetero dimerize to form a fully functional transporter (Martinoia et al., 2002; Rea, 2007; Rees, Johnson, & Lewinson, 2009).

The ABC transporter family, although ubiquitously present in all organisms, was noted to have considerably expanded in plants (Jasinski, Ducos, Martinoia, & Boutry, 2003; Sánchez-Fernández, Davies, Coleman, & Rea, 2001). According to Sanchez-Fernandez et al., a disproportionately large allocation of the genome to ABC transporters, concomitant with the expansion of secondary metabolite diversity in plants may reflect their need for a constant dialogue with their chemically

complex, microbially rich, immediate environment (Sánchez-Fernández et al., 2001). ABC transporters are particularly well equipped to deal with this chemical diversity firstly because they are known to transport a remarkably wide variety of substrates. These range from alkaloids such as catharanthine (Yu & De Luca, 2013), isoprenoids such as the hormone abscisic acid (Kang et al., 2010), to phenolics like anthocyanidin-3-O-glucosides (Francisco et al., 2013). In fact, mere heterologous expression of a yeast ABC transporter in tobacco was sufficient to increase export of plant secondary metabolites into suspension cell cultures (Goossens, Hakkinen, Laakso, Oksman-Caldentey, & Inze, 2003). Secondly, a single transporter can have 'multispecificity', meaning the same transporter can be responsible for movement of more than one substance. The *Arabidopsis* ABCC1 is involved in vacuolar sequestration of folates in addition to phytochelatin metalloid complexes of various potentially toxic metals (Mendoza-Cozatl, Jobe, Hauser, & Schroeder, 2011; Raichaudhuri et al., 2009). A feature of the ABCs is that, half ABC transporters can further form homo and hetero dimers, combinations of which possibly add to the set of substrates that they transport. As an example, the *Arabidopsis* ABCG11 was shown to form homodimers with itself and heterodimers with ABCG12 to form a full functional transporter (McFarlane, Shin, Bird, & Samuels, 2010). Consequently, even though the amino acid sequence of the transmembrane region is thought to provide substrate specificity, homology-based classification is not enough to predict transporter function. Nevertheless, the promiscuity of these ABC transporters necessitates a strict systematic ordering of ABC transporters as a first step to genetic and biochemical dissection of function.

1.4.2 Analysis of the *Medicago* ABC transporter family reveals an expansion of all sub-families

In providing an analysis of the important genes involved in symbiosis we first consider the ABC complement of three model plants with differing lifestyles and varying abilities to interact with plant microbes. *Arabidopsis* and rice are well established model systems to study plant microbe interactions. While *Arabidopsis* serves as a prototype for fundamental research in plant-pathogen interactions (Nishimura & Dangl, 2010), the monocot rice provides a genetically amenable system to study interactions with beneficial mycorrhizae (Gutjahr et al., 2008). In an early comparison between the ABCs encoded by their genomes it was noted that *Arabidopsis* and rice both have a similar number of genes allocated to ABC

transporters, each containing around 54 and 45 full-molecule transporter genes respectively (Garcia, Bouige, Forestier, & Dassa, 2004; Jasinski et al., 2003). Differences in the number of homologues between the two model plants were thought to have arisen as a result of sub-functionalization after the monocot-dicot split. One such instance is the loss of mycorrhiza-related transporters in the Brassicaceae (see below). Legume evolution, including the ability to nodulate, is marked by a whole-genome duplication that took place 60 MYA prior to the radiation of most, if not all, legume species (Young et al., 2011). The recently sequenced *Medicago truncatula* genome (Tang et al., 2014) encodes 99 full-molecule transporters some of which are predicted to play important roles in root nodule symbiosis (RNS) and arbuscular mycorrhizal symbiosis (AMS) based on analyses of their transcriptional profiles (Benedito et al., 2010; Z. Miao et al., 2012) . All sub-families from ABCA to ABCI, classified based on homology to ABC transporters in the human genome, were represented in the *Medicago* genome except ABCH which characteristically is absent from plants (Verrier et al., 2008). Notably, the size of sub-family G, of which numerous genes are known to function in plant-microbe interactions, is twice as large in *Medicago* compared to *Arabidopsis* (Figure 1). Sub-family G is unique in the organization of the two NBD and TMD domains and in plants comprises exclusively of 'reverse' oriented molecules (NBD-TMD) (Verrier et al., 2008). Though the significance of this observation may not be clear at present, future discoveries might shed light on possible inherent structural features of this sub-family that make it advantageous for the plant to use with incoming microbes. Comparison between the three model systems is likely to provide interesting candidate genes critical for microbial associations.

Over the past four years there have been several studies in both legumes and non-legumes uncovering critical roles for ABC transporters in symbiosis development. It is emerging now, that ABC transporters possibly play roles from the initial signal exchange through development of infection structures up to maintenance of the interaction. We draw examples from both, root nodule symbiosis and arbuscular mycorrhizal symbiosis and when relevant, supplement it with examples from interactions with pathogens and attempt to consolidate these findings to put them in perspective of the distinct stages of symbiosis that they are involved in.

1.5 Section III: ABC transporters involved in different stages of plant microbe interactions

Transporters with roles in metabolite secretion can serve several purposes, chemoattraction and antibiosis, formation of defence barriers or specialized microbial accommodation structures and nutrient provision, with significant potential for overlap between categories. Transporters involved in surveillance, which perceive environmental cues, both biotic and abiotic, may be constitutively expressed or induced by environmental cues such as nutrient deficiency (i.e. flavonoids, strigolactones). In either case it serves to induce corresponding signals from the microbe that can be subsequently detected by the plant. In a similar fashion, the other transporter classes can be regulated upon perception of signals from the symbionts while preparing to accommodate the incoming microbe and to establish a suitable nutrient exchange interface. Ultimately, functional interactions that involve transporter functions include the modulation of defence responses, exchange of signals and nutrients and developmental events required for microbe accommodation. We classify plant ABC transporters studied so far in plant microbe interactions based on the above mentioned criteria into the following three categories.

1.5.1 Plant signalling to microbes

Formation of tailored ecological niches requires energy-expending host cells (Bulgarelli et al., 2012). Plants accomplish this by releasing metabolites into their surroundings. If energy expenditure is pharmacologically blocked, for example with the use of an inhibitor of ABC efflux pumps such as sodium orthovanadate, diagnostic fractions of *Arabidopsis* root secretions are qualitatively altered in a dose-dependent manner (Loyola-Vargas, Broeckling, Badri, & Vivanco, 2007).

Furthermore, an alteration in the composition of exudates caused by the *Arabidopsis abcg30* mutation retarded the growth of microbes *in vitro* and also dramatically changed the identity of rhizosphere microflora (Badri et al., 2009). Although this may be due to pleiotropic effects of the mutation on multiple metabolic pathways, it suggests ABC transporters are important players in host-controlled design of their environs.

From the standpoint of host-microbe communications, it can be argued that the most agronomically important secretions of legumes belong to a class of phenolic compounds, the flavonoids and iso-flavonoids. Each legume species deploys a combination of flavonoids to attract compatible symbionts. These chemo-attractants can be detected in exudates under low nitrogen conditions (Maxwell, Hartwig, Joseph, & Phillips, 1989). Conditional secretion of these chemoattractants might indicate the plant's underlying need for conservation of ATP that is otherwise needed for exudation of these substances into the rhizosphere. Although their transport machinery has been elusive so far (Hassan & Mathesius, 2012), ABC transporters have been implicated repeatedly in transport of these and related phenylpropanoid pathway derivatives (Buer, Muday, & Djordjevic, 2007; Goodman, Casati, & Walbot, 2004). Translocation of the soybean signalling flavonoid, genistein, was shown to be MgATP dependent and could be inhibited by sodium orthovanadate indicative of the involvement of an ABC transporter. In the absence of any further transcriptional induction by low nitrogen conditions the authors conclude that the transporter is probably expressed constitutively and that increased levels of flavonoids secreted under low nitrogen conditions are likely to be due to biosynthetic changes (Sugiyama, Shitan, & Yazaki, 2007). The ABC transporter gene responsible, however, is yet to be identified.

The phytohormone strigolactone which inhibits shoot branching in plants can also act as a signal for mycorrhiza (Akiyama et al., 2005). Strigolactone induced spore germination and hyphal branching is accompanied by an increase in size and number of the fungal mitochondria (Besserer et al., 2006). The recently discovered transport machinery for these sesquiterpene lactones in *Petunia x hybrida* involves the *PhPDR1* gene, a ABCG type plasma-membrane-localized ABC transporter, induced in response to phosphate deficiency in hypodermal passage cells of the root (Kretschmar et al., 2012). The transcript level of this transporter is correlated with the early stages mycorrhizal colonization but is decreased at later stages, possibly reflecting the decreased requirements for the chemoattractant in the root

exudates. Interestingly, the *P. x hybrida pdr1* mutant showed reduced mycorrhizal colonization although the infection structures developed normally. Given that strigolactones are also produced during nodulation (Liu et al., 2011), analysis of the *Medicago* orthologue of *PhPDR1* might provide useful insights into the role of strigolactones in rhizobial infection.

Another plant-to-mycorrhiza signalling molecule are cutin monomers produced by the *M. truncatula* glycerol-3-phosphate acyl transferase *RAM2* (REQUIRED FOR ARBUSCULAR MYCORRHIZATION); these cutin monomers are also important for invasion by the hemibiotrophic oomycete *P. palmivora* (Wang et al., 2012). The *ram2* mutant is defective in formation of fungal and oomycete hyphopodia and mycorrhizal appressoria. Since external addition of cutin monomers alone is enough to restore infection by either microbe, the authors concluded that cutin is involved in signalling rather than structural aspects of the interaction. Induction of the *RAM2* transcript requires the central regulator of symbiosis signalling, CCaMK. However, the *ccamk* mutant, although blocked in mycorrhizal colonization can still form hyphopodia at the root surface and so basal expression of *RAM2* at the epidermis is thought to be independent of CCaMK (Murray, Cousins, Jackson, & Liu, 2013). Moreover, successful infection by *P. palmivora* does not require CCaMK indicating that the product of the *RAM2* biosynthetic pathway is constitutively present at the root surface. Although it is not known how these cutin monomers are transported in symbiosis, there are several reports implicating half ABCG transporters in the transport of cuticular lipids (G. Chen et al., 2011; McFarlane et al., 2010; Panikashvili, Shi, Schreiber, & Aharoni, 2011; Pighin et al., 2004). Based on these observations, a hypothetical *Medicago* cutin transporter can be predicted to be an ABCG transporter which is plasma membrane localized and is active constitutively but is transcriptionally induced by mycorrhizae.

Maintenance of defence barriers and prevention of disease requires active secretion. Legumes responding to beneficial symbionts release phytoalexins like medicarpin and formononetin which quite possibly evolved to detain opportunistic soil pathogens in the soil. Previously found to be secreted under low nitrogen conditions, secretion of these isoflavonoids was reported to be induced by elicitors from *Phytophthora medicagenis* (Banasiak et al., 2013). Silencing of *ABCG10* in *Medicago* led to increased infection by *P. medicagenis* while levels of detected isoflavonoids correspondingly decreased. The authors also reported *MtABCG10* to be induced by liquiritigenin and iso-liquiritigenin, suggesting a wide chemical variety

of isoflavonoids as substrate. However, no direct transport assays support this hypothesis.

Pre-infection defences include numerous anti-microbial compounds which can be secreted constitutively or are pathogen induced. Tobacco leaf exudates are composed of various phytochemicals, including the solanaceous terpenoid sclareol. A *Nicotiana plumbaginifolia* plasma-membrane ABC transporter *NpPDR1*, which can be induced by sclareol and its analogue sclareolide is perhaps the first ABC transporter identified as having a role in plant defence (Jasinski et al., 2001). Addition of ATP synthesis inhibitors increased retention of a radioactively-labelled sclareolide derivative in cultured cells of *Nicotiana*, confirming that export of sclareol is ATP dependent. *NpPDR1* was expressed constitutively in leaf trichomes (the primary sites of sclareol biosynthesis) and throughout the root except in the root tips. However, upon attack by necrotrophic fungal pathogens such as *Botrytis cinerea*, which causes soft rot, expression was immediately detected in whole leaves. Knockdown of *NpPDR1* by RNAi rendered *N. plumbaginifolia* *NpPDR1* susceptible to this normally incompatible pathogen indicating a role for the transporter in non-host resistance. Transcriptional control by the jasmonic acid pathway shed light on its regulation by the defense signalling pathway (Stukkens et al., 2005) and was followed up by studies of the orthologous *AtPDR12* in *Arabidopsis*. Orthologues of *Arabidopsis AtPDR12*, *N. plumbaginifolia (NpPDR1)* in *N. tabacum (NtPDR1)* and *soybean (GmPDR12)* are all inducible by methyl jasmonate and to an extent salicylic acid (Eichhorn, Klinghammer, Becht, & Tenhaken, 2006; Sasabe, Toyoda, Shiraishi, Inagaki, & Ichinose, 2002; van den Brule, Muller, Fleming, & Smart, 2002) demonstrating ABC transporters as conserved molecular players in defence signalling pathways across species.

Localized secretion of anti-microbial metabolites at the site of microbial entry is possibly mediated by the *Arabidopsis AtPDR8* full-molecule transporter belonging to sub-family G. *AtABCG36/AtPDR8/AtPEN3* (penetration 3) is perhaps the best studied full ABCG transporter in non-host resistance. Although present ubiquitously in all organs and polarly-localized in root epidermal cells (Langowski, Ruzicka, Naramoto, Kleine-Vehn, & Friml, 2010), PEN3 accumulates at sites surrounding localized infection pockets upon pathogen recognition at the cell surface. In fact, application of PAMPs is enough to trigger the actin cytoskeleton-mediated recruitment of these transporters to the site of application (Underwood & Somerville, 2013). Targeted focal localization of this transporter at the penetration site suggests

a targeted secretion of anti-microbial metabolites but no substrate has yet been identified. The *atpdr8* mutant allows the entry and development of fungal papillae of normally incompatible pathogens which include the necrotrophic fungus *Blumeria graminis* pv. *hordei*, *Erysiphe pisi* and the oomycete *P. infestans*. The pathogen's growth is eventually restricted by post-penetration defence mechanisms that include callose depositions around the infection structure (Stein et al., 2006). MLO based resistance to powdery mildew, specifically *Golovinomyces orontii* is also PEN3 dependant (Consonni et al., 2006). *mlo* mutants show complete immunity to the fungal pathogen in contrast to the wild type where the fungus penetrates susceptible cells and hyphae extend throughout the leaf. The double mutant *Atmlo2 Atpen3* reverts to wild type levels of infection and displays the yellow chlorotic patches associated with *pen3* related susceptibility. *AtPDR7* which is the closest homologue of *AtPDR8* was shown to not be involved in penetration resistance to non-host pathogens demonstrating a unique role for AtPDR8 in generalized non-host resistance.

Finally, the wheat gene *Lr34* (Leaf rust 34) which has provided durable partial resistance for over 50 years to the two rust causing fungi *Puccinia triticina* and *P. striiformis* has recently been revealed to encode an ABC transporter. *Lr34* was mapped to the seventh chromosome of the D genome of polyploid wheat and identified as a 1401 amino acid long ABCG transporter (Krattinger et al., 2009). Although marked by senescing leaf tips, *Lr34* if present in the genome provides heritable, long term resistance in the adult plant to not only the two above mentioned rust fungi but also to stem rust causing fungus and the powdery mildew *B. graminis*. The characteristic necrotic leaf tips also indicate that *Lr34* is constitutively expressed. (Krattinger et al., 2011) Interestingly, some senescence related marker genes were found to be upregulated in *Lr34* lines especially the flag leaves which was also found to be the most resistant organ in the plant.

1.5.2 Cellular accommodation of microbes

Once the microbe is in contact with the host, the host can take measures to allow entry providing the proper signals are present. Often, purified elicitors are sufficient to trigger a cellular reprogramming of the contacted host cell. In the case of Nod-factors, entire developmental programmes can be initiated such as root hair branching, the formation of the pre-infection thread, and nodule organogenesis. Upon rhizobial attachment, root hairs curl to entrap the bacteria following which the

plasma membrane invaginates and extends down through the root hair forming the so called 'infection thread' which provides a conduit for the rhizobia to colonize the nodule cortex (Murray, 2011). Finally an entire new organ in the form of a nodule develops to house the incoming bacteria. During the mycorrhizal interaction, the plant plasma surrounds the appressoria and following cortical penetration it extends manifold to firstly surround the incoming hyphae; at later stages it encases the primary sites of nutrient exchange, the fungal arbuscules and is now called the periarbuscular membrane (Parniske, 2008). Inhibition of pathogen entry after protective physical barriers have been overcome as well as formation and function of host-pathogen interfaces such as the extra-haustorial membrane is also supported by energy dependent active processes involving transporters.

Gradients of the plant hormone auxin trigger developmental changes ranging from organ initiation to cell expansion including root hair growth. A role for auxin in nodulation has been hypothesized since the finding that application of auxin transport inhibitors like NPA and TIBA to legume roots can create nodule-like structures called 'pseudonodules' in the absence of rhizobia (A. M. Hirsch et al., 1989; Rightmyer & Long, 2011). Nod-Factor alone can also initiate organogenic events in some legumes perhaps using the same cellular machinery. A screen for NPA binding sites in *Arabidopsis* led to the discovery of ABCB transporters which were subsequently shown to efflux auxin (Noh et al., 2001). Since then a number of ABCB transporters have been shown to transport indole-acetic acid. This includes the *Arabidopsis ABCB4* which is a facultative importer and exporter of auxin (Cho, Lee, & Cho, 2007; Santelia et al., 2005). Several ABC transporters have been implicated in nodulation and mycorrhization. The expression of *LjABCB4* which is an orthologue of the auxin-transporting *AtABCB4* was associated specifically with uninfected cells of the nodule. The *Lotus* ABC family was defined for the incompletely sequenced legume (Sugiyama et al., 2006) and the authors uncovered two sub-groups of homologous genes encoding *Lotus* orthologues of *Arabidopsis* MRP14 (Subfamily C) and PDR12 (Subfamily G) ABC transporters which were highly induced after inoculation by the *Lotus* symbiont *Mesorhizobium loti*.

A forward genetics screen for *Medicago* mutants with defects in mycorrhizal colonization led to the identification of *STR1* and *STR2* (*STUNTED ARBUSCULE*), two half ABCG transporters that when knocked down had compromised arbuscule development but intact pre-symbiotic signalling (Q. Zhang, Blaylock, & Harrison, 2010). The knockdown roots showed shrivelled infection structures which, unlike

arbuscules in the wild type root, did not fill the entire infected cortical cell. The fungus had difficulty initiating the arbuscule as well as in hyphal branching required to form the arbuscule. All events prior to arbuscule development from signalling to hyphopodia formation and intracellular hyphal extension appeared to be normal. The functional conservation of these transporters in all mycorrhizal angiosperms was demonstrated by an ensuing study in rice which observed a similar extent of morphological defect if either gene was mutated (Gutjahr et al., 2012). Presence of nurse plants in the vicinity did not overcome the deficiency ruling out a rhizospheric secreted signal as a candidate substrate. Both transporters co-localized to the peri-arbuscular membrane which has a unique molecular identity (Pumplin et al., 2012) showing that the two transporters dimerize to form the full functional ABC transporter. Knockdown of *str2* in the *str1* mutant background did not further enhance the severity of the phenotype supporting the idea of coordinated transport of a common substrate. Dissimilarities with arbuscule phenotypes of strigolactone biosynthetic mutants are enough to rule strigolactones out as a substrate. Cutin monomers have been suggested as possible substrates but the hypothesis remains to be tested (Wang et al., 2012). Another *Medicago* ABC transporter, *MtABCB1*, responsive to mycorrhiza was identified in transcriptomic studies of laser dissected cortical cells containing arbuscules. Spatial expression patterns of this full molecule transporter belonging to sub-family B showed an association with arbuscules but unlike the *STRs* it was also present in adjacent cortical cells three weeks post inoculation (Gaude, Bortfeld, Duensing, Lohse, & Krajinski, 2012).

1.5.3 Nutrient exchange and additional processes

Maintenance of symbiotic associations is important for mutualistic and (hemi) biotrophic interactions which require the host plant to remain alive for the entire duration or part of the microbe's life cycle. One aspect of this is the sequestration of potentially toxic chemicals such as phytoalexins across the tonoplast which can be considered as 'storage excretion'. The majority of ABC transporters of sub-family C studied except AtMRP4 localize to the plant vacuolar membrane (Klein, Burla, & Martinoia, 2006). These ABCC transporters function as glutathione-S-conjugate pumps that move substrates into the vacuole only in the conjugated form (Rea, Li, Lu, Drozdowicz, & Martinoia, 1998). The previously mentioned isoflavonoid medicarpin when conjugated with glutathione proved to be an excellent substrate for MgATP dependent, vanadate sensitive uptake into vacuolar membrane vesicles of

the legume *Vigna mungo*. Non glutathionated medicarpin was transported with an efficiency four times lower than GS-medicarpin and this influx was independent of MgATP (Z. S. Li, Alfenito, Rea, Walbot, & Dixon, 1997). The authors speculate that non-infected neighbouring cells sequester the toxic medicarpin into vacuoles to prevent cellular damage and maintain healthy cells while at the same time they are prepared to remobilize the isoflavonoid if the infection spreads.

Ultimately, a sustained successful relationship requires exchange of nutrients between the host and the symbiont. However, no plant ABC transporters have been implicated in nutrient transfer to the microbe at present. For pathogens, leakage of sugars may serve as a susceptibility factor. Mutations in transporters which release sugars to the plants surface may provide resistance but there is no information at present about the chemical nature of substrate for any of the ABC transporters involved in plant-pathogen interactions. This remains one of the major challenges in the future both for academic and agronomic interest.

1. 6 Conclusion and future challenges

1. The ABC transporter family contains key members which decide the outcome of many plant-microbe interactions. With advances in genome sequencing technologies, inventories of ABC transporter genes in diverse plants are increasing. A large proportion of the transporters with known function seem to be involved in plant-microbe interactions highlighting a need to consolidate what is known at present. Integrating current knowledge might reveal conserved mechanisms involved in host-microbe interactions.
2. Linking transporters to their substrate remains one of the primary challenges in ABC transporter research. So far only one symbiotic ABC transporter namely, PhPDR1, has been described whose substrate as well as role in infection progression is known. Further biochemical studies are required to uncover specific substrates of important ABC transporters like *Medicago* STR1/2 and the *Arabidopsis* PDR8 (PEN3) and wheat LR34 to conclusively ascribe function for agricultural exploitation. On the other hand, it is also a priority to identify ABC transporters likely to transfer known substrates essential to the development of symbiosis like auxin and malate, for which ABCs have been identified in other tissues and organisms.

1.7 Summary

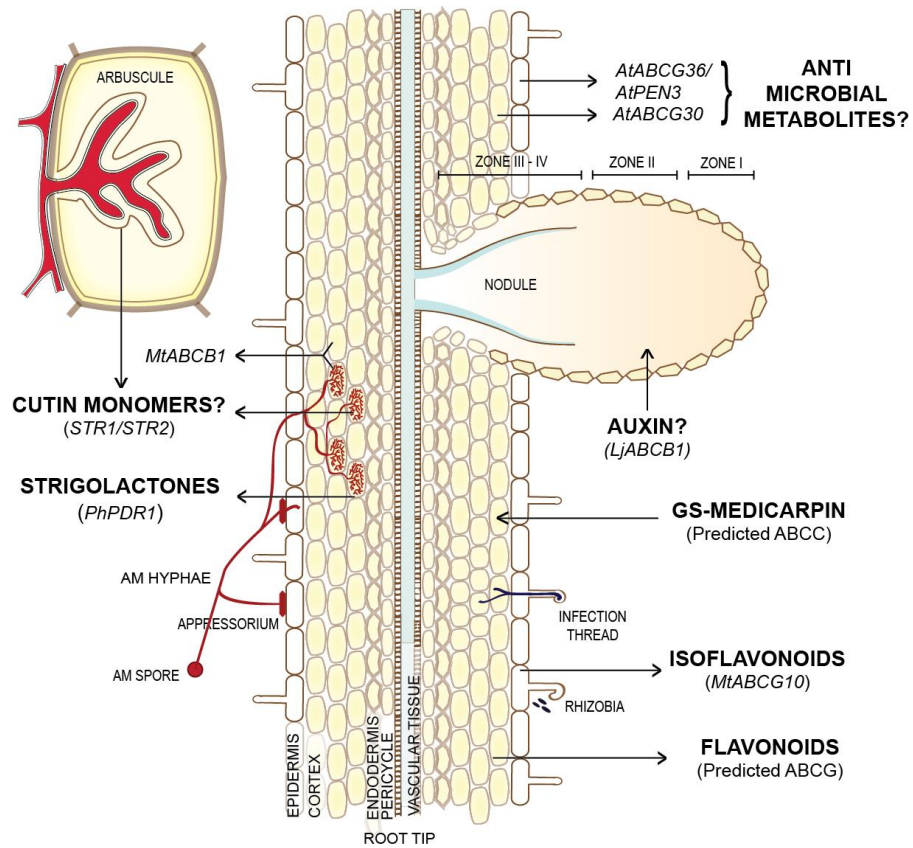


Figure 1.4: Summary diagram showing ABC transporters associated with Root nodule symbiosis and Arbuscular mycorrhizal symbiosis studied to date.

Labels in bold denote substrates identified or predicted. Gene names are given in parentheses below the substrate.

ABC transporters are involved in many different processes and are associated with almost all stages of plant-microbe interactions (Figure 1.4). To date however, no such transporter common to both bacterial and fungal symbiotic associations have been identified and/or characterized in any species. Understanding their regulation and function will shed light on transport processes fundamental to the establishment of symbioses and reveal how the common symbiosis pathway differentially regulates a core set of genes to accommodate microbes with vastly different life-styles.

AIMS AND OBJECTIVES

Through the research described in this thesis, I aim to investigate the role of different transporters involved in symbiotic infection processes; in particular, the ATP binding cassette (ABC) transporter family, members of which have been shown to play important roles in plant-microbe interactions (Chapter 3-4). Specifically, I attempt to

(1) Identify ABC transporters common to both Root nodule symbiosis (RNS) and arbuscular mycorrhizal symbiosis (AMS) in *Medicago* using *in silico* tools and evaluate spatio-temporal activity of candidate genes using promoter-GUS fusions and semi-quantitative RT PCR.

(2) Understand the role of the candidate transporters in symbiotic interactions by identifying and characterizing single mutants and subsequently generating double and triple mutants, in addition to using RNAi and gene overexpression strategies.

(3) Discern the key regulatory genes of the common symbiosis signalling pathway that control the specificity of expression of the transporters during rhizobial and mycorrhizal infection.

In the last chapter of my thesis (Chapter 5) I present results that address the single question – Does the phytohormone Auxin play a role in root nodule symbiosis? My objectives thus were

(1) Using pharmacological, physiological and molecular biological experiments understand how manipulating the endogenous auxin stream can alter rhizobial infection events.

(2) Find key genes in the auxin transport and signalling pathway that control nodule organogenesis.

CHAPTER TWO:

Materials and Methods

2.1 Plant Methods

2.1.1.1 *Medicago truncatula* lines and growth conditions

Medicago truncatula ecotypes Jemalong A17 (Barker et al., 1990) and R108 seedlings (Hoffmann, Trinh, Leung, Kondorosi, & Kondorosi, 1997) were used in this study. All mutants and transgenic plants described in this study were derivatives of either ecotype. Plants were grown in a 1:1 mixture of Terra green and sharp sand (TG::SS) or in John Innes Cereal Mix (loam based) or Barley mix (N100 P200 K200). Plants were watered regularly as needed and kept in controlled environment chambers with a 16 hour photoperiod at 20°C and 80% humidity.

On plates, seedlings were either grown on distilled water agar (DWA) or Fahraeus plant medium (FP) using a filter paper sandwich method. Briefly, Whatman paper (Grade 0858 Cellulose Qualitative Filter Paper) was cut to size to fit square tissue culture dishes (Fischer scientific) and sterilized. Seedlings were grown vertically on 1.5% agarose slants between two filter paper squares.

The following *M. truncatula* lines were used for this study.

Lines	Description	Background	Reference
A17 Jemalong	Wild type		
R108	Wild type		
<i>nfp-1</i>	Mutation C 31	Jemalong A17	(Ben Amor, 2003)
<i>dmi3-1</i>	A 14-bp deletion in the gene caused translational termination after approximately two-third of the kinase domain.	Jemalong A17	(Wais et al., 2000)

<i>nsp1-1</i>	Contains a premature stop codon and encodes a truncated protein of 239, instead of 554, amino acids	Jemalong A17	(Catoira et al., 2000)
<i>nsp2-2</i>	Contains a 435 bp deletion that removes a major portion of the conserved GRAS domain.	Jemalong A 17	(G. E. D. Oldroyd & Long, 2003)
<i>ram1-1</i>	induced by fast neutron mutagenesis, deletion was approximately 71 kb and contained ten predicted genes	Jemalong A 17	(Gobbato et al., 2012)
<i>nin-1</i>	11-bp deletion starting at position 1850	Jemalong A17	(Marsh et al., 2007)
NF5606 (<i>amn1-1</i>)	<i>tnt1</i> insertion in exon 1, Backcrossed once to WT R-108	R108	This study
NF17134 (<i>amn1-2</i>)	<i>tnt1</i> insertion in exon 6 backcrossed once to WT R-108	R108	This study
NF 9733 (<i>amn2-1</i>)	<i>tnt1</i> insertion in exon 3	R108	This study
NF18154 (<i>amn3-1</i>)	<i>tnt1</i> insertion in exon 1, Backcrossed once to WT R-108	R108	This study
NF8444 (<i>amn3-2</i>)	<i>tnt1</i> insertion in exon 1, Backcrossed once to WT R-108	R108	This study
NF12598(<i>amn3-3</i>)	<i>tnt1</i> insertion in exon 4	R108	This study
NF 19099(<i>amn3-4</i>)	<i>tnt1</i> insertion in exon 5	R108	This study
NF 10070 (<i>iaa8-1</i>)	<i>tnt1</i> insertion in exon 1	R108	This study
NF 14494 (<i>lax2-1</i>)	<i>tnt1</i> insertion in exon 4	R108	This study
NF 16662 (<i>lax2-2</i>)	<i>tnt1</i> insertion in exon 4	R108	This study
<i>amn1-1 amn2-1</i>	double mutant	R108	This study
<i>amn1-2 amn2-1</i>	double mutant	R108	This study
<i>amn1-1 amn3-1</i>	double mutant	R108	This study
<i>amn1-1 amn3-2</i>	double mutant	R108	This study
<i>amn2-1 amn3-1</i>	double mutant	R108	This study
<i>amn2-1 amn3-2</i>	double mutant	R108	This study
<i>amn1-1 amn2-1 amn3-1</i>	triple mutant	R108	This study
<i>lax2-1 DR5-GUS</i>	double cross generated by crossing <i>lax2-1</i> with transgenic DR5-GUS (R-108)	R108	This study
<i>iaa8-1 DR5-GUS</i>	double cross generated by crossing <i>iaa8-1</i> with transgenic DR-5GUS (R-108)	R108	This study
<i>DR5-GUS</i>		R108	(Zhou et al., 2011)
<i>GH3-GUS</i>		A17	(Mathesius et al., 1998)

Table 2.1: List of *M. truncatula* lines used in this study

2.1.1.2 Seed sterilization, scarification and vernalisation

M. truncatula pods were split open by grinding and seeds collected. To disrupt the seed coat, seeds were scarified using concentrated sulphuric acid for eight minutes and rinsed with distilled water a minimum of five times in universal glass jars. Under sterile conditions, sodium hypochlorite (Sigma Aldrich reagent grade 10-15% active chlorine) was added to each bottle for two minutes after which the bleach was decanted and the seeds rinsed repeatedly until no traces of the bleach remained. Alternatively, seeds were scratched between two sheets of sand paper to scarify the seed coat and then treated with bleach. Sterilized seeds were left in sterile water for 2-3 hours till they imbibed water and swelled up. They were then individually placed on DWA medium in deep dish petri dishes. The petri dishes were wrapped in aluminium foil and transferred to 4°C. For most experiments, the seeds were vernalized for a minimum of three days for most experiments to synchronize germination or 14 days for early flowering of plants (<https://www.noble.org/Medicago-handbook/>).

2.1.1.3. Cross fertilizations

To generate different allelic combinations between mutant plants or transgenics, flowers were first emasculated and then hand pollinated with pollen from the desired parent under a dissection microscope. The recipient (ovule donor) flowers were selected for a stage when the petals had not yet unfurled but were longer than five millimetres. A single incision was made in the petals to free the anthers and the stigma without damaging them. Crossing was carried out only if anthers of the female parent had not yet dehisced. Anthers were then removed from the recipient flower, either using fine forceps or suction generated from a pump, to avoid self-fertilization. Pollen from the desired male parent was carefully placed on the tip of the stigma and the flower petals gently replaced to maintain humidity. In addition, the crossed flower was carefully lowered into a humidified chamber (falcon tube containing distilled water) and plugged with cotton. For a successful cross, the pod started developing within days and once the pod stopped coiling, it was taken out of the tube and covered with a net bag. The seed pod was allowed to develop to maturity and seeds collected once they turned brown and fell off the branch naturally. The F1 seeds were sterilized as described above and grown in soil. Homozygous F2 progeny were selected by polymerase chain reaction (PCR) screening of the required gene and segregation ratio was analysed.

2.1.1.4 Generation of stably transformed hairy roots of *M. truncatula*

Seeds were sterilized and vernalized for three days as described above. The night before transformation the petri dishes containing WT seeds were placed at RT in an inverted position. Under sterile conditions, the entire meristematic root tip was excised and the cut end of the remaining seedling dipped in the *Agrobacterium rhizogenes* culture. Twelve seedlings each were placed on modified FP (MOD-FP) medium agar plates and kept upright in controlled environment chambers for 7-10 days. The untransformed roots were excised and discarded while the remaining roots were placed onto selection medium containing 20µg/ml kanamycin if antibiotic transformation selection was used. If ds RED transformation marker was used for selection, only positively fluorescing plants were transferred onto fresh medium. The plants were grown on plates till transformed hairy roots developed and then transferred to soil for nodulation assays or on water agar plates for infection assays.

2.2. Microbiological methods

2.2.1 Bacterial methods

2.2.1.1 Bacterial strains and growth conditions

Escherichia coli cultures were grown at 37°C for 16 hours overnight at 250 RPM in 10 ml cultures. *A. rhizogenes* strain AR1193 (Stougaard, Abildsten, & Marcker, 1987) was used for hairy root transformations of *M. truncatula* and *A. tumefaciens* GV3101 was used for transient transformations. Single colonies were used for inoculating 5 ml TY medium and grown on shaking cultures at 28°C as required. *Sino rhizobium maillot* strains were grown overnight at 28°C under shaking conditions. Long term storage of bacteria was done at a final concentration of 15% glycerol at -80°C.

The following bacterial strains were used in this study

Bacterial Strains	Genotype	Purpose	Source	Reference
<i>E. coli</i> DH 5a	<i>F endA1 glnV44 thi-1 recA1 relA1 gyrA96 deoR nupG Φ80dlacZΔM15 Δ(lacZYA-argF)U169, hsdR17(r_K⁻ m_K⁺), λ-</i>	General purpose plasmid amplification and cloning	Invitrogen (Life technologies)	

<i>E. coli</i> SCS110	<i>rpsL (Strr) thr leu endA thi-1 lacY galk galT ara tonA tsx dam dcm supE44 Δ (lac-proAB) [F' traD36 proAB lacIq ZΔM15]</i>	Methylation free plasmid preparations	Phil Poole, JIC
<i>E. coli</i> JM 109	<i>endA1 glnV44 thi-1 relA1 gyrA96 recA1 mcrB⁺ Δ(lac-proAB) e14- [F' traD36 proAB⁺ lac^f lacZΔM15] hsdR17(r_K⁻m_K⁺)</i>	Endonuclease A minus strain for propagation of large plasmids	Invitrogen (Life technologies)
<i>E. coli</i> DB 3.1	<i>F- gyrA462 endA1 glnV44 Δ(sr1-recA) mcrB mrr hsdS20(r_B⁻, m_B⁻) ara14 galk2 lacY1 proA2 rpsL20(Sm^r) xyl5 Δleu mtl1</i>	ccdB resistant propagation of gateway destination vectors	J. Allan Downie, JIC
<i>A. rhizogenes</i> AR1193		Gene transfer to plants	(Stougaard et al., 1987)
<i>A. tumefaciens</i> GV3101		Transient expression of genes	
<i>S. meliloti</i> 1021		Symbiotic partner of <i>M. truncatula</i>	J. Allan Downie, JIC
<i>S. meliloti</i> 2011		Symbiotic partner of <i>M. truncatula</i>	J. Allan Downie, JIC
<i>S. meliloti</i> SL44 (nodAD1ABC)		Non-nod factor producing strain of <i>S. meliloti</i> 1021	J. Allan Downie, JIC

Table 2.2: List of bacterial strains used in this study

2.2.1.2 Bacterial plasmid preparation and transformation by heat-shock or electroporation

Overnight grown cultures of *E. coli* were pelleted at 10,000 RPM for 10 minutes in 2 ml Eppendorf tubes. Plasmid was isolated by the alkaline lysis method using the Qiagen miniprep kit following manufacturer instructions. *E. coli* chemically competent cells were transformed by a 45 second heat shock at 42°C followed by an immediate cold shock on ice. SOC medium was added to each aliquot and

transformed cells allowed to recover for an hour on a shaker at 37°C. The cells were pelleted by centrifugation and transformed cells selected on medium containing desired antibiotic. *Agrobacterium* cells were transformed by electroporation. In individual sterile cuvettes (Geneflow), 40 µl competent cell and approximately 100 ng plasmid were added. Current was applied at 2.5V for 10 seconds at a resistance of 200 ohms and SOC medium added immediately after. The transformed cells were allowed to recover at 28°C on a shaker for one hour and selected on TY medium containing appropriate antibiotics.

The following vectors, plasmids and constructs were used in this study.

Name	Insert/Description	Backbone	Reference
	Gateway ENTRY vector	pDONR201	
	Gateway ENTRY vector	pGEMT Easy	Invitrogen
	Gateway ENTRY vector	pENTR/dTOPO	Invitrogen
pAMN1-GUS	1.06 Kb upstream of Medtr3g086420	pKGWFS7	This study
pAMN2-GUS	1.78 Kb upstream of Medtr4g081190	pKGWFS7	This study
pAMN3-GUS	2.1 Kb upstream of Medtr8g022270	pKGWFS7	This study
pMtLAX2-GUS	2.8 Kb upstream of Medtr7g067450	pKGWFS7	This study
pMtiAA8-GUS	1.9 Kb upstream of MTR_5g067350	pKGWFS7	This study
pEXPA7:CDSMtLAX2:T35S	CDS Medtr7g067450	pK7WG2-R*- pExpa7	
pEXPA7:CDSAMN2:T35S	CDS Medtr4g081190	pK7WG2-R*- pExpa7	
pEXPA7:GUS:T35S	pENTR™-gus <i>Arabidopsis thaliana</i> β-glucuronidase (gus) gene	pK7WG2-R*- pExpa7	
p35S:CDSAMN2:egfp:T35S	CDS Medtr4g081190	pK7WG2-R	
p35S:eGFP:egfp:T35S	free gfp	pK7WG2-R	
pGAL:AMN2	CDS Medtr4g081190	pYESDEST-52	
pGAL:MtLAX2	CDS Medtr7g067450	pYESDEST-52	
pGAL:AMN2:eGFP	CDS Medtr4g081190	pAG306GAL- ccdB-eGFP	Addgene corp.

pENOD11:AtIAA17:T35S	AtIAA17 WT	pAGM4723
pENOD11: AtIAA17mll:T35S	AtIAA17 negative	dominant pAGM4723
pENOD11: AtIAA17mllMsc1: T35S	AtIAA17 Control	pAGM4723

Table 2.3: Table of vectors, plasmids and constructs used in the study

2.2.1.3 Plasmid mobilization by Tri-parental mating

Tri-parental mating is based on the principle that a conjugative plasmid existing in one bacterial strain (helper) aids in the transfer of the desired plasmid (donor) present in another bacterial strain into a third (acceptor) strain. On a TY agar plate containing no antibiotic, the strain containing the desired donor plasmid, the acceptor strain and the helper strain were streaked out separately. On the same plate, these strains were streaked in a patch where all three were mixed. This mating plate was incubated overnight at 37°C. The next day, the patch was replica plated onto a sterile velvet cloth and bacterial colonies transferred onto a fresh TY plate containing antibiotics for selection of the acceptor strain transformed with the plasmid of interest. This plate was incubated at 28°C for three days or till colonies appeared. The colonies were re-streaked onto a fresh plate to obtain single colonies which were used for further experiments.

2.2.1.4 Blue White Screening

To screen for recombinant clones containing the gene of interest, blue white screening was performed in which white colonies identify clones with a disrupted *lacZ* gene in the plasmid backbone indicating the presence of an insert. Blue-white selection is only possible in *E. coli* strains such as DH5 α which contain the amino-terminal fragment of the LacZ product allowing for α -complementation. To the growth medium, X-GAL (Formedium) a chromogenic substrate for β -galactosidase and a Lac operon inducer – IPTG (Isopropyl β -D-1-thiogalactopyranoside) were added to a final concentration of 40 μ g/ml and 100 μ M respectively along with the antibiotic. Plates were incubated overnight and colonies screened visually for colour development.

2.2.2 *Saccharomyces cerevisiae* transformation and culture

2.2.2.1 Yeast strains and growth conditions

All yeast strains were derivatives of the BY4742 background and were obtained from the Euroscarf collection (<http://web.uni-frankfurt.de/fb15/mikro/euroscarf/>). Cells were grown at 28°C for the desired amount of time in either the YPD or SD medium with suitable dropouts and carbon source. Long term storage was in 15% glycerol.

2.2.2.2 Yeast competent cell preparation and transformation

A single colony was used to inoculate 10 ml cultures of YPAD medium and grown overnight at 28°C on a shaker at 250 RPM. The next day, the overnight culture was adjusted to an absorbance 0.2 OD₆₀₀ in YPD medium. The sub-cultured cells were allowed to grow up to absorbance at OD₆₀₀ 0.6 to 0.8. The cells were pelleted by centrifugation at 2500 RPM for 5 minutes. The resultant cell pellet was re-suspended in 2 ml of sterile distilled water. Per transformation, 240 µl 50% PEG (MW 3350), 36 µl 1 M Lithium acetate and 30 µl of 2 mg/ml single stranded DNA was added to 100 µl of re-suspended yeast cells in a sterile tube. 150-300 ng of the desired plasmid was added per tube and mixed by vortexing. The tube was incubated at 42°C for 45 minutes in a water bath. The cells were pelleted and re-suspended in 100 µl of sterile 0.9% NaCl and plated onto appropriate auxotrophic selection medium.

2.2.2.3 Yeast drop test

A single yeast colony containing the desired construct was grown overnight in 5 mL SD dropout medium. The next day, all cultures were diluted in water to ~0.6 absorbance at OD₆₀₀. In a sterile 96 well cell culture dish (Thermo) cells were serially diluted five times. Using a multichannel pipette, 5 µl of each culture was pipetted onto the selection medium and the plate allowed to dry. The plate was then incubated at 28°C for 3-5 days and a photograph was taken.

The following yeast strains were used in this study.

Strain	Mutation	Genotype	Accession number	Reference
YML070w	<i>yap1-1</i>	BY4742; <i>Mat a</i> ; <i>his3D1</i> ; <i>leu2D0</i> ; <i>lys2D0</i> ; <i>ura3D0</i> ; <i>YML070w::kanMX4</i>	Y16483	R. Prusty (2004)
YJR040w	<i>gef1</i>	BY4742; <i>Mat a</i> ; <i>his3D1</i> ; <i>leu2D0</i> ; <i>lys2D0</i> ; <i>ura3D0</i> ; <i>YJR040w::kanMX4</i>	Y16838	
Wild type	BY4742	<i>MATα</i> ; <i>his3Δ 1</i> ; <i>leu2Δ 0</i> ; <i>lys2Δ 0</i> ; <i>ura3Δ 0</i>	Y10000	

Table 2.4: Yeast strains used in the present study

Medium	Recipe for 1 litre
Farhaeus Plant (FP) medium	0.1 g CaCl ₂ . 2H ₂ O, 0.12 g MgSO ₄ , 0.01g KHPO ₄ , 0.150 g NaHPO ₄ .12H ₂ O, 5 mg ferric citrate, 2.86 g H ₃ BO ₃ , 2.03 g MnSO ₄ , 0.22 g ZnSO ₄ .7H ₂ O, 0.08 g CuSO ₄ .5H ₂ O, 0.08 g H ₂ MoO ₄ .4H ₂ O, pH 6.3-6.7. For solid medium 0.5% (w/v) LabM No. 1 agar was added.
Modified FP medium	FP medium containing 0.5 mM NH ₄ NO ₃
Buffered (BNM) medium	Nodulation 390 mg MES, 344 mg CaSO ₄ .2H ₂ O, 0.125 g KH ₂ PO ₄ , 122 mg MgSO ₄ .7H ₂ O, 18.65 mg Na ₂ EDTA, 13.9 mg FeSO ₄ .7H ₂ O, 4.6 mg ZnSO ₄ .7H ₂ O, 3.1 mg H ₃ BO ₃ , 8.45 mg MnSO ₄ .H ₂ O, 0.25 mg Na ₂ MoO ₄ .2H ₂ O, 0.016 mg CuSO ₄ .5H ₂ O, 0.025 mg CoCl ₂ .6H ₂ O, pH 6.5. For solid medium 11.5 % (w/v) LabM No. 1 agar (Formedium) was added.
Distilled water agar (DWA) medium	1.5 % (w/v) Lab M No. 1 agar (Formedium, UK, pH 5.7 (adjusted with KOH).
LB medium	(Luria-Bertani) Tryptone 10.0g Yeast Extract 5.0g NaCl 10.0g pH 7.0 10g added for solid medium

TY (Tryptone-Yeast agar medium)	Tryptone 5.0g Yeast Extract 3.0g CaCl ₂ 6H ₂ O 1.32g
SOC (Super optimal broth with catabolite repressor medium)	Tryptone 20.0g Yeast Extract 5.0g NaCl 0.58g KCl 0.19g MgCl ₂ 2.03g MgSO ₄ 7H ₂ O 2.46g Glucose 3.6g
YPAD medium (YPD with adenine)	Yeast Extract 10g Peptone 20g Glucose 20g Adenine 20mg
SD (Synthetic Defined) medium	Yeast Nitrogen Base without Ammonium Sulphate and Amino Acids (Formedium) 1.9g (NH ₄) ₂ SO ₄ (Ammonium Sulphate) 5g Dropout Uracil Glucose/Galactose/Xylose Carbon source

Table 2.5: Recipe for preparation of media used in this study

Buffers	Recipe for 1 litre
Z Buffer	100 mM Sodium phosphate buffer (100 mM Na ₂ HPO ₄ , NaH ₂ PO ₄ each) 10 mM KCl, 1 mM MgCl ₂ pH 7.4
GUS Buffer	50 mM Sodium phosphate buffer, 1 mM EDTA, 1% Triton-X
PIPES (piperazine-N,N'bis[2-ethanesulfonic acid]) Buffer	5.8 g NaCl, 30 g PIPES, 1M NaOH, 2 g MgCl ₂ •6H ₂ O

Table 4.5: Recipe for preparation of buffers used in this study

Antibiotic	Solvent	Final-concentration (µg/ml)
Carbenicillin	Water	100
Kanamycin	Water	100
Rifampicin	Ethanol	50
Spectinomycin	Water	100
Streptomycin	Water	200
Tetracycline	Ethanol	5

Table 2.6: Antibiotics used in this study

2.3 Molecular Biological methods

2.3.1 DNA Methods

2.3.1.1 Agarose gel electrophoresis

DNA fragments were resolved by running the samples on a 1% agarose gel at 100 V in 1x TAE (Tris acetate EDTA). An ethidium bromide bath prepared at a concentration of 0.5 µg/ml was used for visualization of the DNA bands. Analytical gels were photographed using GeneFlash Syngene Bioimaging system.

2.3.1.2 PCR cycling conditions

All PCR reactions were carried out using the G-Storm or PTC 225 Peltier thermal cyclers. For all cloning purposes the hi-fidelity Phusion taq (New England Biolabs) was used, using manufacture recommended concentrations. For general purpose genotyping and colony PCRs the GoTaq green master mix was used.

Stage	Temperature (°C)	Time-period (Phusion)	Time-period (GoTaq)	Number of cycles
Initial Denaturation	96	5 minutes	5 minutes	x1
Denaturation	96	30 sec	30 sec	
Annealing	55-60	30 sec	30 sec	x30-35
Extension	72	30 sec per Kb	1 minute per Kb	
Final extension	72	10 minutes	10 minutes	x1

Table 2.7: Standard PCR cycling Parameters

2.3.1.3 Restriction digestion

Sequence specific digestion of DNA was carried out using restriction enzymes from NEB or Roche. The reaction was setup with 1 µg plasmid or PCR purified fragments. Wherever compatible a double digest was setup in the same buffer otherwise sequential digest carried out.

2.3.1.4 DNA gel extraction

Ethidium bromide stained DNA was visualised on a long wavelength UV transilluminator and the required section excised using a scalpel blade. Fragments were purified using the QIAquick gel extraction kit (Qiagen) following the manufacturer's instructions.

2.3.1.5 Sequencing using BigDye V3.1

Sequencing ready-reactions were performed using gene-specific primers: 1.6 µl 2 µM gene-specific primer, 1.5 µl 5x sequencing buffer, 4.9 µl dH₂O, 1 µl DNA from miniprep (typically >200 ng/µl), 1 µl Big Dye v3.1 (10 µl final volume). PCR cycling conditions were as follows: 25 cycles at 96 °C for 10 s, 55 °C for 5 s and 60 °C for 4 min. Sequencing ready-reactions were submitted to Genome Enterprise Ltd (Norwich, UK) or MWG operon (Eurofins, Germany) and results were analysed using ContigExpress (Vector NTI Advance 10, Invitrogen).

2.3.1.6 Gateway Cloning: BP reaction and LR reaction

Gateway technology is based on the ability of "site-specific recombinases to catalyse a reciprocal double-stranded DNA exchange between two DNA segments provided both DNA segments carry very specific sequences" (SB Primrose, R Twyman – 2009 7th Ed.). To create entry clones, the required gene fragment was amplified using primers containing gateway compatible end sequences. The forward primer started with 5'-GGGGACAAGTTTGTACAAAAAAGCAGGCT-3' while the reverse primer had the sequence 5'-GGGGACCACTTTGTACAAGAAAGCTGGGT-3'. The purified fragment was sequenced and cloned into the *ccdB* 'suicide gene' containing pDONR201 vector backbone. A ligation reaction was setup using a 1::3 vector::insert molecular ratio in an 8 µl reaction and 2 µl of enzyme BP clonase added (Invitrogen). Ligation was allowed to proceed overnight at 25°C and terminated the next day by addition of 1 µl proteinase K. The entire ligation mix was used to transform 50 µl of chemically competent *E. coli* cells. In case of the pENTR/dTOPO vector (Invitrogen) a four base pair CACC tag on the forward primer was added for cloning. The purified fragment was used for cloning according to the manufactures protocol. The reaction was allowed to proceed overnight and 2-5 µl was used for transforming 50 µl of competent cells. Colonies were screened by restriction digestion or colony PCR and confirmed by sequencing.

For the LR reaction, the desired entry clone and the destination vector plasmid were purified and the concentrations noted using the Nanodrop 2000 UV-Vis spectrophotometer. 150 ng of each vector was added to a thin walled pcr tube along with 2 µl of LR clonase and the volume made upto 10 µl. The reaction was allowed to proceed overnight at 25°C and terminated the next day by addition of 1 µl of Proteinase K. 2-5 µl of the reaction was used for transforming chemically competent cells and plated onto appropriate selection medium. Colonies were screened by restriction digestion and confirmed by end sequencing of clones insert.

2.3.1.7 Golden gate assembly: Level 1 and Level 2 (Binary) vector assembly

The protocol was adapted from (ref). Individual components to be assembled were synthesised from life technologies GeneArt^R. To construct 'level 1' vectors a thin walled PCR tube, 100 ng of the linearized vector backbone and equimolar amounts of the other assembly pieces were added to a 15 µl total reaction mixture volume. The reaction mixture contained a final concentration of 1x NEB T4 buffer, 1x BSA, and 1 µl of *BsaI* and T4 ligase (New England Biolabs) each. The tube was placed into a thermocycler and cycling parameters setup as follows. (37°C/3min//16°C/4min) x25 cycles (50°C/5min//80°C/5min) x1 cycle. 2 µl of the assembly reaction was transformed into 20 µl of competent *E. coli* cells. Only white colonies selected on the basis of blue white screening were screened by restriction digestion and confirmed by sequencing. Construction of level two vectors was done using the same protocol but the *BsaI* was replaced with *BpiI* restrictions enzyme. Selection of untransformed colonies was based on red-white selection; the untransformed colonies appeared red.

2.3.2 RNA methods

All gene expression analyses were performed with Microsoft Excel 2010 and the *M. truncatula* Gene Expression Atlas (<http://mtgea.noble.org/jic/>). Further statistical analyses were performed with the Genstat 16th Ed software package.

2.3.2.1 General sample collection and RNA isolation

Tissue was collected post the desired treatment in 2 mL Eppendorf tubes or wrapped in aluminium foil and immediately snap frozen in liquid nitrogen. The samples were ground in liquid nitrogen in a pre-chilled mortar and pestle treated

with RNaseZAP (Invitrogen). The ground samples were collected in 2 mL Eppendorf tubes. RNA was isolated using RNeasy plant mini kit (QIAGEN) following the manufacturer's protocol. The eluted RNA was treated with DNase (Invitrogen) following the manufacturer's protocol and the quality evaluated by agarose gel electrophoresis.

2.3.2.2. Root hair tissue collection and RNA isolation

A root hair harvesting protocol was adapted from Ramos and Bisseling (Ramos & Bisseling, 2003). Root tips were removed and the roots plunged into liquid nitrogen contained in a Teflon-coated loaf tin (Dunelm Mill). A Daler Rowney number 2 filbert paint brush (Dunelm Mill) was used to brush root hairs and collected in the tin. Around 120-150 roots were used per RNA sample and the remaining nitrogen was poured into a 45 ml PTFE-coated conical centrifuge tube (VWR) and the nitrogen left to boil off. RNA was isolated from this purified root hair sample using RNeasy plant micro kit (QIAGEN) according to the manufacturer's protocol and quality analysed using a Bioanalyser.

2.3.2.3 Complimentary DNA (cDNA) synthesis

RNA samples were placed on ice at all times and quantified on the same day the synthesis was performed. 1 µg of total RNA was used per sample unless stated otherwise. To a final volume of 13 µl, 1 µg RNA and dNTPs and oligo dT primers were added. For gene specific priming, antisense primers were designed and used at a final concentration of 2 pmol. The tubes were incubated at 65 °C for 5 minutes and immediately placed on ice for at least one minute. To this, buffer and DTT were added to a final concentration of 1x and 0.1 mM respectively. Finally, 40 units of the enzyme RNaseout and 200 units of Superscript III were added. The tubes were placed in the thermocycler and cycling parameters were as follows 50°C/60 min//70°C/15 min. If the sample was intended for amplification of full length cDNA, 1 µl RNaseH was added to remove DNA RNA hybrids.

2.3.2.4 Primer efficiency calculations and quantitative PCR

To calculate the efficiency of the qPCR primers used in this study, serially diluted cDNA samples were used and quantitative PCR carried out to determine their Ct value and corresponding dilution ratio as described below.

Quantitative PCR was carried out to compare the relative abundance of a transcript across different sample types and treatment conditions. The cDNA was prepared as above (2.3.2.3) and diluted 20 fold in sterile double distilled water. Forward and reverse primers up to a final concentration of 0.2 mM in 5 µl, 5 µl of the diluted cDNA and 10 µl of SYBR Green Taq Ready Mix (Sigma) was added to a total reaction volume of 20 µl. A minimum of three technical replicates each were used for three biological replicates per experiment. The plate was carefully sealed with Biorad transparent qPCR lids and samples mixed by flicking the wells. The samples were collected by a brief spin and placed into the Biorad 96 CFX Real time cycler. The cycling parameters used were 96°/5min// (96°C/10sec/60°C/15sec/72°C/20sec) x41// unless stated otherwise and followed up by a melt curve analysis from 65°C to 95°C. The resultant threshold cycle Ct values were exported to Microsoft Excel 2010 and the data analysed.

2.4 Assays used in this study

2.4.1 Bacterial growth curve assay

The requisite strain(s) of bacteria was grown overnight in 5 ml culture with appropriate antibiotics. The following day, the absorbance at OD600 was measured using an Eppendorf biophotometer and the CFU (colony forming units) calculated and noted. This culture was diluted in fresh medium to 10^{-5} CFU. In a 48 well plate, 360 µl of sterile medium containing the desired dilution of the chemical to be tested was added. A minimum of five replicates were used per treatment and the wells were randomly assigned per treatment. 40 µl of the diluted culture was added to each well containing 360 µl of the medium to get a final volume of 400 µl per well. The plate was placed into the infinite 2000 plate reader under shaking conditions and the OD600 absorbance measured at an interval of 1 hour upto 50 hours. The data was exported to Microsoft Excel 2010 and the average of all replicates per treatment plotted on a graph.

2.4.2 Root hair length measurement

Root hair length was measured using the Leica DFC 420 stereo microscope and the Leica application suite Version 4.2.0 software. *Medicago* seedlings were germinated as described earlier. Overnight germinated seedlings were selected only if the root tip was not curved and 5 seedlings per plate per treatment were placed between

filter paper sandwiches on square petri dishes. The seedlings were allowed to grow for seven days under long day conditions. To measure the root hair length, the top filter paper was removed carefully with forceps without moving the roots and placed under the microscope. Five consecutive root hairs on each side of the root were measured by specifying the base and the tip of the hair using the software. Average of all root hairs was calculated and compared.

2.4.3 Histochemical localization of GUS

To visualize spatial patterns of gene expression, X-GlcA staining of β -Glucuronidase activity was performed. To 50 ml of GUS buffer, 196 μ l of 250 mg/ml X-GlcA (Melford) in DMF (Dimethyl formamide) was added and finally mixed. Tissue samples were taken in small petri dishes and covered in the staining solution and the plates kept at 28 °C in dark. After the desired colour intensity developed, the staining solution was removed and the samples washed with fresh GUS buffer.

2.4.4 Infection assay and β -Galactosidase staining

Roots infected with pXLGD4 (*phemA:LacZ*) containing plasmids could be stained with X-GAL a chromogenic dye which acts as a substrate for the enzyme β -galactosidase encoded by the bacterial gene *lacZ*. 25% Gluteraldehyde (Sigma) was diluted to 2.5% in Z-buffer and tissue submerged in this solution. The samples were then subjected to a vacuum for 10 minutes after which the tissues were allowed to stay in the solution for an hour in dark at RT. The tissue was then washed repeatedly with buffer a minimum of three times and 1 ml of the staining solution added (or enough to cover the samples). For 1 mL of the staining solution 50 μ l each of 100 mM potassium ferrocyanide and potassium ferricyanide and 20 μ l of 40 mg/ml of X-gal in DMF was made up in Z-buffer. The samples were then placed at 28 °C in the dark overnight (16 hours). The reaction was stopped by disposing the staining solution and washing at least three times with Z-buffer. The roots were then analysed under a microscope and the number of infection threads quantified or images captured.

2.4.5 SYTO13 Green-Fluorescent staining to visualize rhizobia

SYTO13 stains (Invitrogen) nucleic acids, and thus can be used to localize rhizobia accurately in plant tissue such as nodule sections. Nodule sections were incubated

in 1 $\mu\text{L}/\text{mL}$ SYTO13 green in PIPES buffer and visualized directly under a fluorescent filter and images captured.

2.4.6 Nodulation assay

To compare nodule number between different genotypes seeds were sterilized, scarified and vernalized as described before. Overnight germinated seedlings were transferred to sterile terragreen and sharp sand mixed to a 1:1 ratio and covered by a transparent lid to maintain humidity. Specifically, P40 (2 inch diagonals) trays were used for all nodulation assays. After allowing seven days of growth, plants were inoculated with 1 ml of rhizobia at a final absorbance of 0.02-0.05 at OD600 diluted in water. The plants were allowed to grow for three weeks under long day conditions and watered regularly. To count the number of nodules, soil was completely removed from each pot without damaging the roots and the roots gently washed in water. Pink (Nitrogen fixing) and white nodules were scored separately and the numbers recorded.

2.4.7 Mycorrhization assay and Ink staining

To compare differences in percentage colonisation by the fungus *Rhizophagus irregularis*, seedlings were germinated as described. The seedlings were allowed to grow on plates for seven days on DWA medium and gently removed from the plates with forceps without damaging the roots. They were then transferred to TG::SS low nutrient growth medium mixed with 25-30% chive inoculum containing roots of chive plants infected with spores of the mycorrhizal fungus. Alternatively, seedlings were transferred to inoculum containing growth medium directly after germination. Plants were covered with a lid to maintain humidity and allowed to grow for 4-5 weeks before harvesting the root tissue. Roots were washed and approximately one inch of each sample from around two third of the total root length was collected for analysis. The fungus was visualized using an ink staining protocol (Q. Zhang et al., 2010). Roots were placed in float racks containing 2 ml eppendorf tubes with holes at the bottom to allow drainage. The rack was placed in boiling 10% w/v potassium hydroxide solution for 12 minutes to clear the roots and the excess solution allowed to drain off by blotting onto a blue roll. It was then placed into the staining solution containing 5% ink and 10% acetic acid at 96°C for 6 minutes. Finally, the samples were washed with distilled water to remove excess stain.

2.4.8 Wheat germ agglutinin (WGA) staining of fungus

Harvested roots were washed with water to remove soil and transferred to 50% ethanol for 4 hours. The ethanol was removed and samples transferred to a 20% w/v KOH solution at 28°C. After 2 days the solution was removed and samples washed thoroughly with distilled water. 0.1 M HCl was then added for 1-2 hours and rinsed again with distilled water and once with buffer PBS. WGA-AlexaFlour 568 was added to PBS buffer at a final concentration of 0.2 µg/mL and samples immersed in this staining solution overnight at 28°C in dark. The next day, samples were rinsed and observed under the microscope.

2.5 Bioinformatics Analyses

2.5.1 Defining the *M. truncatula* ABC transporter family

To define the complete *M. truncatula* ABC transporter family two approaches were taken. In the first one, all *M. truncatula* annotated protein sequences of IMGAG version 3.5 (http://bioinfo3.noble.org/Medicago/index_MT3.html) were analysed for the presence of (ATP Binding cassette) ABC signature motifs and transmembrane domains (TMD) and Nucleotide binding domains (NBD) using PFAM search (<http://pfam.xfam.org/>). Only those genes with two NBDs and two TMDs were termed full transporters and those with only one of each were termed as half transporters. In the second approach, full *Arabidopsis* ABC transporter sequences were retrieved from (ref) and the sequences used to run BLAST against the entire *Medicago* genome database deposited in (http://bioinfo3.noble.org/Medicago/index_MT3.html) and retrieve the top 10 hits for each gene. This was repeated 4 times for each of the hits found in the searches. All genes retrieved in this manner were reverse blasted to the *A. thaliana* genome and a list was compiled of only those genes which matched an *A. thaliana* ABC transporter. Probeset IDs were obtained for the genes and used for expression analysis whenever necessary.

2.5.2 Retrieving orthologues of candidate genes from different species

Individual protein sequences were utilized for BLAST searches against the entire database of protein sequences on NCBI. Additionally for *Lotus* and *Oryza* <http://www.kazusa.or.jp/e/> and <http://plants.ensembl.org/index.html> were searched. A reciprocal BLAST was used to validate the putative orthologues. In case of rice,

the transcriptome in response to mycorrhiza was analysed for ABC transporters which were co-regulated and their functional orthologues in *M. truncatula* retrieved.

2.5.3 Co-regulation Analysis

Publically available expression data for *AMN 1*, *AMN2* and *AMN3* were downloaded from <http://mtgea.noble.org/v3/>. Expression was analysed across vegetative conditions, in nodules and upon infection by arbuscular mycorrhiza. In a separate analysis, a list of genes were compiled which was induced in root hairs upon infection with compatible rhizobia and not negatively controlled by the transcription factors NIN, ERN1 and NFYA1. Genes common to both lists were said to be co-regulated with the candidate genes.

2.6 Microscopy Techniques

2.6.1 Light Microscopy

All images were captured using the Nikon Eclipse 800 microscope and the InStudio software. Images were processed using ImageJ.

2.6.2 Confocal Laser Scanning Microscopy

Nodule sections stained with SYTO13 fluorescent dye were observed using the Leica SP5 Confocal Microscope (Leica Microsystems, Wetzlar, Germany). After excitation at 488 nm, eGFP emission were detected using >660 nm filter set. All samples were imaged with the 20x objectives.

	Primer name	5' to 3' Sequence
P_1	Tnt_amn1_F	CTC ATC GGT TCG AAC TGT TTA CTC G
P_2	Tnt_amn1_R	TGGTTCCAGCAAAGAGTGTAGGCT
P_3	AMN1_CDS_F	ATGGGAAACAAAGGTGGATT
P_4	AMN1_CDS_R	TCAAGTTGAATGACTTTGTTGTAGCC
P_5	qAMN1_F	ATGTTTATTGATACATGCAGGAGA
P_6	qAMN1_R	CAA CTG CTC TGG GGG AAA CCA AT
P_7	Tnt_amn2_F	ATATGATCAAGTAAAATTCTTTATCTT
P_8	Tnt_amn2_R	AAAGCCTTTCTTTCTTCTC
P_9	AMN2_CDS_F	ATGGGGAGCAATAGCATGTTTCGTT
P_10	AMN2_CDS_R	TCACCTAGGGGAGCTACCATGTTGAAG
P_11	qAMN2_F_1	CATGAATTCATAAGTGGAATGAATGA
P_12	qAMN2_R_1	AGC TCT GGC TAA GGC TAT TCT TTG T

P_13	Tnt_AMN3_F	GACAATCCGAGAAGACACTATCCAAC
P_14	Tnt_AMN3_R	TTGGTGGCCCTAGCAACATG
P_15	AMN3_CDS_F	ATGGCTGATTCTTCCTTTGAGATAGA
P_16	AMN3_CDS_R	TGCTTACGGTGCGAATATGAGTG
P_17	qAMN3_R_1	GTTATGAAACACAGGTTGGTGAAAGT
P_18	qAMN3_R_1	G ATT CCA AGT CTA ATG CAC TGC TT
P_19	AMN1_antisense_cDNA	GTGGACTCCCATATACTGAAATAATATAACC
P_20	RNAi_128_F	CACCGGAGTATGCTGGACAAGAACT
P_21	RNAi_128_R	ACTTGAAGGTTGTAGAAGAG
P_22	MtLAX2_Tnt_F	TGAAACAGTAACATCTACTACATAAATG
P_23	MtLAX2_Tnt_R	TCGGTTCAATTAATTCATGTCATTT
P_24	MtLAX_CDS_F	ATGTTGCCACAAAAACAAGG
P_25	MtLAX_CDS_R	TCATGTGTCTAATTGAACAAACT
P_26	pMtLAX2_F	TCTCTATTATGATGATAACTTGAGTTCTAC
P_27	pMtLAX2_R	TGTTTCTCTCTTTTCTTAACAAAACC
P_28	pIAA8_F	CACCATTACATTGAGTAGTAGTAG
P_29	pIAA8_R	CACAATGAATACAAAGTTTC
P_30	Tnt_IAA8_F	CATTTTTCTCTCTTCTATGTTACTAA
P_31	Tnt_IAA8_R	TATAGTTCTAAATTGCAGTCCG
P_32	TntF	TCCTTGTTGGATTGGTAGCC
P_33	TntR	CAGTGAACGAGCAGAACCTGTG
P_34	pAMN1_F	AGC CTT AGG GGG TGT TTG TTT CCT
P_35	pAMN1_R	CAATCGTGACACGATTTTGGATG
P_36	pAMN2_F	GACATACCCCATCAACCACA
P_37	pAMN2_R	TTTCCCTATAGACTCTCCCTTTTGG
P_38	pAMN3_F	CCTATGATTTAGTTAGTCATGGTTGTG
P_39	pAMN3_R	GCTAGCTAGCTACCTAGCAGCCAGTG
P_40	AMN1_CDSseq_F3	CAATGGAAGCTACTACCAACCACAGGAC
P_41	HISTONE H3_F	CCCTGGAAGTGTGCTCTTC
P_42	HISTONE H3_R	CCTGAGCAATTTACGAACC
P_43	TIP41-F	GCTTTGCCACCTGTTGAAGT
P_44	TIP41-R	AGCACCGCTTCCACAATAAG
P_45	Ubiquitin-F	GCCGGAAAACAGCTAGAAGA
P_46	Ubiquitin-R	GGAGACGGAGAACAAGGTGA
P_47	MtPT4_F	GGATTCTTTTGCACGTTCTTGG
P_48	Mt PT4_R	CCTGTCATTTGGTGTTCAGTG
P_49	MtIAA8_F	ATGTCTCTACCAAGGCTAGG
P_50	MtIAA8_R	TTAGTTCCTGCTTTTACTTT

Table 2.8: List of primers used in this study

CHAPTER THREE:

Analysing the phylogeny and expression of *M. truncatula* ABC subfamily B transporters during root nodule symbiosis (RNS) and arbuscular mycorrhizal symbiosis (AMS)

3. 1 Introduction

Several studies in the past five years have reported ABC transporters to be important players in symbiosis. Members of subfamily G, in particular, have been found to play diverse roles in arbuscular mycorrhizal symbiosis at different stages of the association. One example is the *Petunia x hybrida* strigolactone transporter *PhPDR1* was shown to be required for initial establishment of symbiosis with mycorrhizae (Kretzschmar et al., 2012). A second example is the two periarbuscular membrane localized half ABCG transporters, *STR1* and *STR2* which were shown to be essential for arbuscule development, mutations in which, lead to prematurely degenerating arbuscules (Kall, Krogh, & Sonnhammer, 2004; Q. Zhang et al., 2010). Mutants of the orthologous transporters in rice, also phenocopied the stunted arbuscule morphology observed in the *str1* mutants (Gutjahr et al., 2012) indicating an evolutionarily conserved function across all angiosperms. It is likely that ABCGs are also important for nodulation. Based on pharmacological studies, transport of genistein, a potent nod-gene inducing flavonoid in soybean is predicted to be through members of ABC transporter family other than sub-family B or C (Sugiyama et al., 2007). In keeping with this observation, knockdown of the *M. truncatula* ABC transporter *MtABCG10* using RNA interference reduced the amount of isoflavonoids released into the root exudate (Banasiak et al., 2013). Other ABC transporters are also likely involved in the symbioses. During nodule development *LjABCB1* was shown to be expressed in uninfected cells of the nodule and yeast cells accumulated less auxin when the transporter was expressed in this heterologous system suggesting it was an auxin efflux transporter (Takanashi et al.,

2012). However, no ABC transporters have been reported which have a role in both symbioses (Bapaume & Reinhardt, 2012; Udvardi & Poole, 2013) . The recent completion of genome sequencing for *M. truncatula* and legumes has made the study of complete gene families possible. The genome sequence, along with the availability of a large volume of transcriptomic data under symbiotic and non-symbiotic conditions means it is now possible to identify ABC transporters specific to symbiosis (Tang et al., 2014; Young et al., 2011) . To address this I defined and then analysed the expression of the ABC transporter family in *M. truncatula in silico* to identify a set of three ABC-B transporters expressed during both nodulation and mycorrhization. I then followed up these candidates by analysing their temporal and spatial expression, gene regulation and by investigating their role in symbiosis.

In plants, the complete ABC transporter family has been described for *Arabidopsis* (Sanchez-Fernandez, Davies, Coleman, & Rea, 2001), *Oryza* (Jasinski et al., 2003), *Vitis* (Cakir & Kilickaya, 2013), *Zea mays* (Pang, Li, Liu, Meng, & Yu, 2013) and the partial family for *Lotus japonicus* (Sugiyama et al., 2006) which is still not completely sequenced. I defined the complete ABC transporter family for *M. truncatula*. Next I reasoned that transporters which were exclusively responsive to Nod-factor or Myc-factor alone would play highly specialized roles in symbiosis and would be important candidate genes to investigate. Root hairs as the primary sites of infection are the first cell layer to perceive microbes and are an attractive tissue to study pre-infection and infection related processes. At the start of this project, since there was no transcriptomic data available for root hairs treated with nod-factor I isolated root hairs after 24 hours of treatment with high concentrations of (10 nM) Nod-factor (NF prepared by Giulia Morieri, Allan Downie) and then I extracted RNA which was then used for microarray analyses (Affymetrix GeneChip® *Medicago* Genome Array).

From these analyses I identified three novel ABC sub-family B transporter genes which were specifically induced in response to rhizobia in nodules or infected root hairs and in roots in response to mycorrhiza. We named these three transporters as for ABCB in Mycorrhization and Nodulation. Even though the arbuscular mycorrhizal symbiosis (AMS) is 450 million years old, the AMNs have evolved roles in the relatively recent root nodule symbiosis (RNS) indicating that these transporters possibly perform important roles central to the development of symbiotic associations. In agreement with this idea, I further found homologues of these transporters in both monocotyledonous and dicotyledonous plants and established

that the AMNs are probably conserved across angiosperms. I then confirmed the symbiotic expression of these genes using different approaches.

3. 2 Results and discussion

3.2.1 The complete *M. truncatula* ABC transporter family comprises of 167 putative members

The *Medicago* genome has eight chromosomes and has a total size of 465 Mb. Perhaps the most significant finding from the analysis of the genome was that around 60 MYA, the same time as RNS evolved, there was a whole-genome duplication (Young et al., 2011). According to the authors, this duplication led to the split of the papilionoids, the taxonomic clade under which *Medicago* and most other legumes are classified, from asterids, resulting in specialisation and the evolution of nodulation in the former. They noted that many gene families considerably expanded, possibly due to higher rates of local gene duplication in *Medicago* that allowed for specialization between homeologues. In keeping with these observations, I found that that the total number of full ABC transporters in *Medicago* is almost double, 99 in comparison to the 54 in *Arabidopsis*. This significant expansion of this group of transporters might indicate specialized roles for some members of this family which may be involved in rhizobial symbiosis. The total number of genes encoding both half and full ABC transporters is not double compared to *Arabidopsis*, possibly because of loss of copies of genes during evolution. This exercise also provided evidence for local gene duplications with clusters on chromosome 6 and 7 consisting of 4-5 members (Figure 3.1). These genes show more than 90 % homology to each other at the amino acid level.

A comparison of the total number of ABC transporters in *Medicago* and *Arabidopsis* and their classification further into sub-families is given in Table 3.1. The HUGO nomenclature is followed as recommended by Verrier et al (Verrier et al., 2008). I found that the *Medicago* genome encodes for 167 putative ABC domain containing ORFs of which 146 genes have at least one intrinsic membrane domain. All eight plant sub-families including sub-family ABC-I are represented in the legume genome. As the assignment of families was based on reverse (reciprocal) BLAST to the *Arabidopsis* genome, there are no members in the ABCH sub-family as none exist in plants. Importantly, as in *Arabidopsis*, the ABC-G family with 60 members including full and half transporters, remains the largest sub-family in *Medicago* however there is a twofold increase in the membership to this family. Since most of the ABC transporters found to be involved in plant-microbe interactions are ABCG transporters, this observation might indicate further roles for hitherto unstudied members of this sub-family in symbiosis.

Phylogenetic relationships between all full molecule transporters, containing two NBD and two TMDs each, are shown in figure 3.1. All five families of full molecule transporters are represented and each forms a distinct cluster in the unrooted tree generated using clustal omega.

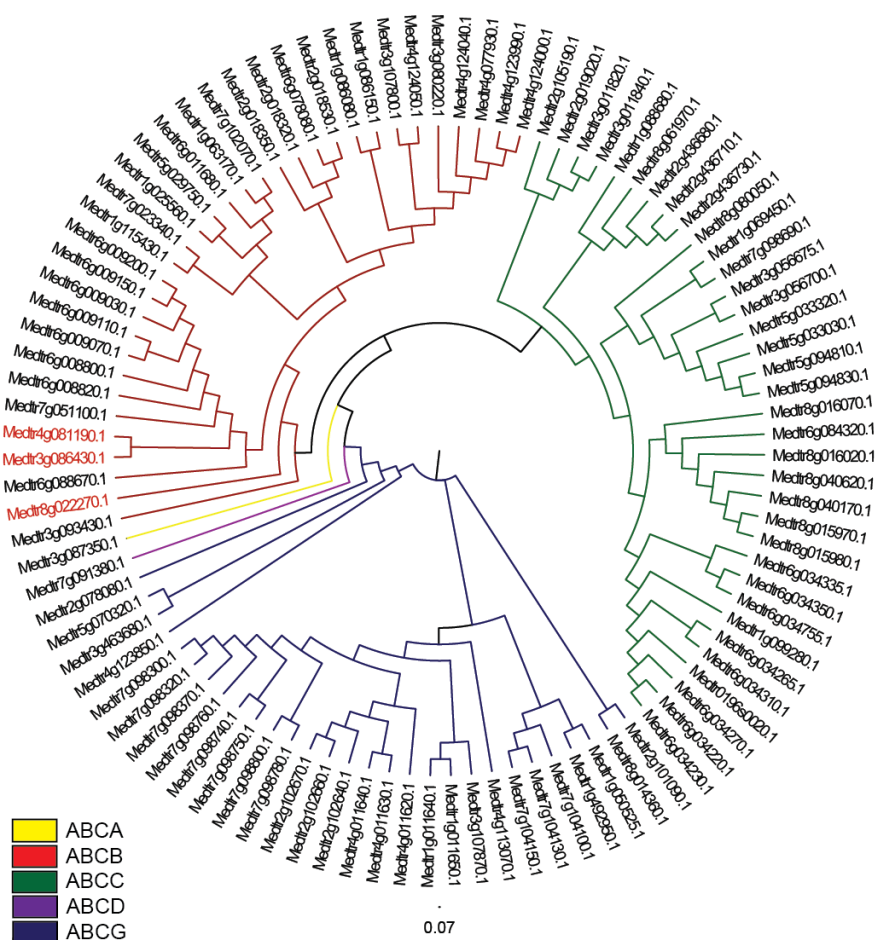


Figure 3. 1: An unrooted cladogram showing phylogenetic relationships between members of full-molecule ABC transporter sub-families of *M. truncatula*.

The *M. truncatula* ABC transporter full molecule family comprises of 99 ORFs each containing two ABC transporter domains and transmembrane domains. Each protein is represented by the corresponding gene IMGAG ID. The largest sub-family for full molecules is the sub-family C with 35 members, closely followed by ABCB with 33 members. ABCA and ABCD each contain a single representative member. Each sub-family forms distinct clusters with different branch colours representing each clade as shown in the key provided. Tree was constructed using amino-acid sequences in clustal omega (<http://www.ebi.ac.uk/Tools/msa/clustalo/>). The AMNs are highlighted in red. AMN1 (Medtr3g084630.1), AMN2 (Medtr4g081190.1) and AMN3 (Medtr8g022270.1) The figure was modified using the Figtree software.

HUGO sub-family	Sanchez-Fernandez sub-family	Domain Organization	<i>Arabidopsis</i>	<i>Medicago</i>
ABCA	ABC1 Homologue (AOH)	(TMD-NBD) ₂	1	1
	ABC2 Homologue (ATH)	TMD-NBD	12	6
ABCB	Multidrug resistance (MDR)	(TMD-NBD) ₂	22	33
	Transporter associated with antigen processing (TAP), ABC transporter of the mitochondria (ATM), Lipid-A like exporter	TMD-NBD	7	10
ABCC	Multidrug resistance associated protein (MRP)	(TMD-NBD) ₂	15	35
		TMD-NBD		1
ABCD	Peroxisomal membrane protein (PMP)	(TMD-NBD) ₂	1	1
		TMD-NBD	1	1
ABCE	RNAse L inhibitor (RLI)	NBD-NBD	3	4
ABCF	General control non-repressible (GCN)	NBD-NBD	5	6
ABCG	Pleiotropic drug resistance (PDR)	(NBD-TMD) ₂	15	29
	White brown complex homologue (WBC)	NBD-TMD	28	31
ABCH		NBD-TMD	0	0
ABCI	Non-intrinsic proteins (NAP), Structural maintenance of chromosomes (SMC)	NBD	21	9
TOTAL			131	167

Table 3.1: A comparison of ABC transporters in *Arabidopsis* and *Medicago*.

(Updated from (Verrier et al., 2008))

3.2.2 Three ABC sub-family B members are induced specifically in response to symbiosis

To next analyse the expression pattern of the identified list of transporters, I retrieved the transcript sequences for all of the 167 genes and identified the microarray probeset IDs with potential matches to the transcripts. I only considered those with a 99% and above identity match with the target. This resulted in a list of 220 probeset IDs for 124 genes since more than one ID can exist for any one gene. For 43 ABC transporters I thus could not find any probeset. I then then examined

the expression pattern of the genes for which probesets were available to identify those which were symbiosis specific, meaning they were induced under conditions in which a beneficial microbe was present but were not otherwise expressed under vegetative conditions. I obtained the average expression values for these probesets under the following experimental conditions Vegetative: leaf, stem, flower, pod, seed 10 dap (days after pollination), root-non mycorrhized, root 0 dpi, root hair 3 dpi uninfected, root hair 5 dpi uninfected. The symbiotic conditions considered were nodule 4 dpi, nodule 10dpi, nodule 14 dpi, nodule 16 dpi, nodule 28 dpi, root mycorrhized, root hair 3 dpi infected and root hair 5 dpi infected. I devised a mathematical index based on the expression values to designate specificity of expression with a unitless number, called the specificity number (SN).

$$\frac{(\text{Maximum symbiotic} - \text{Maximum non symbiotic}) \text{ expression value}}{\text{Average non symbiotic expression value}} = \text{Specificity number}$$

The higher the ratio between the symbiotic and non-symbiotic conditions the more 'specific' the expression. Of the 124 genes I selected those with a SN higher than 2. The list of 18 genes is presented in Table 3. 2. The robustness of this method was proved by the presence of the *STR2* transporter on this short list of 17 *Medicago* genes specific to symbiosis. No probeset could be found for the *STR1* transporter. Of most interest to us were three ABC transporters belonging to sub-family B, *AMN1* (Medtr3g084630.1), *AMN2* (Medtr4g081190.1) and *AMN3* (Medtr8g022270.1), that were responsive to both, rhizobia in infected root hairs only and mycorrhizal infection in whole roots. I chose to study these transporters because of initial microarray experiments performed in my group on infected root hairs which indicated two of the transporters, *AMN1* and *AMN2* to be exclusively induced upon rhizobial infection. I identified *AMN3* during bioinformatics analyses of the rest of the ABC-B sub-family. There were four other ABCB transporters which showed induction upon either mycorrhization or nodulation only. These genes were induced by mycorrhizae irrespective of the strain used to infect the roots implying a fundamental role in infection by members of Glomeromycota; but importantly no pathogens were noted to induce these genes, further emphasizing the role of the AMNs (for ABCB in Mycorrhization and Nodulation) specifically in symbiotic infection and not infection by pathogens.

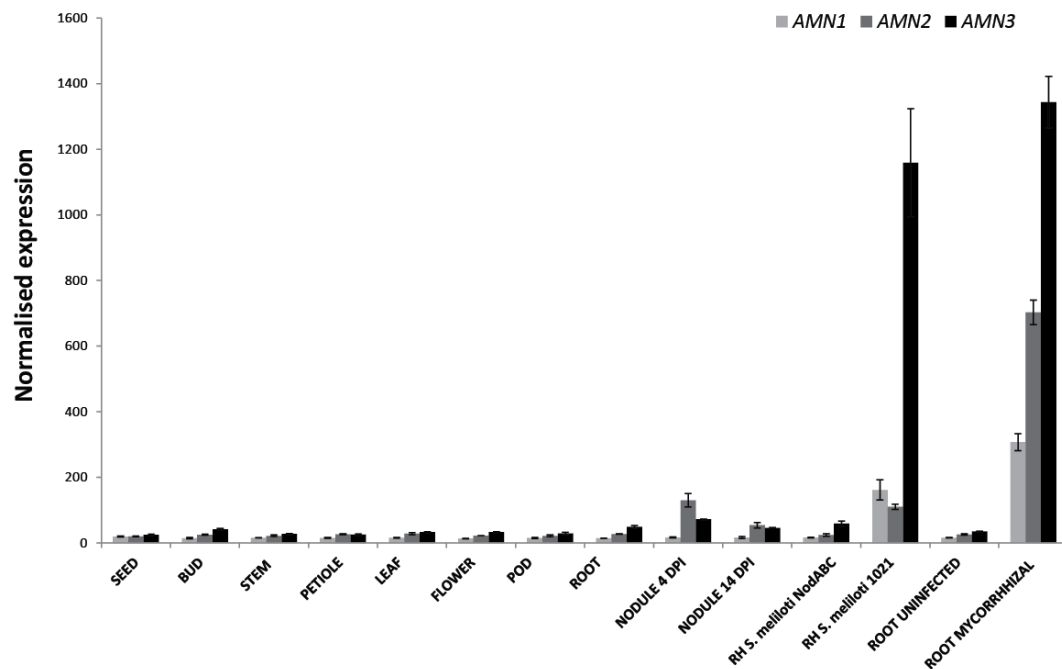


Figure 3. 2: Expression of *M. truncatula* AMN1, AMN2, and AMN3 in different tissues.

AMN1 (Mtr.1103.1.S1_at), *AMN2* (Mtr.44070.1.S1_at) and *AMN3* (Mtr.46524.1.S1_at) are specifically induced in root hairs infected with *S. meliloti* and in whole roots inoculated with *R. irregularis*. These are not expressed in tissues under non-symbiotic conditions. Expression values were taken from the *Medicago* Gene Expression Atlas and represent average of three biological replicates. Error bars denote standard error of the mean (S.E). This strong and striking induction of *AMN1* and *AMN2* transcripts in root hairs formed the basis for selection of these two genes as candidate genes to be studied further. *AMN3* was identified upon further inventorization of all ABC-B subfamily members of *Medicago truncatula* when it showed an identical expression pattern.

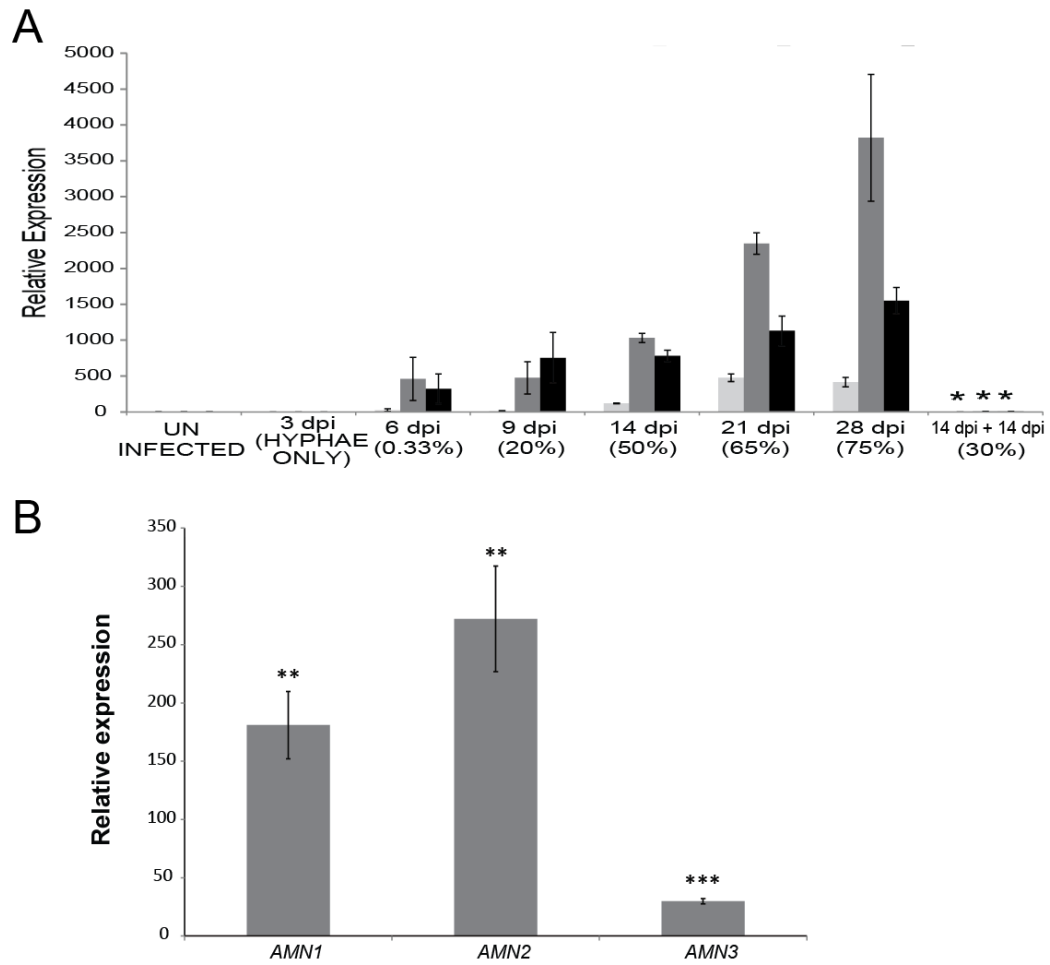


Figure 3.3: Expression of *M. truncatula* AMN1, AMN2, and AMN3 in different tissues upon infection by either mycorrhiza or rhizobia.

(A) Quantitative RT-PCR expression data showing *AMN1*, *AMN2*, and *AMN3* increase over time in WT *M. truncatula* Jemalong A17 roots, inoculated with *R. irregularis*. Approximate percentage colonization of three representative samples is indicated within brackets next to the time point used for harvesting root tissue. For the 14 dpi + 14 dpi time point, colonization was allowed to proceed for 2 weeks after which the plants were transferred to full nutrient containing soil. (B) Quantitative RT-PCR data showing induction of *AMN1*, *AMN2*, and *AMN3* in root hairs (RH) infected with *S. meliloti* and a control strain, which is unable to produce Nod factors.

Primers for *AMN1* (P_5 and P_6) *AMN2* (P_11 and P_12) and *AMN3* (P_17 and P_18) Values represent average of three biological replicates each. Error bars depict standard error of mean (S.E) Asterisks indicate * $p = 0.05$ ** $p < 0.05$ *** $p < 0.01$ using Student's t-test

Two of the transporters, *AMN1* and *AMN2*, are the closest homologues to each other in *Medicago* while the third *AMN3* was different from all other *Medicago* sub-family B members (Figure 3.5). All three transporters were forward oriented full molecule ABC transporters containing the characteristic Walker A and Walker B motif in addition to the ABC signature motif (Figure 3.3). *AMN1*, *AMN2*, and *AMN3* are predicted to have 12 integral membrane spanning domains (Figure 3.4) each and are predicted to localize to the plasma membrane using pLOC (Chou & Shen, 2008).

Since the AMNs seemed to have a role in early stages of symbiotic infection, it was essential to understand whether they were simply induced by Nod-Factors and Myc-factors alone. 24 hours post treatment with high concentrations of Nod factor, all three *AMNs* could be detected in root hairs and whole roots of *Medicago truncatula* (Figure 3.2). They were also highly induced by Myc factors alone (S. Bensmihen personal communication) suggesting a very early role in both symbioses.

```

AMN3  MADSSFEIDNPRRHYPTPVSYQSISSSSFTNSASRSNATPRRRTRRRNRIPSTPFASDD
AMN2  -----
AMN1  -----

AMN3  DRSWQGEVSWKFEPTGLREHSTNFGSVLSPWPTNSTSDRSRVFROSANDYILSRIIGFRN
AMN2  -----
AMN1  -----

AMN3  LFNSSNDHSSYGRVELKSHVARATNDHSYFDQYSGFSKLCIIEKGVNSGNRHIKKASPL
AMN2  -----
AMN1  -----

AMN3  AEEDELSGIDYSISDEHVKHDHGHGVPYGRKSPSQIYGGGGGYSHYEKMASGYDDDEG
AMN2  -----
AMN1  -----

AMN3  DEDMDEDDVVPPKNVGLFSLFRYTRNWDWLLVFIGCIGALINGGSLPWYSYLFGNLVNK
AMN2  -----MGSNSMFRYADGFDKLLMFFGTGLGSLDGLQNPLMMYILSDVINA
AMN1  -----MGNKGGFLRYADGVDKLLFFGTGLGCIIGDGIQTPLTMLVLGSLIDD
          .:.*: * **.*: :.: * . * :.:.:

AMN3  LSREAKNDKQMLKDVEQICIFMTGLAAVVVVGAYMEITCWRLVGERSAQRIRTEYLRAI
AMN2  YGDK--NSR-LNQHDVNFALKLLCVAIGVIGSAFIEGICWNRTAERQASRMRYEYLKSV
AMN1  YARGGSEHI-VSIHNINKYALKLLGIALGVAFAFIVGVCWTRTAERQTSRMRIEYLSI
          . : :.:. : : * * ..*.: ** ..**.:*:* **.:

AMN3  LRQDISFFDTDINTG---DIMHGIASDVAQIQEVMGEKMAHFHHVFTFICGYAVGFRR
AMN2  LRQEVGFFDQTAGSSTTYQVVSLSISSDANTVQSALCEKIPDCLTYMSTFFFCHIFAFVL
AMN1  LRQEVGFFDQTN-SSTTFQVIATITSDAQTIQDTMSDKVPNCLVHLSAFFSSFIVALFL
          **.:.*.*.: . :.: *.*. :*.: :*: . :.:

AMN3  SWKVS LVVFSVTP LTMFCGMAYKALYGG LTAKEEAS YRKAGSIAEQAISSIRTVFSFVAE
AMN2  SWRLALAAIPLSIMFIVPALVFGKIMLDVTMKMIESYGVAGGIAEQAISSIRTVFSYVGE
AMN1  SWRLAVAAPF SIMMIMPALIFGNAMKELGGKMKDAFGVAGSIAEQAISSVRTVSYVGE
          **.:.:. : : : : : * : : ** .*****:*:*:*.*

AMN3  SQLGEKYSELLQKSAPIGAKIGFAKGAGMGVIYLVTYSTWALAFWYGSILIARGELDGGGS
AMN2  NQTLKRFSTALEKTMEFGIKQGFAGKGLMLGSM-GVIYVSWGFQAWVGTFLISDKGEKGGH
AMN1  KQTLKRFSSALETCMQLGIKQGQTKGVVGSF-GLLYATWAFQSWVGSVLVTRTKGEKGGK
          .* :.:* *.: . : * * * :** :* : : * :.: * *.:. : **

```



```

AMN3      LDLESEKHIQEALKNVSKEATTIIVAHRLSTIREADKIAVMRNGEVVEYGSHDTLISSIQ
AMN2      LDSASEVLVQEALEKIMVGRTCIAVAHRLSTIQNSNSIAVIKNGKVVEQGSHNELISLGR
AMN1      LDSVSENLVQEALEKMMVGRTCVVIHRLSTIQSVDSIAVIKNGKVVEQGSQSLLNDRS
          **  **  :****:..:  *  :*****:.. :.***:.*:*:**  **  .  *:.
AMN3      NGLYASLVRAETEANAFS*
AMN2      NGAYHSLVKLQHGSSPR*-
AMN1      NGTYYSLIRLQQSHST*--
          ** * **:::  :  .

```

Figure 3 4: Amino acid sequence alignment of AMN1, AMN2, and AMN3 showing characteristic domains of a Full ABC transporter

AMN1, AMN2, AMN3 are three forward oriented, full-molecule ATP Binding Cassette domain containing intrinsic membrane proteins comprising two transmembrane domains and two nucleotide binding domains (highlighted in grey and dark grey respectively). The nucleotide binding domain is highly conserved and amino acid residues of characteristic signature motifs such as the Walker A (Q-loop) and the Walker B motifs (highlighted in red) are present, ~120 amino acids apart. The ABC signature motif (named C), characteristic of all ATP binding proteins is situated between the two Walker motifs (marked in red). A short stretch of aromatic amino acid, the A-loop, containing sub-domain 25 residues upstream of the Walker A motif is highlighted in green. AMN3 is unique in containing a stretch of serine rich hydrophilic residues highlighted in pink, at the N terminus which makes it different from all other ABCs present in sub-family B. It is of unknown significance. The domains were determined using pfam and NCBI annotations and alignment generated using Clustal omega.

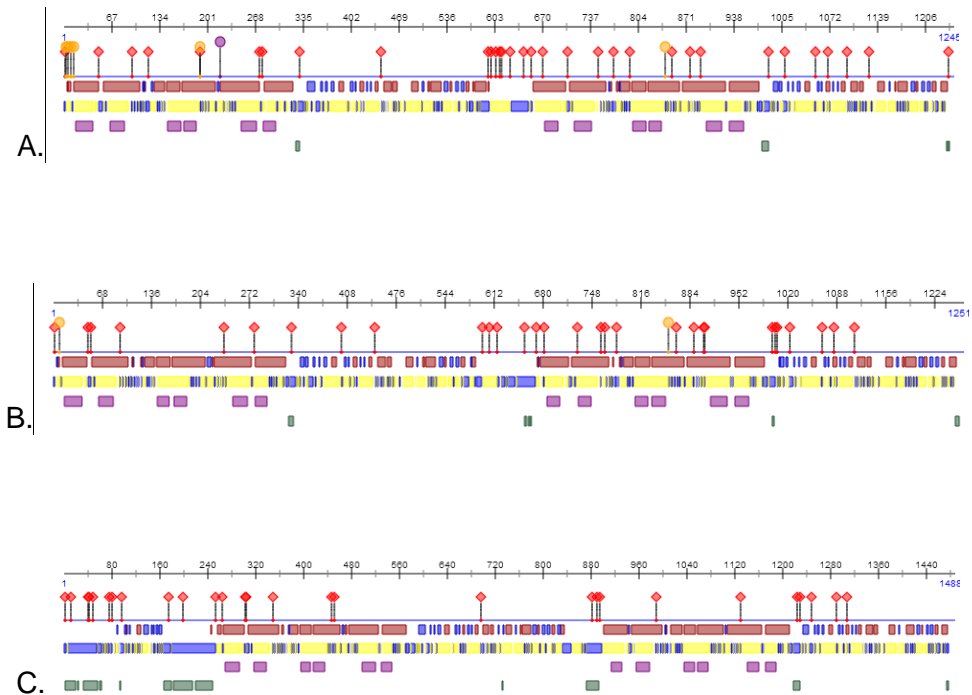


Figure 3.5: Hydrophobicity plots showing predicted transmembrane regions for AMN1, AMN2, and AMN3

AMN1 (A), AMN2 (B) and AMN3 (C) were predicted to have 12 transmembrane regions each using PredictProtein (<https://www.predictprotein.org/>) as shown. Magenta boxes designate the position of the transmembrane helix. The N terminal region was predicted to be cytoplasmic for all three transporters. Boxes in green represent hydrophilic residues. *AMN* gene identifiers are as follows *AMN1* (Medtr3g084630.1), *AMN2* (Medtr4g081190.1) and *AMN3* (Medtr8g022270.1)

Gene Model	Probeset ID	Domain Organization	Sub-family	SN	Expression
Medtr5g07032 0.1	Mtr.5725.1.S1_s _at	(TMD-NBD)2	ABCG	80	RNS: Nodule 10 dpi,14dpi,16dpi,28dpi
	Mtr.5725.1.S1_a t	(TMD-NBD)2	ABCG	20	RNS: Nodule 10 dpi,14dpi,16dpi
Medtr8g02227 0.1 (AMN3)	Mtr.46524.1.S1_ at	(TMD-NBD)2	ABCB	36	RNS: Infected root hair 3dpi,5dpi, 10 nM Nod Factor AMS: Mycorrhized root, Arbusculated and adjacent cells
Medtr4g08119 0.1 (AMN2)	Mtr.44070.1.S1_ at	(TMD-NBD)2	ABCB	29	RNS: Infected root hair 3dpi,5dpi, Nodule Zone 2, 10 nM Nod Factor AMS: Mycorrhized root, Arbusculated and adjacent cells
Medtr4g10817 0.1	Mtr.49882.1.S1_ at	TMD-NBD	ABCA	25	RNS: Nodule all stages, Nodule Zone 2, Vegetative: Seed
Medtr3g08643 0.1 (AMN1)	Mtr.1103.1.S1_a t	(TMD-NBD)2	ABCB	21	RNS: Infected root hair 3dpi,5dpi, 10 nM Nod Factor AMS: Mycorrhized root, Arbusculated and adjacent cells
Medtr4g12404 0.1	Mtr.43343.1.S1_ at	(TMD-NBD)2	ABCB	11	RNS: Nodule 16 dpi , Pathogen: Phytophthora,Ralstonia , Vegetative: Root tip,
	Mtr.6889.1.S1_a t	(TMD-NBD)2	ABCB	5	RNS: 16 dpi, 28 dpi, Pathogen: Phymatotrichum, Vegetative: Full Nitrogen whole root ,
Medtr4g07793 0.1	Mtr.9965.1.S1_a t	(TMD-NBD)2	ABCB	8	RNS: Nodule 10dpi, 16dpi, 28 dpi Pathogen: Phymatotrichum , Vegetative: Root hairs
Medtr1g05052 5.1	Mtr.2427.1.S1_a t	(TMD-NBD)2	ABCG	6	RNS: Nodule all stages, AMS: Mycorrhized root cortical cells
Medtr5g09483 0.1	Mtr.41168.1.S1_ at	(TMD-NBD)2	ABCC	6	RNS: Nodule all stages, Vegetative: Root and Root hairs
Medtr3g09343 0.1	Mtr.4782.1.S1_a t	(TMD-NBD)2	ABCB	6	AMS: Root mycorrhizal (induced) Vegetative: Root non-mycorrhizal
	Mtr.27228.1.S1_ at	(TMD-NBD)2	ABCB	2	AMS: Root mycorrhizal (induced) Vegetative: Root non-mycorrhizal, Full Nitrogen root
Medtr6g08867 0.1	Mtr.11576.1.S1_ at	(TMD-NBD)2	ABCB	4	RNS: Nodule all stages
Medtr5g03091 0.1	Mtr.51195.1.S1_ at	TMD-NBD	ABCG	3	RNS: Nodule 16 dpi, AMS: Mycorrhized root, Arbusculated cells Vegetative: Root hair 5 dpi, Hypocotyl, Root

Medtr8g10741 0.1	Mtr.39481.1.S1_ at	NBD	ABCI	3	RNS: Nodule 3 dpi, Vegetative: Root, Leaf,
Medtr4g01163 0.1	Mtr.32240.1.S1_ at	(NBD-TMD)2	ABCG	2	RNS: Nodule all stages Vegetative: Root, Hypocotyl
Medtr1g09466 0.1	Mtr.19183.1.S1_ s_at	(NBD-TMD)2	ABCG	2	RNS: 10 nM Nod Factor Vegetative: Constitutive in root hair, Root border cell
Medtr1g01164 0.1	Mtr.18815.1.S1_ at	(NBD-TMD)2	ABCG	2	RNS: Nodule, AMS: Mycorrhized root, Vegetative: Leaf, Root ,
Medtr3g01182 0.1	Mtr.7160.1.S1_a t	(TMD-NBD)2	ABCC	2	RNS: Nodule Vegetative: Root, Leaf, Shoot

Table 3. 2: *Medicago* ABC transporters induced either during Root Nodule Symbiosis (RNS) or Arbuscular Mycorrhizal Symbiosis (AMS)

Specificity of transporters is reported in descending order except when two probeset IDs correspond to the same gene model (Genome V4). Expression data were taken from MtGEA and the unpublished microarray data.

3.2.3 *AMN1*, *AMN2*, and *AMN3* are not present in *Arabidopsis* but are evolutionarily conserved across all mycorrhizal angiosperms

To identify a role for the AMNs in symbiosis we looked for orthologues in the model plant *Arabidopsis* by constructing a phylogenetic tree consisting of all members of the full-molecule sub-family B shown in Figure 3. 5. The AMNs had no orthologues in *Arabidopsis* and did not cluster together with any previously characterized members of the family. This further substantiated our observation that the AMNs are symbiosis-specific since the Brassicaceae family members including *Arabidopsis* cannot nodulate or mycorrhize and would be expected to have lost symbiosis related genes.

I could find the AMNs in all dicotyledonous plants which possess the ability to mycorrhize and/or nodulate and whose sequences are available on NCBI/Phytozome (Figure 3.6). With monocots however, the reverse BLAST criteria for identification of an orthologue was not satisfied for either of the genes. We thus looked for ABC transporters induced upon mycorrhization in rice transcriptomic studies and identified an ABCB transporter, the closest homologue of which in *Medicago* was *AMN2* closely followed by *AMN1*. Using this sequence I was able to identify homologous sequences in other monocotyledonous species all of which were full ABCB transporters. Further, inclusion of rice ABCB transporters in

phylogenetic tree construction showed them as clear orthologues for AMN1 and AMN2 Figure 3.5.

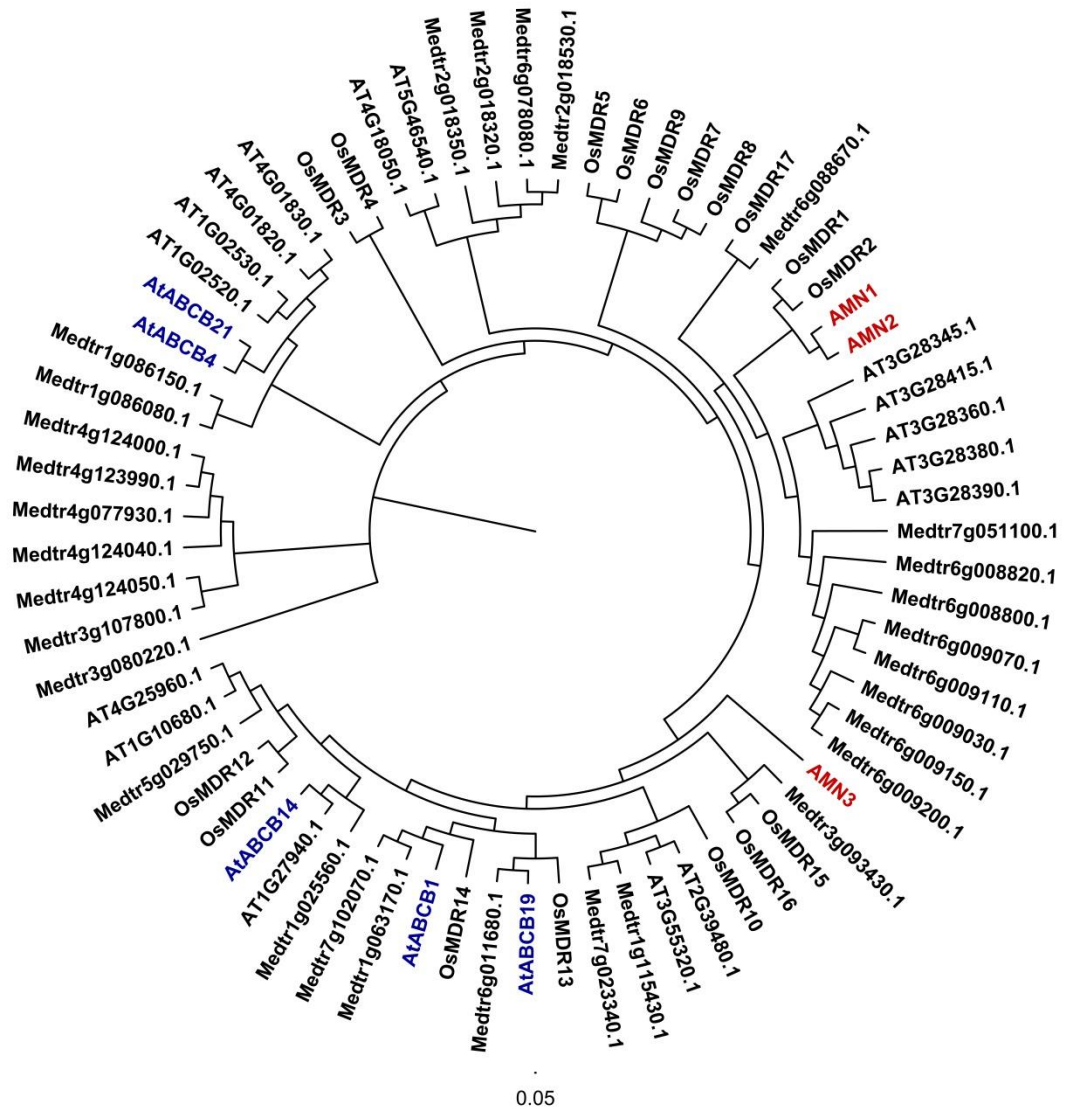


Figure 3.6: Phylogenetic relationships between sub-family B full-molecule ABC transporters of *Arabidopsis*, *Medicago* and *Oryza*.

M. truncatula and *Arabidopsis* and *O. sativa* protein sequences were retrieved from their respective databases. A rooted phylogram was created using CLUSTAL OMEGA. AMN1, AMN2, AMN3 are highlighted in red. Notably AMN1, AMN2, and AMN3 have no direct orthologues in *Arabidopsis*. In addition, all *Arabidopsis* ABCBs studied so far (highlighted here in blue) form separate subclades suggesting un-relatedness in the type of substrate transported,

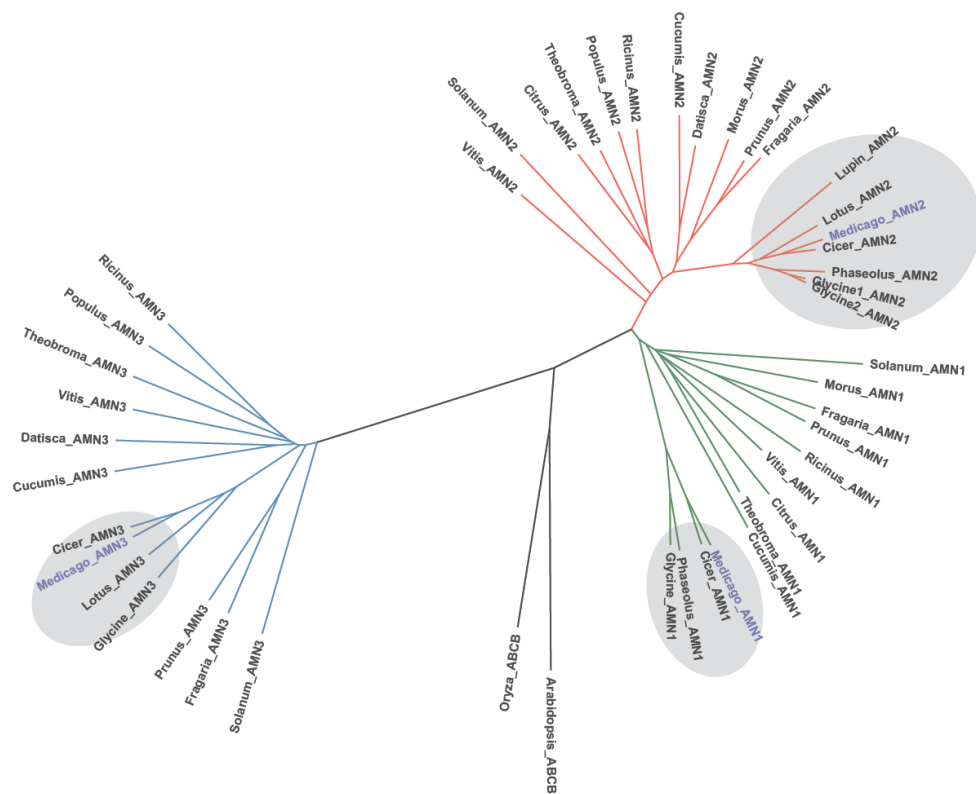


Figure 3.7: *Medicago truncatula* AMN1, AMN2, and AMN3 orthologues are conserved in dicots which can nodulate or mycorrhize.

M. truncatula protein sequences were used to retrieve orthologous sequences on NCBI. A rooted phylogram was created using CLUSTAL omega. AMN1, AMN2, AMN3 orthologues form distinct clusters comprising of dicotyledonous plant species which can form beneficial fungal and bacterial associations. Members of family Leguminosae, which can nodulate, further form sub-clusters, shown here encircled in grey. AMN2 but not AMN1 and AMN3 was found in *Lupinus*, which can nodulate but does not mycorrhize. *Arabidopsis thaliana* ABCB transporter ABCB15 and an unrelated *Oryza sativa* ABCB transporter were used as outgroups. Scientific names and accession numbers are provided in supplemental table 3.1.

functionalization of the transporters in legumes or alternatively may simply reflect the shared ancestry of the legumes. The fact that *Lupinus*, which can nodulate but not mycorrhize, has retained AMN2 suggests that this protein may be important for RNS. This could suggest neo or sub functionalization of the transporters in legumes or alternatively may simply reflect the shared ancestry of the legumes. Secondly, AMN3 did not have a clear orthologue in either *Arabidopsis* or rice. This could indicate a sub-functionalization requirement during rhizobial infection. Thirdly, AMN2 seems to be the best conserved amongst the three AMNs and could be found over a wider range of species. In addition, Soybean was found to have two copies of this transporter. Lastly, AMN2 and AMN3 could also be found in an actinorhizal angiosperm, *Datisca* which forms associations with filamentous bacteria called *Frankia*. It will be interesting to test whether the AMNs are also involved in actinorhizal symbiosis.

3.2.4 AMNs are expressed in *M. truncatula* upon infection with symbionts

To confirm the validity of the microarray data I used quantitative PCR. Using root hair cDNA provided by A. Breakspear, I estimated the transcript abundance corresponding to these genes in *M. truncatula* WT Jemalong A17 root hairs infected with WT Nod-factor producing *S. meliloti* 1021 and compared them to root hairs infected with the non-Nod factor producing strain SL44. The *AMN* transcripts could be detected in control treated root hairs at very low abundance and was significantly increased upon infection (Figure 3.2 C).

To quantitate expression during mycorrhizal colonization I monitored the expression of the *AMNs* along with the progression of infection over time. I harvested three samples of which I scored the number of arbuscules and vesicles to get a rough estimate of the percentage colonization. Each biological replicate consisted of a pooled sample of three plants each. The transcript levels were determined for 8 time points (Figure 3.2 B) including one time point (14dpi +14 dpi) in which the plants were grown for two weeks in low nutrient soil and then were transferred to full nutrient containing soil. Upon initial contact at 3 dpi, where the plants were just beginning to get colonized and showed approximately 0.33% colonization, the *AMNs* were not induced indicating a role in the later stages of mycorrhizal colonization. The increase in expression of all three *AMNs* correlated with a proportionate increase in colonization. When infected plants were transferred to full

nutrient containing soil after an initial two weeks in low nutrient soil, the expression of the *AMNs* reduced dramatically and was almost completely switched off. After this treatment, there were still internal arbuscules and vesicles present inside the root. This indicated that expression of *AMNs* is associated with actively progressing infection.

3.2.5 Promoters of *AMN1*, *AMN2*, and *AMN3* are associated with rhizobial infection

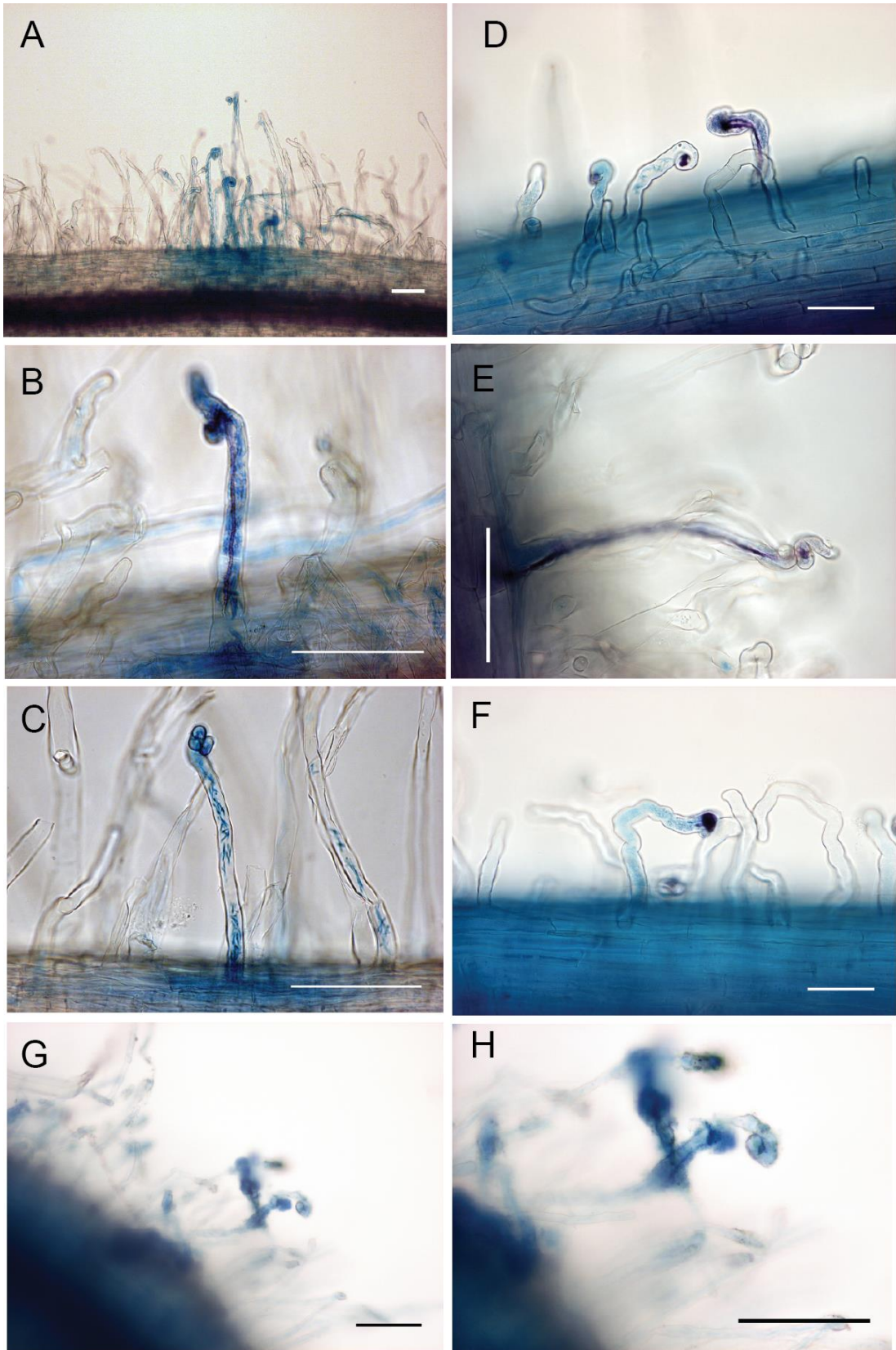
The *AMN1*, *AMN2*, *AMN3* promoters were assessed for their spatio temporal expression patterns using promoter GUS fusions. In general, *AMN1* and *AMN2* promoters showed overlapping patterns of expression with variations in the spread and the strength of the expression in tissue. Gene expression of *AMN2* and *AMN3* could be detected within a few hours of staining whereas *AMN1* required longer staining procedures to detect low levels of GUS expression. Upon infection with rhizobia, at 10 dpi *AMN1* expression was associated with root hairs forming an infection pocket or those containing an infection thread (Figure 3.6). A few root hairs surrounding the infected root hairs also showed *GUS* activity. *AMN2* showed a similar pattern of expression and was also associated with infection structure containing root hair cells. *AMN3* showed the most divergent pattern of expression even though it was also associated with infected root hairs. The expression of *AMN3* was spread over a zone of the root responding to Nod-factor responsive root hairs but was induced in infection containing cells (Figure 3.6). This explains why the expression of *AMN3* is the easiest to detect. In uninfected plants, all three *AMNs* could be detected in low levels in vascular tissue and lateral root primordia as well as the root tip. *AMN1* could be detected in root cap cells as well (Figure 3.7).

FIGURE 3.8: Spatial expression pattern of *AMN1*, *AMN2*, and *AMN3* promoter ten days post inoculation with *S. meliloti*

M. truncatula A-17 WT hairy roots transformed with the Gateway destination vector pKGWFS7 containing the *AMNs* promoter-GUS reporter sequence stained for GUS activity using the chromogenic substrate X-GlcA (in blue). Rhizobia carrying the pXLGD4 plasmid for *pHemA:LacZ*, stained in Magenta.

Bright field image showing GUS staining (**A,B,C**) expression associated with *pAMN1-GUS* expression in rhizobially infected roots. *pAMN2-GUS* (**D,E,F**) *pAMN3-GUS* (**G,H**) showing micro-colony containing root hair cell stained blue in comparison to cells nearby

Scale bar denotes 100 μ m



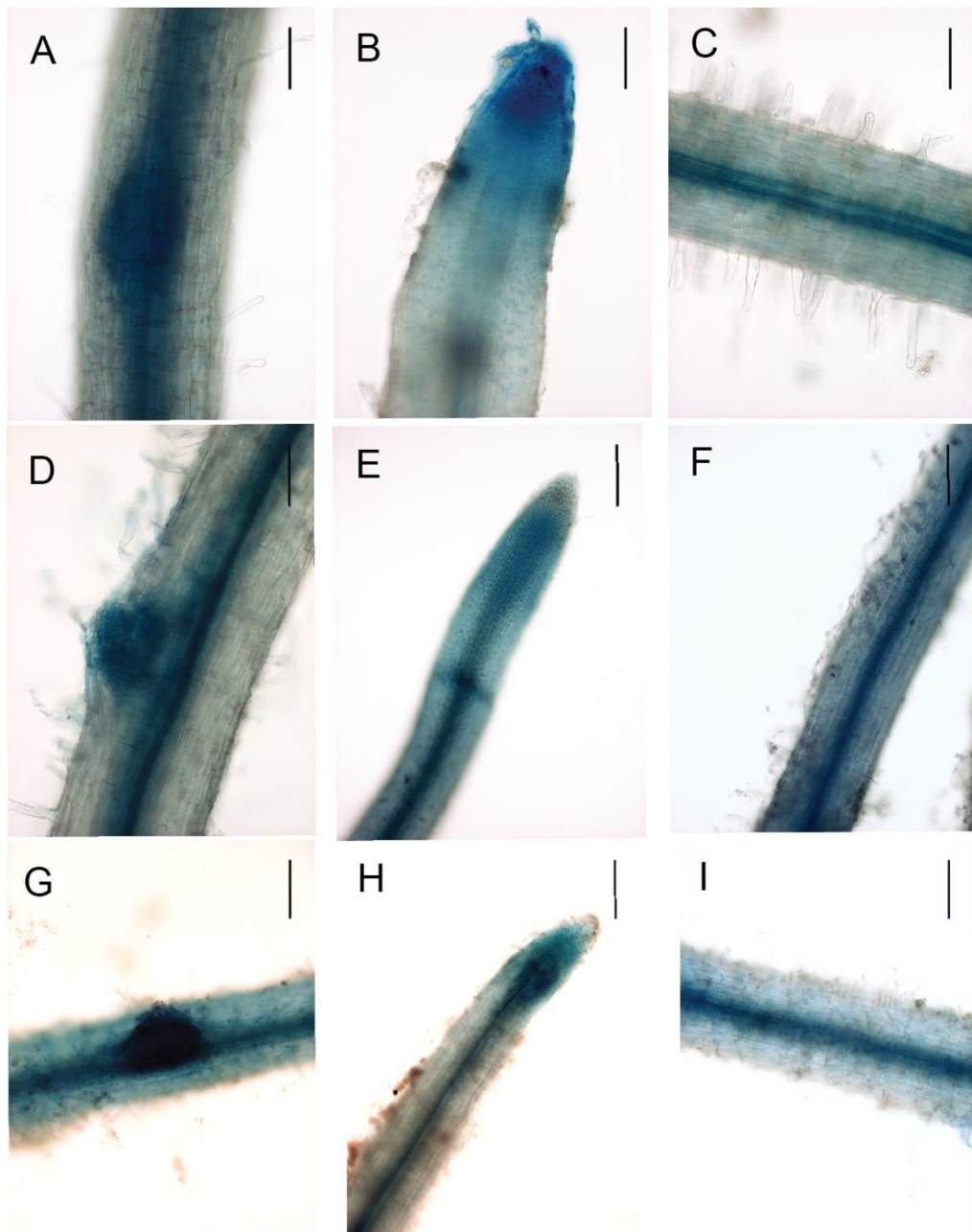


Figure 3.9: Non-symbiotic expression pattern of *AMN1*, *AMN2*, and *AMN3*

M. truncatula Jemalong A-17 WT hairy roots transformed with the Gateway destination vector pKGWFS7 containing upstream promoter sequence of the *AMNs* stained for GUS activity using the chromogenic substrate X-GlcA (in blue).

(**A,B,C**) Bright field image showing GUS staining associated with *pAMN1*-GUS expression in the emergent lateral root, root tip and vascular bundle. (**D,E,F**) *pAMN2*-GUS (**G,H,I**) *pAMN3*-GUS. Scale bar denotes 100 μ m

3.2.6 Promoters of *AMN1*, *AMN2*, and *AMN3* are associated with mycorrhizal infection

Previous studies classify mycorrhizal responsive genes to fall under **early** (responsive to myc factor, appressoria formation and hyphal penetration), **arbuscule associated**, and **adjacent cell associated** the latter referring to cells adjacent to cells containing arbuscules. Consistent with the qPCR and microarray studies, I noted that of the three genes *AMN1* is the gene most weakly expressed in roots. After 4 weeks I could note induction in arbuscule containing cells but found that it was not associated with intercellular hyphae or vesicles. No expression of *pAMN1:GUS* was observed upon hyphal penetration of the root surface (Figure 3.8 E,F). This weak induction might be because the cloned promoter consists of only 1000 bps upstream of the ATG start site and therefore might be missing some upstream regulatory elements. *AMN2* expression was also not associated with intercellular hyphae through the cortex (Figure 3.9) but was induced very strongly in arbuscule containing cells. *AMN3* mirrored the expression of *AMN2* and was not induced upon initial contact and was instead upregulated in arbusculated cells (Figure 3.10). In addition, a constitutive expression was seen throughout the root. I also observed expression at 4 wpi which reproduced the expression pattern seen at 2 wpi for both the *AMN2* and *AMN3* promoters.

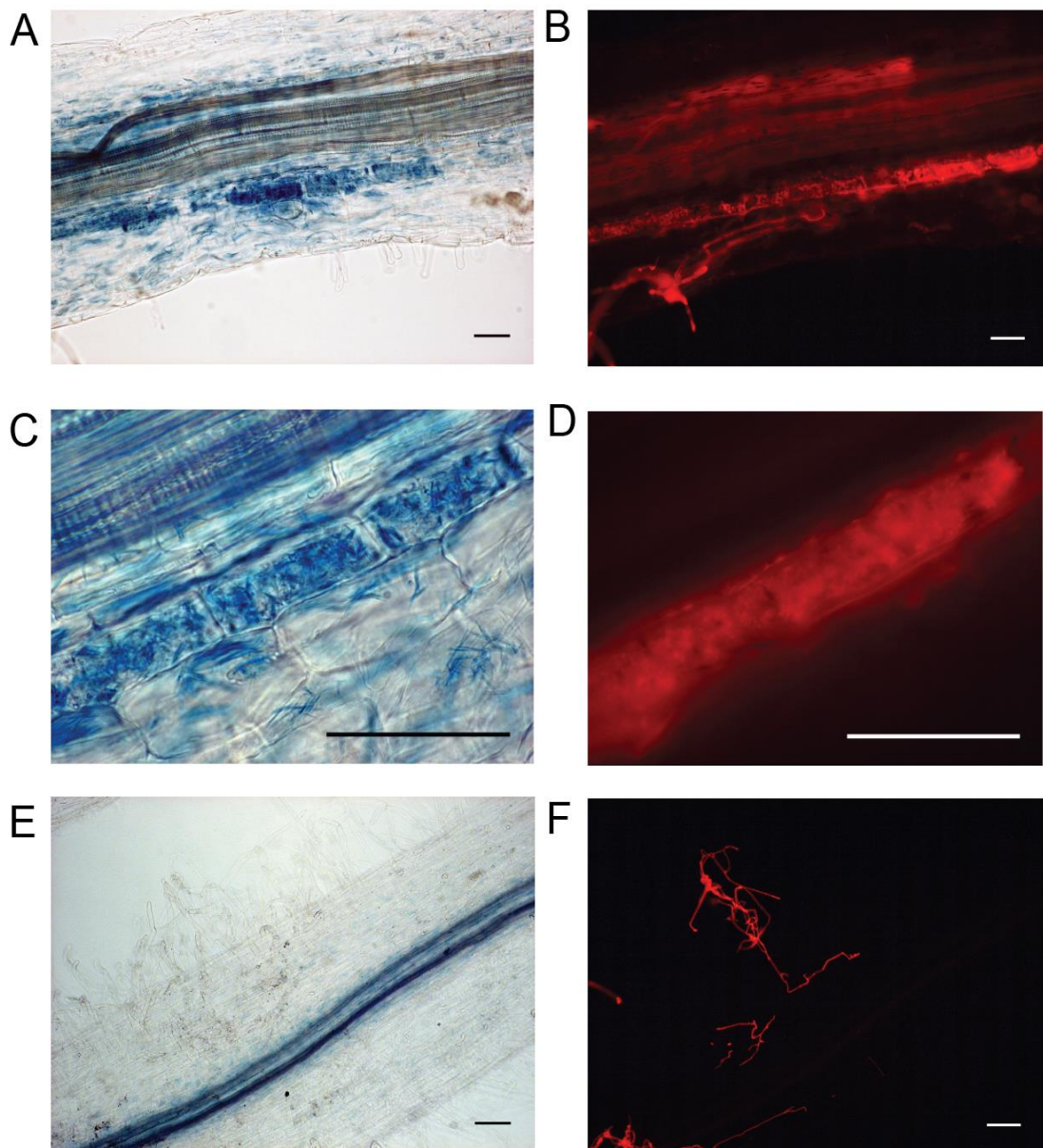


Figure 3.10: Spatial expression pattern of the *AMN1* promoter four weeks post inoculation with *R. irregularis*

M. truncatula A-17 WT hairy roots transformed with the Gateway destination vector pKGWFS7 containing 1006 bps upstream of ATG were stained for GUS activity using the chromogenic substrate X-GlcA (in blue). The fungus, *R. irregularis*, was stained with WGA Alexa Fluor 568 (in red).

(A,B) Bright field image showing GUS activity associated with a cell hosting an arbuscule. Corresponding fluorescent image showing mycorrhiza on the right.
 (C,D) Individual arbuscule containing cells shown at 100x magnification
 (E,F) No GUS activity was detected upon initial contact with hyphae.
 Scale bar denotes 50 μ m

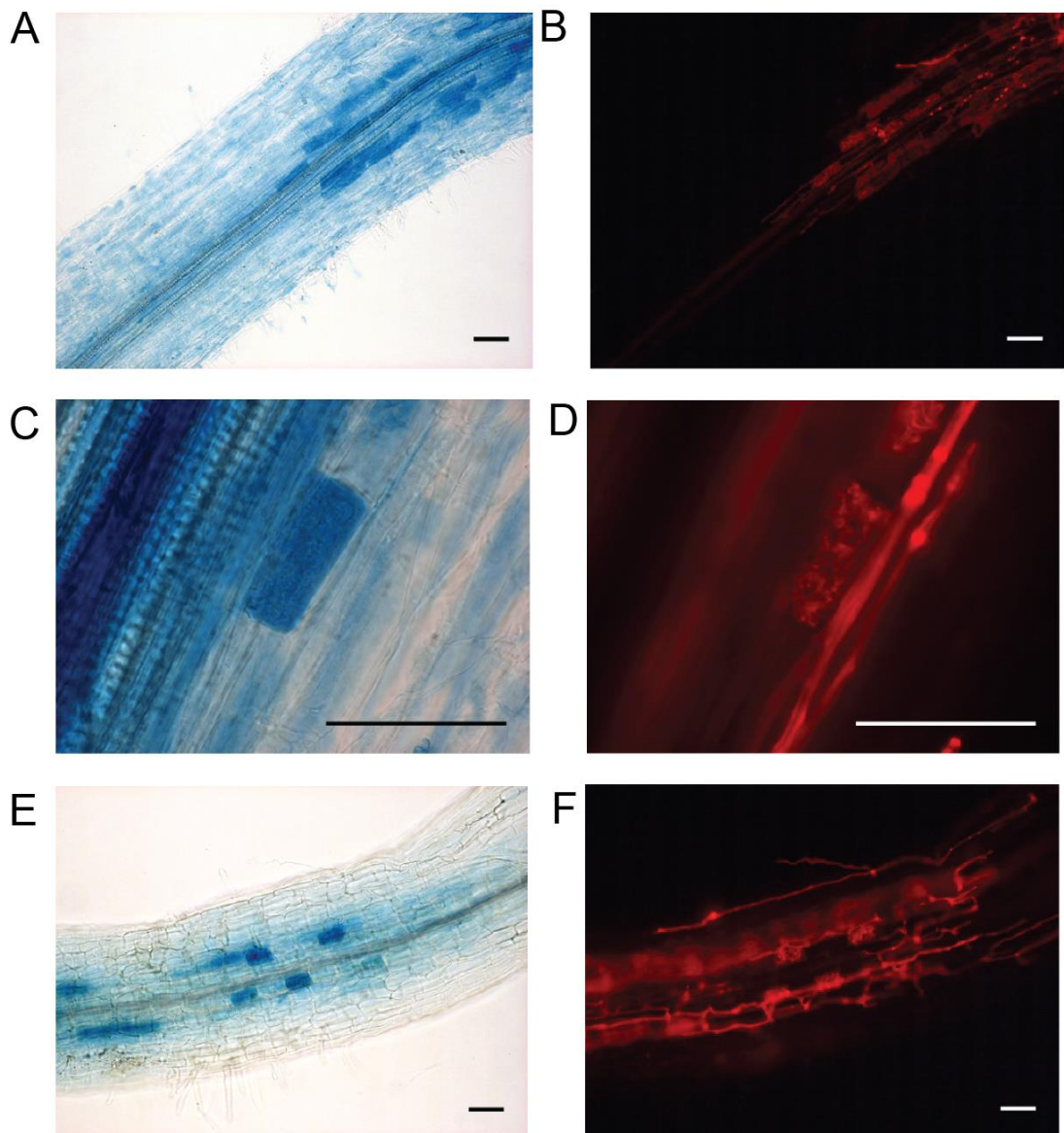


Figure 3.11: Spatial expression pattern of the *AMN2* promoter two weeks post inoculation with *R. irregularis*

M. truncatula A-17 WT hairy roots transformed with the Gateway destination vector pKGWFS7 containing 1773 bps upstream of ATG were stained for GUS activity using the chromogenic substrate X-GlcA (in blue). The fungus, *R. irregularis*, was stained with WGA Alexa Fluor 568 (in red).

(A,B) Bright field image showing GUS activity associated with cell hosting an arbuscule. Corresponding fluorescent image showing mycorrhiza on the right.

(C,D) Individual arbuscule containing cells shown at 100x magnification

(E,F) No GUS expression was detected upon initial contact with hyphae.

Scale bar denotes 50 μm

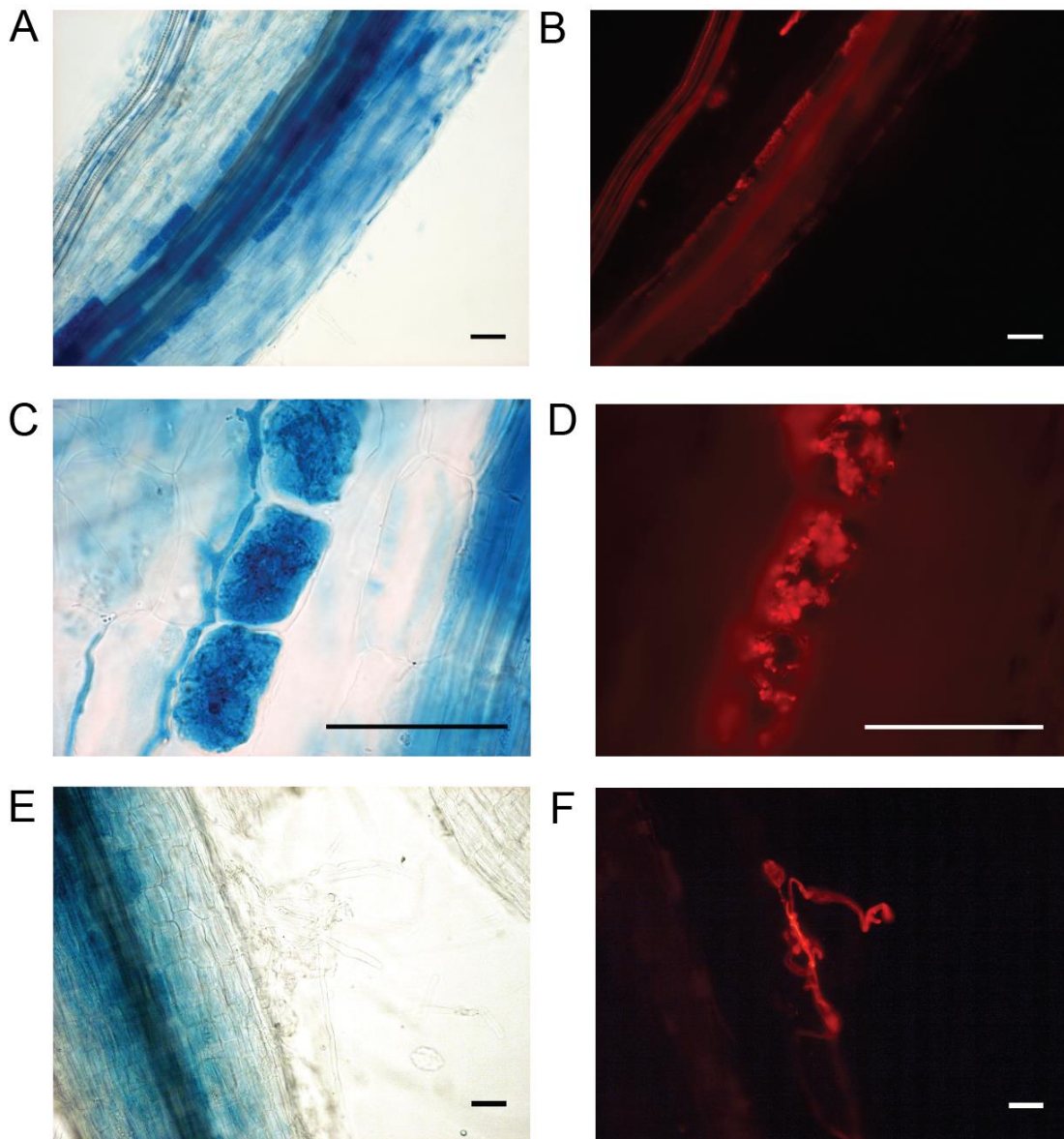


Figure 3.12: Spatial expression pattern of the *AMN3* promoter two weeks post inoculation with *R. irregularis*

M. truncatula A-17 WT hairy roots transformed with the Gateway destination vector pKGWFS7 containing 2006 bps upstream of ATG were stained for GUS activity using the chromogenic substrate X-GlcA (in blue). The fungus, *R. irregularis*, was stained with WGA Alexa Fluor 568 (in red).

(A,B) Bright field image showing GUS activity associated with cell hosting an arbuscule. Corresponding fluorescent image showing mycorrhiza on the right. Arrowheads indicate arbuscules.

(C,D) Individual arbuscule containing cells shown at 100x magnification.

(E,F) Extracellular hyphae extending over the surface of the root before entering the root did not induce expression of p*AMN3*.

Scale bar denotes 50 μ m



Figure 3.13: Staining pattern of vector control hairy root lines

M. truncatula WT hairy roots transformed with an empty binary vector and stained for GUS activity for 48 hours.

(A.) Bright field image showing GUS activity at the base of the hypocotyl.

(B) Primary root tip showing absence of GUS expression in vascular bundle and root apical meristem.

(C) Bright field image showing absence of GUS activity in vascular bundle and root hairs.

(C) Bright field image showing absence of GUS activity in lateral roots.

Scale bar denotes 100 μm

3.3 Conclusion

Together using transcriptomic and expression studies I confirmed that *AMN1*, *AMN2*, and *AMN3* are three novel, functionally uncharacterized ABC sub-family B type transporters in *M. truncatula*. They are conserved across angiosperms and are specifically induced upon infection by both rhizobia and mycorrhizae in infected cells. Admittedly, there might be more ABCB transporters not a part of the presently available genome that are specific to symbiosis. In addition, the *in silico* approach taken to find the find symbiosis specific transporters were based on available transcriptomic data for specific probesets. It is estimated that only about 85% of transcribed genes are represented on the *Medicago* Affymetrix chip. A possible shortcoming of using this method therefore is overlooking genes for which no probesets can be found or which have a poor correlation to actual levels of transcript. The method would also overlook any gene which is not strongly transcriptionally regulated, for instance having dual roles in symbiosis and vegetative tissues as it will have a very low SN value.

The phylogenetic analyses of the AMNs and the presence of the homologues of these transporters in mycorrhizal angiosperms provide compelling evidence that the AMNs likely play an important role in symbiosis. Although these three transporters are symbiosis specific there might be other more 'constitutive' ABCBs that transport the same substrate in vegetative tissues. One such candidate is the Medtr6g088670.1 transporter, tentatively called *MtABCB4* which I identified using the latest release of *Medicago* genome sequence (Version 4.0) (Tang et al., 2014). This transporter shares sequence similarity to all three AMNs at the nucleotide and the protein level as evidenced by its phylogenetic position in the tree (Figure 3.5).

AMNs have been identified in several transcriptomic studies designed to identify mycorrhizal genes. The first mention of these mycorrhizal ABCB transporters was in a study designed to identify mycorrhiza responsive genes in whole roots at 4 wpi with *Glomus intraradices* (*R. irregularis*). The study grouped them with 37 other genes which were found to be specifically mycorrhiza responsive (Gomez et al., 2009). Another transcriptomic study which aimed to differentiate between the arbuscule containing and the adjacent cortical cells using laser capture microdissection microscopy found the *AMNs* in arbusculated cells but noted that these transporters were also expressed in cells adjacent to those containing

arbuscules (Gaude et al., 2012). They noted that other arbuscule markers, such as *MtPT4* were not present in this sample therefore making it seem less likely that this was due to contamination. An independent research report validated this using promoter-GUS for *AMN3* which they reported as ABCB1 but with a different gene identifier from a previous version of the *M. truncatula* genome annotation endeavour. A recent study noticed that all three *AMNs* are induced by early contact where they defined early contact as 3 wpi, however they could not rule out the possibility that there were arbuscules present in the tissue harvested (Ortu et al., 2012).

I used quantitative real time PCR and promoter GUS analyses and could establish that the *AMNs* are associated with actively progressing rhizobial and mycorrhiza infection. The expression is spatially restricted to infection structure containing cells. Taken together, the three *AMNs* described in this chapter are exciting candidates for further functional genetic studies in *Medicago truncatula*.

CHAPTER FOUR:

Genetic analyses of function and regulation of three ABC sub-family B transporters in mycorrhization and nodulation (AMNs)

4.1 Introduction

Medicago truncatula is a model legume used to study rhizobial and mycorrhizal interactions. Its small genome size of around 500 Mb extending over 8 chromosomes, inbreeding nature and ease of transformation by tissue culture methods makes it an attractive genetic model (Cook, 1999; G. E. Oldroyd & Geurts, 2001). With the recent completion of the *Medicago* genome sequence (Tang et al., 2014; Young et al., 2011), the availability of extensive EST sequences transcriptomic data and a large population of *Tnt1* mutants, *Medicago* is amenable to reverse genetic techniques. Tobacco *Tnt1*, a copy-and-paste DNA-retrotransposon mobilizes during regeneration in tissue culture in *Medicago* but is otherwise stable (d'Erfurth et al., 2003). This ability was exploited to create a population of *Tnt1* mutants by somatic embryogenesis from *M. truncatula* ecotype R-108. The parental line contained five *Tnt1* inserts and over 20,000 lines were derived from it (Pislariu et al., 2012). We took a genetic approach to determine the function of the AMNs in symbiosis and identified *Tnt1* insertion mutants from the *M. truncatula* R-108 collection.

An alternative genetic approach is the use of RNA interference (RNAi). RNAi has been used widely in legumes to provide genetic evidence of function in the absence of a mutant. It is based on the ability of the endogenous silencing machinery to cleave double stranded RNA into short sequences using the endonuclease Dicer;

followed by cleavage of complementary target mRNAs, by the RISC (RNA induced gene silencing) complex containing the ARGONAUTE protein (Waterhouse & Helliwell, 2003). In *Medicago*, the double stranded hairpin RNA can be introduced into the cell by *A. rhizogenes* mediated hairy root transformation using a Gateway binary vector. Transgenic hairy roots can both nodulate and mycorrhizize if inoculated by a compatible symbiotic partner. However, a disadvantage of using the hairy root system in *Medicago* is that often the roots are chimeric and contain both transformed and untransformed roots. Also, as the transgenes are randomly inserted into the genome they are subject to position effects and can therefore vary greatly in their expression. Since generation of stably transformed lines is a time and resource intensive process however, hairy roots provide a quick alternative. The hairy root transformation system is also useful to studying gene function using overexpression. In this chapter I describe the isolation and characterization of *Tnt1* mutant lines and RNAi lines; and overexpression studies to study the role of the AMNs.

Genes with related functions are often expressed under the same conditions and in the same tissues. It follows from this that by determining what genes are co-regulated with our genes of interest we can derive information about their function. In addition, analyses of promoter motifs can provide critical information about transcription factors that regulate gene expression. I combined both approaches and identified regulatory genes which provide clues to the function of the AMNs. With the exception of *Coptis japonicus* CjMDR1 and CjMDR2 which are ABCB transporters involved in transport of an isoquinoline alkaloid berberine (Shitan et al., 2003; Shitan et al., 2013), all *Arabidopsis* full molecule ABCB transporters studied so far have been implicated in transport of auxin including AtABCB19 (Noh et al., 2001), AtABCB21 (Kamimoto et al., 2012) and AtABCB14 (Kaneda et al., 2011) and also a *Lotus japonicus* LjABCB1 (Takanashi et al., 2012). The AMNs which also belong to this sub-family are therefore putative auxin transporters. Presence of many AuxREs (Auxin responsive elements) upto 2 kb upstream of the translation start site of all three genes together with the observation that often the expression of ABC transporter genes can be substrate inducible implicated auxin as a possible substrate of the AMNs. In addition, several auxin signalling markers have expression patterns that closely resemble those of the AMNs including being expressed specifically in infected root hair cells (Breakspear et al., 2014). To address this hypothesis, I tested several potential substrates by applying candidate

chemicals to WT roots and performing qRT-PCR to determine if the *AMNs* were transcriptionally responsive.

Both nodulation and mycorrhization utilize a common set of core regulatory genes which control the outcome of both symbioses. These genes belong to the common symbiotic pathway as described in Chapter 1. With the availability of these mutants and other symbiotic mutants in *Medicago*, it is possible to query where the *AMNs* are positioned relative to other members in the pathway. I thus performed qPCR in various SYM pathway mutants infected by either microbe or treated with its elicitor and identified genes regulating the expression of the *AMNs* during symbiosis.

4.2 Results and Discussion

4.2.1 The intron-exon structure of *AMN1* and *AMN2* is conserved

The available sequence of *AMN1*, *AMN2*, and *AMN3* were confirmed by amplifying and sequencing their cDNA from mycorrhized roots of *Medicago truncatula* ecotype A17. I was unable to amplify the *AMN1* full length transcript from infected root tissue upon repeated attempts. Closer analysis of the gene arrangement around the predicted locus showed an orphan ORF encoding ABC membrane fragment (predicted as gene Medtr3g086420) ~1.5 Kb upstream of the predicted start of *AMN1* (Medtr3g086430). This gene fragment shared >80% homology to the first TMD of *AMN2*. I therefore used the gene prediction server GENSCAN (Burge & Karlin, 1997) using sequence upstream of Medtr3g086420 and included the entire *AMN1* downstream sequence (Medtr3g086430). The resultant gene provided a gene model for a full ABC-B transporter with homology to *AMN2* including in the first transmembrane domain. I designed primers for this predicted *AMN1* CDS using the now corrected model and was able to amplify and verify the sequence using RT PCR amplified product. Since the transcript is not highly abundant (as determined by qRT-PCR), it was necessary to use an antisense gene specific primer designed at the 3' UTR to prime cDNA synthesis using 3 µg total RNA. I could then amplify full length *AMN1* using this cDNA. The full length *AMN2* transcript on the other hand was readily amplified using as little as 1 µg of total RNA as template. Upon sequencing of the product, I found that the *AMN2* predicted gene model included an extra 33 bps at the 5' end of the third exon and predicted a false intron in the now 6th exon. *AMN1* and *AMN2* were thus, both mis-annotated and the corrected sequence is provided in Appendix 1.1 and Appendix 1.2. Based on this information,

AMN1 and *AMN2* were both predicted to be made up of six introns and seven exons. The *AMN3* CDS sequenced product was found to be identical to the 4.7 Kb CDS encoding *AMN3* predicted gene model. On average, eukaryotic genes contain approximately 3.7 introns per Kb of DNA (Deutsch & Long, 1999). Although some intronic sequences have been shown to exert a regulatory effect on the gene, the reason why introns are retained is not well understood. However intron-exon positions have been routinely used to derive evolutionary relations between genes, orthologous genes have been found to have more conserved intron positions than non-orthologous genes (Henricson, Forslund, & Sonnhhammer, 2010). Although the intron lengths vary the exon lengths between *AMN1* and *AMN2* are conserved suggesting that these genes have a common ancestor (Figure 4.1 A). *AMN1* and *AMN2* encode two ABC transporters of 137.06 kDa and 137.72 kDa while *AMN3* encodes a 163.60 kDa protein.

4.2.2 Two mutant alleles each of *AMN1* and *AMN3* and one for *AMN2* were identified

Two *Tnt1* insertion mutant lines each representing different alleles for all three *AMNs* were obtained from the Samuel Roberts Noble foundation: *amn1-1* (NF5606), *amn1-2* (NF17134), *amn2-1* (NF9733), *amn3-1* (NF18154) and *amn3-2* (NF8444). The identified insertions were at positions 2291 bps, 4616 bps, 1548 bps, 361 bps, 408 bps away from the ATG start site of their respective genes. The inserted *Tnt1* transposon sequence introduces a series of missense mutations and followed by a stop codon in the transcript of the gene it is inserted in. The resultant hybrid transcript introduces a premature stop during translation thereby forming truncated non-functional proteins. Heterozygous or homozygous plants were identified from these lines for each allele except for one *AMN2* line (Figure 4.1 A). Heterozygous plants were allowed to self-fertilize and a homozygous plant was selected from this progeny before further experiments were carried out. All identified insertions were in exons and no gross morphological changes could be seen in the mutants (Figure 4.1 C). However, qPCR data consistently showed a two-to-ten times higher expression of *AMN1* in the mutant background relative to WT upon mycorrhization (supplementary). I therefore decided to use RT-PCR to try and amplify the full length gene using RNA samples from mycorrhized roots since the *AMNs* are hardly detected in uninfected root tissue. *UBIQUITIN* was used as a positive control and it amplified from all samples. Oligo-dT primed cDNA was sufficient to amplify full

length *AMN2* transcript from the wild type samples but not from the mutant *amn2-1* (NF9733). This could happen if the entire 5.2 Kb *Tnt1* retrotransposon was transcribed while integrated within the gene of interest. This was confirmed by using a *Tnt1* specific forward primer and the gene specific reverse primer and was also able to amplify the hybrid transcript in the mutants but understandably never from wild type control plants. In case of *amn1-2* (NF17134) and *amn3-1* (NF18154), I had to increase the starting amount of RNA and use antisense gene specific primers to prime cDNA synthesis. Again, I was able to confirm the presence of the hybrid transcript in the mutants but not the full length WT transcripts conclusively ascertaining that the *M. truncatula* lines were mutants (Figure 4.2 B). qPCR detection of the incorrect hybrid transcripts thus could imply a regulatory feedback mechanism used by the plant to create a functional AMN transporter when challenged by microbes.

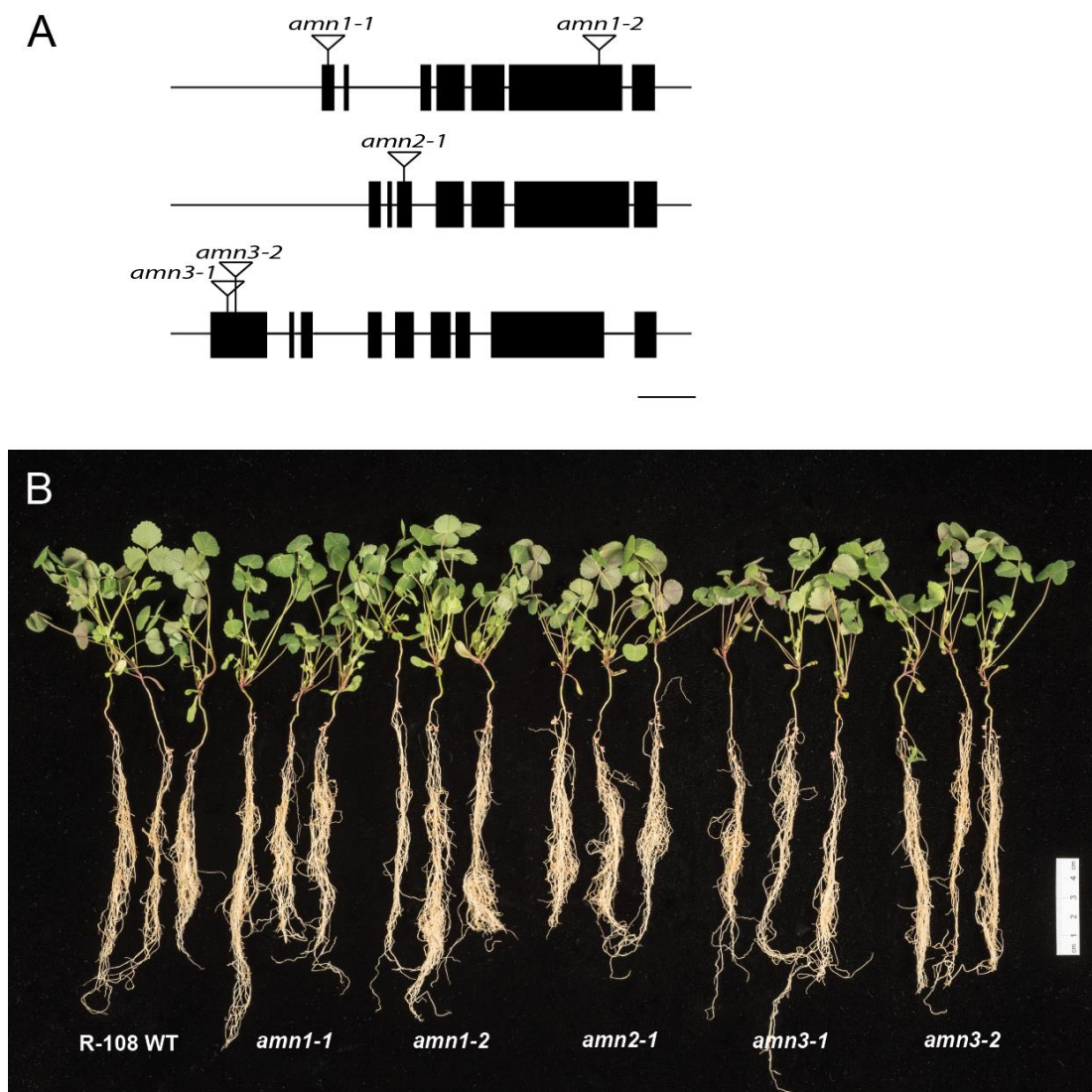


Figure 4. 1: Identification of *amn1*, *amn2*, and *amn3* mutant alleles of *M. truncatula*

A. Gene structure diagram of *AMN1*, *AMN2*, and *AMN3* showing positions of the *Tnt1* inserts in exon one (*amn1-1*) and exon six (*amn1-2*) of *AMN1* and a single allele for *AMN2* in exon three (*amn2-1*) and two alleles for *AMN3* both in exon 1 (*amn3-1*, *amn3-2*). Alleles are numbered according to their position in the gene. Note also a similar exon intron arrangement for *AMN1* and *AMN2*, each with seven exons and six introns. **C.** Backcrossed *M. truncatula* R-108 mutant lines for *amn1*, *amn2*, and *amn3* alleles show no obvious morphological phenotypic abnormalities three weeks after infection with *S. melliloti* 1021 compared to the wild type.

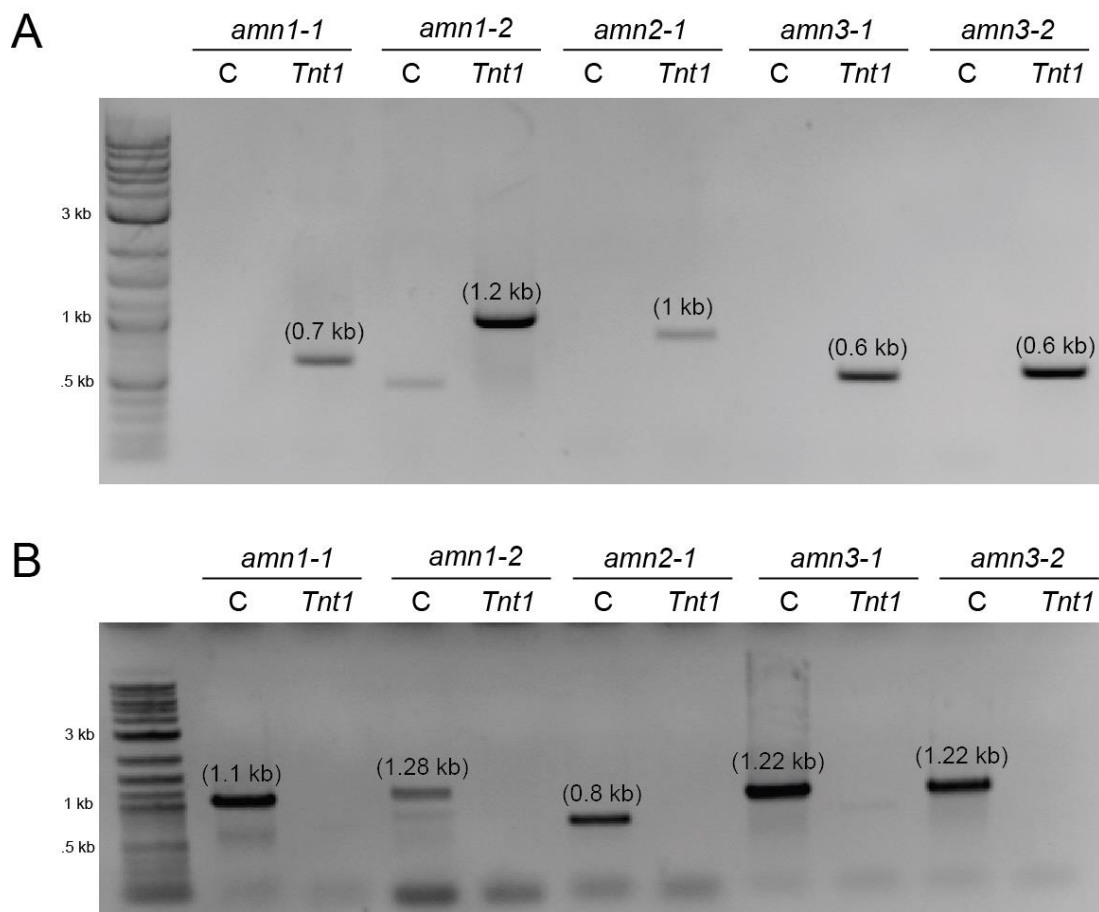


Figure 4.2: DNA Polymerase Chain Reaction confirmation of *Tnt1* insertion mutant lines

A. Gel image confirming presence of *tnt1* insertions at predicted sites. Bands represent PCR amplified products with a forward or reverse *tnt1* primer combined with a gene specific primer using DNA extracted from mutant lines. *amn1-1* (P₃₂ and P₂) *amn1-2* (P₃₃ and P₄) *amn2-1* (P₃₂ and P₈) *amn3-1* and *amn3-2* (P₃₂ and P₁₄) Faint band in lane 3 control is a non-specific product. B. Gel image confirming absence of WT gene sequence in mutant lines. Bands represent PCR amplified products with gene specific primers. *amn1-1* (P₁ and P₂) *amn1-2* (P₄₀ and P₄) *amn2-1* (P₇ and P₈) *amn3-1* and *amn3-2* (P₁₃ and P₁₄)

C: Control. Expected sizes are indicated on top of the bands. Lane 1 represents a 1 kb DNA marker.

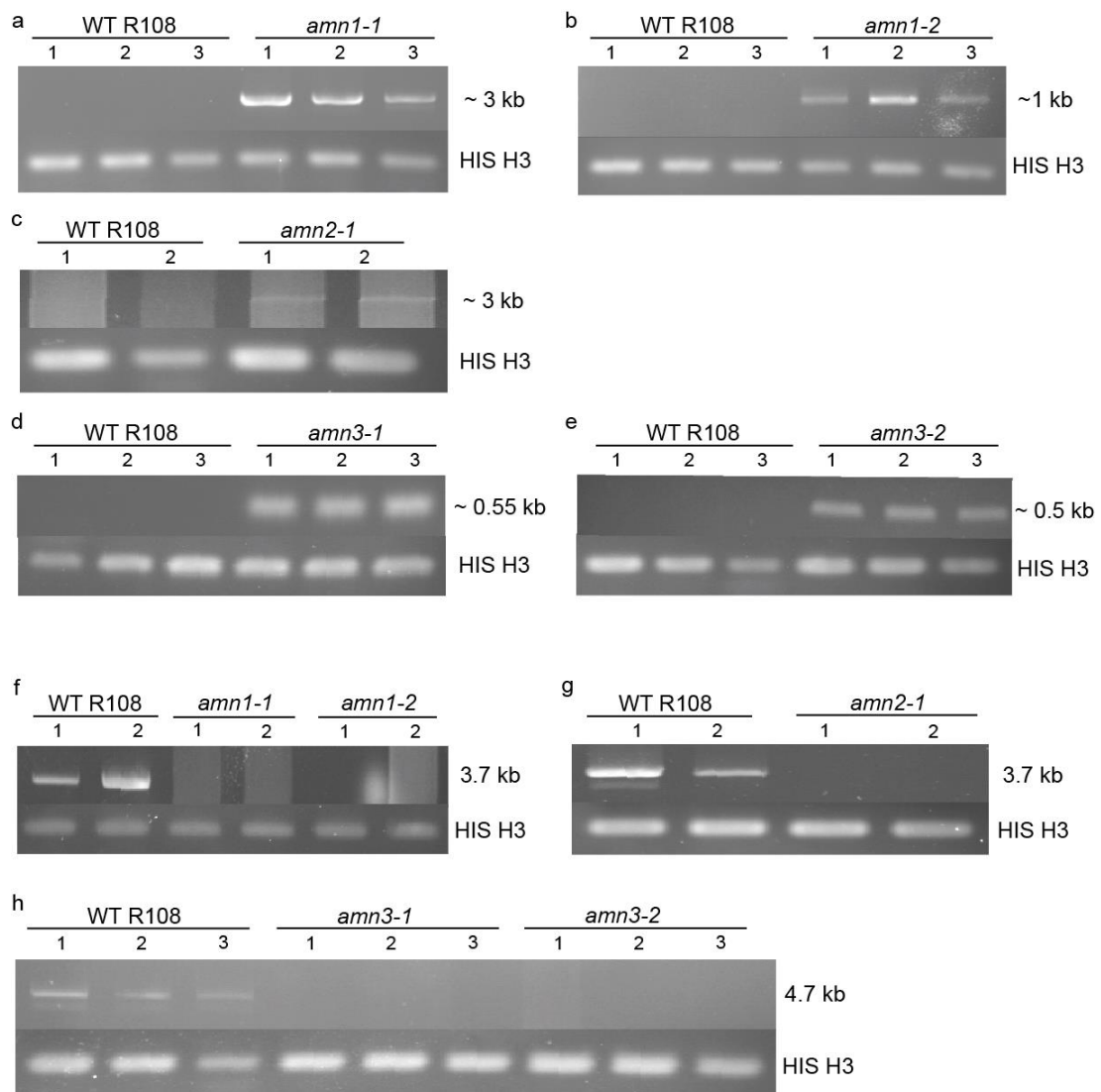


Figure 4.3: Semi quantitative RT-PCR confirmation of *Tnt1* insertion mutant lines

(a,b,c,d,e). Gel image confirming presence of *tnt1* insertions at predicted sites. Bands represent PCR amplified products using cDNA generated from RNA extracted using mutant lines with a forward or reverse *tnt1* primer combined with a gene specific primer. *amn1-1* (P_32 and P_4) *amn1-2* (P_33 and P_4) *amn2-1* (P_32 and P_10) *amn3-1* and *amn3-2* (P_32 and P_14) (f,g,h). Gel image confirming absence of WT full-length transcript in mutant lines. Bands represent PCR amplified products with gene specific primers on cDNA generated using RNA extracted from mutant lines. *AMN1* (P_3 and P_4) *AMN2* (P_9 and P_10) *AMN3* (P_15 and P_16) Expected sizes are indicated on the right. *Histone H3* (P_41 and P_42) amplifies from all samples as shown, validating the quality of the cDNA was comparable.

4.2.3 Single mutants of *AMN1*, *AMN2* and *AMN3* are unaffected in their ability to form symbiotic associations with both rhizobia and arbuscular mycorrhizae

Tnt1 lines typically contain many background insertion events which can complicate phenotypic analyses. All mutants were thus backcrossed to the parental WT R-108 lines with the exception of *amn2-1* and homozygotes identified prior to further characterization. Nodulation was tested at 3 wpi with *S. meliloti* strain Sm1021 (Figure 4.2 A). There was also no experimentally reproducible difference consistent across alleles for any mutant in the number of nitrogen fixing 'pink' nodules and developing uninfected 'white' nodules compared to WT. Nodules also showed no gross morphological differences. Colonization was then tested with *Rhizophagus irregularis* 5 weeks post inoculation in the mutants. No differences in total colonization percentage consistent between alleles were observed for the single mutants (Figure 4.2 B). There were no obvious changes in arbuscule structures which filled up the entire cell as in the WT.

When the ratio of pink/white nodules was calculated for the same experiment, using a Student's t-test I found that there was a statistically significant decrease in *amn2-1* (1.83), *amn3-1* (1.50) and *amn3-2* (1.43) compared to WT R108 (4.14) but not in *amn1-1* (3.91) and *amn1-2* (3.78) mutant alleles (Supplementary Figure 5.6). Numbers in brackets represent average of the ratios calculated. Using a paired t-test I found the p values were equal to 0.02, 0.009, 0.008 for *amn2-1* and *amn3-1* and *amn3-2* respectively when compared to the WT plants. Plants in which the denominator (white nodules) was 0 were not included in the calculation; these findings should therefore be considered cautiously. The reduction in this ratio could indicate that the nodules which do develop on mutant alleles of *AMN2* and *AMN3* have a slight delay in commencement of nitrogen fixation given that the pink colour indicates nitrogen fixing nodules. Possibly, absence of the AMNs might impede the passage of the bacteria through the infection thread, delaying nitrogen fixation.

The absence of an obvious defect in nodule number in the single mutants could be explained by genetic redundancy amongst the *AMNs*. I thus proceeded to cross the single mutants with each other in multiple allelic combinations. Since we might expect *AMN3* also to contribute to the flux of the transported substrate or a close chemical relative, I also generated double and triple crosses with *amn3* alleles. However, it takes 5 months from germination to seed harvest in *M. truncatula*;

therefore it takes approximately 12-14 months from the time of making the cross before one obtains sufficient seed from homozygous double mutants for phenotype testing. I therefore decided to use RNA interference technology to knockdown both *AMN1* and *AMN2* to simulate a double mutant in transgenic hairy roots. IN addition, I tested the RNAi construct in the *amn3* mutant background to simulate a triple mutant.

4.2.4 RNAi knockdown of *AMN1* and *AMN2* has a negative effect on nodule number and mycorrhizal percentage colonization

Considering the large size of the ABC transporter family, off target silencing is a potential problem when using RNA interference technology. To circumvent this possibility I identified a probe for the RNAi from the *AMN1* sequence extending over 128 bps complementary to a highly conserved region of the first transmembrane domain that is common between *AMN1* and *AMN2*. It was essential to avoid the nucleotide binding domain which is highly conserved across all sub-families. A discontinuous mega BLAST, which is sensitive to alignments with a low degree of identity, of the probe sequence against the *Medicago* genome retrieved only the corresponding homologous region of the *AMN2* gene, supporting its specificity. The symbiotic phenotypes were then used in *AMN1/AMN2* RNAi knockdown roots. The number of nodules 3 wpi were reduced by 50% in transgenic hairy roots expressing this RNAi construct, compared to the empty vector controls. Nodules in RNAi lines appeared to be small and triangular in shape but they appeared to be infected normally (Appendix 1.6). This phenotype for the double knockdown was observed in two independent experiments but could not be reproduced in the third trial. To simulate a triple mutant the same RNAi construct was used in *amn3-1* and *amn3-2*. The *AMN1/AMN2* knockdown in the *amn3-2* mutants did not have a further additive effect on the observed reduction in total nodule number (Figure 4.3 A).

The same strategy was then used to evaluate mycorrhization. The total percentage colonization was noted to be reduced by ~18% five weeks post colonization by *R. irregularis* (Figure 4.3 B). Fewer arbuscules were noted in the roots expressing the RNAi construct although they developed normally once they initiated in a cortical cell (Appendix 1.6). This phenotype was only observed in one experimental trial. Similar to the nodulation experiment, knockdown of *AMN1* and *AMN2* in the *amn3-2* background did not further enhance the phenotype suggesting that *AMN3* is not involved in the same function as *AMN1* and *AMN2*.

Mycorrhized root samples from four independent transgenic RNAi knockdown roots were tested by qPCR to determine the efficiency of knockdown using the described construct. Since the construct was designed to be specific for *AMN1* and *AMN2*, gene expression of *AMN3* was checked as a negative control. In all four lines, relative expression of *AMN1* and *AMN2* was lower than in empty vector controls even when the percentage colonization was approximately equal (EV-2 and KD-3) confirming the efficiency of the knockdown (Figure 4.4 A). However, expression of *AMN3* was also lower in the RNAi lines as compared to the controls. One reason could be that off-target silencing caused by the RNAi construct might be knocking down *AMN3*. Alternatively, the observed decrease in *AMN3* expression in RNAi lines could be a reflection of lower percentage colonization of those lines.

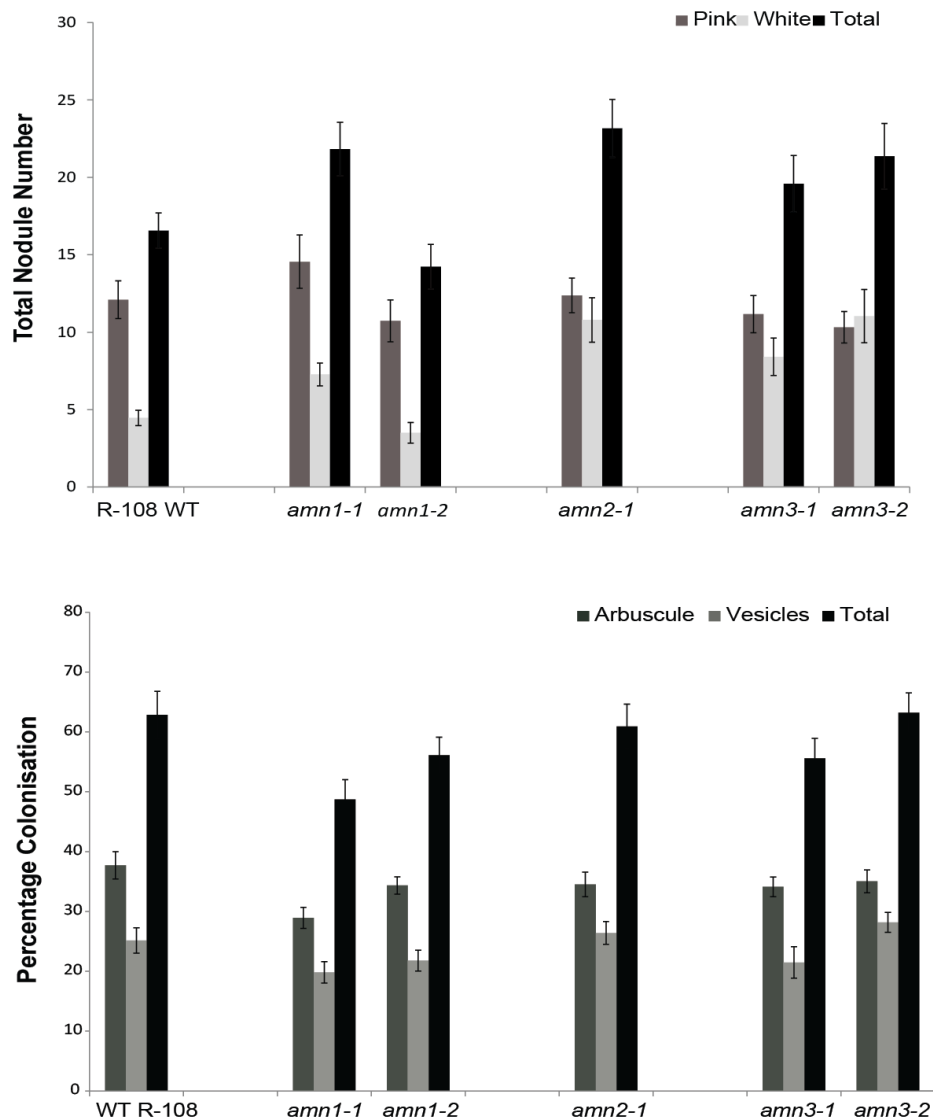


Figure 4.4: Symbiotic phenotypes of single mutant alleles of *AMN1*, *AMN2*, and *AMN3*

A. No statistically significant difference in total nodule number that was consistent between mutant alleles could be observed 3 weeks post infection (wpi) with *S. meliloti* 1021 using Student's t-test. Values represent average of the mean. 24-30 plants per line were scored. Error bars depict Standard error of the mean (S.E). Number of pink, nitrogen fixing nodules and white, uninfected nodules was also comparable between all lines tested. A statistically significant difference in ratios of pink/ white nodules is discussed in section 4.2.2 **B.** WT and *AMN* mutant alleles are normally colonized by the fungal symbiont *R. irregularis* four weeks post inoculation. No difference in total arbuscule number was recorded. 23-25 plants were scored for each line. A Student's t-test was performed for either experiment. Values represent average percentage colonization. Error bars depict standard error of the mean (S.E).

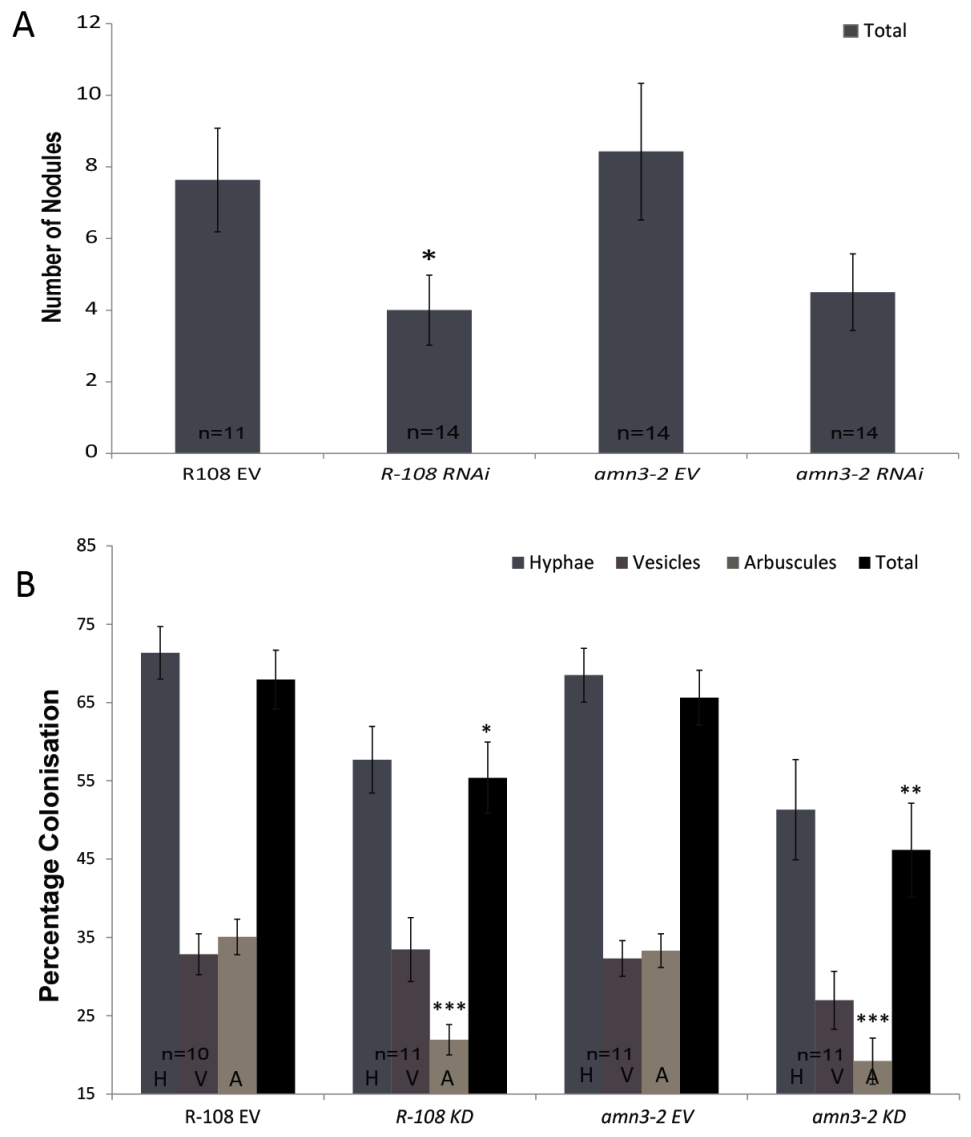


Figure 4.5: Double knockdown of *AMN1* and *AMN2* negatively affects both rhizobial and mycorrhizal associations

A. Average number of nodules is decreased by ~50% in *AMN1*-antisense lines three wpi with Sm 1021. This phenotype is not further enhanced in the *amn3-2* mutant allele. Number of plants (n) is indicated at the base of each bar. **B.** Percentage colonization of *M. truncatula* RNAi lines by *Rhizophagus irregularis* five wpi is lower than empty vector controls. Arbuscule development is further affected in these lines. Number of plants varied between 10 to 11 for each line.

H: Hyphae V: Vesicle A: Arbuscule. Error bars denote standard error of the mean (S.E). A Student's t-test was used to determine statistical significance of the differences. Asterisks denote * $p < 0.05$, ** $p < 0.01$, *** $p < 0.001$

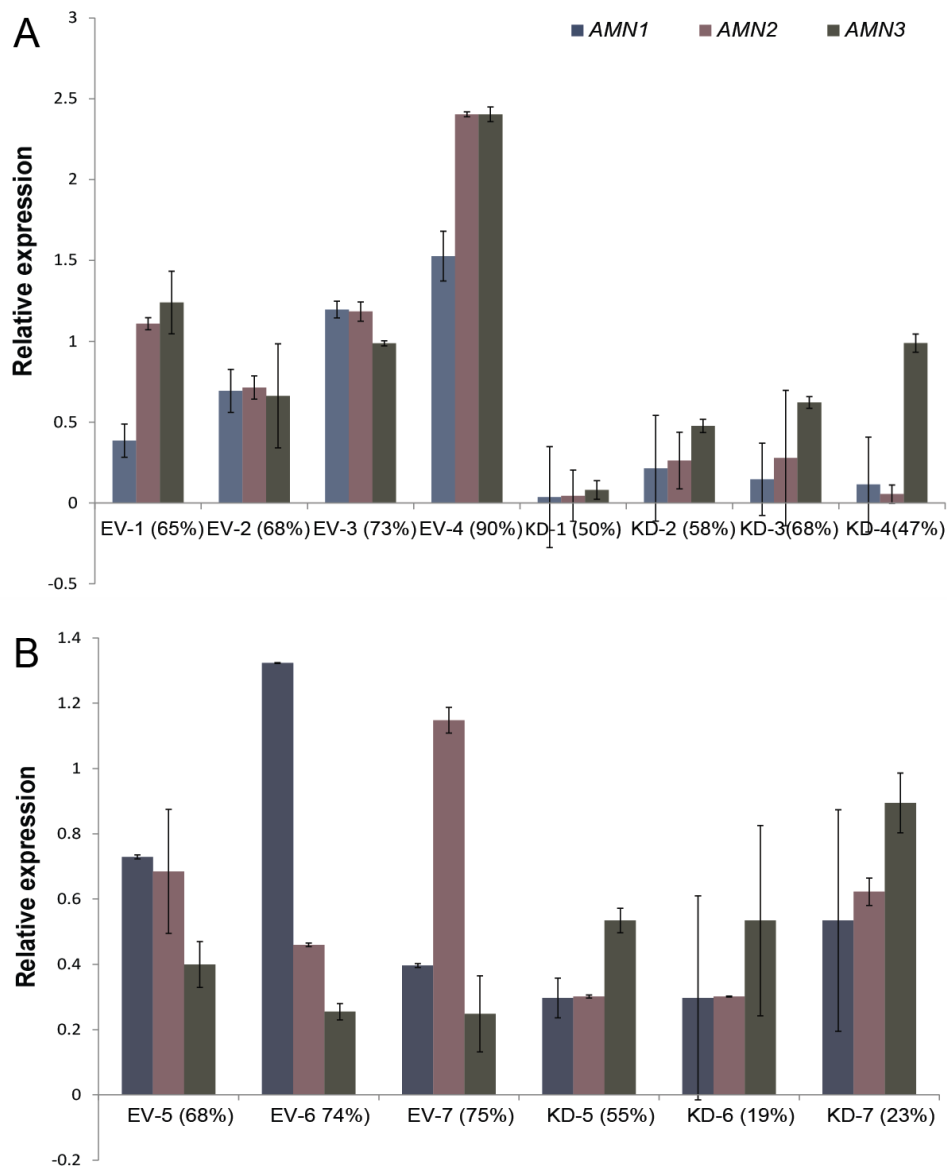


Figure 4.6: Relative expression of *AMN1*, *AMN2*, and *AMN3* in RNAi expressing lines

A. quantitative RT-PCR values comparing Empty vector (EV 1-4) and Knockdown RNAi (KD 1-4) expressing lines in *M. truncatula* A17. Wild type shows reduced expression of *AMN1* and *AMN2* in knockdown lines. Expression of *AMN3* is also reduced. **B.** Expression of the RNAi antisense construct in *amn3-2* background (KD 5-7) replicates the reduction in *AMN1*, *AMN2* transcript levels seen in A. Error bars denote standard error between technical replicates.

Primers used in the experiment *AMN1* (P_5 and P_6), *AMN2* (P_11 and P_12), *AMN3* (P_17 and P_18), *Tip41* (P_43 and P_44), *Ubiquitin* (P_45 and P_46). Values represent average of three technical replicates. Error bars depict standard error of mean (S.E).

The effects of *AMN1*, *AMN2* knockdown in the *amn3-2* mutant background were also monitored by qPCR (Figure 4.4 B). Mycorrhized root tissue from three independent root samples each from empty vector control and RNAi expressing transgenics in the *amn3-2 tnt1* mutant background were tested for relative expression of the three *AMNs*. As seen in the WT background, the RNAi construct did indeed reduce the expression of *AMN1* and *AMN2*. *AMN3* expression in the *amn3-2* mutant background did not correlate with colonization percentage. Since the entire *AMN3* transcript containing the *Tnt1* insert is transcribed (Section 4.2.1), we can expect to detect the transcript by qPCR even in the mutant background.

4.2.5 Double mutants of *AMN1* and *AMN2* do not show any change in nodule number and mycorrhizal colonization

Six allelic double mutants were generated and so far one combination representing *amn1 amn2*, *amn1 amn3* and *amn2 amn3* for defects in mycorrhizal associations. Mutations segregated in a mendelian fashion with two exceptions wherein I had to increase the sample size to find a double mutant (Table 4.1). No growth defects or other non-symbiotic phenotypes were seen in any of the mutant combinations. I did not have enough seeds to phenotype *amn2 amn3* for nodulation yet. Allelic combinations *amn1-1 amn2-1*, *amn1-2 amn2-1* and *amn1-1 amn3-1* had nodule numbers comparable to WT (Figure 4.5 A, C). Nodules were also morphologically indistinguishable from WT.

Many mycorrhizal mutant phenotypes can be overcome with application of high inoculum concentrations. Therefore I used a weaker *R. irregularis* inoculum (5% v/v compared with the normal 25% v/v) and allowed the plants to grow till WT plants were ~20% colonized. No difference in total percentage colonization could be observed for all mutants and arbuscules developed normally (Figure 4.5 B, D). In *amn2 amn3* however, there was a decrease in frequency of vesicles. To confirm this phenotype, the second allelic combination will be tested for consistency.

F1 seeds for the *amn1-1 amn2-1 amn3-2* triple mutants are awaited presently and will be screened for homozygotes before a phenotype is tested.

	Gene 1 (Homozygous)	Gene2 (Homozygous)	Double Homozygous plants	Total	Ratio
<i>amn1-1</i> xWT R-108			4	19	4.75:1
<i>amn1-2</i> xWT R-108			3	24	8:1
<i>amn3-1</i> xWT R-108			5	49	9.8:1
<i>amn3-2</i> xWT R-108			9	28	3.11:1
<i>amn1-1</i> x <i>amn3-1</i>	10	9	3	46	15.33:1
<i>amn1-1</i> x <i>amn3-2</i>	12	6	2	34	17:1
<i>amn1-1</i> x <i>amn2-1</i>	38	38	4	165	41.25:1
<i>amn1-2</i> x <i>amn2-1</i>	6	5	1	44	44:1
<i>amn1-2</i> BCx <i>amn2-1</i>	16	27	4	72	18:1
<i>amn2-1</i> x <i>amn3-1</i>	36	39	8	141	17.63:1
<i>amn2-1</i> x <i>amn3-2</i>	24	15	4	71	17.75:1
<i>lax2-1</i> xDR5-GUS	8	Taken forward to next generation	-	44	
<i>iaa8-1</i> xDR5-GUS	5	Taken forward to next generation	-	24	

Table 4.1: Genotypic ratios of the crosses tested and described in this thesis.

BC stands for backcrossed line

4.2.6 Constitutive root hair expression of *AMN2* blocks cortical penetration of Infection threads

Overexpression of ABC transporters can confer phenotypes associated with the endogenous function of the gene *in planta* (Kuromori et al., 2010). Overexpression of a transporter may provide a phenotype if the substrate is already present in the cell. For instance it could promote excess secretion and possibly overproduction of the substrate through positive feedback on the biosynthetic pathway. I hypothesized that constitutive expression of the *AMNs* in all root hairs might affect rhizobial infection frequency or structure through excess secretion. To test this hypothesis I expressed *AMN2* from the *M. truncatula* *Expansin A7* (*pExpA7:AMN2*) promoter shown previously in the lab to be expressed in a constitutive fashion in the epidermis including root hairs. Three weeks after infection with Sm1021 transgenic plants were scored for nodule number and changes in morphology of the infection threads were investigated.

Total nodule number in *pExpA7-AMN2* transgenic roots was not changed compared to those transformed with the empty vector. However, there was a statistically significant increase in the number of white, uninfected nodules in hairy roots overexpressing the *AMN2* transporter (Figure 4.6 A). On an average, only 1.5 nodules were uninfected in the EV vector control roots in contrast to approximately 5 in *pExpA7-AMN2* transgenic roots and this appeared to be due to an increase in total nodule number in the overexpression roots, although this increase was not significant ($p=0.037$). In addition, infection threads in the overexpressed roots initiated and developed normally like in the WT until they reached the cortex. At a stage when the infection threads in the WT were ramifying into underlying nodule primordia (Figure 4.6 B-E), infection threads showed irregular, distorted tips which seemed to have difficulty penetrating into the cortex.

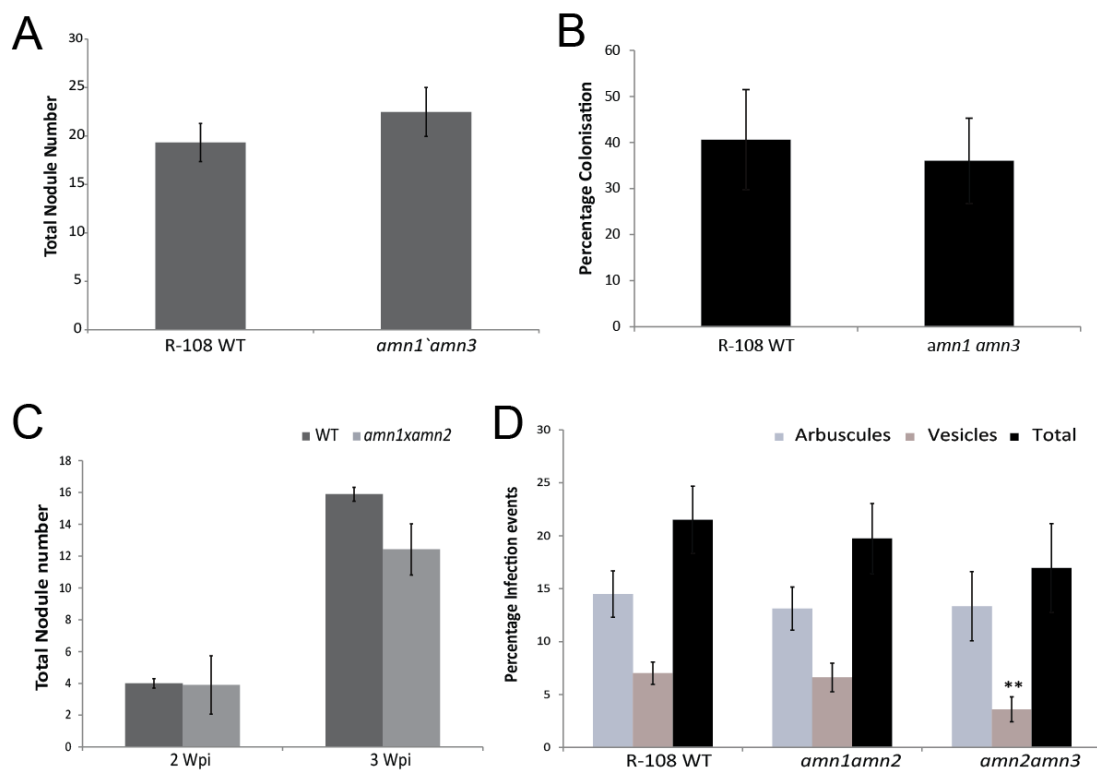


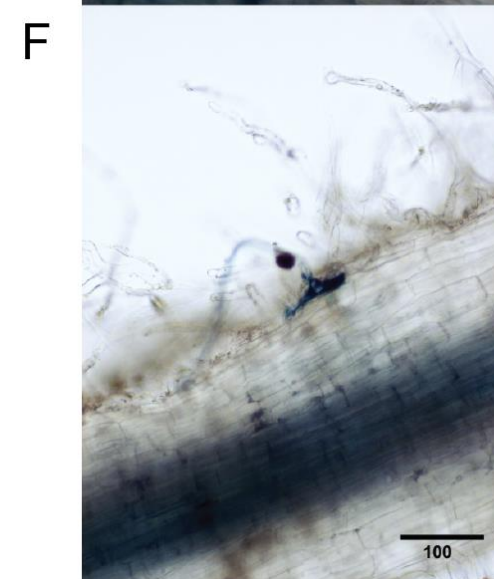
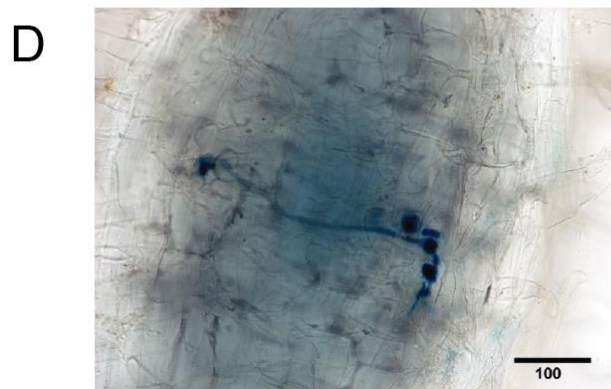
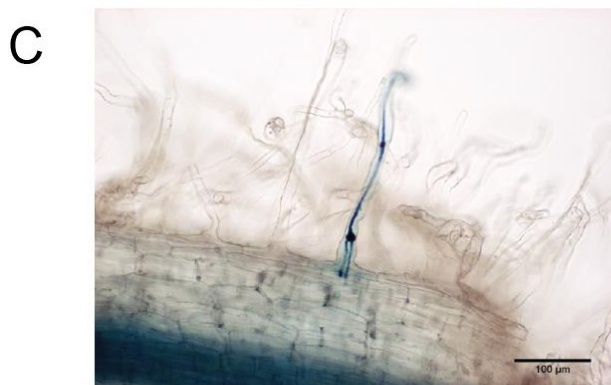
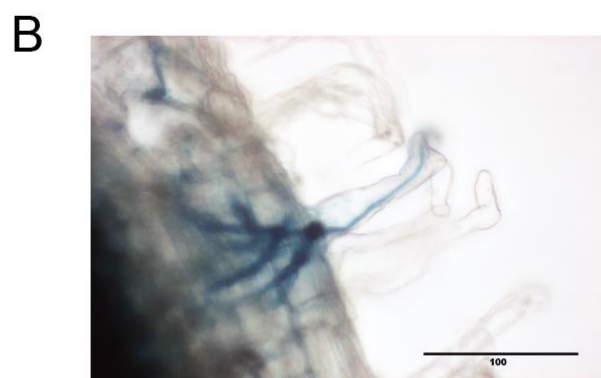
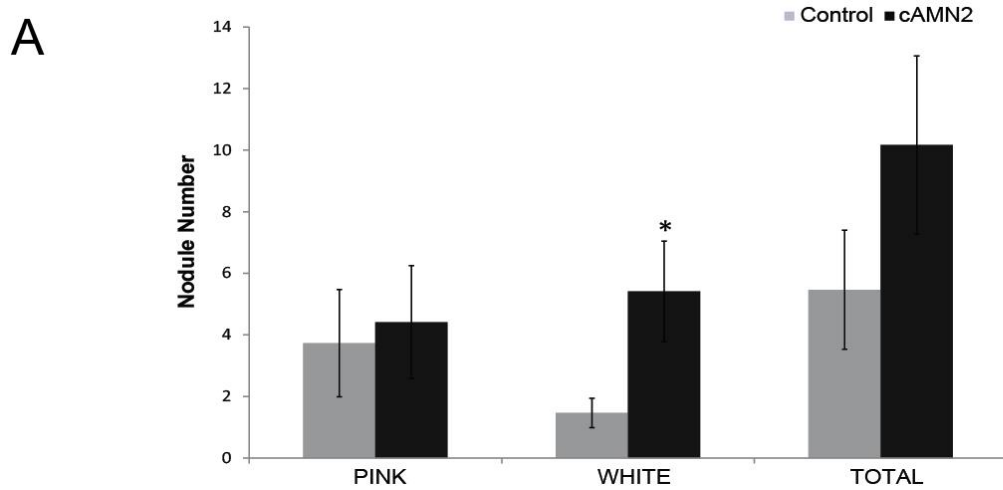
Figure 4.7: Symbiotic phenotypes of *AMN* double mutant combinations

No change in average nodule number **A.** or average mycorrhizal percentage colonization **B.** in *amn1 amn3* double mutants (n=23) **C.** Number of nodules is comparable to WT at 2 wpi and 3 wpi in *amn1 amn2* double mutants (n=25) **D.** Total percentage colonization upon inoculation with *R. irregularis* is the same in *amn2 amn3* and *amn1 amn2*. Vesicle frequency is lower than WT in *amn2 amn3* (n=15 for each). A Student's t-test was used to test statistical significance. Asterisks denote ** $p < 0.01$ Error bars denote standard error of mean.

Figure 4.8: *Expansin A7* driven constitutive expression of *AMN2* affects nodule number and Infection thread structure.

A. No difference in total nodule number of *M. truncatula* A17 WT transgenic roots containing the empty vector construct or expressing *pExpA7::AMN2*. Values represent average of N=15 and N=11 for Control and *AMN2* overexpressing lines respectively. A Student's t-test was used to determine statistical significance. Asterisks denote * $p < 0.05$. Error bars denote standard error of mean. **B,C.** Infection threads in control EV expressing lines branch normally and ramify into the cortex. The tip of the thread is not affected once it reaches the cortex (E,F) **D-F** ITs do not colonize underlying nodules (E) Aberrant tip structures are visible as the infection thread reaches the root cortex. *S. meliloti* 1021 (pXLGD4 expressing *HemA::LacZ*) stained in blue.

Scale bars denote 100 μm .



These phenotypes of failed epidermal-cortical progression of ITs and uninfected nodules may point towards a primary defect in IT formation in the outer cortex. This result could be explained if the transported substrate is either a negative regulator of infection thread development or a positive regulator which negatively affects structural development of IT growth at high concentrations. This experiment was only carried out once and therefore needs to be repeated. The effect of *AMN1* overexpression could be tested in a similar manner to provide a separate line of evidence.

4.2.7 *AMN1*, *AMN2*, and *AMN3* co-regulation analyses

As described above, these genes are all induced in rhizobial and mycorrhizal infected tissues, and an initial analysis showed that the expression profiles of *AMN1*, *AMN2*, and *AMN3* are highly correlated across symbiotic treatments raising the possibility that they may transport the same or related substrates. I theorized that the metabolic pathway associated with biosynthesis of the substrate for AMNs may be transcriptionally co-regulated with these genes. To test this hypothesis, I retrieved probesets 70% correlated with *AMN1*, *AMN2*, and *AMN3* across rhizobial and mycorrhizal experimental treatments from the MtGEA. A list of genes co-regulated with probeset IDs co-regulated with the AMNs is presented in Table 4.1. Of the 23 genes co-regulated with the *AMNs*, eight encode enzymes involved in different metabolic reactions (Table 4.1 – V.). Of these, two genes were previously studied to be symbiosis related. The *DXS2* gene is a chloroplast localized enzyme which catabolizes the first rate limiting step in the methylethritol-4-phosphate (MEP) pathway for biosynthesis of isoprenoids. Previously shown to be mycorrhiza induced, this gene is expressed only in arbuscule containing cells (Floss et al., 2008). It is absent from *Arabidopsis*, further supporting its role as a symbiosis specific gene. Knockdown of *DXS2* by RNAi results in reduced levels of C27 apocarotenoids in mycorrhized roots such as mycorradicin and a higher proportion of degenerating arbuscules were seen. Interestingly, a recent report has revealed a role for apocarotenoids in soybean nodulation and data from our group shows expression of *DXS2* in root hairs of *M. truncatula* seedlings infected with *S. meliloti* 1021 (Kim et al., 2013). If *DXS2* is required for the biosynthesis of AMN substrates, it would suggest they are transporting an apocarotenoids with a role in both symbioses. In addition, a second gene involved in *DWARF27* was also co-regulated (Table 4.1 - V).

Another co-regulated gene of noteworthy mention is the chalcone-o-methyltransferase which is required for methylation of isoliquiritigenin to form a Nod-factor inducing flavonoid, 4,4'-dihydroxy-2'-methoxychalcone (Maxwell, Harrison, & Dixon, 1993). Isoliquiritigenin also acts as a precursor to another Nod gene inducing flavonoid called liquiritigenin (Jez, Bowman, & Noel, 2002). Liquiritigenin in turn can be converted to another Nod gene inducing flavone, dihydroxyflavone (J. Zhang, Subramanian, Stacey, & Yu, 2009). A role for flavonoids is well established in a symbiotic context and both rhizobia and mycorrhizae sense these chemoattractants and initiate a dialogue with the host plant. Infection by rhizobia is known to cause massive changes in phenylpropanoid pathway derivatives (Breakspear et al., 2014) including *PAL* (*PHENYLAMMONIA LYASE*) which catalyses the first committed step in this pathway and *CHS* (*CHALCONE SYNTHASE*) and these very same genes are also expressed in arbuscule containing cortical cells (Harrison Dixon 2003). It is also worth mentioning here that the *Medicago BLUE COPPER PROTEIN1* (*MtBCP1*) previously shown to localize to the plasma membrane around the trunk of the arbuscule and around the hyphae was also co-regulated with the *AMNs*.

	PROBESET ID	GENE DESCRIPTION	REMARKS
I.	UNKNOWN PROTEINS		
1	Mtr.11271.1.S1_at	PREDICTED: Cicer arietinum uncharacterized LOC101497077 (LOC101497077), mRNA	
2	Mtr.25607.1.S1_s_at	Cysteine rich protein of unknown function	
3	Mtr.43814.1.S1_s_at	<i>Medicago truncatula</i> hypothetical protein (MTR_5g075400) mRNA, complete cds	
II.	ELECTRON CHAIN		
4	Mtr.14172.1.S1_at	<i>Medicago truncatula</i> Cytochrome P450 (MTR_7g092620) mRNA, complete cds	
5	Mtr.15627.1.S1_s_at	<i>Medicago truncatula</i> Blue copper protein (MTR_7g086190) mRNA, complete cds	Blue copper protein (MtBcp1b)
6	Mtr.31863.1.S1_at		Cytochrome b
7	Mtr.51106.1.S1_at	<i>Medicago truncatula</i> Blue copper protein (MTR_7g086100) mRNA, complete cds	Blue copper protein
III.	LECTIN RELATED		
8	Mtr.45646.1.S1_at	<i>Medicago truncatula</i> Lectin receptor-like kinase Tg-20 (MTR_8g068050) mRNA, complete cds	

9	Mtr.7279.1.S1_s_at	<i>Medicago truncatula</i> Lectin receptor-like kinase Tg-20 (MTR_8g068050) mRNA, complete cds	
10	Mtr.37152.1.S1_at	<i>Medicago truncatula</i> lectin-like (Lec10) pseudogene mRNA, complete sequence	
11	Mtr.35524.1.S1_at	<i>Medicago truncatula</i> Subtilisin-like protease (MTR_4g053780) mRNA, complete cds	
12	Mtr.40286.1.S1_at	<i>Medicago truncatula</i> Serine carboxypeptidase II-3 (MTR_3g079570) mRNA, complete cds	
IV. TRANSPORT			
13	Mtr.24353.1.S1_at	PREDICTED: <i>Cicer arietinum</i> SPX domain-containing protein 2-like	Vacuolar transporter chaperone 4
14	Mtr.33871.1.S1_at	PREDICTED: <i>Cicer arietinum</i> peptide transporter PTR1-like	Peptide transport-like protein - <i>Arabidopsis thaliana</i>
V. ENZYMES			
15	Mtr.18066.1.S1_s_at	<i>Medicago truncatula</i> O-methyltransferase (MTR_3g021440) mRNA, complete cds	Chalcone-O-methyltransferase
16	Mtr.31229.1.S1_at	<i>Medicago truncatula</i> Dehydrogenase/reductase SDR family member (MTR_4g097510) mRNA, complete cds	
17	Mtr.49672.1.S1_s_at	<i>Medicago truncatula</i> Anthocyanidin 3-O-glucosyltransferase (MTR_7g070860) mRNA	Flavonol 3-O-glucosyltransferase
18	Mtr.43585.1.S1_at	<i>Medicago truncatula</i> mRNA for 1-deoxy-D-xylulose 5-phosphate synthase 2	DXS2 gene
19	Mtr.37912.1.S1_at	PREDICTED: <i>Cicer arietinum</i> NADP-dependent alkenal double bond reductase P1-like	Allyl alcohol dehydrogenase
20	Mtr.38546.1.S1_at	PREDICTED: <i>Cicer arietinum</i> UDP-arabinopyranose mutase 3-like	xylan glucuronosyltransferases
21	Mtr.4797.1.S1_s_at	PREDICTED: <i>Cicer arietinum</i> beta-carotene isomerase D27, chloroplastic-like (LOC101489176), mRNA	Carotenoid biosynthesis
22	Mtr.11343.1.S1_at	PREDICTED: <i>Cicer arietinum</i> beta-carotene isomerase D27, chloroplastic-like (LOC101489176), mRNA	
VI. RECEPTOR			
23	Mtr.35414.1.S1_at	PREDICTED: <i>Cicer arietinum</i> probable inactive receptor kinase At2g26730-like	Receptor-like kinase

Table 4.2: List of genes co-regulated with *AMN1*, *AMN2*, and *AMN3*

4.2.8 Promoter analyses of 2kb upstream region of the *AMNs* reveals putative hormone regulatory sites

I identified *cis* regulatory elements controlling the coordinated expression of the three *AMN* genes using the MatInspector software and shortlisted the shared regulatory elements (Cartharius et al., 2005). As would be expected of symbiosis related genes, regulatory elements included the Nodulin consensus 1 and 2 found in promoters of leghaemoglobin genes (Ramlov, Laursen, Stougaard, & Marcker, 1993). MYB and NAC transcription factor binding sites with a role in secondary wall development and sugar responsive motifs were also present among a total of 40 common regulatory elements in the promoters of *AMN1*, *AMN2*, and *AMN3*. However, the most interesting group of regulatory elements included the hormone related transcription factor binding sites.

In the *AMNs* an incomplete TGTCT auxin responsive element (AuxRE) sequence could be found but studies show that the last base pair is not strictly required for recognition by ARFs (Ulmasov et al., 1999). This finding is interesting for two reasons. Firstly, a suite of auxin signalling genes, which include *MtIAA8*, *MtIAA9*, *MtARF16* and *MtGH3.1* are all specifically induced in infected root hair cells similar to the *AMNs* and loss of ARF16a reduces rhizobial infection (Murray group, unpublished). Secondly, ABCBs including AtABCB1, and AtABCB19 have been shown to efflux auxin in *Arabidopsis* (Geisler et al., 2005; Noh et al., 2001). Although, classification into a sub-family is not criteria alone for assignment of a substrate, presence of AuxREs may suggest a regulatory role for auxin in control of the three *AMNs*.

Perfect TAACAAA consensus sequence (GAMYB) found in promoters of some gibberellic acid (GA) responsive genes were found within 2kb upstream sequence of the start codon.

The last three hormones which had conserved regulatory elements in the promoter of the *AMNs* are the three typical defense responsive hormones, salicylic acid, jasmonic acid and ethylene. All three of these hormones have negative effects on nodulation and both ET and JA inhibit calcium oscillations and therefore block the common symbiotic signalling pathway (Sun, Miwa, Downie, & Oldroyd, 2007). Presence of binding sites for WRKY transcription factors which are controlled by

these defense hormones further supports a role for these hormones in control of the AMNs. Although studies in *Arabidopsis* and other model systems for plant pathogen interactions evidence that ABC transporters in plant-microbe interactions are controlled by either of the three hormones, studies in mutualistic symbioses are lacking.

4.2.9 Expression of *AMN1*, *AMN2*, and *AMN3* is not affected by Indole acetic Acid

Presence of AuxREs in the promoters of all three *AMNs* further implicated a role of Auxin in control of the *AMNs*. I therefore checked inducibility of the *AMNs* by IAA as a first indication, since several ABC transporters including the auxin efflux transporter AtABCB19 and AtABCB1 are auxin inducible. Treatment of 2 day old seedlings with 1 μ M auxin failed to induce the *AMNs* (Figure 4.8 A) even though other auxin-regulated genes were induced (Appendix 1.7). Presence of AuxREs in the promoters of all three *AMNs* further implicated a role of Auxin in control of the *AMNs*. No statistically relevant increment in *AMNs* transcript levels were noted when 3 day old seedlings were treated with 1 μ M IAA for three hours only (Figure 4.9C). In addition, since I could also detect GA-MYB binding transcription factor binding sites in the promoters of all three *AMNs*, I also tested the inducibility upon treatment with GA. However as shown in Figure 4.9 C, the *AMNs* were not induced. In addition, since co-regulation analyses suggested that *AMNs* might be transporting the phenylpropanoid pathway derivatives flavonoids or isoflavonoids. I also used naringenin and liquiritigenin which are Nod-gene inducing flavonoids and isoflavonoids respectively. Neither naringenin nor liquiritigenin could induce the *AMNs* (Figure 4.8 A).

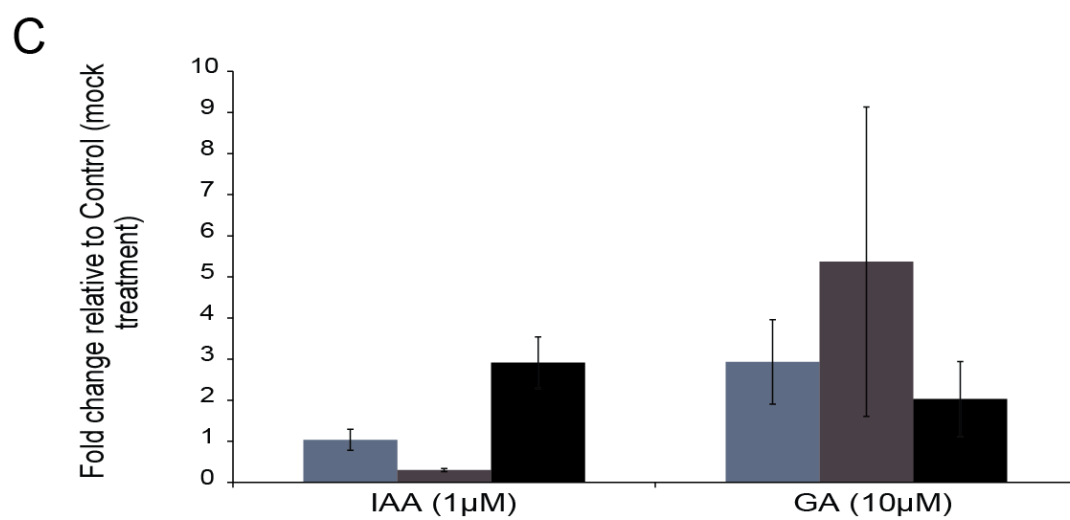
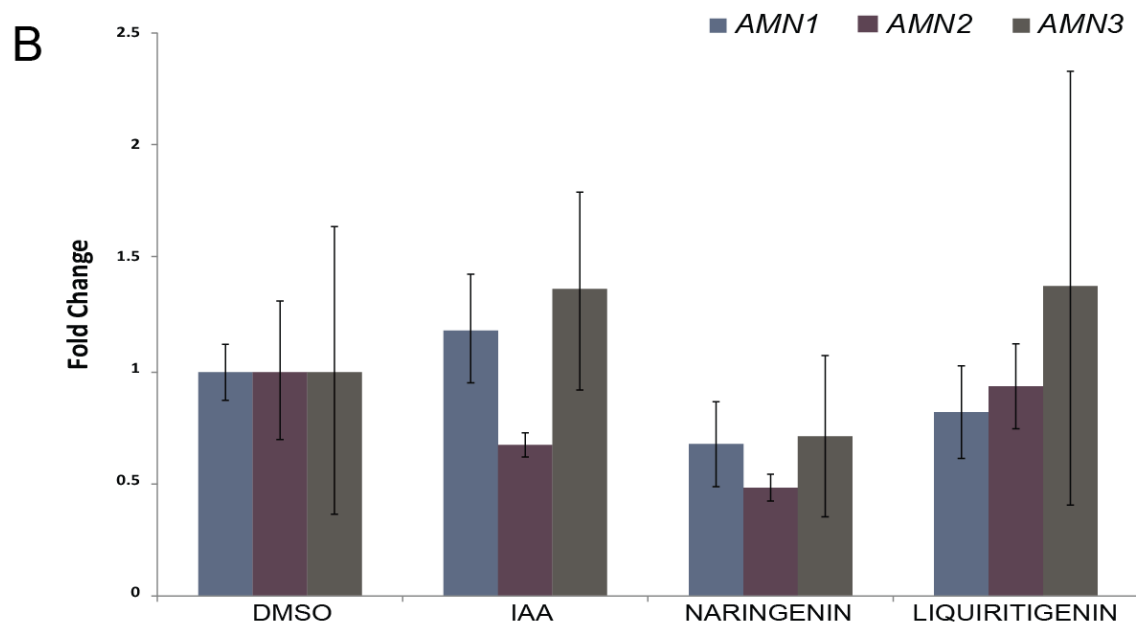
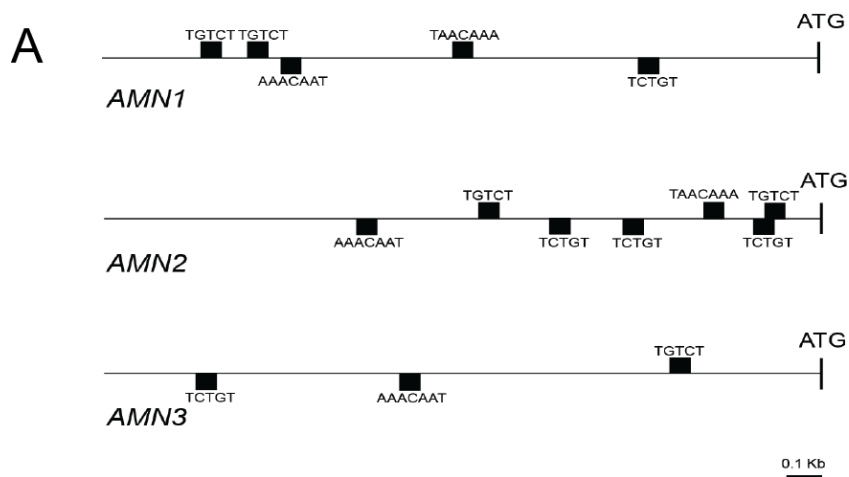


Figure 4.9: Candidate substrates for *AMN1*, *AMN2*, and *AMN3*

A. Incomplete Auxin Response Elements could be found upstream of all three *AMNs* in both orientations as depicted. Perfect conservation of the GA MYB transcription factor binding site is also shown here. **B.** quantitative RT PCR expression comparing gene expression profiles of *AMN1*, *AMN2*, and *AMN3* upon treatment with IAA, the flavonoid Naringenin and the isoflavonoid liquiritigenin. Data are representative of 3 biological replicates each comprised of 8 seedlings. **C.** quantitative RT PCR expression comparing gene expression profiles of *AMN1*, *AMN2* and *AMN3* 3 hours post treatment with IAA and GA. Concentrations are indicated in brackets. Fold change related to mock treated control. Data are representative of 3 biological replicates each comprised of 9 seedlings. Error bars denote standard error of mean. A Student's t-test was carried out to determine whether difference is statistically relevant. Primers used in the experiment *AMN1* (P_5 and P_6), *AMN2* (P_11 and P_12), *AMN3* (P_17 and P_18), *Tip41* (P_43 and P_44), *Ubiquitin* (P_45 and P_46).

4.2.10 *AMN1*, *AMN2*, and *AMN3* are *DMI3* dependent

As the expression of the *AMNs* is symbiosis specific I hypothesized that these genes are controlled by the common symbiotic pathway. To test this hypothesis and place the *AMNs* relative to other genes in the pathway, I tested expression of the *AMNs* in different SYM gene mutants. These included mutants for the receptor for *Nod Factor Perception* (*NFP*), the central regulator of symbiosis signalling – *CCaMK* (*Calcium and Calmodulin Kinase*) or *DMI3* (*Doesn't Make Infections*), the three GRAS domain containing transcription factors *NSP1*, *NSP2* (*nodulation signalling pathway 1 and 2*) and *RAM1* (*Reduced Arbuscular Mycorrhization*), and the transcription factor *NIN* (*Nodulation inception*). *DMI3* is the only gene amongst these required for colonization by both microbes. *NSP1* and *NSP2* are essential for nodulation (S. Hirsch & Oldroyd, 2009) but have also been shown to control strigolactone production hence exerting an effect on mycorrhization (Liu et al., 2011). I used the same set of mutants to determine the regulation of the *AMNs* during symbiotic signalling.

To determine their regulation during nodulation, I treated 3 day old seedlings with 10 nM Nod-factors for 24 hours and assessed the changes in the transcript levels

relative to the control. WT plants treated with Nod Factor showed an average induction of 3 fold, 8 fold and 4 fold increase in expression of *AMN1*, *AMN2*, and *AMN3* respectively across three biological replicates (Figure 4.8 B). Absence of *AMN2* induction in the *nfp* and *dmi3* mutant backgrounds suggested that its expression is dependent on NFP and CCaMK. *AMN1* and *AMN3* were not statistically significant but showed the same trend. Mutations in the three GRAS domain transcription factors *NSP1*, *NSP2* and *RAM1* did not affect induction of the *AMNs*. The transcription factor *NIN* on the other hand caused a hyper induction of all three genes although only *AMN1* was statistically significant. This is not surprising since positive feedback in the *nin* mutant affects several infection related genes including *ENOD11* resulting in their up-regulation. This results in a wider zone of *ENOD11* expression and hyper curling of root hairs containing infection pockets in the absence of nodule development (Schauser et al., 1999). As the use of high concentration of NF yielded variable expression I tested regulation in whole roots infected with *S. meliloti* at 3 dpi. Relative to the water treated controls, the hyper induction of all three *AMNs* was registered at a statistically relevant 90% confidence interval (Figure 4.9 C).

Colonization of *dmi3* and *ram1* mutants by mycorrhizae is strongly compromised (Gobbato et al., 2012). Accordingly, all three *AMNs* failed to get induced in *dmi3* and *ram1* mutants infected with *R.irregularis* for 4 weeks, confirming their dependence on the regulatory kinase and the GRAS domain containing transcription factor. An ANOVA F-test across the mutants confirmed that the results were statistically significant (Figure 4.9 A).

4.3 Conclusions

This section explores the function and regulation of the three ABCB transporters called *AMNs*. To this end I isolated and characterized single mutants for their nodulation and mycorrhizal phenotypes. In the absence of any clear phenotypes, I generated double mutants and used RNAi technology to knockdown both *AMN1* and *AMN2*. This resulted in a 50% reduction of nodule number and 20% reduction in total percentage colonization upon mycorrhization. However, this phenotype was not consistent with the double mutant phenotypes suggesting that additional members of the ABCB family can compensate for the absence of *AMN1* and *AMN2*. This is unlikely to be *AMN3* since *AMN1/AMN2* knockdown in the *amn3* mutant did not further strengthen the phenotype. Seeds from the F1 generation of the triple

cross are now available and will be further phenotyped. However, constitutive expression of *AMN2* in the epidermis blocked entry of the rhizobia into the outer cortex. This suggested that the AMN substrate is possibly detrimental to infection when present ectopically.

I was able to bioinformatically determine that the *AMNs* are co-regulated with biosynthetic genes of the phenylpropanoid pathway and isoprenoid pathway. However, they were not induced by precursors of flavonoids and isoflavonoids i.e naringenin and liquiritigenin potentially eliminating at least these flavonoids as substrates. Auxin as a candidate substrate cannot be conclusively eliminated although IAA also failed to induce these transporters

Importantly, I was able to show that induction of *AMN1*, *AMN2*, and *AMN3* is DMI3/CCaMK dependent. This finding positions the AMNs downstream of the common symbiotic pathway but upstream of the nodulation regulator NIN. In addition, the GRAS domain transcription factor RAM1 is required for the expression of these genes during mycorrhization. This could be due to direct transcriptional regulation of the AMNs by RAM1 or could be a secondary consequence of reduced infection which was found to have a strong impact on *AMN* expression. Expression of the *AMNs* is higher in the *nin* mutant background as are other marker genes and Nod-factor responses in the epidermis of this transcription factor mutant.

A modest phenotype in the *amn2 amn3* double mutant upon mycorrhization suggests that the triple *amn1 amn2 amn3* mutant might have a more severe phenotype. Identification and characterization of this line will be important for finding a function for the AMNs. In addition, screening of double mutants for sensitivity to various flavonoids and lignin pre-cursors would help move towards substrate identification.

Another approach to studying transporter function is the use of heterologous systems such as *E. coli* or yeast and in the case of transporters it can be used to test potential substrates. For instance, AtABCB1, an auxin efflux transporter confers IAA resistance to the *Saccharomyces cerevisiae yap1-1* mutant that is sensitive to low concentrations of IAA (Geisler et al., 2005; Prusty, Grisafi, & Fink, 2004). AtABCB4 expressing *yap1-1* on the other hand is more sensitive to IAA consistent with its auxin importer activity (Santelia et al., 2005). (Prusty et al., 2004). To further address this hypothesis, *AMN2* can be expressed in yeast strains sensitive to IAA or its toxic analogue 5-Fluoroindole.

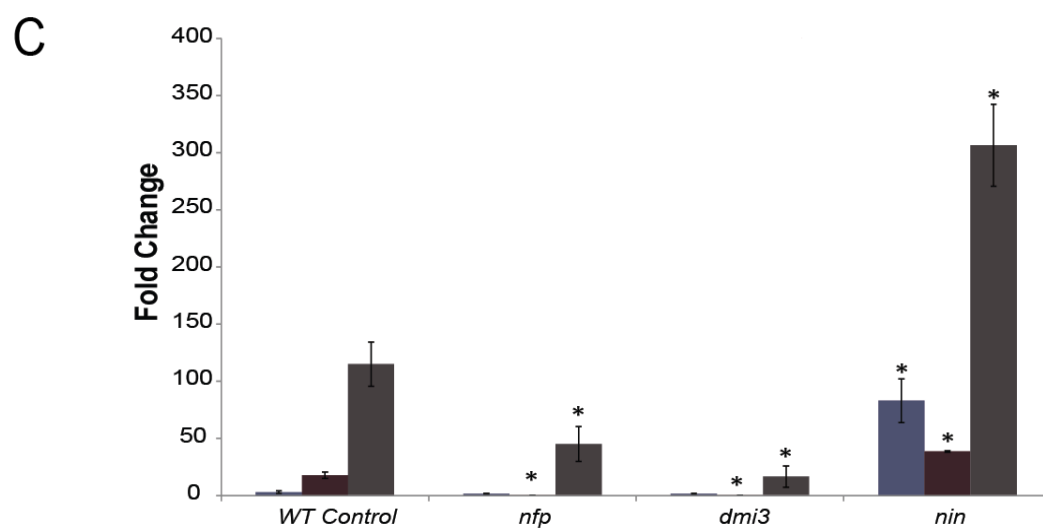
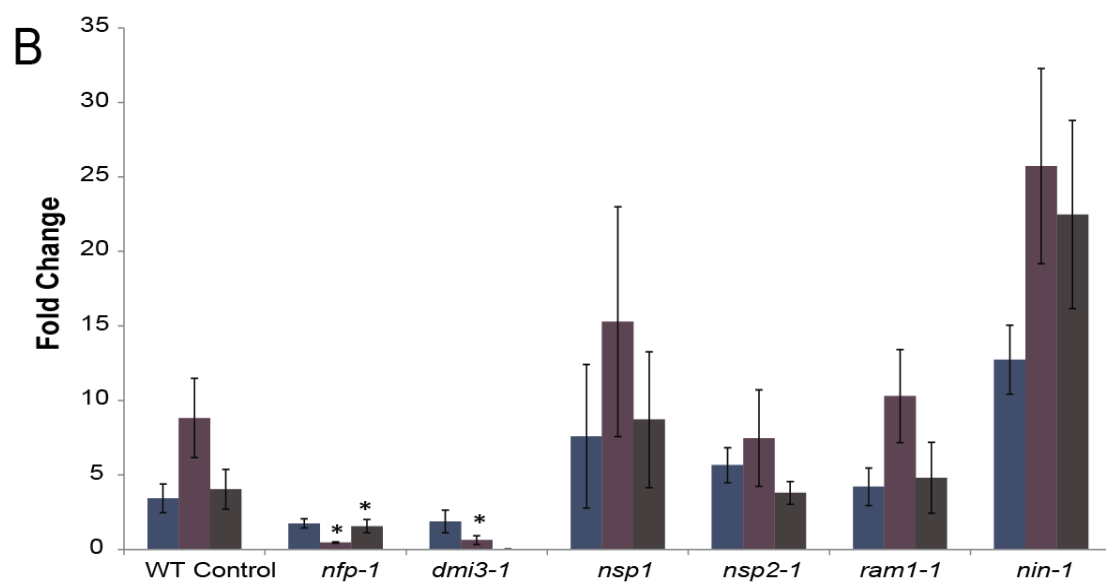
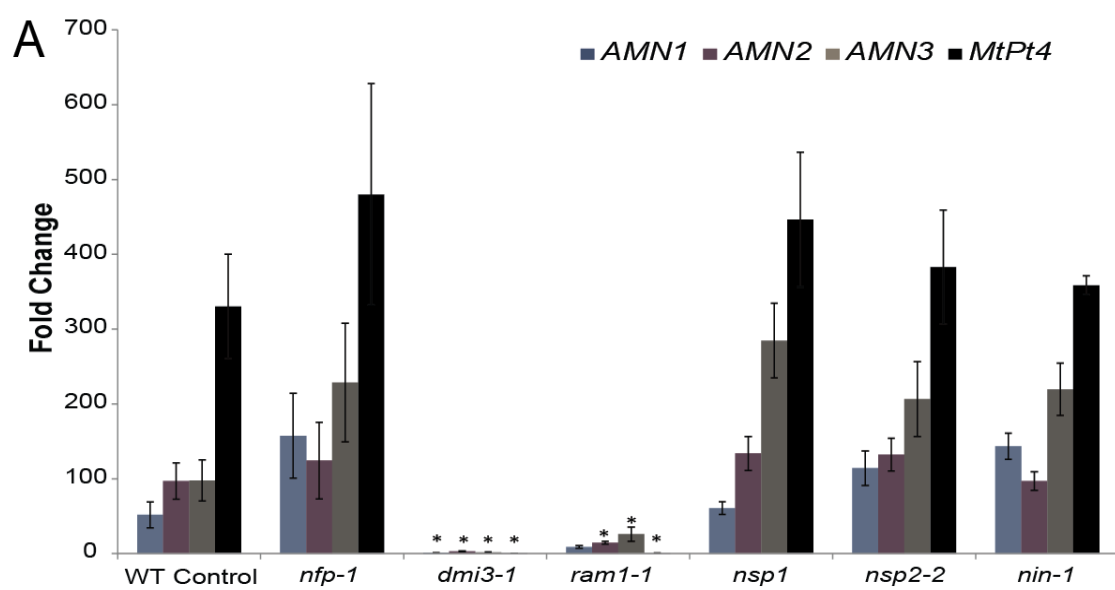


Figure 4.10: Expression of *AMN1*, *AMN2*, and *AMN3* in different symbiotic pathway mutants.

A. Fold change relative to uninfected control roots in Wild type *M. truncatula* compared to six SYM pathway mutants inoculated with *R. irregularis* four wpi. Comparable expression of the positive control *MtPT4* in five mutants suggests colonization levels were similar between mutants and WT. Failure of *dmi3* and *ram1-1* mutants to get colonized correlated with an absence of induction for all four tested genes exhibiting a dependence on the said genes for full functional expression. **B.** Fold change relative to uninfected control roots in Wild type compared to six SYM pathway mutants treated with high concentrations (10 nM) of *S. meliloti* 1021 nod factor in comparison to *S. meliloti* SL44. Induction of gene expression is dependent on *nfp* and *dmi3* and negatively regulated by the transcription factor NIN. **C.** Rhizobial inoculation of mutants mimics effects caused by 10 nM nod factor treatment.

Data are representative of three biological replicates each comprised of 3 plants (mycorrhizal inoculation) or 10 seedlings (NF treatment and rhizobial inoculation). Asterisks indicate significance at the 90% confidence interval or higher using a Student's t-test. * $p < 0.05$. Error bars depict standard error of mean (S.E). Primers used in the experiment *AMN1* (P_5 and P_6), *AMN2* (P_11 and P_12), *AMN3* (P_17 and P_18), *Tip41* (P_43 and P_44), *Ubiquitin* (P_45 and P_46), *MtPT4* (P_47 and P_48)

CHAPTER FIVE: A role for auxin transport in rhizobial Infection

5.1 Introduction

The phytohormone auxin plays diverse roles in plant development and its action is dependent on auxin levels within the cell. IAA itself can diffuse freely into a cell, wherein it dissociates into an anionic form which then cannot efflux out of the cell without using energy (Zazimalova, Murphy, Yang, Hoyerova, & Hosek, 2010). Auxin transport is mediated by efflux and influx carriers like the *Arabidopsis* AUX1 influx permease, PIN family of efflux transporters and ABCB transporters which are known to both efflux and influx auxin (Friml, 2003). Auxin transport inhibitors are routinely used to study the role of auxin in different physiological processes. 1-Naphthylthalamic acid (NPA) blocks efflux of auxin presumably by interacting with ABCBs (Bailly et al., 2008). Although 1-NOA (1-naphthoxyacetic acid) is considered to be a useful inhibitor of auxin influx (Parry et al., 2001), a recent study suggests it can inhibit both efflux and influx of IAA (Lankova et al., 2010). Given Auxin's role in almost every aspect of plant growth, it is not unreasonable to hypothesize a role for auxin in symbiosis which involves development of a completely new organ - the nodule to house the invading rhizobia. In addition to nodule formation itself, root nodule symbiosis also involves a second developmental programme also likely to require auxin; rhizobial infection involves a re-direction of root hair growth to trap the rhizobia and subsequent formation of a tubular plasma-membrane enclosed cell wall structure called the infection thread are likely to involve auxin. Studies in symbiosis have primarily researched a role for auxin during organogenesis.

Noteworthy findings include the observation that high concentration of auxin transport inhibitors (ATIs) like (NPA) and 2,3,5-triiodobenzoic acid (TIBA) can induce formation of nodule-like structures called 'pseudonodules' in the absence of rhizobia (A. M. Hirsch et al., 1989; Rightmyer & Long, 2011). Knockdown of the pathways encoding endogenous ATIs i.e the flavonoids, blocks nodule formation, indicating an important role for the inhibition of auxin transport in initiation of nodules (Wasson et al., 2006; J. Zhang et al., 2009). A role for auxin transport is further supported by studies using the soybean GH3 promoter which shows a dynamic change in expression at the site of NF application (Mathesius et al., 1998). Auxins role in infection has also been studied during nodulation in non-legumes, specifically the *Casuarina-Frankia* symbiosis. Although, mechanisms of infection are vastly different between the symbiotic association of filamentous bacteria *Frankia* with its actinorhizal host *Casuarina* and that of the legume-rhizobia symbiosis; some components of the symbiotic signalling pathway are conserved in the host plants (Gherbi et al., 2008; Svistoonoff et al., 2013; Svistoonoff, Hocher, & Gherbi, 2014). Detection of auxins in infected cells of the actinorhizal nodule using antibodies along with expression of the auxin influx transporter *CgAUX1* in infected cells including infected root hair cells is associative evidence for auxin's role in infection during symbiosis (Peret et al., 2007; Perrine-Walker et al., 2010). Although, the decrease in nodule number in *Casuarina glauca* upon treatment with the auxin influx inhibitor 2-NOA provides an indication that the auxin influx machinery might be involved in organogenesis, to date, no functional genetic evidence exists for its role in nodulation.

To investigate a role for auxin in infection I used pharmacological and physiological assays and complemented them with molecular and genetic studies. The effects of external application of IAA and the efflux inhibitor, NPA have been recorded previously for nodule organogenesis in *Medicago* (Prayitno et al., 2006; van Noorden et al., 2006). I tested the effects of ATIs, both efflux and influx inhibitors, on infection frequency in *M. truncatula* seedlings. Removal of the shoot apical meristem has strong effects on auxin mediated physiological processes such as root growth which can be restored by addition of IAA (Fu & Harberd, 2003).

In addition to endogenous auxin, plant growth is also responsive to auxin produced by bacteria. Since more than 80% of rhizospheric bacteria including rhizobia, can produce their own IAA (Sahasrabudhe, 2011) it is possible that they directly manipulate host auxin gradients to facilitate their entry. Previous reports using

rhizobial strains transformed with an auxin overproducing construct showed differences in nodule number which varied depending on the bacterial strain and plant host studied. In the *M. truncatula*-*S. meliloti* symbiosis the use of auxin overproducing bacteria increased the number of nodules while in the *Phaseolus* and *Vicia* symbiosis with *R. leguminosarum* the nodule numbers were lowered (Camerini et al., 2008; Pii, Crimi, Cremonese, Spena, & Pandolfini, 2007). To date, no mutant of *S. meliloti* has been identified which cannot synthesize IAA.

Upon perception of auxin by the auxin receptor TIR1, AUX/IAA repressors are targeted for cellular degradation by ubiquitination (Calderon Villalobos et al., 2012; Gray, Kepinski, Rouse, Leyser, & Estelle, 2001). AUX/IAA proteins have four domains wherein domain III and IV are responsible for forming homodimers or inactive heterodimers with auxin transcription factors (ARFs) that mediate auxin responses. A point mutation in domain II of the AUX/IAA proteins inhibits binding to ubiquitin, which prevent de-repression of ARF activity. In *Arabidopsis*, root architecture and root hair length could be manipulated using a stabilized version of the AUX/IAA co-receptor, AtIAA17 (H. Li, Cheng, Murphy, Hagen, & Guilfoyle, 2009). The *Arabidopsis* AXR3/IAA17 protein is involved in initiation and expansion of root hairs (Knox, Grierson, & Leyser, 2003). CaMV 35S driven IAA17 repressor lines (IAA17mII repressor), containing a stabilizing mutation in domain II, have shorter roots and very few or no root hairs. This gain-of-function substitution in the domain II of IAA17 prevents targeting to the 26S proteasome thereby enhancing its repressor activity leading to a block in root hair initiation and elongation (Knox et al., 2003). Conversely, IAA17 fused to an N terminal VP16 activation domain (VP16-IAA17mII activator) results in an increase in root hair length (H. Li et al., 2009). The N terminus fusion of the VP16 activation domain was sufficient to confer properties of a stable transcriptional activator to the fusion. The authors utilized this ability to generate gene fusions that stably activated or repressed the *DR5-GUS* reporter promoter (H. Li et al., 2009; Tiwari, Hagen, & Guilfoyle, 2003). To test a role for auxin in infection I expressed the *Arabidopsis* IAA17 synthetic activator and repressor constructs under the *ENOD11* promoter. The p*ENOD11* (early nodulin) promoter is an early marker of nodulin gene expression that is initially expressed in all root hairs that perceive rhizobially produced Nod factor and then gets restricted to root hair cells undergoing infection and is also expressed in young nodules (Journet et al., 2001). By driving the expression of these fusions using an infection responsive *ENOD11* promoter I could bypass the changes in growth induced by

these constructs while testing the effects of repression and activation of auxin signalling on rhizobial infection.

Auxin can bring about its effects by degradation, conjugation and activation of its signalling components. In addition auxin transport has been found to be crucial to its effects by the creation of localized maximas/minimas (Woodward and Bartel 2005). *CgAUX1* plays a role in infection by the actinomycete *Frankia* of its symbiont *Casuarina* (Peret et al., 2007). *P. sativum* stable lines transformed with the *AtAUX1* promoter, show GUS expression throughout the cortex in developing nodules but is restricted to the meristem in mature nodules (Simon A. Walker, Thesis 2000). Using expression data from infected root hairs I noted that none of the 10 PINS encoded in *M. truncatula* genome but the homologue of the *AtAUX1* influx transporter, named *MtLAX2* (Schnabel & Frugoli, 2004) is up-regulated three days post inoculation. The following chapter describes the isolation of the *MtLAX2* mutant along with an infection specific AUX/IAA gene *MtIAA8* and characterization of their symbiotic phenotypes.

5.2 Results and Discussion

5.2.1 Treatments with auxin efflux and influx inhibitors decrease the frequency of rhizobial infection but do not affect early symbiotic signalling

To test for a role of auxin in infection, I first established concentrations of chemicals at which growth of root and root hair were affected but the seedlings were not severely stunted and no cellular toxicity was observed. Using 100 nM of NAA, 1 μ M each of IAA, NPA, 10 μ M CHPAA and 30 μ M of 1-NOA, the root hair length changed (Figure 5.1 B) and recapitulated the trends seen in *Arabidopsis* root hairs (Rahman et al., 2002). None of the chemicals, at the concentrations used affected the growth of *S. meliloti* over a 48 hour time period (Figure 5.1 A). For the infection assay, seedlings were pre-treated with inhibitors for 24 hours prior to inoculation and then maintained on treatment plates for 7 days before being stained for LacZ activity. Both efflux (NPA) and influx (1-NOA) transport inhibitors reduced the number of micro-colonies, infection threads and nodules. The change in nodule number was consistent over two independent experiments and was statistically significant from control solvent treated plants. Seedlings treated with external IAA did not cause a change in infection frequency (Figure 5.1 C). Interestingly, external addition of IAA has been reported to reduce nodule number in *M. truncatula* seedlings at these concentrations (van Noorden et al., 2006) and the present study shows a similar trend although the differences were not significant. Auxin thus, might play differing roles in infection and organogenesis. However, we can conclude that perturbation of either efflux or influx transport is detrimental to both infection rates and nodule organogenesis.

ENOD11 is routinely used as a marker for activation of early NF signalling. It encodes a secreted protein transcripts of which can be detected 30 minutes to 3 hours after rhizobial infection or NF treatment (Journet et al., 2001). Interference with NF signalling affects the development of GUS expression in *pENOD11*-GUS transgenic lines and thus is used as a visual marker for activity of the symbiotic signalling pathway (G. E. Oldroyd, Engstrom, & Long, 2001). I pre-treated 2 day old seedlings for 24 hours using the inhibitor concentrations described above. Subsequent treatment of seedlings with additional 1 nM Nod factor did not affect development of *pENOD11*-GUS expression. Together with the observation that a synthetic auxin 2,4-D did not affect initial calcium spiking (Yiliang Ding, personal

communication) characteristic of activation of symbiotic signalling, we conclude that auxin does not affect the signalling events required to establish symbiosis but is required for downstream events.

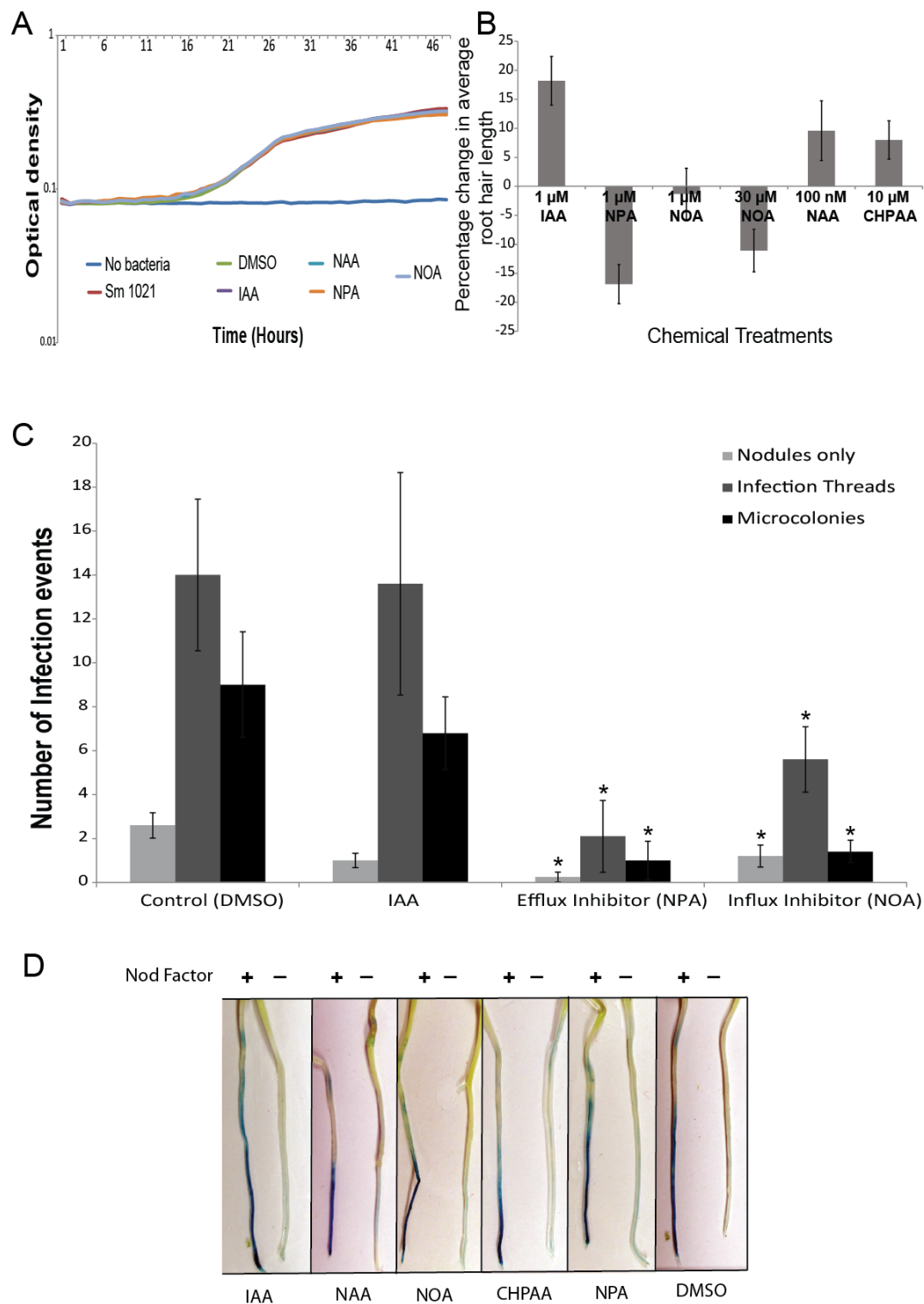


Figure 5. 1: Pharmacological dissection of auxin's role in rhizobial infection of *M. truncatula*

A. Growth curve of *S. meliloti* 1021 over 48 hours in media supplemented with IAA, NAA and other Auxin transport inhibitors (ATIs). **B.** Average percentage change in root hair length of *M. truncatula* seedlings 7 days post treatments with IAA, NAA, NPA, 1-NOA, CHPAA over four different experiments. **C.** Bar graph showing average change in infection events in seedlings treated with 1 μ M IAA (n=8), 1 μ M NPA (n=9) and 30 μ M NOA (n=10) on infection rates 7 days post infection with *S. meliloti* in comparison to solvent DMSO (n=9). Error bars represent standard error of mean (S.E). Student's t-test was used to determine statistical significance * $p < 0.05$ **D.** Representative roots showing pENOD11 expression in the presence and absence of NF in 3 day old seedlings pre-treated with IAA and other ATIs.

5.2.2 MtLAX2 expression is not associated with infection threads

In a further attempt to provide genetic support for a role for auxin in infection or nodule organogenesis we chose to study a member of the LAX family of auxin influx transporters. A role for this family was suggested by the finding that a *Casuarina glauca* AUX1 homologue is expressed in infection containing cells including the infected root hair. Phylogenetic analysis revealed that the *M. truncatula* orthologue of the CgAUX1 and the AtAUX1 is MtLAX2 (Figure 5.2 A), named by (Schnabel & Frugoli, 2004). Of the 5 LAX family members in *Medicago*, MtLAX2 is transcriptionally induced in infected root hair cells (Figure 5.2 B) although the fold change is not statistically significant. I generated transgenic roots containing a pMtLAX2-GUS construct to analyse its spatial expression pattern during nodulation. In addition I re-examined a previously studied *Pisum sativum* stable lines transformed with the AtAUX1 promoter (Simon A. Walker, Allan Downie unpublished) for infection associated expression. This is consistent with microarray studies which show a progressive decrease in transcript levels of LAX2 in nodules over time, as the meristem stays a defined size and the nitrogen fixation zone continues to grow (Figure 5.2 C). However in both systems, I could not detect promoter activity in root hairs containing infection structures (supplementary figure 5.1). An *M. truncatula* line transformed with a soybean GH3 has often been used as a marker for early responses of auxin to Nod factor and rhizobia (Mathesius et al., 1998). Again no expression could be detected in infection containing root hair cells

(Supplementary Figure 5.1). Interestingly, I noticed isolated promoter activity of the *AtAUX1/MtLAX2* in either plant system, just below root hairs on infected plants which was not always associated with curled root hairs. In *Arabidopsis*, activity of *AUX1* in atrichoblast cells has been proposed to play a role in root hair elongation (Jones et al., 2009). Further experiments are required to investigate whether the promoter activity at the base of uninfected root hair cells is nod-factor dependent to find a role for *LAX2* in infection induced root hair curling. Taken together, *MtLAX2* possibly plays a role in both rhizobial infection and organogenesis and is a good candidate for genetic dissection of a role for auxin during symbiosis

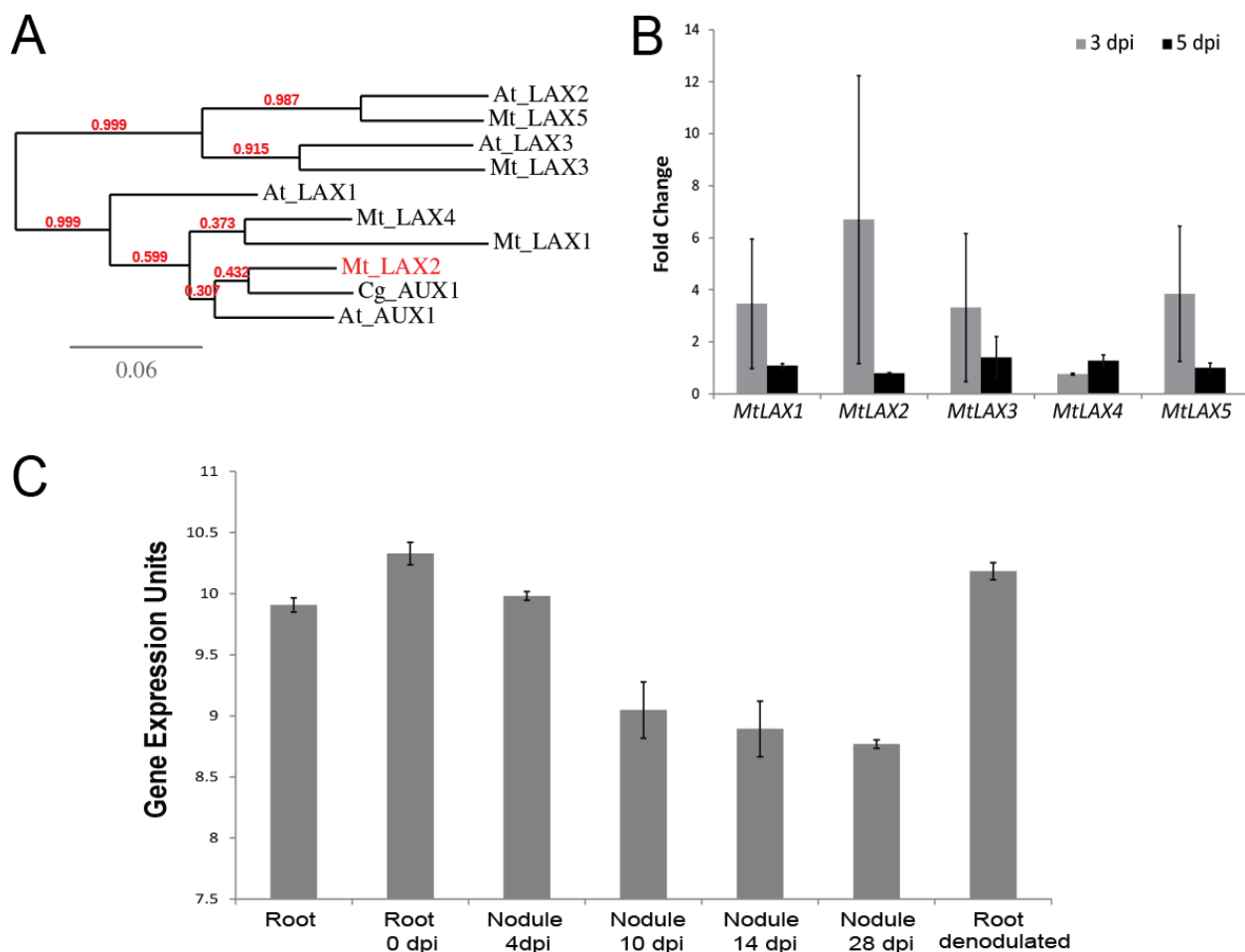


Figure 5.2: Phylogenetic and Expression studies of *M. truncatula* LAX2

A. Phylogenetic tree showing interrelations between five *M. truncatula* LAX family of influx transporters and *AtAUX1* and *CgAUX1*. Numbers in red indicate bootstrap values **B.** Expression data for all five members of the *M. truncatula* LAX influx transporters in infected root hairs compared to root hairs infected with the non-Nod factor producing strain of *S. meliloti* (Murray lab, unpublished) *MtLAX1* (Mtr.13440.1.S1_at) *MtLAX2* (Mtr.41246.1.S1_at) *MtLAX3* (Mtr.8766.1.S1_at) *MtLAX4* (Mtr.29499.1.S1_at) *MtLAX5* (Mtr.12078.1.S1_at). **C.** Expression of *MtLAX2* in nodules of *M. truncatula* from 4 dpi upto 28 days post infection with *S. meliloti* (Benedito et al., 2008) Denodulated root refers to the root after nodule excision.

Values represent average of three biological replicates each. Error bars depict Standard error of mean (S.E).

5.2.3 The *mtlax2* mutant has reduced nodule numbers

To determine whether infection was affected by LAX2, I expressed the *MtLAX2* CDS under the EXPANSIN A7 promoter in *M. truncatula* hairy roots. No significant changes in nodule number were observed (Figure 5.3 C). To further investigate a role of MtLAX2 in nodulation, I isolated two *Tnt1* insertion mutant alleles of *MtLAX2* with insertions in exon 4 (Figure 5.6 A). Sensitivity of root growth to auxin and nodulation phenotypes was tested. Growth of *MtLax2-1* was insensitive to 1 μm IAA on plates similar to the effect of 0.1 μm 2,4-D on *ataux1* (Figure 5.6 B also see Supplementary figure 5.5) (Bennett et al., 1996) suggesting a conserved function for this transporter in *M. truncatula* roots. Neither allele showed any apparent growth defects (5.3 F). At 10 dpi with Sm 1021 the number of nodules is reduced by ~40% in *mtlax2-1*. This can result from fewer nodules being initiated or delayed nodule development. At 3 wpi, both *lax2-1* and *lax2-2* show a consistent reduction in nodule number in comparison to WT. LAX2 is therefore required for nodule initiation or emergence or both. To gain insights into possible changes in the distribution of auxin signalling in the mutant I crossed *lax2-1* to a DR5-GUS reporter containing transgenic line of *Medicago* and identified lines homozygous for the *Tnt1* insertion. However, due to time restrictions I could not further characterize and compare responses in these lines during nodulation. In the *lax2* mutants, although the infection structures develop normally (Supplementary Figure 5.1), a more detailed analysis is needed to determine if a decrease in the number of micro-colonies and elongating infection threads might indicate the cause for the higher number of uninfected white nodules observed.

5.2.4 Mutation in an AUX/IAA gene *MtIAA8* reduces nodule number

Auxin transporters such as LAX2 generate auxin gradients which trigger morphogenetic events through the auxin signalling pathway. The AUX/IAA proteins form heterodimers with members of Auxin response factors (ARFs) and prevent them from activating the transcription of early auxin responsive genes. Changes in root hair transcriptome upon infection with *S. meliloti* identified two homologous AUX/IAA genes *MtIAA8* (Medtr5g067350) and *MtIAA9* (Medtr8g67530) which are induced in infected root hairs. Along with other infection induced genes, *MtIAA9* was confirmed to be IAA inducible (Supplementary Figure 5.2). Expression of *MtIAA8* was monitored by constructing *pIAA8-GUS* fusions which showed the characteristic expression of auxin responsive genes in the root tip (Figure 5.7 B v), lateral root

initials (Figure 5.7 B iv) and vascular bundle (Figure 5.7 B vi). In addition, *MtIAA8* expression was associated with infection thread containing root hairs (Figure 5.7 B i,ii). In mature nodules, expression was associated with the meristematic nodule tip (Figure 5.7 B iii) but was expressed throughout the primordia in developing nodules. A genetic role for the AUX/IAA gene was investigated by identification of a single allele of the gene *iaa8-1*. At 10 dpi a reduction of ~30% in nodule number was seen which increased at 3 wpi to ~50% (Figure 5.7 C). To assess auxin responses in the mutant background I crossed the *iaa8-1* mutant to the *DR5-GUS* lines. The homozygous F2 progeny remain to be characterized. Expression of *IAA8* in infected root hairs suggests a role in infection; therefore an infection thread count is necessary to complete the characterization of this mutant.

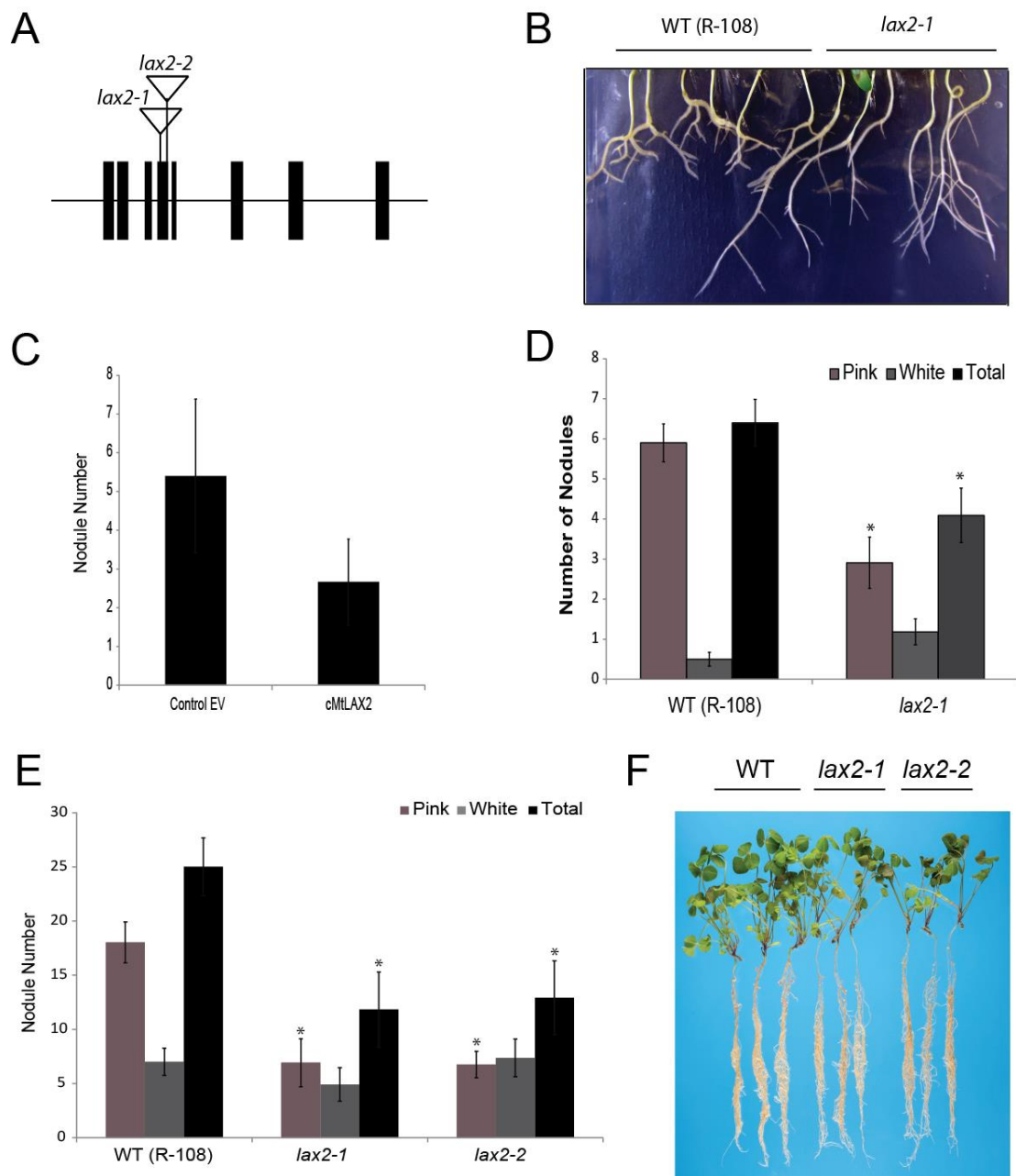


Figure 5.3: Characterization of *lax2* mutants

A. Diagram showing position of *Tnt1* insertion alleles of *lax2-1* and *lax2-2* in *MtLAX2*. Black boxes represent exons. **B.** Growth of *lax2-1* in media supplemented with 1 μm IAA (Also see Supplementary Figure 5.5) **C.** Bar graph comparing average nodule number in *M. truncatula* hairy roots transformed with control empty EV (n=15) and *EXPANSIN A7* driven *MtLAX2* (n= 12) **D** Bar graph comparing average nodule number between WT (n=21) and *lax2-1* (n= 11) plants 10 dpi **E** and 3 wpi WT (n= 32) *lax2-1* (n= 12) and *lax2-2* (n= 11) with Sm 1021 **F.** Representative plants of WT compared to *lax2-1* and *lax2-2* show no defects in plant growth 3 wpi with Sm 1021. Error bars represent standard error. Asterisks denote $p < 0.05$ using Student's t-test.

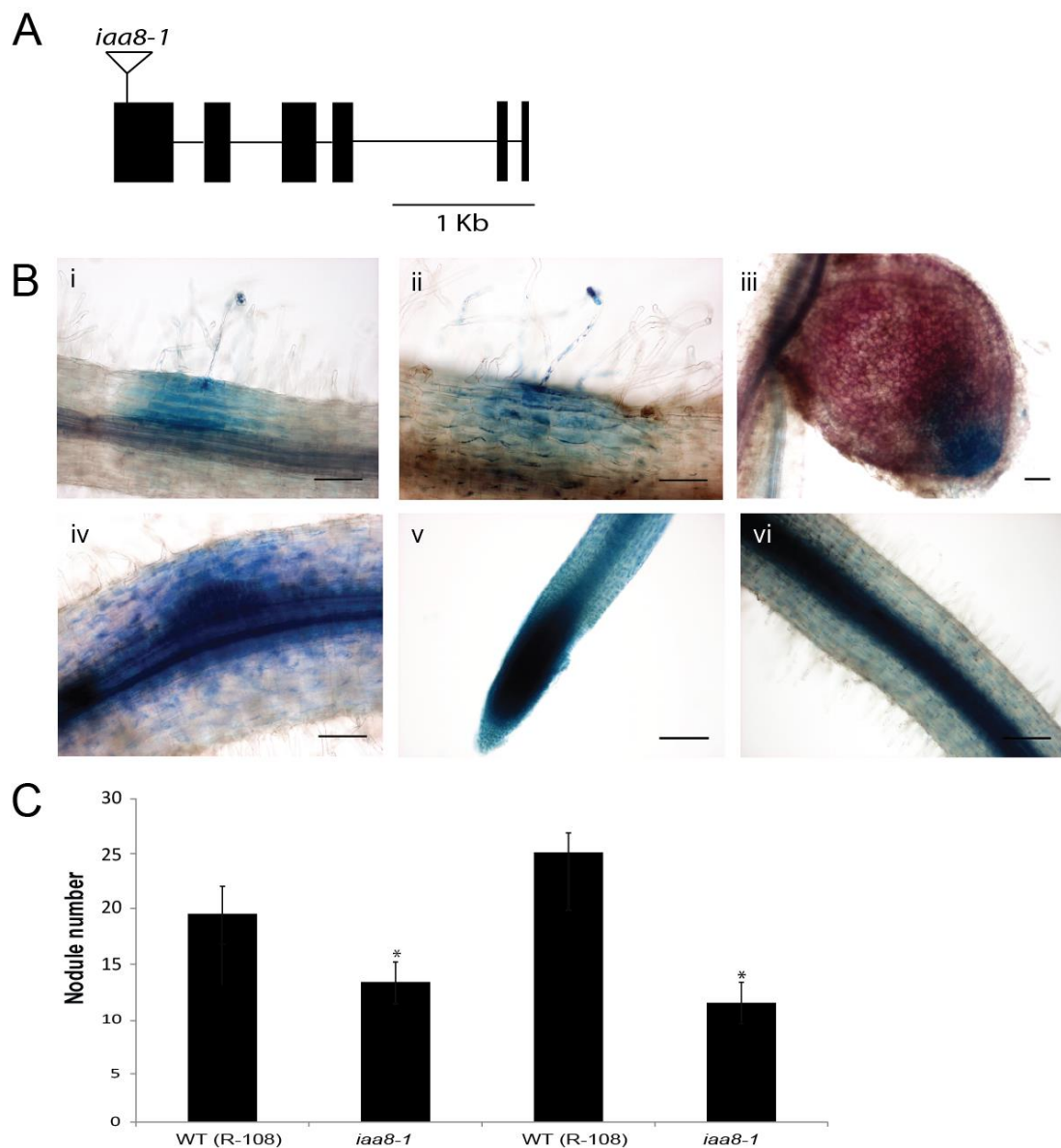


Figure 5.4: Characterization of *iaa8* mutants

A. Diagram showing position of *Tnt1* insertion allele *iaa8-1* in *MtIAA8*. Black boxes represent exons. **B.** Promoter-GUS analysis showing expression is associated with infected root hair cells Sm1021 LacZ stained with Magenta-Gal (i-iii) *GUS* expression in uninfected plants is associated with emerging lateral roots (iv) the root tip (v) and the vascular bundle (vi) **C.** Bar graph comparing average nodule number 2 wpi (n=16, n=19) 3 wpi (n=32, n=18) between WT and *iaa8-1* plants respectively. Asterisks denote $*p < 0.05$ using a Student's t-test. Error bars denote SEM.

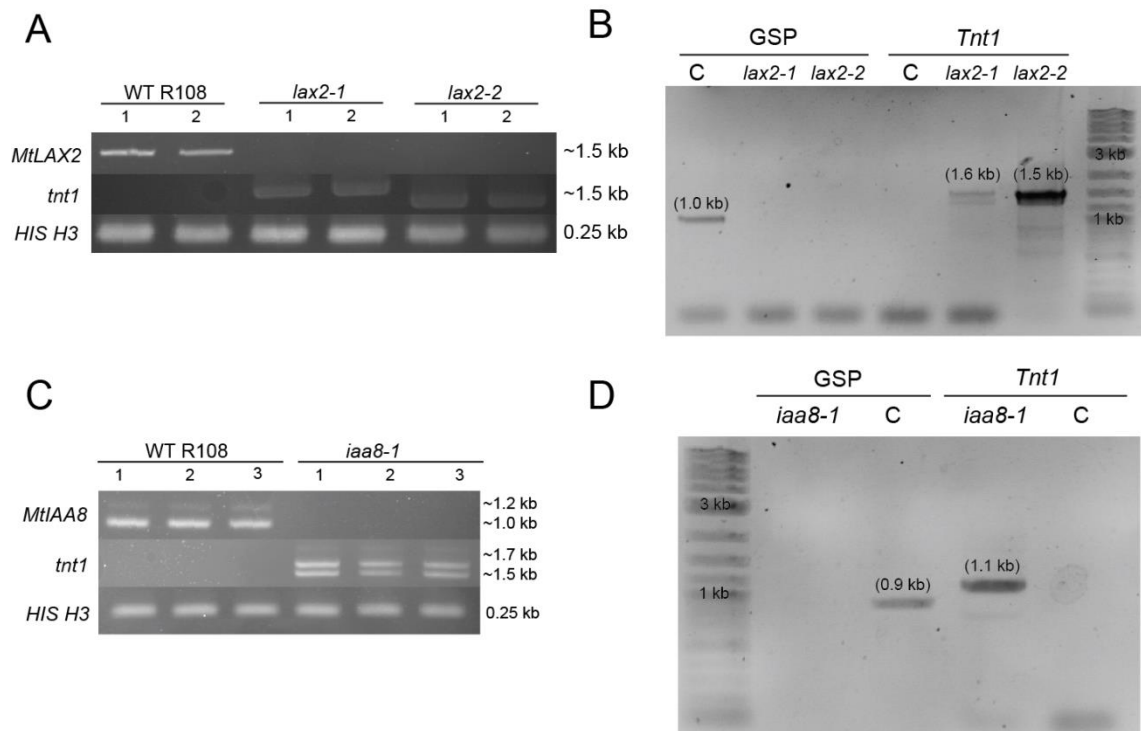


Figure 5.5: Confirmation of *tnt1* mutants described in this chapter

Agarose gel image confirming presence of *tnt1* insertions at predicted sites. **A,C** Semi-quantitative RT-PCR comparing *lax2-1*, *lax2-2* mutants (A) and *iaa8-1* mutant (C) with WT R108 control. RNA was extracted from 2-3 separate individual plants. Full-length transcript amplifies from WT but not from the mutants. *Tnt1* inserts can be amplified from mutant lines but not WT. Amplicon sizes are indicated to the right. Multiple bands in C represent splice variants. Primers used *MtLAX2* CDS (P_24 and P_25) *Tnt1* insert (P_32 and P_25) *MtIAA8* CDS (P_49 and P_50) *Tnt1* Insert (P_32 and P_50) *Histone H3* (P_41 and P_42) **B, D** Gel images showing PCR amplified products using template DNA isolated from mutants and WT control R108 as indicated. *Tnt1* insert amplifies from mutant lines but not in control plants. WT gene sequence amplifies from control but not mutant lines. Expected sizes are indicated on top of the bands. DNA marker represents 1 Kb ladder. Primers used *MtLAX2* (P_22 and P_23) *Tnt1* insert in *lax2-1*, *lax2-2* (P_32 and P_23) *MtIAA8* (P_30 and P_31) *Tnt1* Insert in *iaa8-1* (P_32 and P_31).

5.2.5 Decapitation of the shoot apical meristem (SAM) reduces rhizobial infection frequency and this phenotype can be rescued by IAA

Decapitation of *Arabidopsis* seedlings cause a reduction in root length which can be complemented by external addition of IAA at the shoot apical meristem (SAM) (Fu & Harberd, 2003). A more severe removal of the aerial auxin source as demonstrated by Swarup et al. showed that only early lateral root primordia could emerge in decapitated seedlings compared to control (Swarup et al., 2008). I therefore hypothesized that reduced auxin levels in the root resulting from shoot decapitation would reduce infection frequency if the hormone has a role in this process. Decapitation of *Medicago* seedlings produced the same effect as in *Arabidopsis* and provision of 0.5 μ l of 1 ng/L IAA was sufficient to restore root length (Figure 5. 5 A). I then tested the effects of decapitation on infection and nodule formation with and without supplementation of IAA. Decapitation had a pronounced repressive effect on microcolony formation, but didn't alter nodule number. Remarkably, IAA treatment was sufficient to restore the number of micro-colonies to WT levels (Figure 5.5 B). Together these results suggest a role for auxin during directional curling of the root hair around attached bacteria required for formation of an infection pocket.

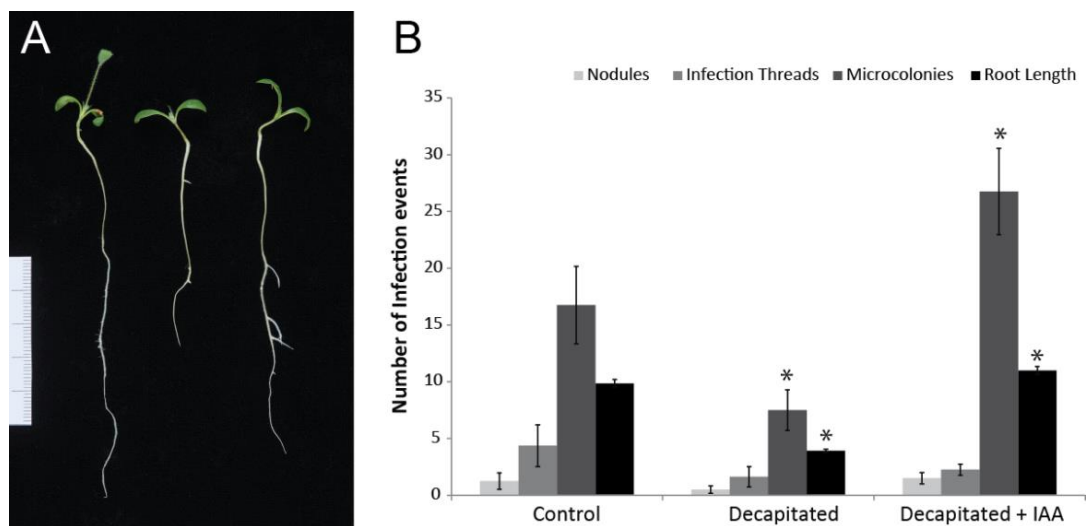


Figure 5.6: Effects of decapitation of the shoot apical meristem (SAM) on *S. meliloti* – *M. truncatula* interaction

A. *M. truncatula* seedlings (from left to right) control seedling, decapitated seedling with shorter primary root and decapitated seedling supplemented with 1 ng/L IAA showing full recovery of root length **B.** Bar graph comparing the average number of infection events in the three experimental sets of 8-10 seedlings each. Error bars depict standard error (S.E). Infection events were scored 7 days post infection. Root length in centimetres. Asterisks denote $*p < 0.05$ using Student's t-test.

5.2.6 Introduction of a dominant negative copy of the *Arabidopsis* IAA17 does not affect infection structures or nodule number

To test whether activation and repression of auxin signalling can mimic the effects caused by pharmacological experiments, I introduced the IAA17 repressor (IAA17mlmII repressor), and IAA17 activator (VP16-IAA17mlmII Activator) into *M. truncatula* using the hairy root transformation system. mII stands for a single bp mutation in domain II of the IAA17 transcript that stabilizes the protein and prevents ubiquitin mediated degradation. mI denotes a mutation in domain I that reduces the severity that the mII mutation has on protein degradation rates (Tiwari et al., 2003). The *pENOD11* promoter which is highly expressed in infected root tissues was used to drive expression of the gene fusions as depicted in Figure 5.6 A. A version of the IAA17 repressor construct with deletions in domain II and III was used as a control (IAA17mlmII MscI digest Control). An HA tag was introduced in the N-terminal region of the repressor and control constructs in place of the VP16 activation domain in the activator construct.

S. meliloti infection structures initiated normally as the root hair curled around the attached rhizobia to form infection pockets in all three sets of transformants. The infection threads elongated normally down the root hair and no abnormal structures were formed (Figure 5.6 B i-vi). At 3 wpi, the number of nodules was comparable across the different set of transformants even though there were very few lines (data not shown). Thus, infection induced modulation of AtIAA17 mediated auxin signalling did not qualitatively affect nodule formation or infection structures.

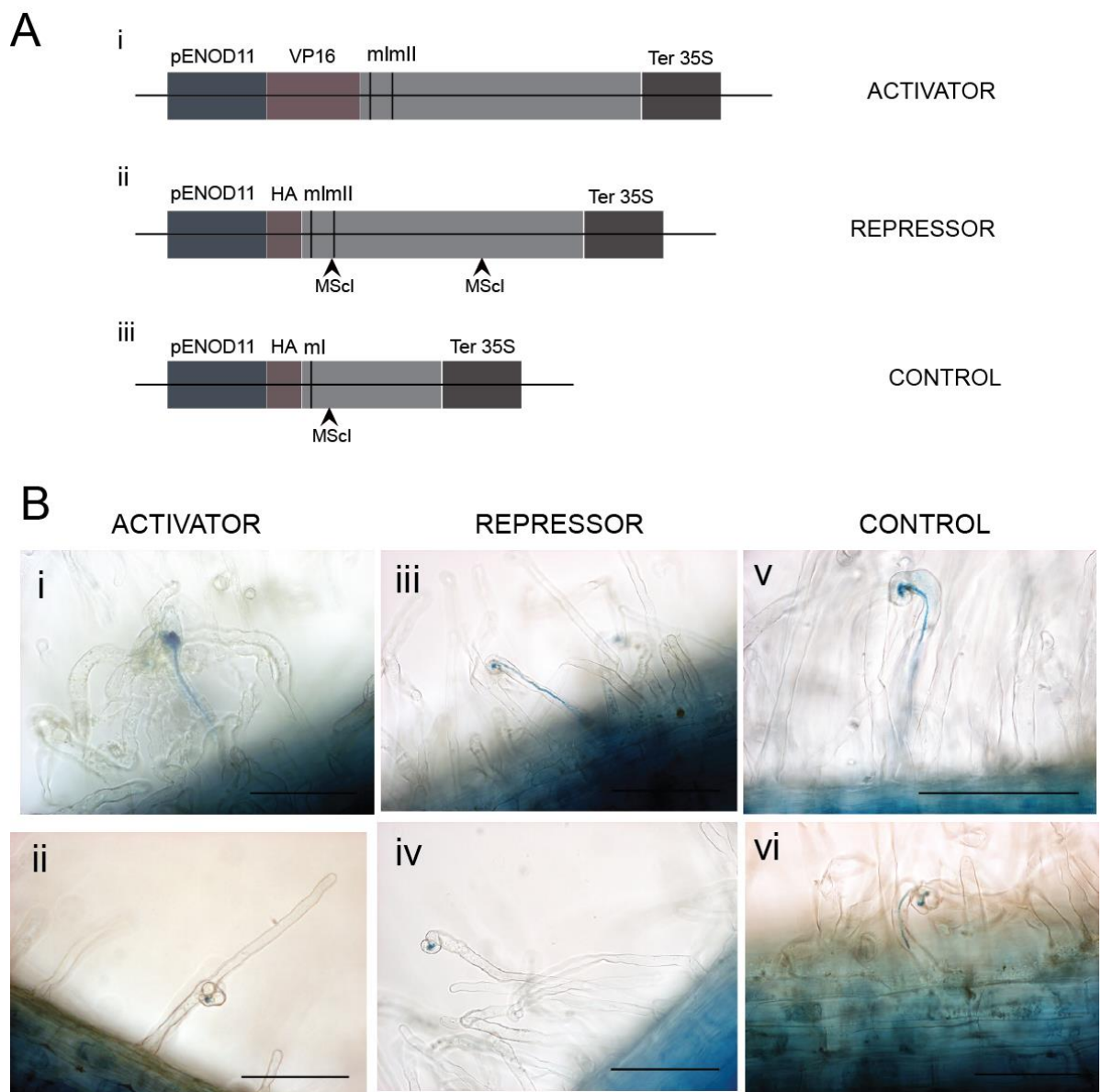


Figure 5.7: Effects of Infection induced repression and activation of Auxin signalling on *S. meliloti*-*M.truncatula* interaction

A. Diagram showing construct design for pENOD11 induced (i) VP16-IAA17mI mII activator (ii) IAA17mI mII repressor and (iii) IAA17mI control MScI digested vector control. Lines represent mutated base pair. mII refers to the stabilizing mutation in domain II and mI refers to a single mutation in domain I which reduces severity of mII mutation. All vectors have a ds Red transformation marker **B.** Infection structures in hairy roots transformed with (i,ii) activator construct (iii,iv) repressor construct and (v,vi) vector control 7 days post infection with Sm 1021 are normal and do not show any aberrant morphology. Scale bars denote 100 μ m.

5.2.7 Enhancement of rhizobially produced auxin does not affect the number of infections but decreases nodule number

To address the hypothesis that bacterially produced auxin might contribute to the rhizobial infection; I obtained a previously studied, auxin over producing construct and introduced it into Sm1021 carrying the *pHemA-LacZ* marker. This *rolA-iaaM-tms2* chimeric construct consists of the *iaaM* (tryptophan monooxygenase) gene from *Pseudomonas syringae* and *tms2* (IAA hydrolase) gene from *Agrobacterium tumefaciens*, that convert tryptophan to indole acetamide and then to indole acetic acid in a two-step process. I generated a control plasmid with a large deletion spanning most of the *iaaM-tms2* genes as described in the materials and methods. These plasmids were then introduced into strain *S. meliloti* 1021 and these strains not show any difference in growth rates in culture relative to WT (Figure 5.7 A, B). There was no change in the number of infection events between the WT *S. meliloti* strain and the IAA over-producing strain (Figure 5.7 D), consistent with the results from the addition of exogenous IAA described above (Figure 5.7 C). Infection with the IAA overproducing strain also caused a root shortening comparable to the addition of external IAA on plates (data not shown). However, I observed a ~50% reduction in nodule number upon infection by *S. meliloti* containing the auxin overexpressing plasmid (Figure 5.7 C) in contrast to previous studies using *M. truncatula* (Pii et al., 2007) which show a doubling of nodule number. We repeated the experiment in soil with the same concentration of inoculum but saw a reduction in nodule number. Other symbiotic hosts like *Phaseolus vulgaris* and *Vicia hirsuta* also show a decrease in nodule number upon infection by compatible rhizobial strains carrying this construct (Camerini et al., 2008; Pii et al., 2007). I confirmed the identity of the transformed plasmids by restriction digestion (data not shown) and physiological changes in root growth. It is possible that the basal levels of IAA produced by the host strains differ from the original laboratory. Therefore a more informative experiment would involve an *S. meliloti* mutant defective in auxin production, which has not been described in literature so far. From my experiment I can therefore only conclude that, constitutive over-production of auxin by rhizobia does not affect the frequency or development of ITs and micro-colonies.

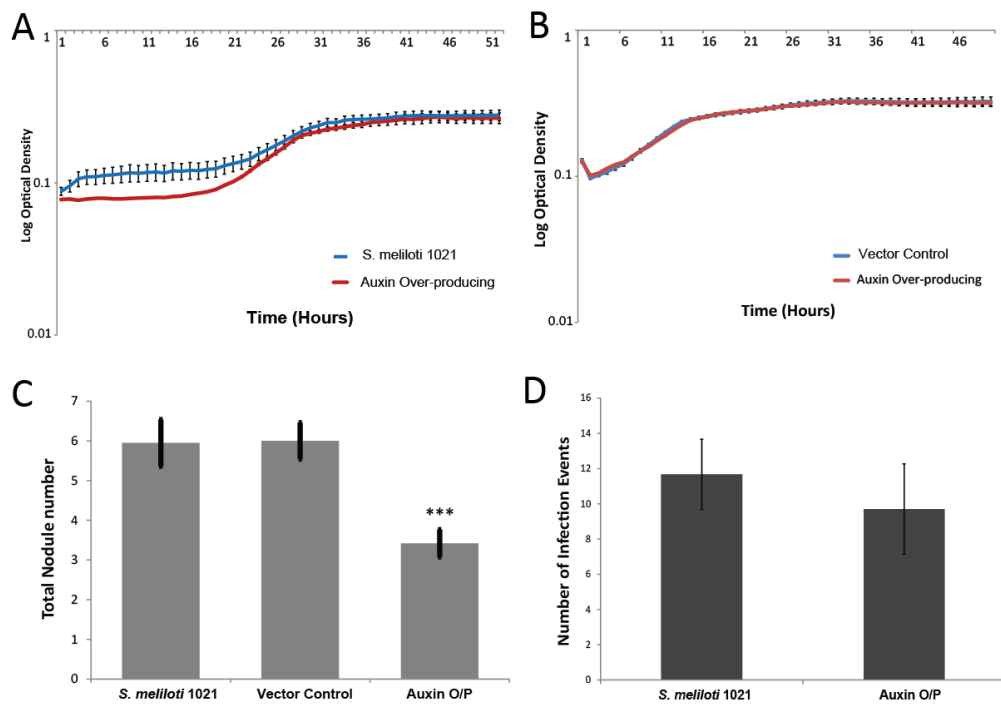


Figure 5.8: Effects of rhizobially produced auxin on infection

A. Growth rates of Sm 1021 strains containing the pXLGD4 plasmid and the *rolA-iaaM-tms2* construct and **B.** Growth rates of *rolA-iaaM-tms2* transformed strain and an *EcoRI* digested vector control. Values represent average measured optical density of 6 technical replicates. Error bars represent standard error of the mean of six replicates at each time point **C.** Nodule number in *M. truncatula* seedlings infected with auxin overproducing strain 10 days post infection. Values represent average nodule number of N=15-20 plants. Error bars depict standard error. Asterisks represent *** $p < 0.001$ **D.** Total number of infection events in seedlings infected with *S. meliloti* 1021 control and auxin overproducing strain 7 days post infection. 8-10 seedlings per rhizobial transformant were used for this experiment.

5.3 Conclusion

This study makes advances towards understanding of the role of the phytohormone auxins in rhizobial infection. Previous studies in this and other legume model systems have focussed on nodule organogenesis rather than infection. I was able to show that perturbing auxin transport by use of either efflux or influx inhibitors were sufficient to inhibit rhizobial infection. Since auxin exerts its influence on most development programs by creating gradients using its extensive transport machinery this result is not surprising. Furthermore, removal of the shoot apical meristem results in less auxin being transported to the roots which results in fewer infections. Previous studies in soybean have shown that removal of shoot apex lowers total nodule number without affecting nodule morphology or size (Delves, Higgins, & Gresshoff, 1992). Although a similar trend is seen in the present experiment, the difference in nodule number is not statistically significant, perhaps due to having used early time points and a small population size. Taken together we can conclude that the polar auxin transport machinery exerts a positive role on infection during symbiosis.

My results supported earlier work showing that addition of IAA to the growth medium was detrimental to organogenesis (van Noorden et al., 2006). In contrast, I observed that external addition of IAA did not affect the number of infection events, namely infection pocket (microcolony) and infection thread formation. The seemingly independent responses of organogenesis and infection to manipulations of auxin in these experiments suggest that auxin has dual roles in both of these distinct developmental programmes. This is supported by the recent finding in our lab that an *mtarf16* mutant has reduced number of infections but the number of nodules is the same as in WT (Breakspear et al., 2014). In natural soil conditions, external IAA can be contributed by rhizobia which produce their own IAA. Inoculation with an IAA overproducing rhizobial strain resulted in an increase in the number of nodules in *M. truncatula* but not in the *Phaseolus vulgaris* interaction with *R. leguminosarum* was reported. Pii et al. used same construct used to infect *Vicia hirsuta* which resulted in a lower number of nodules being formed. Different Sm 1021 strains used between our lab and the published study having different basal levels of IAA production could explain this discrepancy. However, the authors also reported an increase in primary root length contrary to the decrease in root length observed in the present study. Since we know that external application of auxin causes root shortening on plates, bacterially produced IAA can also be expected to cause root shortening. Therefore, similar effects on infection rates by both IAA

addition to external medium and rhizobial overproduction of IAA using the present Sm 1021 strain suggests that bacterially produced auxin does not contribute to rhizobial infection. However we cannot rule out that rhizobially contribute auxin at the correct concentration has an effect on this interaction. The observation that NF alone can initiate organogenesis, it is likely that the inherent plant machinery is sufficient for nodule formation. However, it is very difficult to conclude in general about all symbioses because using *Bradyrhizobium* strains deficient in IAA production, lowers the number of nodules on its host plant (Fukuhara, Minakawa, Akao, & Minamisawa, 1994).

Artificial simulation of constitutive activation and repression of auxin signalling in *Medicago* did not provide clear results about auxins role in symbiosis. No developmental defects were observed in the composite plants presumably due to the use of an infection inducible. Even though there were no differences in nodule number, the sample size was too small to conclusively eliminate a role in organogenesis. Moreover, results from the pharmacological and physiological experiments indicate that auxin might affect infection independently of organogenesis. This study was challenged by the difficulty in counting infections on hairy roots which can vary greatly in both their size and in the expression levels of the transgenes and in which the auxin-cytokinin balance has been altered by *A. rhizogenes*. An ideal experiment would thus involve stable transgenics expressing the constructs developed in this study.

Using data from transcriptomic studies available in the lab, I noted that none of the 10 *M. truncatula* PIN transporters were transcriptionally affected in root hairs upon infection, while *MtLAX2* showed an induction although it was not statistically significant. The experiments described here show expression based association and genetic evidence for an involvement of *MtLAX2* in nodule organogenesis. This finding is not surprising since nodules are believed to be modified lateral roots employing a similar subset of molecular players for initiation and emergence (Couzigou et al., 2012). *ataux1* mutants have a reduced number of lateral roots and in the *Arabidopsis* double mutant *aux1 lax3* lateral roots fail to emerge (Bennett et al., 1996; Marchant et al., 2002; Peret et al., 2007). In *Medicago* as well there is a reduction in nodule number at the two time points tested. *iaa8-1* showed a comparable lowering of nodule number. *MtIAA8* encoding a primary auxin response AUX/IAA protein is expected to act in relevant tissue. A role during infection was not investigated in the present study due to the limitation of time, but is an interesting avenue to explore considering the expression pattern of this gene and my data

suggesting a direct role for auxin in infection. In addition, a better understanding of the changes in auxin signalling resulting in reduced nodule number in these mutants can be explored by using the *DR5-GUS* lines generated during the course of this study. This study thus has set the stage and generated tools for exploring the role of auxin in rhizobial infection and nodule organogenesis.

CHAPTER SIX: General Discussion

6.1 AMNs are novel ABC transporters with conserved roles in rhizobial and mycorrhizal infection

The work presented here describes the identification of three previously uncharacterized ABC transporters named *AMNs* for *ABC* in *Mycorrhization and Nodulation*; which were chosen for this study based on their exclusivity of expression across more than 120 experimental microarray conditions (<http://mtgea.noble.org/jic/>). In light of the presently studied overlap between the two symbioses (Oldroyd, 2013), identification of these transporters involved in rhizobial and mycorrhizal infection promises revelation of hitherto unknown processes basal to development of either symbiosis. Of the 146 full and half molecule ABC transporters encoded in the *M. truncatula* genome for which expression data is presently available, these three are transcriptional induced in both symbioses. The absence of any obvious developmental defect in both single and double mutants suggests that the primary role of these transporters is symbiotic but a low level of expression in the vascular bundles, root apical meristem and lateral root initials found using promoter GUS analyses suggest they might have additional roles in root growth. On the other hand, a low level of expression in vascular bundles, root apical meristem and lateral root initials as detected by promoter-GUS fusions suggests they might have additional roles in root growth. Quantification of root length and lateral root numbers in double and triple mutants will help address these questions.

Upon infection, expression of the AMNs is induced in cells housing infection structures (infected root hair cells and arbusculated cells) (Chapter 3 Figure 3.8, 3.9, 3.10, and 3.11). This partly contradicts an earlier study that used microarray data from laser capture micro-dissected roots and promoter GUS analyses and found the expression of *AMN3* in arbuscule containing cells as found in this study but also in adjacent cells (Gaude, Bortfeld, Duensing, Lohse, & Krajinski, 2012). The authors use 1 kb of the upstream region in contrast to the ~2.4 kb used in the present study which might offer an explanation for the differences observed. Another reason could be different staining times for the GUS assays or simply that an earlier infection time point was analysed in this study. Further expression studies using qPCR over time reveals that expression of the AMNs is associated only with actively progressing mycorrhizal infection. Transfer to phosphorus-replete soil was enough to abolish the expression of these genes (Figure 3.3). This could indicate a role for the AMNs in development of infection structures or nutrient exchange. The AMNs are the first ABC-B transporters in plants identified with a role in symbiotic infection, on which functional genetic studies have been carried out. *AMN1* and *AMN2* are the closest homologues of each other in the *Medicago* genome while *AMN3* stands out among all ABCBs due to the presence of an extra stretch of hydrophilic residues at the N terminus.

Conservation of the AMNs in diverse plant species emphasizes an evolutionarily important role in symbiosis. The presence of *AMN2* and *AMN3* in the actinorhizal plant *Datisca* which forms a root nodule symbiosis with filamentous *Frankia* bacteria and the absence of *AMN* gene induction during infections with root pathogens such as *Phytophthora palmivora* and *Ralstonia solanacearum*, suggests that these transporters are required for processes specific to symbiotic infection. The presence of the AMNs across all mycorrhizal angiosperms including monocots further corroborates their role in symbiotic infection. Interestingly, *Lupinus* as the only non-mycorrhizal legume (Oba, Tawaray, & Wagatsuma, 2001) retained *AMN2* suggesting this gene is necessary for nodulation (Akiyama, Tanigawa, Kashihara, & Hayashi, 2010).

A reverse genetic approach was followed during the course of this study to uncover a functional role for the AMNs in symbiosis. Although the number of pink or white nodules were not significantly reduced in the mutant alleles, a difference in ratios of the Pink/White nodules was found. This might suggest a slight delay in rhizobial progression down the infection thread (Gurich & Gonzalez, 2009). The apparent lack of a symbiotic phenotype in the *amn1amn2* double mutants also raises the

possibility that other functionally redundant transporters are present in the genome which is complicated by the large size of the ABC transporter family and that sequence conservation does not always indicate transport of common substrate. The obvious candidate for a functional homologue as suggested by expression profiles is *AMN3*. A reduction in vesicle number in *amn2 amn3* double mutants is the only mycorrhizal symbiotic phenotype observed in this study from the analysis of stable mutants, however further assessment of the second allelic combination and reproducibility of the observed phenotype are required before any conclusions can be drawn. Vesicles are primarily nutrient storage bodies of the fungus. It is possible that an inability to establish a functional beneficial interaction might cause a shortage in the stored food reserve in vesicles. The triple mutant generated during the course of this study will help overcome the apparent functional redundancy seen amongst the AMNs. Another transporter which could act redundantly is *MtABCB4* which is homologous to *AMN3* and is expressed in root under low phosphate conditions. Expression of *MtABCB4* (Medtr.3g093430.1) according to the *M. truncatula* gene expression atlas, is dramatically induced by mycorrhiza. Therefore we can expect a mild phenotype for the triple mutant.

Localization of these transporters will also give clues as to the function of these transporters. Although, attempts to localize these transporters during the course of this study failed, the AMNs are predicted to be integral to the plasma membrane (PM) using Plant-mPLOC (<http://www.csbio.sjtu.edu.cn/bioinf/plant-multi/>). Additionally, all plant ABCB transporters whose localization has been studied are found in the PM (Rea, 2007). Similar to the *MtPT4* phosphate transporter which localizes exclusively to the peri-arbuscular membrane (Pumplin, Zhang, Noar, & Harrison, 2012) the AMNs might be specifically localized to the infection thread or the peri-arbuscular membrane which are extensions of the main plasma membrane making possible a role in secretion into the Infection thread (IT) lumen or across the peri-arbuscular membrane.

Lastly, attempts were made to identify the transported substrate of the AMNs. All three *AMNs* have at-least one auxin response element (AuxRE) in their promoter. IAA transporting *AtABCB1* and *AtABCB19* are IAA inducible but the three *AMNs* are not at two different time points tested. This could indicate that the *AMNs* do not transport auxin. However further transport assays are required to confirm this hypothesis. A good experimental system would be the *yap1-1* and *gef-1* strains of *S. cerevisiae* which have been established in previous studies to test transport ability

of ABCB transporters (Prusty, Grisafi, & Fink, 2004) (Takanashi, 2011), could be used.

6.2 AMNs are dependent on the Common Symbiosis Signalling pathway for correct expression during either symbiosis

Bacterial symbionts such as rhizobia and fungal symbionts such as mycorrhiza have vastly differing lifestyles. Nevertheless, these symbionts seem to respond to a similar set of plant signals (flavonoids), induce calcium spiking, and utilize a core set of signalling components (*DMI1*, *DMI2*, *CCamK*, *CYCLOPS/IPD3*) (Catoira et al., 2000; Singh, Katzer, Lambert, Cerri, & Parniske, 2014) and structural genes downstream of the pathway such as *VAPYRIN* to establish a beneficial interaction (Murray et al., 2011). However, depending on the microbial signal perceived the developmental outputs are strikingly different. For instance, rhizobia induce the formation of macroscopic nodules containing giant cells that harbour thousands of nitrogen fixing bacteria, while mycorrhizae invade the root cortical cells to form nutrient exchange sites called arbuscules. In addition, autoactivation of the central regulator of symbiosis signalling, *CCaMK* induces the formation of nodule-like structures yet these structures (Gleason et al., 2006) do not develop when host plants are infected with mycorrhizae. These observations suggest that there exists a tight and finely tuned signalling pathway that discriminates between the incoming symbionts and then regulates the activity of downstream genes to bring about developmental changes specific to the needs of one symbiont while at the same time repressing genes involved in associations with the other. Given the existence of such an intricate signalling pathway, it is imperative to understand the regulation of genes which are involved in both rhizobial and mycorrhizal symbioses. The *AMNs* represent an interesting case, described in Chapter 4 I demonstrated that symbiotic induction of the *AMNs* is dependent on the Common symbiosis signalling pathway, using *M. truncatula* mutants of key transcriptional regulators.

Perception of microbial signals such as Nod factors and Myc factors ultimately lead to signature peri-nuclear calcium spiking which are decoded by the kinase, CALCIUM AND CALMODULIN KINASE (*CCaMK*). If *CCaMK* is activated in the absence of these signals, nodule like structures and pre-penetration structures can still be initiated implying that *CCaMK* acts as a master regulator controlling key genes of the symbiosis pathway. Understandably thus, my experiments show that the expression of the *AMNs* upon either rhizobial or mycorrhizal inoculation was completely abolished in the *dmi3 (ccamk)* mutant background (Figure 4.10).

Although a decrease in *AMN1* transcript levels upon mycorrhizal colonization and not rhizobial inoculation or nod factor treatment was statistically significant, it shows a similar trend as both *AMN2* and *AMN3*. It is therefore a reasonable statement to conclude that the induction in gene expression of *AMN1*, *AMN2* and *AMN3* is dependent on CCaMK. Since we know that the AMNs are associated with actively progressing infection (Figure 3.3), no change in *AMN* gene induction in the *dmi3* mutant background which is not colonized at all, might simply be reflecting the absence of infection structures.

I also examined expression of the *AMNs* in the different symbiotic contexts using mutants of key transcriptional regulators. The specificity of the output from the common signalling pathway must depend on the transcriptional regulators acting downstream or parallel to CCaMK. This includes the GRAS transcription factors *NSP1*, *NSP2* and *RAM1* (Gobbato et al., 2012; Hirsch & Oldroyd, 2009). Knockdown of *NSP1* or *NSP2* alone can interfere with nodulation and slightly reduce mycorrhization while a mutation in *RAM1* is sufficient to abolish mycorrhizal colonization but has no effect on mycorrhization. During mycorrhization, *RAM1* is clearly required for the expression of the *AMNs* (Figure 4.10). Surprisingly, neither *NSP1* nor *NSP2* seemed to be required for induction of the *AMNs* during mycorrhization or by Nod factors alone. This contradicts the model that has been proposed, in which *RAM2* and *NSP2* may have analogous functions in the two symbioses and may compete for interactions with *NSP1* (Gobbato et al. 2012). As the case with the regulation by CCaMK, the control of *AMN* expression by *RAM1* may not be direct. However, this could imply the presence of another GRAS transcription factor that control *AMN* expression during nodulation.

Downstream of CCaMK, there are also two nodulation specific transcription factors *NIN* and *ERN1*, mutations in which can impede progression in rhizobial infection. Infection is blocked very early in the *nin* mutant where ITs do not progress beyond the micro-colony stage and root hairs are hyper curled. Higher transcript levels of the *AMNs* in the *nin-1* mutant background could be explained by a negative regulation of the *AMNs* by *NIN*. Alternatively, the *AMNs* might be involved in processes such as root hair curling which is exaggerated in the *nin-1* mutant background. Since many genes normally induced during infection including *NIN* itself are further upregulated in *nin-1* during infection, it is likely due to loss of feedback regulation in the mutants which suggests that control of *AMN* expression is either upstream or parallel to *NIN*. We conclude that, *NIN* is required for optimal expression of the *AMNs*.

My work has therefore shown that the *AMNs* are under the control of the Common Symbiotic signalling pathway and the induction of their expression during symbiosis is dependent on CCaMK. Specifically during mycorrhization but not during nodulation, *AMNs* require the GRAS transcription factor RAM1. Ultimately, the study of *AMN* gene induction will be useful to dissect the two branches of the signalling pathway and help us understand how one pathway can be used to control two symbioses.

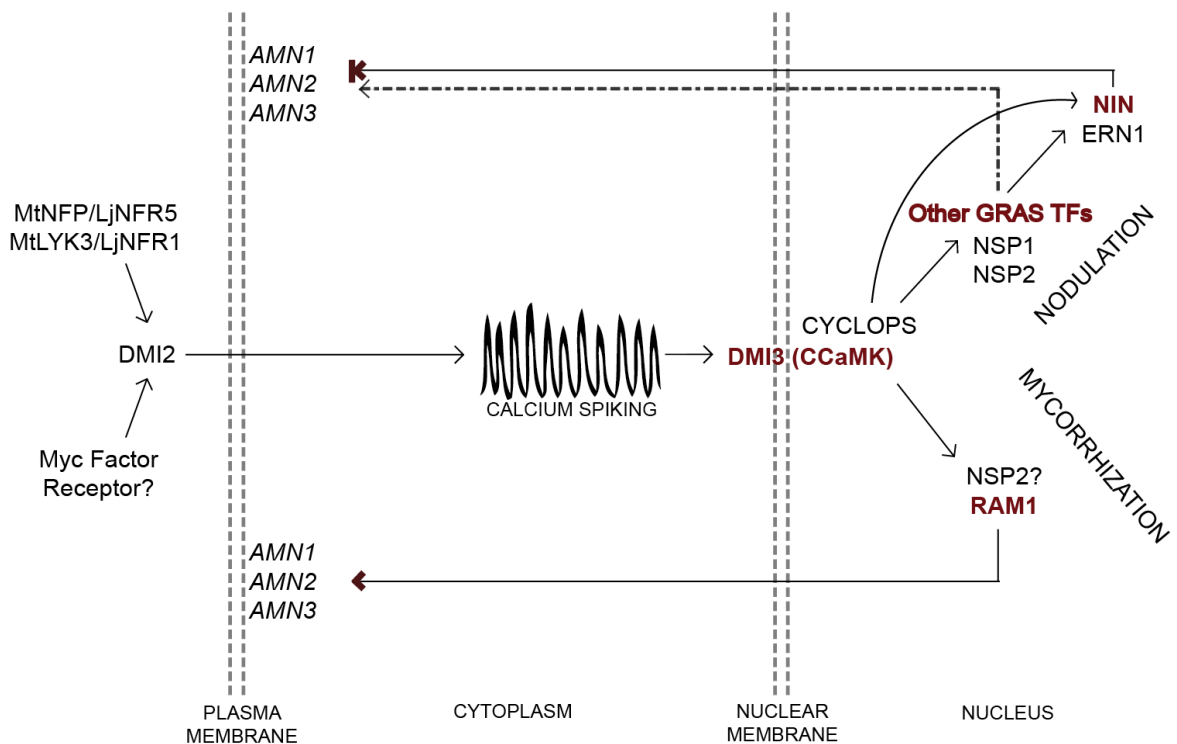


Figure 6.1: A schematic representation of the common symbiosis signalling pathways showing the position of the AMNs

AMN1, *AMN2*, *AMN3* are predicted plasma-membrane ABC transporters that are dependent on components of this pathway. Genes controlling expression of the *AMNs* are highlighted in red. Dashed arrow represents hypothetical pathway as discussed in the text.

6.3 Auxin transport plays an important role in root nodule symbiosis

Root nodule symbiosis can be genetically separated into two distinct developmental programmes – Infection thread development and nodule organogenesis. Although, auxin has been implicated in nodule organogenesis, at present there is no auxin signalling or transport mutant described in the literature, which shows defects in nodule development. Auxin is also thought to have a role associated with bacterial infection during symbiosis between the actinorhizal plant *Casuarina* and the actinomycete *Frankia* (Chapter 1). Our lab has provided the first genetic evidence for auxin's involvement in rhizobial infection in the form of the *mtarf16a* mutant, which has reduced number of ITs but no change in nodule number (Breakspear Liu et al. 2014); however the molecular mechanism is not understood. My research made inroads towards addressing the role of auxin in both rhizobial infection and nodule organogenesis.

I found that mutation in a single gene *MtLAX2*, the orthologue of *AtAUX1*, is sufficient to reduce the total nodule number in *M. truncatula* (Chapter 5). Since nodule organogenesis and lateral root development share many common themes, including the apparent requirement for an auxin influx transporter as shown here, The reduction in nodule number might also reflect a requirement of shoot derived auxin for nodule organogenesis (Marchant et al., 2002). This is therefore the first genetic evidence that auxin transport plays a major role in nodulation. This conclusion is also supported by pharmacological experiments (Figure 5.1) which show that both efflux and influx auxin transport inhibitors are sufficient to alter total nodule number. A reduction in nodule number can occur if there is a defect in nodule initiation, emergence or both. The total number of infections and hence the total nodule number is limited for any particular plant, controlled by the phenomenon of auto regulation of nodule number (AON) (Stougaard 2000); therefore a defect in nodule emergence would be hypothesized to be eventually overcome in symbiosis progression while a defect in nodule initiation would show a persistently lowered number of nodules. The severity of the *MtLAX2* knockdown increases from 30% to 50% over the course of infection indicating that initiation is defective in the mutant. To discriminate between the two, we first need to test whether lateral root phenotype is the same in *Medicago lax2* alleles as this would be a starting point for extrapolating the results from experiments in *Arabidopsis* to *Medicago*. Next, to determine if the *lax2* defect is in nodule initiation nodule count at an early timepoint coinciding with nodule initiation should be done on seedlings stained with a bacterial

visual marker like *lacZ* (necessary to distinguish between nodule and lateral root primordia). If a decrease in nodule primordia is noted even at this time point, *lax2* could be conclusively ascribed to have a defect in nodule initiation. In addition, nodule sections comparing cell size between WT and *lax2* mutants would help determine if cell expansion is compromised in the mutant. Finally, the two *lax2* mutant alleles should be compared to WT plants for differences in total nodule number over time. This is important to ascertain whether the observed defect in total nodule number is sustained with increasing infections at later time points conclusively determining defective nodule initiation or emergence as the cause of reduced nodule numbers in the *lax2* mutants. Developing nodule size could also be monitored to directly assess nodule growth.

Although *lax2* mutant alleles had normally developing ITs (Supplementary Figure 5.2) and *pMtLAX2* expression was not associated with IT progression, we cannot yet dismiss the possibility that auxin has a role in rhizobial infection based on results from pharmacological and physiological experiments. Use of both auxin influx and efflux transporter inhibitors decreased the number of infection threads and infection pockets (Figure 5.1). It could be that the increase auxin signalling in infected root hairs is not dependent on auxin influx, or is dependent on other AUX family members. Removal of the primary source of auxin, the shoot apical meristem, also resulted in decreased number of micro-colonies (Figure 5.4). Together, these results suggest that auxin, specifically auxin transport also influences rhizobial infection. Most rhizobia that produce IAA could act as a source of auxin in nature and therefore contribute to infection (Pii, Crimi, Cremonese, Spena, & Pandolfini, 2007; Zahir, Shah, Naveed, & Akhter, 2010). Surprisingly, auxin supplemented directly to the medium in plates or via auxin overproducing rhizobia did not affect the number of infection threads at the concentrations used (Figure 5.10). This suggests that perturbation of endogenous auxin transport contributes to the frequency of infections and infection progression rather than the overall tissue auxin level. IAA biosynthetic mutants of *S. meliloti*, unidentified to date are needed, to investigate the role of bacterially produced auxin in rhizobial infection and nodule organogenesis.

Of the five members of the LAX family of influx transporters *MtLAX2* is the only one which responds transcriptionally to rhizobial infection in spot inoculated root segments of *M. truncatula* (Jodi Lilley, personal communication), with a presumed role of redistributing auxin to sites of nodule initiation. Changes in auxin concentration at these sites must thus bring about changes in downstream

signalling pathways (Leyser, 2006). Is it then possible that these transporters indirectly control the accumulation of transcription regulators such as ARFs, SAURs and AUX-IAAs which respond to changes in auxin concentrations within minutes. One such candidate supporting this hypothesis would be *MtIAA8* described in Chapter 5 which shows strong expression in infected root hair cells with micro-colonies and progressing ITs. A 30-50% reduction in nodule number is comparable to that seen in *lax2-1* and *lax2-2* mutants. It supports the earlier stated hypothesis that MtLAX2 controls local accumulation of these transcription regulators to affect nodule development (Figure 6.2). This hypothesis can be tested by a simple qPCR experiment comparing expression of *MtIAA8* in *lax2-1* and *lax2-2* mutants to the WT R-108 upon rhizobial infection. Together we will have conclusive proof that auxin controls both rhizobial infection and nodule organogenesis by manipulating its transport.

The expression of *MtIAA8* in infected root hair cells cannot be explained by LAX2 activity. This warrants further investigation, in particular scoring the number of ITs in the *mtiaa8* mutant. Possible functional redundancy of IAA8 function may exist with a close homologue, *MtIAA9*, which responds even more strongly to infection (Breakspear et al., 2014). Therefore an *iaa8 iaa9* double mutant might be needed. This could be achieved either by transcript knock-down in hairy roots, or through isolation of an *iaa9 Tnt1* mutant for crossing with *iaa8*. Together, these results present the first genetic evidence of a role for auxin in nodulation and put forward a mechanistic model connecting auxin transport and auxin signalling in nodule organogenesis.

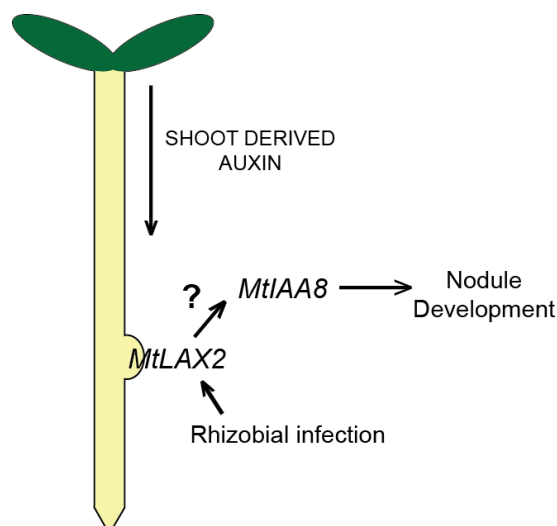


Figure 6.2: Hypothetical model of Auxin transport and its role in symbiotic nodule organogenesis

6.5 Conclusions

Rhizobial infection causes major transcriptional changes in root hairs. The findings here show that some of the molecular machinery is also conserved in mycorrhizal infection. Genes which are shared between the two symbioses are just beginning to be identified and characterized in model legumes. In particular secretion and transport are important physiological processes active at or nearby the site of the interaction be it root hairs or hypodermal passage cells. AMN1 AMN2 and AMN3 are three novel ABCB transporters involved in both rhizobial and mycorrhizal infection. The symbiotic induction of expression which is DMI3 dependent and their absence in non-symbiotic plants supports their role as symbiosis specific transporters while the control of their expression by RAM1 during mycorrhization promises insights into how two very different microbial symbioses are served by a single pathway. While expression and phylogenetic studies have revealed exciting features of these transporters genetic evidence for a functional role remains elusive, with no reduction in total nodule number or mycorrhizal colonization percentage in single mutants, and a modest reduction in vesicle formation in the *amn2 amn3* double mutant. A triple mutant has been generated and its characterization will provide insights into the symbiotic role of the transporters. Whether the AMNs can transport IAA like other ABCBs remains an open question.

The work described here also successfully makes inroads into our present understanding of auxin and its role in nodulation. It shows for the first time, the requirement of an auxin transporter and a component of auxin signalling in nodule organogenesis, and reveals an apparent link between auxin signalling and rhizobial infection. The identification of the genetic components involved and the tools that have been developed should further contribute to the mechanistic understanding of auxin's role in nodulation.

APPENDICES

Appendix 1.1 *AMN1* sequence (As obtained from cDNA sequencing)

atgggaaacaaaggtggattttacgttatgcagatggtgtgacaagtgctattattcttggaaacttgggttgattgg
 tgatggcatacaaactccactcactatgctgttcttggcagtttgatagatgattatgctcgtggtggttctgaacatattg
 gtccattcataatatcaacaagatgctctcaagctacttggtattgccctggagttgcttttctgctttattgttgagat
 gctggacaagaactgcagaaagacaaacttcgaggatgaggattgaatatctaaaatcaatcctaagacaagaa
 gttggttcttggacaagcaaaactaactcttctacaacctccaagtaattgccaccataaactctgatgctcaacaatc
 caagacaccatgctgataaggttcttaattgcttctcagcattttctctagctttatagtgccactcttctctc
 ctgggagactgtagtagctgctttccatttcaattatgatgatcatgccagcactcatattggaaatgctatgaaagag
 ctgggtggtaaaatgaaggatgattcggagttgctggtagcatagcagaacaagcaatctcatcggttcaactggt
 tactcgtacgtaggtgagaagcaaacactgaagagattcagttctgctcttgaacatgatgcagctggcataaag
 caaggtcagacaaagggagtggtggtggaagtttgggtggttatatgctacctgggcattccaatcttgggttgaagt
 gttctggttaggaccaaaaggagaaaaggggtgcaaggtgtttgtgctgaaatatgtattttggggaggattgtctct
 gatgagtgactaccaaatctggctccatattagaggcgacaatagcagctacgaggattttcgagatgattgacag
 aaagccaaccataaactctacaaaagaaaaggaaggtttgaagcatacaagaggagagattacatttaag
 atgtgagtttagttaccctcaaggccagataccctgatttccaaggactcaatctaaagttcaggcatgtaaaca
 gtggcctggttgaggaaagtggttctggaaaatctactataatctttgcttgaagattctatgatcctacatgtggtg
 agatattgctgatggtttgacataaaaagactacaccttaagtgttttagtccctgataggattggtaaatcaagag
 ccaattctattgcaactccataagagagaaacattctatttggaaaggaaggagctcaatggaagatgcataacc
 gcagcaaaaagcagcgaatgcacatgatttcattgtcaaaactccaaatggctatgaaactcaagtaggacaactag
 gagctcaattgtctggaggacaaaacaaaggattgctattgcaagggcttaataagagatcctaaaattctactac
 ttgatgaagccaccagtgcttggattcacaatctgaaagagtgtgacaagatgcactgacttgcttctagaggtag
 aacaacaatcatcatcgtcatcgcttccacgattcgtgaaggctgattcaatagtagttctcaatcaggaaggggtg
 gttgaaagtgttctcacaatgagctactccaactgaacaatggacaaggtgggtttacaccgaaatgctaaattg
 cagcaaaacagcaaaatgaaaatgcacagcatcaataaacaagagccctcgtgcaatggaaaatccaataa
 caagttcaaatccaagccgaaaagtactccaattcatcatgcatttagccctgcacaaccatttagtccatattc
 aatcagtggtatcggctctagctttagatgactacagcagtgaaaacgtggagaaaccttacaatcaaacatctct
 cactggcgttctacaaaatgaatgctcctgagtggaagtagcttgtttggatgtttagggccattggctcaggaata
 tgccaaccattttattcctattgcttaggaatagttgcttctgtctatttcattgatgataatgctcggatcaaatcaaaatc
 aggtgtactcaatcatcttctgctgcatatcggtgtgaactcgtctcaggcctcattcagcatcacaatfttccatcat
 gggagagcgttctgaaaaggggtgcgagagaatttctcagagaaagtgttaacfttgagataggatggttgatca
 agaggagaacacaagtgcagtaactgtgcacgctggcgaccgaagctaacttggtcgtccctcgttcgagaa
 agaatgctggtttagttcaagtctccgttactgcattgctggctttgtacttggttaactggtacatggagggttagctattg

tcatgattgctatgcagcctttgatcattcatgtctctattcaaaaaccgttctcatgaagagtatgacaggaaaagcaa
 aaaatgctcaaagagatgctagtagcaattagcaatggaagctactaccaaccacaggactatcgccgatttcatct
 gagaaaaggatactaaattgttcaaaactgctatggatggccctaagatggaaagcatcaagcaatcatggatttc
 aggttccatattgtctatgtcacagttcataacaacagcatctatagctttgacttttggtagcggaggcatattataaatc
 gtaacaagtcgaatcaaagcaactctgcaagtttctcattttgatgggaactggtagacaaattgctgatacagg
 aagcatgacttctgacatagctaaaagtggaagccattagttcagatattgcaatactggataggaaaactcagat
 tgaacctgaagatactagacacacaaaagtttaaaaagagtatgaagggatgataaaaactgaaagatgtgttttctc
 atactctgcaaggccagaccaaattgattctcaagggtctcagttctgagattgaagccggcaaaaacaattgcattagt
 cggacaaaagtggtcaggaaaatccaccatcattggcttaattgaaagattttatgacctattaagggatccatattc
 atagacaattgtgacatcaaagaacttattgaaaagttgagatcacatattgcattggtagtcaagagcctacac
 tcttctggaaccatacgcgacaacattgtatcgggaaggaagatgcatcagaggctgaaataagaaaagccg
 cacgtctgcaaatgctcatgactttataagtgaatgagagaagggatgatacactgtggagaaaggaggatg
 cagctatcaggaggacagaagcaaaaggatagcaatagctagagcaatgtgaagaatccaccaatacttctgtta
 gatgaggcaacaagtgtcttgacagtgatcagagaatctgtacaagaagcattggagaaaatgatggttgaa
 gaacatgtgtagttatagctaccgttgtcaacaatacaaaagttgattccatagctgtgataaaaatggaaagggtg
 gtggaacaaggttctcattcacagttactgaatgatagatcaaatgggacttattactcttaattagggtacaacaag
 tcattcaactga

Appendix 1.2 *AMN2* sequence (As obtained from cDNA sequencing)

atggggagcaatagcatgttctggtatgcagatggattcgataaattgttgatgttcttcgggactcttggaaagtcttggtg
 atggtctgcagaatcctctcatgatgtacattcttagtgatgtgatcaatgcttatggagataagaatagccgtttaaate
 aacatgatgtgaacaagtttgattgaagctattatgtgtgcaattggagttggaattcagctttattgaaggaatatgt
 tggatagaacagcagagagacaggctcaagaatgagagtggaataacctaaaatcagcttaagacaagaagtt
 ggttctttgacacacaaaactgctggttctcaacaacataccaagttgtctcactcatctcctctgatgcaatacagtc
 caatctgcctgtgtgagaagataccagactgctgacttcatgtcaacattcttttctgccacatcttgcattgtacttt
 catggagactggcattagcagctataccactctccatcatgttcattgtcccggcgttgtattggaaagatcatgttgg
 atgcaaatgaaaatgatagagtcttatggtgtgctgggtggattgcagagcaagcaatatctcaataagaactgtt
 ttctctatgttggggagaatcaaacactaaaaagatttagcactgcacttgaaaaaactatggagtttgaataaagc
 aaggtttgcaaaaggggtgatgttaggaagtatgggagttattatgtaagttggggtttcaagcttgggttgaacttt
 ttgatatccgataaaggagagaaaggtggcatgtattgtagctggcttaacatcttaatgggaggactgagcatttt
 aagtgcacttcaaatttaactgccatcatggaggcaagtccgcggtcactcgctttatgaaatgattgatagggtg
 ccagttatagattctgaagagaagaaaggaaggcttatcacatgtgagaggagaaatgaatttaagacatata
 ctctgttatccatctaggccagattcaccagcttgcaggaattcaatctcattattccagcaggtaagaggataggctc
 tgtgggggtagtggtcaggaaaatccactataattgactgcttgaagggtttatgacctgtcgaggagaaatata
 tattggacggtcacaagattaatagacttcaattgaaatggtgagatctaacttggttagtgaatcaagagcctgtt
 cttttgccacatcataaaagagaatataattgttggaaaagaaggtgcttcaatggaaagtgtgataagtcagcta
 aatcagcaaatgcacatgattcattgtcaattaccagatggatgaaactcaagttggacagtttggattcaactg

tctggtggacagaagcagcgaatcgccatagctagagcttacttagggatccaaaggttctcctgcttgatgaagca
acaagtgcactggatttcaatccgaaagagtggtacaggcagcgatcgatcaagctcaaaaggaagaacaac
aatcattattgctcatcgactgtccacaataagaacagccgacactattgcagtgtcaagcagggaaagtgattga
aacaggtagtcataatgtgctcatggaatcaatgggtgagaaggaggagagtagcgtcgtatggtcaagttgcaa
caagtaacagctcagaatgatgaaatcaagcattccaatctcaattagaaggaaagagctctcacaggatgagca
ttccacaaagtccaggaatgagttcaaatcaagcacaccgggcactccaatgttgatccctcagccagggatttc
cattggcacgccttactcatattctatccagatgatcatgatgatgatagttatgaagatgattttaaagatcaaacca
tccagctccttcacagtgccgttgctgaaaatgaatgcgcccagtggggaagaggagtggtgggagattggga
gcaataggctcaggagcagtacaacctataaatgcatattgtgttgattacttatatcagttattttgaacctgatacct
ctaagatgaagtctaaagctagagccctgccctcgtttcttaggaattggtgttttaactcttcacaagtattctcaa
cactacaattttgctgcatgggagagaggtgactaaaagaattcgggagaaaatactagaaaaattgatgagttt
gagataggatggttgatcatgaagacaacacaagtgcagctatttgcaagattagcctctgaagccaactggtc
cgttcactcgttggcgaccggatgtctcttctggtcaagcaatcttggatccatcttcttacactgtaggactgtgct
cacatggaggcttctcttgatgattgcagtacagccattagtcattggaagcttttatgaagaagtgtttgatgaag
actatggcggaaaaaacccgtaaagcacaacgggaaggaagccaactgcaagtgaagctgttataaaccaca
gaaccataactgcattcagttctcagaaaagaatgttggcactctcaagctacaatgacaggacctaaacagga
gagattaggcagtcattgattcaggtttgtctttcagctcacaattttcaacacttcatcaacagcattggcatattg
gatggtgggagctcctaataaaaaggccaaatagaaccgacggaaactctcaagcatttttaattgctcttactg
catacatcattgcagaagctggaagcatgactctgacatatctaaaggaagcaatgcagttggatcagtttcgctat
cctagacaggaaaagtgagattgatcctgaaaccttatggggagcagataaaaaaggaaaataaggggcagg
gtggagcttaaaaatgtattcttcttatccctctagacctgagcaaatggtattccagggttgaaatctcaaagttgag
gctggacgaacgggtggcactgttagggcacagtgggtgcgtaaatccactatcattggctgattgaaagggtttatg
atccaatcaagggaaactgatgcatagatgaacaagacatcaagacctataacttaagaatgttgaggtcacatatc
gcttagtaagccaggaaccaaccttttagtggaaacctcgggaaaacatcgcatatggaaaagaaaacgcaa
ctgaatctgagataagaagggctgctaccgttgctaagtctcatgaattcataagtggaaatgaatgaagggtatgaaa
cacactgtggagaaagaggagttcagctatcaggaggacagaaacaaagaatagccttagccagagctatacta
aagaatccagcaattcttctctggatgaagctacaagtgcactgtatagtgcatcagaggttttagtccaagaagcac
ttgagaaaataatggttgaagaacatgtatagcagtgccacataggctatcaacaatacagaattcaactccatt
gctgtgattaagaatgggaaagttgtggaacaaggttcacataatgaattgattcacttgaagaatggagcttatc
attctctgttaactcaacatggtagctcccctagggtga

Appendix 1.3 ABC Domain containing genes encoded in *M. truncatula*

<i>Medicago</i> Gene ID	<i>Arabidopsis</i>	Gene Description (TAIR)
ABCA		
Medtr7g091380.1	AT2G41700.1	(ABCA1)
Half		
Medtr3g099990.1	AT3G47730.1	(ABCA2)
Medtr4g108153.1	AT3G47780.1	(ABCA7)
Medtr4g108163.1	AT3G47780.1	(ABCA7)
Medtr4g108170.1	AT3G47780.1	(ABCA7)
Medtr4g108240.1	AT3G47780.1	(ABCA7)
Medtr4g108210.1	AT3G47780.1	ATATH6, ATH6 ABC2
ABCB		
Medtr1g025560.1	AT1G27940.1	(ABCB13)
Medtr1g063170.1	AT2G36910.1	(ABCB1)
Medtr1g086080.1	AT2G47000.1	(ABCB4)
Medtr1g115430.1	AT3G55320.1	(ABCB20)
Medtr2g018320.1	AT4G18050.1	(PGP9)
Medtr3g080220.1	AT1G02520.1	(ABCB11)
Medtr3g086430.1	AT3G28345.1	(ABCB15)
Medtr3g093430.1	AT3G28860.1	(ABCB19)
Medtr3g107800.1	AT1G02520.1	(ABCB11)
Medtr4g077930.1	AT1G02520.1	(ABCB11)
Medtr4g081190.1	AT3G28345.1	(ABCB15)
Medtr4g123990.1	AT1G02520.1	(ABCB11)
Medtr4g124000.1	AT1G02520.1	(ABCB11)
Medtr4g124050.1	AT1G02520.1	(ABCB11))
Medtr5g029750.1	AT4G25960.1	(ABCB2)
Medtr6g008800.1	AT3G28345.1	(ABCB15)
Medtr6g008820.1	AT3G28345.1	(ABCB15)
Medtr6g009030.1	AT3G28345.1	(ABCB15)
Medtr6g011680.1	AT3G28860.1	(ABCB19)
Medtr6g078080.1	AT4G18050.1	(ABCB9)
Medtr7g023340.1	AT3G55320.1	(ABCB20)
Medtr7g051100.1	AT3G28345.1	(ABCB15)
Medtr8g022270.1	AT3G28860.1	(ABCB19)
Medtr2g018530.1	AT4G18050.1	(ABCB9)
Medtr1g086150.1	AT2G47000.1	MDR4, PGP4, ABCB4

Medtr2g018350.1	AT4G18050.1	PGP9
Medtr4g124040.1	AT1G02520.1	PGP11
Medtr7g102070.1	AT2G36910.1	ABCB1
Medtr6g009070.1	AT3G28345.1	
Medtr6g009110.1	AT3G28345.1	
Medtr6g009150.1	AT3G28345.1	
Medtr6g009200.1	AT3G28345.1	
Medtr6g088670.1	AT3G28345.1	
Half		
Medtr1g059830.1	AT5G03910.1	(ABCB29)
Medtr1g086095.1	AT1G02520.1	(ABCB11)
Medtr4g109720.1	AT5G39040.1	(ABCB27)
Medtr5g033080.1	AT1G70610.1	(ABCB26)
Medtr5g075955.1	AT5G58270.1	(ABCB25)
Medtr5g075960.1	AT5G58270.1	(ABCB25)
Medtr6g009080.1	AT3G28345.1	(ABCB15)
Medtr6g465300.1	AT4G25450.1	(ABCB28)
Medtr7g033710.1	AT1G70610.1	(ABCB26)
Medtr8g066710.1	AT4G25960.1	PGP2
ABCC		
Medtr0196s0020.1	AT3G59140.1	(ABCC10)
Medtr1g069450.1	AT1G04120.1	(ATABCC5)
Medtr1g088680.1	AT2G47800.1	(ABCC4)
Medtr1g099280.1	AT3G59140.1	(ABCC10)
Medtr2g019020.1	AT2G34660.1	(AtABCC2)
Medtr2g105190.1	AT2G07680.1	(ABCC13)
Medtr2g436710.1	AT3G62700.1	(ABCC14)
Medtr2g436730.1	AT3G62700.1	(ABCC14)
Medtr3g011820.1	AT1G30400.2	(ABCC1)
Medtr6g034220.1	AT3G59140.1	(ABCC10)
Medtr6g034335.1	AT3G59140.1	(ABCC10)
Medtr6g034350.1	AT3G59140.1	(ABCC10)
Medtr6g084320.1	AT3G21250.1	(ABCC8)
Medtr8g015970.1	AT3G21250.1	(ABCC8)
Medtr8g016020.1	AT3G21250.1	(ABCC8)
Medtr8g016070.1	AT3G21250.1	(ABCC8)
Medtr8g040170.1	AT3G21250.1	(ABCC8)
Medtr8g040620.1	AT3G21250.1	(ABCC8)

Medtr8g061970.1	AT2G47800.1	(ATMRP4)
Medtr8g080050.1	AT3G13080.1	(ABCC3)
Medtr7g098690.1	AT1G04120.1	(ABCC5)
Medtr3g056675.1	AT3G13080.1	(MRP3)
Medtr5g033030.1	AT3G13080.1	(MRP3)
Medtr2g436680.1	AT3G62700.1	ATMRP10
Medtr3g011840.1	AT1G30410.1	ATMRP13
Medtr3g056700.1	AT3G13080.1	ATMRP3,
Medtr5g033320.1	AT3G13080.1	ATMRP3,
Medtr5g094810.1	AT3G13080.1	ATMRP3,
Medtr5g094830.1	AT3G13080.1	ATMRP3,
Medtr6g034230.1	AT3G59140.1	ATMRP14
Medtr6g034265.1	AT3G59140.1	ATMRP14
Medtr6g034270.1	AT3G59140.1	ATMRP14
Medtr6g034310.1	AT3G59140.1	ATMRP14
Medtr6g034755.1	AT3G59140.1	ATMRP14
Medtr8g015980.1	AT3G21250.1	ATMRP6
Half		
Medtr3g056645.1	AT3G13080.1	(ABCC3)
ABCD		
Medtr3g087350.1	AT4G39850.1	(AtABCD1)
Half		
Medtr2g062790.1	AT1G54350.1	(ABCD2)
ABCE (HALF)		
Medtr4g007890.1	AT4G19210.1	(ATRLI2)
Medtr1g024860.1	AT4G19210.1	(ABCE2)
Medtr1g025075.1	AT4G19210.1	(ABCE2)
Medtr1g114170.1	AT4G19210.1	(ABCE2)
ABCF		
Medtr2g095440.1	AT5G60790.1	(ABCF1)
Medtr3g080970.1	AT1G64550.1	(ABCF3)
Medtr3g095010.1	AT5G64840.1	(ABCF5)
Medtr4g057795.1	AT5G60790.1	(ABCF1)
Medtr7g018380.1	AT3G54540.1	(ABCF4)
Medtr8g075040.1	AT3G54540.1	(ABCF4)
ABCG		
Medtr1g011650.1	AT1G15520.1	PDR12

Medtr2g102660.1	AT1G15520.1	PDR12
Medtr2g102670.1	AT1G15520.1	PDR12
Medtr4g011630.1	AT1G15520.1	PDR12
Medtr4g011640.1	AT1G15520.1	PDR12
Medtr7g098320.1	AT1G15520.1	PDR12
Medtr7g098370.1	AT1G15520.1	PDR12
Medtr7g098750.1	AT1G15520.1	PDR12
Medtr7g098760.1	AT1G15520.1	PDR12
Medtr7g098780.1	AT1G15520.1	PDR12
Medtr7g098800.1	AT1G15520.1	PDR12
Medtr7g104130.1	AT1G66950.1	PDR11
Medtr7g104150.1	AT1G66950.1	PDR11
Medtr1g011640.1	AT1G15520.1	(ATABCG40)
Medtr1g050525.1	AT2G36380.1	(ABCG34)
Medtr1g492950.1	AT2G36380.1	(ABCG34)
Medtr2g078080.1	AT1G53270.1	(ABCG10)
Medtr2g101090.1	AT1G59870.1	(ABCG36)
Medtr2g102640.1	AT1G15520.1	(ATABCG40)
Medtr3g107870.1	AT1G15520.1	(ATABCG40)
Medtr3g463680.1	AT2G29940.1	(ABCG31)
Medtr4g011620.1	AT1G15520.1	(ABCG31)
Medtr4g113070.1	AT2G26910.1	(PDR4)
Medtr4g123850.1	AT3G53480.1	(ABCG37)
Medtr5g070320.1	AT2G29940.1	(ABCG31)
Medtr7g098300.1	AT1G15520.1	(PDR12)
Medtr7g098740.1	AT1G15520.1	(PDR12)
Medtr7g104100.1	AT1G66950.1	(PDR11)
Medtr8g014360.1	AT1G59870.1	(ABCG36)
Half		
Medtr1g054935.1	AT5G06530.1	(ABCG22)
Medtr1g054960.1	AT5G06530.1	ABCG G22 (ABCG22)
Medtr1g093990.1	AT1G31770.1	(ABCG14)
Medtr1g096580.1	AT1G71960.1	(ABCG25)
Medtr1g099570.1	AT5G52860.1	(ABCG8)
Medtr1g108340.1	AT2G01320.2	(ABCG7)
Medtr1g115790.1	AT2G39350.1	(ABCG1)
Medtr2g095390.1	AT2G28070.1	(ABCG3)
Medtr3g096410.1	AT2G13610.1	(ABCG5)
Medtr4g054020.1	AT1G17840.1	(ABCG11)

Medtr4g058000.1	AT5G60740.1	(ABCG28)
Medtr4g076900.1	AT3G21090.1	(ABCG15)
Medtr4g076940.1	AT3G21090.1	(ABCG15)
Medtr4g076970.1	AT3G21090.1	(ABCG15)
Medtr4g093845.1	AT1G17840.1	(ABCG11)
Medtr4g094010.1	AT1G17840.1	(ABCG11)
Medtr4g094050.1	AT1G17840.1	(ABCG11)
Medtr4g094060.1	AT1G17840.1	(ABCG11)
Medtr4g094090.1	AT1G17840.1	(ABCG11)
Medtr5g025470.1	AT1G31770.1	(ABCG14)
Medtr5g096390.1	AT3G13220.1	(ABCG26)
Medtr6g066240.1	AT1G17840.1	(ABCG11)
Medtr7g100120.1	AT2G37360.1	(ABCG2)
Medtr7g106880.1	AT5G06530.1	(ABCG22)
Medtr8g059150.1	AT4G27420.1	(ABCG9)
Medtr8g093840.1	AT2G13610.1	(ABCG5)
Medtr8g107450.1	AT3G55130.1	(ABCG19)
Medtr4g116540.1	AT5G19410.1	ABC-2
Medtr5g030910.1	AT3G55130.1	ATWBC19,
Medtr3g040670.1	AT5G19410.1	(ABCG23)
Medtr1g094660.1	AT1G53390.1	(ABCG24)
ABCH		
None		
ABCI		
Medtr1567s0010.1	AT1G67940.1	(ABCI17)
Medtr1g063920.1	AT2G37010.1	(NAP12)
Medtr3g096300.1	AT4G33460.1	(ABCI10)
Medtr4g131330.1	AT1G63270.1	(ABCI1)
Medtr7g079540.1	AT1G65410.1	(ABCI13)
Medtr7g101780.1	AT2G37010.1	(NAP12)
Medtr8g101390.1	AT3G10670.1	(NAP7)
Medtr8g107410.1	AT1G67940.1	(ABCI17)
Medtr8g442660.1	AT4G33460.1	(ABCI10)

Appendix Table S.1: *M. truncatula* ABC transporters and their closest *Arabidopsis* homologue, identified in this study

Appendix 1.4: Accession numbers of ABC transporters homologous to *AMN1*, *AMN2*, and *AMN3* across dicots which can either nodulate or mycorrhize

NAME	SCIENTIFIC NAME	ACCESSION NUMBER
Cicer_AMN1	<i>Cicer arietinum</i>	XP_004502504.1
Citrus_AMN1	<i>Citrus sinensis</i>	XP_006484330.1
Cucumis_AMN1	<i>Cucumis sativus</i>	XP_004135503.1
Fragaria_AMN1	<i>Fragaria vesca</i> subsp. <i>Vesca</i>	XP_004310162.1
<i>Medicago</i> _AMN1	<i>Medicago truncatula</i>	
Morus_AMN1	<i>Morus notabilis</i>	EXB82471.1
Phaseolus_AMN1	<i>Phaseolus vulgaris</i>	XP_007163694.1
Prunus_AMN1	<i>Prunus persica</i>	XP_007224599.1
Ricinus_AMN1	<i>Ricinus communis</i>	XP_002515049.1
Solanum_AMN1	<i>Solanum lycopersicum</i>	XP_004239490.1
Theobroma_AMN1	<i>Theobroma cacao</i>	XP_007044881.1
Vitis_AMN1	<i>Vitis vinifera</i>	XP_002282137.2
Cicer_AMN2	<i>Cicer arietinum</i>	XP_004505438.1
Citrus_AMN2	<i>Citrus sinensis</i>	XP_006475215.1
Cucumis_AMN2	<i>Cucumis sativus</i>	XP_004151954.1
Datisca_AMN2	<i>Datisca glomerata</i>	
Fragaria_AMN2	<i>Fragaria vesca</i> subsp. <i>Vesca</i>	XP_004295792.1
Glycine_AMN2	<i>Glycine max</i>	XP_003541009.2
Glycine_AMN2	<i>Glycine max</i>	XP_003526190.2
Lotus_AMN2	<i>Lotus japonicus</i>	chr3.CM1543.140.r2.m
Lupin_AMN2	<i>Lupinus</i>	
<i>Medicago</i> _AMN2	<i>Medicago truncatula</i>	XP_003607685.1
Morus_AMN2	<i>Morus notabilis</i>	EXC05113.1
Cicer_AMN3	<i>Cicer arietinum</i>	XP_004510541.1
Cucumis_AMN3	<i>Cucumis sativus</i>	XP_004155963.1
Datisca_AMN3	<i>Datisca</i>	
Fragaria_AMN3	<i>Fragaria vesca</i> subsp. <i>Vesca</i>	XP_004305767.1
glycine_AMN3	<i>Glycine max</i>	XP_003548375.1
Lotus_AMN3	<i>Lotus japonicus</i>	chr3.CM0416.610.r2.a
<i>Medicago</i> _AMN3	<i>Medicago truncatula</i>	XP_003627370.1
Populus_AMN3	<i>Populus trichocarpa</i>	XP_006369112.1
Prunus_AMN3	<i>Prunus persica</i>	XP_007216167.1
Ricinus_AMN3	<i>Ricinus communis</i>	XP_002529182.1
Solanum_AMN3	<i>Solanum lycopersicum</i>	XP_004236380.1
Theobroma_AMN3	<i>Theobroma cacao</i>	XP_007024714.1
Vitis_AMN3	<i>Vitis vinifera</i>	XP_003632759.1
<i>Arabidopsis</i>	<i>Arabidopsis thaliana</i>	NP_189475.1

<i>thaliana</i>		
Oryza	<i>Oryza sativa</i>	Q6YUU5.1

Appendix Table S.2: Accession numbers of all AMN1, AMN2 and AMN3 homologues used to prepare the phylogenetic tree in Figure 3.3

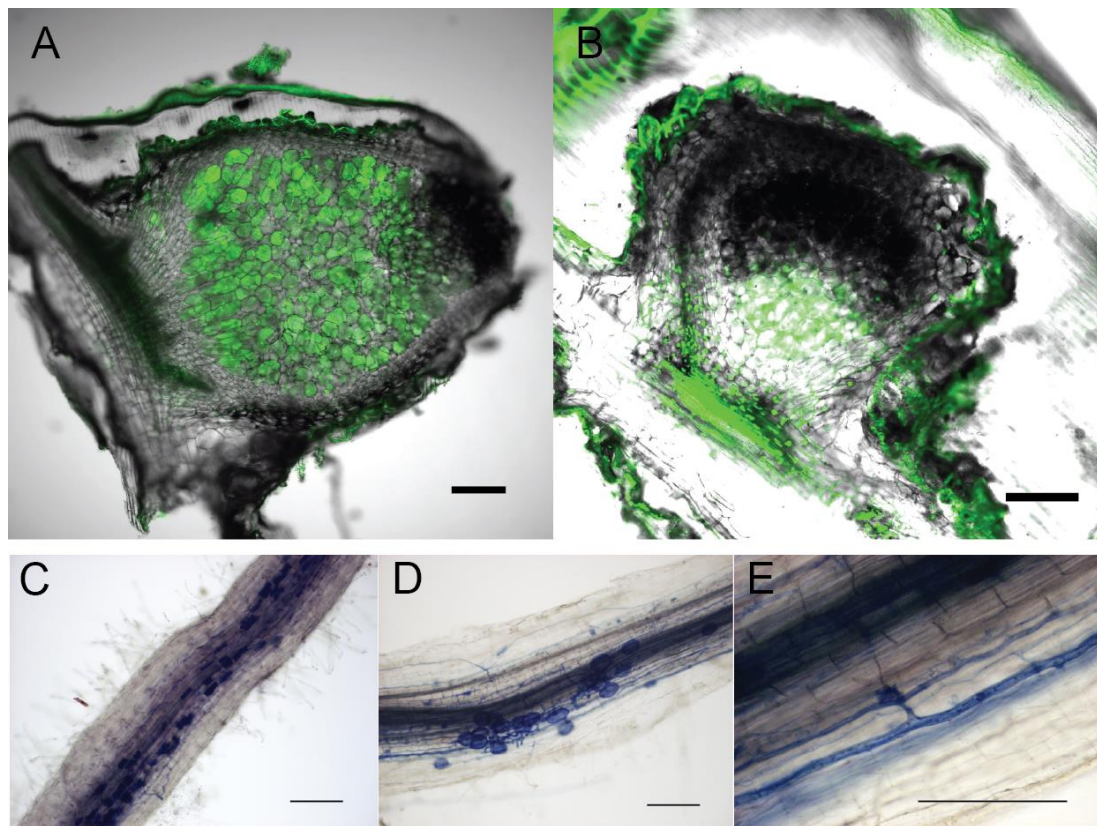
Appendix 1.5: Putative Transcription factor binding sites common to 2 kb Upstream region of *AMN1*, *AMN2*, and *AMN3*

TRANSCRIPTION FACTOR		DESCRIPTION
HORMONE		
1	P\$ARE.01	Auxin Response Element
2	P\$GAMYB.01	GA-regulated myb gene from barley
3	P\$TL1.01	Cis-element involved in SA (salicylic acid) induction of secretion-related genes via NPR1
4	P\$TEIL.01	Ethylene insensitive 3 like factors
5	P\$JARE.01	Jasmonate response element
SYMBIOSIS RELATED		
6	P\$PHR1.01	Phosphate starvation response 1
7	P\$NCS1.01	Nodulin consensus sequence 1
8	P\$NCS2.01	Nodulin consensus sequence 2
9	P\$NRE.01	Nitrate-responsive element
SECONDARY CELL WALL		
10	P\$SNBE.01	Secondary wall NAC binding elements (NAM, ATAF1/2, and CUC2)
11	P\$SMRE.01	Secondary wall MYB-responsive element, MYB46 and MYB83 binding sites
12	P\$CBNAC.02	Calmodulin-binding NAC protein
13	P\$TANAC69.03	Wheat NAC-domain DNA binding factor (DNA binding site II)
SUGAR		
14	P\$STK.01	Storekeeper (STK), plant specific DNA binding protein important for tuber-specific and sucrose-inducible gene expression
15	P\$SUCROSE.01	Sucrose Box- Sequence motif from the promoters of different sugar-responsive genes
WRKY		
16	P\$WRKY.01	WRKY plant specific zinc-finger-type factor associated with pathogen defence, W box
17	P\$WRKY11.01	Calmodulin binding WRKY transcription factor 11
18	P\$SP8BF.01	DNA-binding protein of sweet potato that binds to the SP8a (ACTGTGTA) and SP8b (TACTATT) sequences of sporamin and beta-amylase genes
LIGHT		

19	P\$GAP.01	Cis-element in the GAPDH promoters conferring light inducibility
20	P\$RAP22.01	RAP2.2, involved in carotenoid and tocopherol biosynthesis and in the expression of photosynthesis-related genes
21	P\$GAAA.01	GAAA motif involved in pollen specific transcriptional activation
22	P\$OCSL.01	Enhancer element first identified in the promoter of the octopine synthase gene (OCS) of the <i>Agrobacterium tumefaciens</i> T-DNA
23	P\$TERE.01	Tracheary-element-regulating cis-elements, conferring TE-specific expression
DEVELOPMENT		
24	P\$REVOLUTA.01	Homeobox-leucine zipper protein REVOLUTA (REV, IFL1)
25	P\$WUS.01	Homeodomain protein WUSCHEL
26	P\$RITA1.01	Rice transcription activator-1 (RITA), basic leucine zipper protein, highly expressed during seed development
27	P\$LFY.01	Plant specific floral meristem identity gene LEAFY (LFY)
28	P\$BLR.01	Transcriptional repressor BELLRINGER
29	P\$PIL5.01	Phytochrome interacting factor3-like 5
30	P\$AS1_AS2_II.01	AS1/AS2 repressor complex binding motif II
31	P\$SBP.01	SQUA promoter binding proteins
32	P\$ATHB5.01	HDZip class I protein ATHB5
33	P\$ATHB1.01	<i>Arabidopsis thaliana</i> homeo box protein 1
34	P\$FLC.01	Flowering locus C
35	P\$AP2.01	APETALA2
36	P\$ATML1.01	L1-specific homeodomain protein ATML1 (<i>A. thaliana</i> meristem layer 1)
37	P\$AG.01	Agamous, required for normal flower development, similarity to SRF (human) and MCM (yeast) proteins
38	P\$ATML1.02	<i>Arabidopsis thaliana</i> meristem layer 1
39	P\$AGL15.01	AGL15, <i>Arabidopsis</i> MADS-domain protein AGAMOUS-like 15
40	P\$SOC1.01	Suppressor of overexpression of CO 1 (AGL20)

Appendix Table S.3: List of Transcription factor binding sites common to the 2 Kb region upstream of *AMN1*, *AMN2* and *AMN3*

Appendix 1.6: Infection structures in *AMN1/AMN2* RNAi lines upon nodulation and mycorrhization

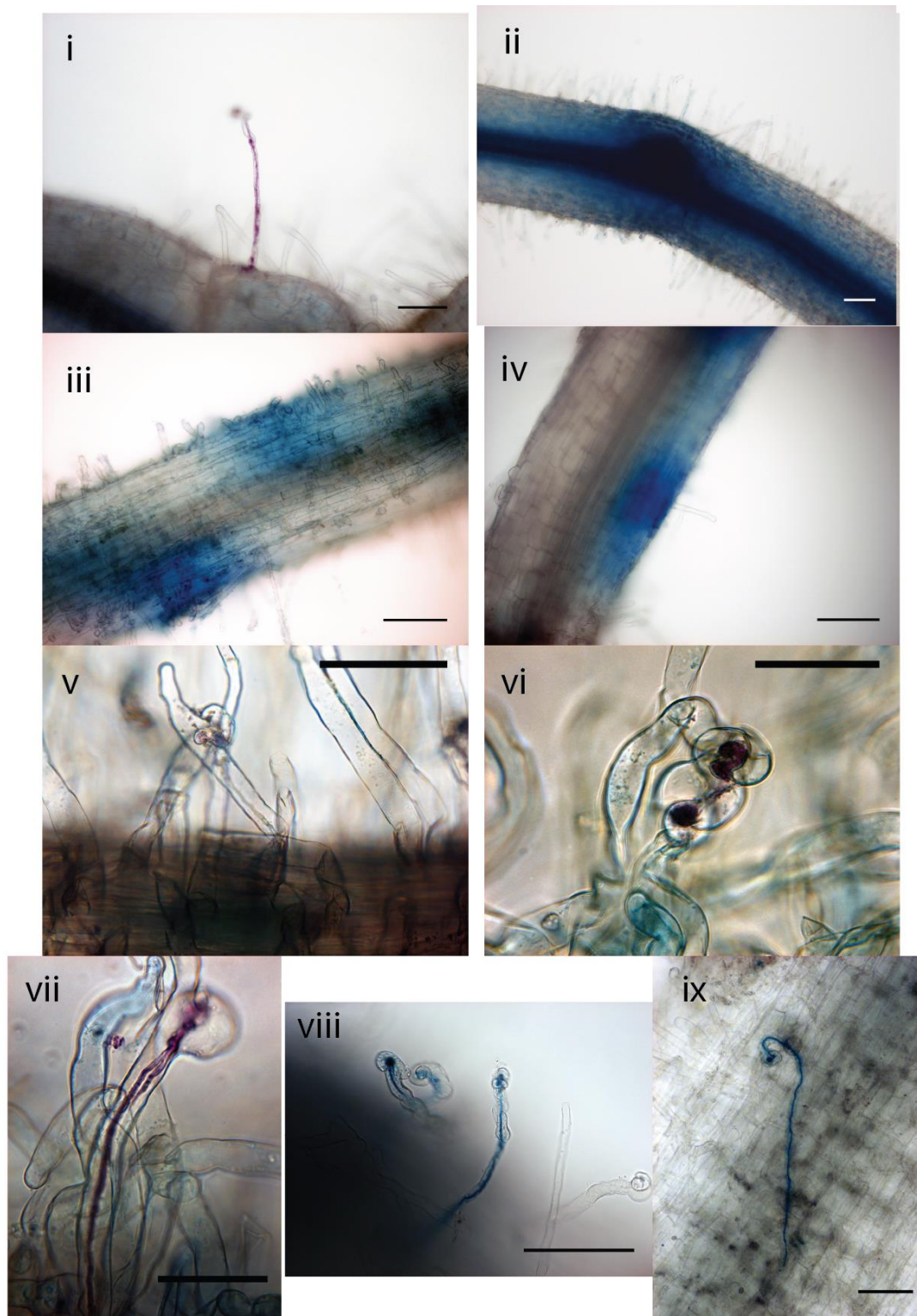


Supplementary Figure 4.1: Infection associated structures in RNAi Knockdown roots

A. WT EV transformed roots develop elongated nodules which are fully colonized by bacteria (stained with SYTO13) B. RNAi Knockdown roots develop small misshapen nodules which get colonized normally C. WT EV transformed root infected with *R. irregularis* are colonized normally and arbuscules are visible in the cortex D. RNAi knockdown roots show fewer arbuscule structures E. Higher magnification of root section in D showing initiating arbuscule

Scale bar represents 100 μm

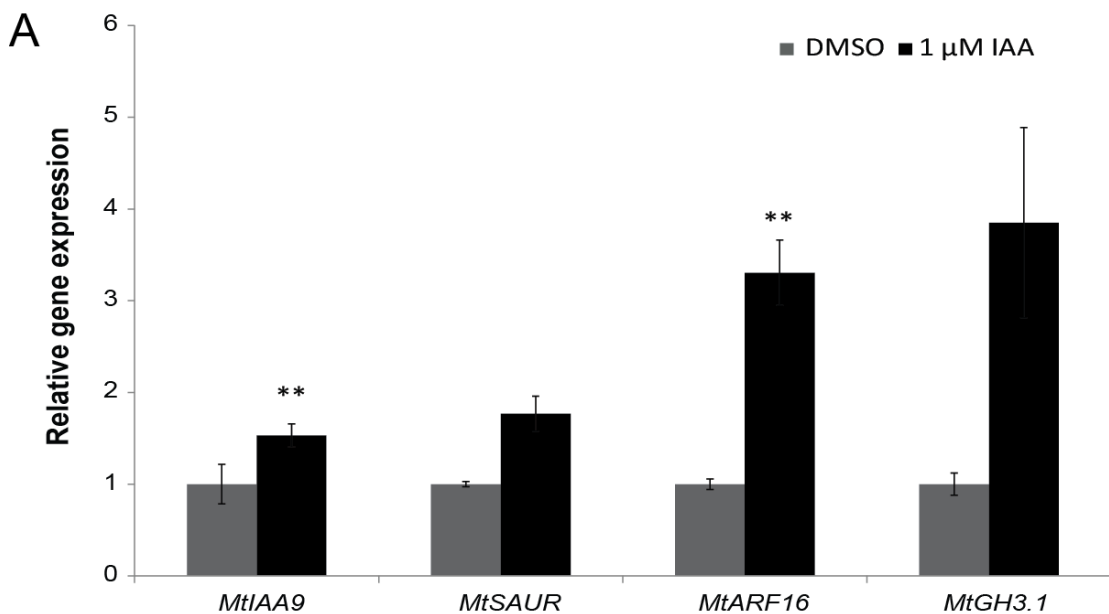
Appendix 1.7 Infection structures on *lax2* mutants and promoter-GUS analyses of auxin markers in *M. truncatula*



Supplementary Figure 5.2: *M. truncatula* roots showing expression of different marker genes

β -glucuronidase enzyme activity is visualized in blue. β -Galactosidase (LacZ) activity in magenta. i *pLAX2* expression is not associated with infection thread containing root hair cells ii *pLAX2* expression is associated with the vascular bundle and lateral root in uninfected roots iii, iv expression of *pLAX2* is associated with epidermal cells not responding to infection 3wpi v *pAtAUX1* in *P. sativum* is expressed below curled root hair 7 dpi vi, vii Expression of soybean *GH3* in *M. truncatula* stable lines is not associated with infection structures viii, ix Infection structures develop normally in *lax2-2* and *lax2-1* mutants of *M. truncatula*. LacZ expressing rhizobia stained in Blue.

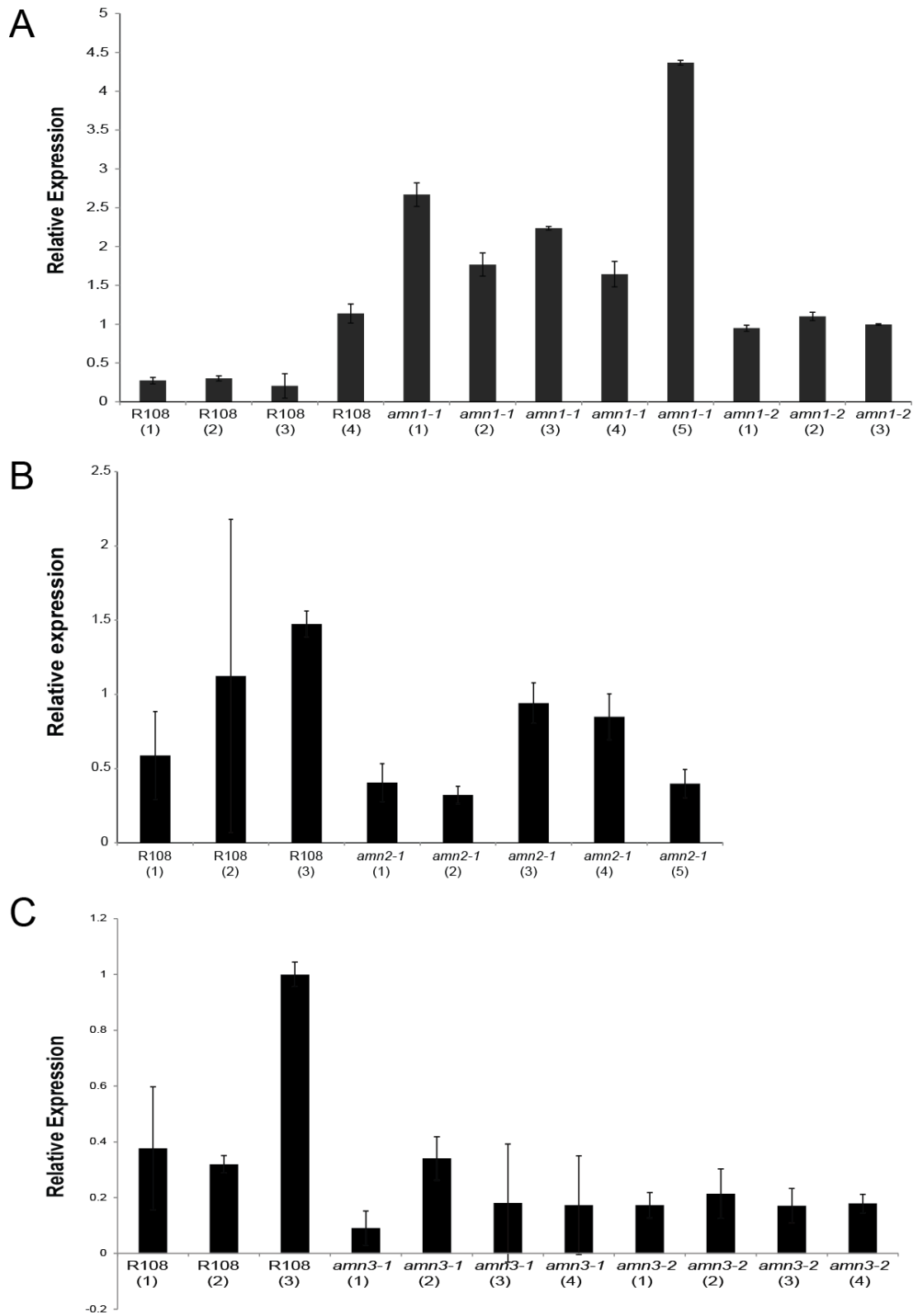
Appendix 1.8 Quantitative RT PCR showing auxin responsiveness of infection induced genes



Supplementary Figure 5.3: Quantitative RT-PCR validation of auxin responsiveness of infection induced genes

Change in gene expression upon IAA treatment of *M. truncatula* roots relative to solvent treated controls. *MtSAUR*, *MtARF16*, *MtGH3.1* were confirmed by promoter GUS experiment to be expressed in infection thread containing root hair cells. Values represent average of three biological replicates each consisting of 10 seedlings each. Error bars depict standard error. Student's t-test was carried out to determine statistical significance, ** $p < 0.01$. All primers used were taken from (Breakspear, Liu et al. 2014).

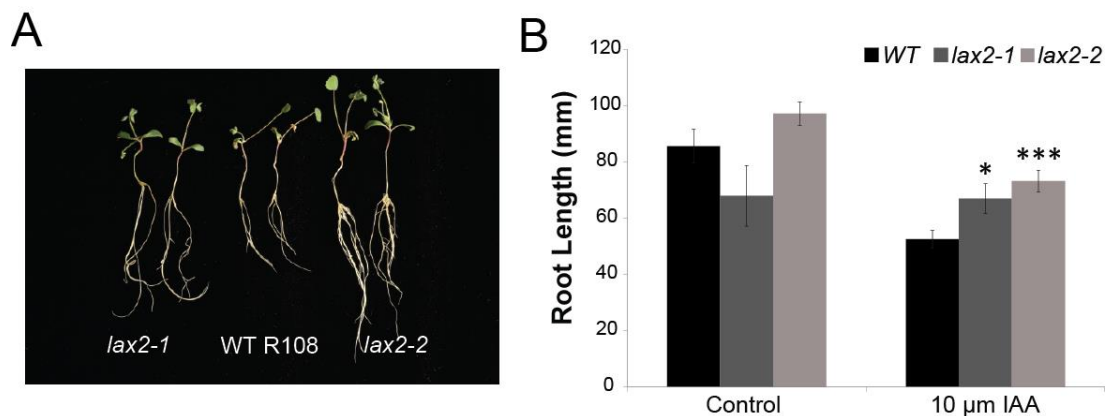
Appendix 1.9 Quantitative RT PCR showing expression of *AMN* transcripts in their respective mutant backgrounds



Supplementary Figure 4.4: Quantitative RT-PCR determination of AMN transcript abundance in their respective mutant backgrounds

Relative transcript abundance in WT R 108 and alleles of (a) *amn1* (b) *amn2* and (c) *amn3* of *Medicago truncatula*. Values represent average of three technical replicates per line. Error bars represent standard error of the mean. Primers used *AMN1* (P_5 and P_6) *AMN2* (P_11 and P_12) and *AMN3* (P_13 and P_14)

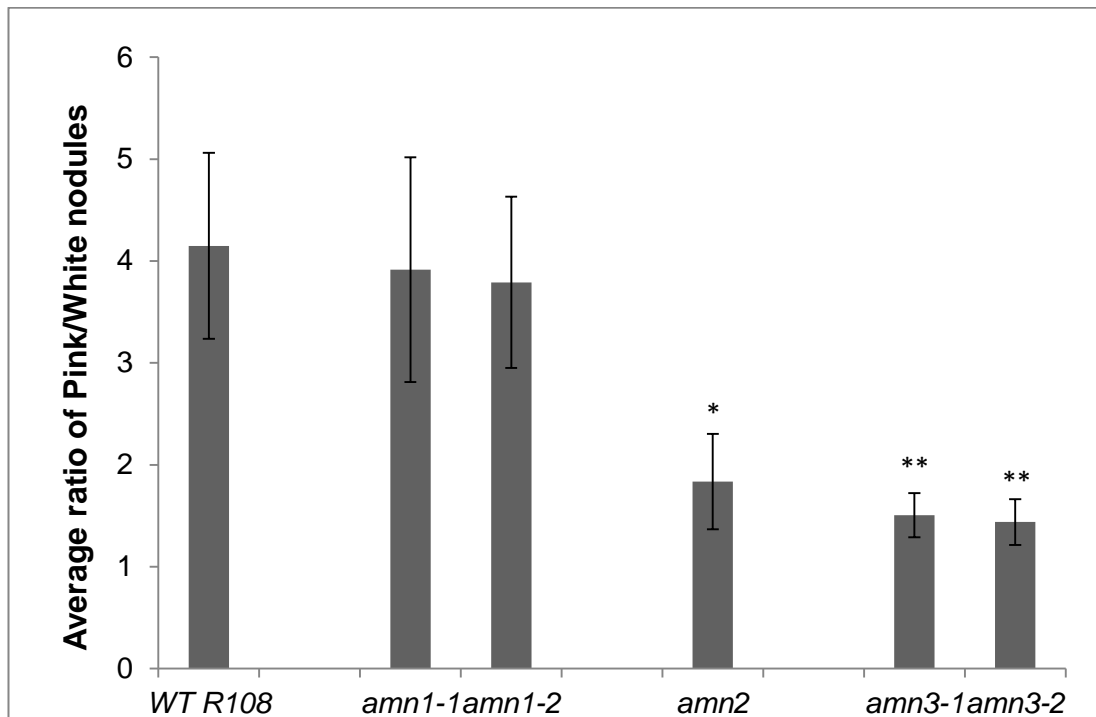
Appendix 1.10 Sensitivity of *lax2-1* and *lax2-2* mutants to IAA compared to WT R108 Control



Supplementary Figure 5.5: *lax2-1* and *lax2-2* mutant seedlings are sensitive to IAA compared to WT R108 Control

A. Representative photograph showing longer root length of *lax2-1* and *lax2-2* seedlings compared to WT R108 grown on 10 µm IAA 15 days post germination.

B. Quantification of root lengths grown with and without 10 µm IAA on water agar plates 15 days post germination. Values represent average of mean (n=4-6). Error bars depict the S.E * $p < 0.01$ *** $p < 0.001$ using a Student's t-test

Appendix 1.11 Ratio of pink/white nodules in *amn* single mutants**Supplementary Figure 5.6: Graph comparing average ratio of pink/white nodules per mutant**

Values represent average of ratios calculated for each individual (n=20-24). Error bars depict the S.E * $p < 0.05$. ** $p < 0.01$ using a Student's t-test

REFERENCES

- Akiyama, K., H. Matsuoka and H. Hayashi. "Isolation and Identification of a Phosphate Deficiency-Induced C-Glycosylflavonoid That Stimulates Arbuscular Mycorrhiza Formation in Melon Roots." *Mol Plant Microbe Interact* 15, no. 4 (2002): 334-40.
- Akiyama, K., K. Matsuzaki and H. Hayashi. "Plant Sesquiterpenes Induce Hyphal Branching in Arbuscular Mycorrhizal Fungi." *Nature* 435, no. 7043 (2005): 824-7.
- Akiyama, K., F. Tanigawa, T. Kashiwara and H. Hayashi. "Lupin Pyranoisoflavones Inhibiting Hyphal Development in Arbuscular Mycorrhizal Fungi." *Phytochemistry* 71, no. 16 (2010): 1865-71.
- Badri, D. V., N. Quintana, E. G. El Kassis, H. K. Kim, Y. H. Choi, A. Sugiyama, R. Verpoorte, E. Martinoia, D. K. Manter and J. M. Vivanco. "An ABC Transporter Mutation Alters Root Exudation of Phytochemicals That Provoke an Overhaul of Natural Soil Microbiota." *Plant Physiol* 151, no. 4 (2009): 2006-17.
- Bailly, A., V. Sovero, V. Vincenzetti, D. Santelia, D. Bartnik, B. W. Koenig, S. Mancuso, E. Martinoia and M. Geisler. "Modulation of P-Glycoproteins by Auxin Transport Inhibitors Is Mediated by Interaction with Immunophilins." *J Biol Chem* 283, no. 31 (2008): 21817-26.
- Banasiak, J., W. Biala, A. Staszko, B. Swarczewicz, E. Kepczynska, M. Figlerowicz and M. Jasinski. "A *Medicago truncatula* ABCTransporter Belonging to Subfamily G Modulates the Level of Isoflavonoids." *Journal of Experimental Botany* 64, no. 4 (2013): 1005-1015.
- Band, L. R., D. M. Wells, J. A. Fozard, T. Ghetiu, A. P. French, M. P. Pound, M. H. Wilson, L. Yu, W. Li, H. I. Hijazi, J. Oh, S. P. Pearce, M. A. Perez-Amador, J. Yun, E. Kramer, J. M. Alonso, C. Godin, T. Vernoux, T. C. Hodgman, T. P. Pridmore, R. Swarup, J. R. King and M. J. Bennett. "Systems Analysis of Auxin Transport in the *Arabidopsis* Root Apex." *Plant Cell* 26, no. 3 (2014): 862-75.
- Bapaume, Laure and Didier Reinhardt. "How Membranes Shape Plant Symbioses: Signaling and Transport in Nodulation and Arbuscular Mycorrhiza." *Frontiers in Plant Science* 3, (2012).
- Barker, David G, Sylvie Bianchi, François Blondon, Yvette Dattée, Gérard Duc, Sadi Essad, Pascal Flament, Philippe Gallusci, Gérard Génier, Pierre Guy, Xavier Muel, Jacques Tourneur, Jean Dénarié and Thierry Huguet. "*Medicago truncatula*, a Model Plant for Studying the Molecular Genetics of The rhizobium-Legume Symbiosis." *Plant Molecular Biology Reporter* 8, no. 1 (1990): 40-49.
- Ben Amor, B. "The *NFP* Locus of *Medicago truncatula* Controls an Early Step of Nod Factor Signal Transduction Upstream of a Rapid Calcium Flux and Root

- Hair Deformation (Vol 34, Pg 495, 2003)." *Plant Journal* 35, no. 1 (2003): 140-140.
- Benedito, V. A., H. Li, X. Dai, M. Wandrey, J. He, R. Kaundal, I. Torres-Jerez, S. K. Gomez, M. J. Harrison, Y. Tang, P. X. Zhao and M. K. Udvardi. "Genomic Inventory and Transcriptional Analysis of *Medicago truncatula* Transporters." *Plant Physiol* 152, no. 3 (2010): 1716-30.
- Benedito, V. A., I. Torres-Jerez, J. D. Murray, A. Andriankaja, S. Allen, K. Kakar, M. Wandrey, J. Verdier, H. Zuber, T. Ott, S. Moreau, A. Niebel, T. Frickey, G. Weiller, J. He, X. B. Dai, P. X. Zhao, Y. H. Tang and M. K. Udvardi. "A Gene Expression Atlas of the Model Legume *Medicago truncatula*." *Plant Journal* 55, no. 3 (2008): 504-513.
- Bennett, M. J., A. Marchant, H. G. Green, S. T. May, S. P. Ward, P. A. Millner, A. R. Walker, B. Schulz and K. A. Feldmann. "*Arabidopsis* AUX1 Gene: A Permease-Like Regulator of Root Gravitropism." *Science* 273, no. 5277 (1996): 948-50.
- Besserer, A., V. Puech-Pages, P. Kiefer, V. Gomez-Roldan, A. Jauneau, S. Roy, J. C. Portais, C. Roux, G. Becard and N. Sejalon-Delmas. "Strigolactones Stimulate Arbuscular Mycorrhizal Fungi by Activating Mitochondria." *PLoS Biol* 4, no. 7 (2006): e226.
- Bonfante, P. and A. Genre. "Mechanisms Underlying Beneficial Plant-Fungus Interactions in Mycorrhizal Symbiosis." *Nat Commun* 1, (2010): 48.
- Boot, Kees J. M., Anton A. N. van Brussel, Teun Tak, Herman P. Spaijk and Jan W. Kijne. "Lipo-chitin Oligosaccharides from *Rhizobium Leguminosarum* Bv. *Viciae* Reduce Auxin Transport Capacity in *Vicia Sativa* Subsp. *Nigra* Roots." *Molecular Plant-Microbe Interactions* 12, no. 10 (1999): 839-844.
- Breakspear, A., C. Liu, S. Roy, N. Stacey, C. Rogers, M. Trick, G. Morieri, K. S. Mysore, J. Wen, G. E. Oldroyd, J. A. Downie and J. D. Murray. "The Root Hair "Infectome" of *Medicago truncatula* Uncovers Changes in Cell Cycle Genes and Reveals a Requirement for Auxin Signaling in Rhizobial Infection." *Plant Cell*, (2014).
- Brechenmacher, L., Z. Lei, M. Libault, S. Findley, M. Sugawara, M. J. Sadowsky, L. W. Sumner and G. Stacey. "Soybean Metabolites Regulated in Root Hairs in Response to the Symbiotic Bacterium *Bradyrhizobium Japonicum*." *Plant Physiol* 153, no. 4 (2010): 1808-22.
- Brewin, Nicholas J. "Plant Cell Wall Remodelling in the Rhizobium–Legume Symbiosis." *Critical Reviews in Plant Sciences* 23, no. 4 (2004): 293-316.
- Brunoud, G., D. M. Wells, M. Oliva, A. Larrieu, V. Mirabet, A. H. Burrow, T. Beeckman, S. Kepinski, J. Traas, M. J. Bennett and T. Vernoux. "A Novel Sensor to Map Auxin Response and Distribution at High Spatio-Temporal Resolution." *Nature* 482, no. 7383 (2012): 103-6.
- Buer, C. S., G. K. Muday and M. A. Djordjevic. "Flavonoids Are Differentially Taken up and Transported Long Distances in *Arabidopsis*." *Plant Physiol* 145, no. 2 (2007): 478-90.
- Bulgarelli, D., M. Rott, K. Schlaeppli, E. Ver Loren van Themaat, N. Ahmadinejad, F. Assenza, P. Rauf, B. Huettel, R. Reinhardt, E. Schmelzer, J. Peplies, F. O.

- Gloeckner, R. Amann, T. Eickhorst and P. Schulze-Lefert. "Revealing Structure and Assembly Cues for *Arabidopsis* Root-Inhabiting Bacterial Microbiota." *Nature* 488, no. 7409 (2012): 91-5.
- Burge, C. and S. Karlin. "Prediction of Complete Gene Structures in Human Genomic DNA." *J Mol Biol* 268, no. 1 (1997): 78-94.
- Cakir, B. and O. Kilickaya. "Whole-Genome Survey of the Putative ATP-Binding Cassette Transporter Family Genes in *Vitis Vinifera*." *Plos One* 8, no. 11 (2013).
- Calderon Villalobos, L. I., S. Lee, C. De Oliveira, A. Ivetac, W. Brandt, L. Armitage, L. B. Sheard, X. Tan, G. Parry, H. Mao, N. Zheng, R. Napier, S. Kepinski and M. Estelle. "A Combinatorial Tir1/Afb-Aux/Iaa Co-Receptor System for Differential Sensing of Auxin." *Nat Chem Biol* 8, no. 5 (2012): 477-85.
- Camerini, S., B. Senatore, E. Lonardo, E. Imperlini, C. Bianco, G. Moschetti, G. L. Rotino, B. Campion and R. Defez. "Introduction of a Novel Pathway for IAA Biosynthesis to Rhizobia Alters Vetch Root Nodule Development." *Arch Microbiol* 190, no. 1 (2008): 67-77.
- Cartharius, K., K. Frech, K. Grote, B. Klocke, M. Haltmeier, A. Klingenhoff, M. Frisch, M. Bayerlein and T. Werner. "MatInspector and Beyond: Promoter Analysis Based on Transcription Factor Binding Sites." *Bioinformatics* 21, no. 13 (2005): 2933-42.
- Catoira, R., C. Galera, F. de Billy, R. V. Penmetsa, E. P. Journet, F. Maillet, C. Rosenberg, D. Cook, C. Gough and J. Denarie. "Four Genes of *Medicago truncatula* Controlling Components of a Nod Factor Transduction Pathway." *Plant Cell* 12, no. 9 (2000): 1647-1665.
- Charpentier, M., R. Bredemeier, G. Wanner, N. Takeda, E. Schleiff and M. Parniske. "*Lotus Japonicus* CASTOR and POLLUX Are Ion Channels Essential for Perinuclear Calcium Spiking in Legume Root Endosymbiosis." *Plant Cell* 20, no. 12 (2008): 3467-79.
- Chen, C., C. Fan, M. Gao and H. Zhu. "Antiquity and Function of *Castor* and *Pollux*, the Twin Ion Channel-Encoding Genes Key to the Evolution of Root Symbioses in Plants." *Plant Physiol* 149, no. 1 (2009): 306-17.
- Chen, G., T. Komatsuda, J. F. Ma, C. Nawrath, M. Pourkheirandish, A. Tagiri, Y. G. Hu, M. Sameri, X. Li, X. Zhao, Y. Liu, C. Li, X. Ma, A. Wang, S. Nair, N. Wang, A. Miyao, S. Sakuma, N. Yamaji, X. Zheng and E. Nevo. "An ATP-Binding Cassette Subfamily G Full Transporter Is Essential for the Retention of Leaf Water in Both Wild Barley and Rice." *Proc Natl Acad Sci U S A* 108, no. 30 (2011): 12354-9.
- Cho, M., S. H. Lee and H. T. Cho. "P-Glycoprotein4 Displays Auxin Efflux Transporter-Like Action in *Arabidopsis* Root Hair Cells and Tobacco Cells." *Plant Cell* 19, no. 12 (2007): 3930-43.
- Chou, K. C. and H. B. Shen. "Cell-Ploc: A Package of Web Servers for Predicting Subcellular Localization of Proteins in Various Organisms." *Nat Protoc* 3, no. 2 (2008): 153-62.
- Consonni, C., M. E. Humphry, H. A. Hartmann, M. Livaja, J. Durner, L. Westphal, J. Vogel, V. Lipka, B. Kemmerling, P. Schulze-Lefert, S. C. Somerville and R.

- Panstruga. "Conserved Requirement for a Plant Host Cell Protein in Powdery Mildew Pathogenesis." *Nat Genet* 38, no. 6 (2006): 716-20.
- Cook, D. R. "*Medicago truncatula*--a Model in the Making!" *Curr Opin Plant Biol* 2, no. 4 (1999): 301-4.
- Couzigou, J. M., V. Zhukov, S. Mondy, G. Abu el Heba, V. Cosson, T. H. Ellis, M. Ambrose, J. Wen, M. Tadege, I. Tikhonovich, K. S. Mysore, J. Putterill, J. Hofer, A. Y. Borisov and P. Ratet. "NODULE ROOT and COCHLEATA Maintain Nodule Development and Are Legume Orthologs of *Arabidopsis* Blade-on-Petiole Genes." *Plant Cell* 24, no. 11 (2012): 4498-510.
- d'Erfurth, I., V. Cosson, A. Eschstruth, H. Lucas, A. Kondorosi and P. Ratet. "Efficient Transposition of the *Tnt1* Tobacco Retrotransposon in the Model Legume *Medicago truncatula*." *Plant J* 34, no. 1 (2003): 95-106.
- Dakora, FD and DA Phillips. "Diverse Functions of Isoflavonoids in Legumes Transcend Anti-Microbial Definitions of Phytoalexins." *Physiological and Molecular Plant Pathology* 49, no. 1 (1996): 1-20.
- de Billy, F., C. Grosjean, S. May, M. Bennett and J. V. Cullimore. "Expression Studies on *Aux1*-Like Genes in *Medicago truncatula* Suggest That Auxin Is Required at Two Steps in Early Nodule Development." *Mol Plant Microbe Interact* 14, no. 3 (2001): 267-77.
- Delves, A. C., A. Higgins and P. Gresshoff. "Shoot Apex Removal Does Not Alter Autoregulation of Nodulation in Soybean." *Plant, Cell & Environment* 15, no. 2 (1992): 249-254.
- Denarie, J., F. Debelle and J. C. Prome. "*Rhizobium* Lipo-Chitooligosaccharide Nodulation Factors: Signaling Molecules Mediating Recognition and Morphogenesis." *Annu Rev Biochem* 65, (1996): 503-35.
- Deutsch, M. and M. Long. "Intron-Exon Structures of Eukaryotic Model Organisms." *Nucleic Acids Res* 27, no. 15 (1999): 3219-28.
- Eichhorn, H., M. Klinghammer, P. Becht and R. Tenhaken. "Isolation of a Novel ABC-Transporter Gene from Soybean Induced by Salicylic Acid." *J Exp Bot* 57, no. 10 (2006): 2193-201.
- Floss, D. S., B. Hause, P. R. Lange, H. Kuster, D. Strack and M. H. Walter. "Knock-Down of the Mep Pathway Isogene *1-Deoxy-D-Xylulose 5-Phosphate Synthase 2* Inhibits Formation of Arbuscular Mycorrhiza-Induced Apocarotenoids, and Abolishes Normal Expression of Mycorrhiza-Specific Plant Marker Genes." *Plant J* 56, no. 1 (2008): 86-100.
- Francisco, R. M., A. Regalado, A. Ageorges, B. J. Burla, B. Bassin, C. Eisenach, O. Zarrouk, S. Vialet, T. Marlin, M. M. Chaves, E. Martinoia and R. Nagy. "*ABCC1*, an Atp Binding Cassette Protein from Grape Berry, Transports Anthocyanidin 3-O-Glucosides." *Plant Cell* 25, no. 5 (2013): 1840-54.
- Friml, J. "Auxin Transport - Shaping the Plant." *Curr Opin Plant Biol* 6, no. 1 (2003): 7-12.
- Fu, X. and N. P. Harberd. "Auxin Promotes *Arabidopsis* Root Growth by Modulating Gibberellin Response." *Nature* 421, no. 6924 (2003): 740-3.

- Fukuhara, Hideyuki, Yasuo Minakawa, Shoichiro Akao and Kiwamu Minamisawa. "The Involvement of Indole-3-Acetic Acid Produced by *Bradyrhizobium Elkanii* in Nodule Formation." *Plant and Cell Physiology* 35, no. 8 (1994): 1261-1265.
- Gage, D. J. "Infection and Invasion of Roots by Symbiotic, Nitrogen-Fixing Rhizobia During Nodulation of Temperate Legumes." *Microbiol Mol Biol Rev* 68, no. 2 (2004): 280-300.
- Garcia-Romera, I, JM Garcia-Garrido and JA Ocampo. "Pectinase Activity in Vesicular-Arbuscular Mycorrhiza During Colonization of Lettuce." *Symbiosis* 12, no. 2 (1992): 189-198.
- Garcia, O., P. Bouige, C. Forestier and E. Dassa. "Inventory and Comparative Analysis of Rice and *Arabidopsis* Atp-Binding Cassette (Abc) Systems." *J Mol Biol* 343, no. 1 (2004): 249-65.
- Gaude, Nicole, Silvia Bortfeld, Nina Duensing, Marc Lohse and Franziska Krajinski. "Arbuscule-Containing and Non-Colonized Cortical Cells of Mycorrhizal Roots Undergo Extensive and Specific Reprogramming During Arbuscular Mycorrhizal Development." *The Plant Journal* 69, no. 3 (2012): 510-528.
- Geisler, M., J. J. Blakeslee, R. Bouchard, O. R. Lee, V. Vincenzetti, A. Bandyopadhyay, B. Titapiwatanakun, W. A. Peer, A. Bailly, E. L. Richards, K. F. Ejendal, A. P. Smith, C. Baroux, U. Grossniklaus, A. Muller, C. A. Hrycyna, R. Dudler, A. S. Murphy and E. Martinoia. "Cellular Efflux of Auxin Catalyzed by the *Arabidopsis* MDR/Pgp Transporter *AtPGP1*." *Plant J* 44, no. 2 (2005): 179-94.
- Gherbi, H., K. Markmann, S. Svistoonoff, J. Estevan, D. Autran, G. Giczey, F. Auguy, B. Peret, L. Laplaze, C. Franche, M. Parniske and D. Bogusz. "SYMRK Defines a Common Genetic Basis for Plant Root Endosymbioses with Arbuscular Mycorrhiza Fungi, Rhizobia, and Frankiobacteria." *Proc Natl Acad Sci U S A* 105, no. 12 (2008): 4928-32.
- Gleason, C., S. Chaudhuri, T. Yang, A. Munoz, B. W. Poovaiah and G. E. Oldroyd. "Nodulation Independent of Rhizobia Induced by a Calcium-Activated Kinase Lacking Autoinhibition." *Nature* 441, no. 7097 (2006): 1149-52.
- Gobbato, E., J. F. Marsh, T. Vernie, E. Wang, F. Maillet, J. Kim, J. B. Miller, J. Sun, S. A. Bano, P. Ratet, K. S. Mysore, J. Denarie, M. Schultze and G. E. Oldroyd. "A GRAS-Type Transcription Factor with a Specific Function in Mycorrhizal Signaling." *Curr Biol* 22, no. 23 (2012): 2236-41.
- Gomez, S. K., H. Javot, P. Deewatthanawong, I. Torres-Jerez, Y. Tang, E. B. Blancaflor, M. K. Udvardi and M. J. Harrison. "*Medicago truncatula* and *Glomus Intraradices* Gene Expression in Cortical Cells Harboring Arbuscules in the Arbuscular Mycorrhizal Symbiosis." *BMC Plant Biol* 9, (2009): 10.
- Goodman, C. D., P. Casati and V. Walbot. "A Multidrug Resistance-Associated Protein Involved in Anthocyanin Transport in *Zea Mays*." *Plant Cell* 16, no. 7 (2004): 1812-26.
- Goossens, A., S. T. Hakkinen, I. Laakso, K. M. Oksman-Caldentey and D. Inze. "Secretion of Secondary Metabolites by ATP-Binding Cassette Transporters in Plant Cell Suspension Cultures." *Plant Physiol* 131, no. 3 (2003): 1161-4.

- Gray, W. M., S. Kepinski, D. Rouse, O. Leyser and M. Estelle. "Auxin Regulates SCF(TIR1)-Dependent Degradation of AUX/IAA Proteins." *Nature* 414, no. 6861 (2001): 271-6.
- Guan, D., N. Stacey, C. Liu, J. Wen, K. S. Mysore, I. Torres-Jerez, T. Vernie, M. Tadege, C. Zhou, Z. Y. Wang, M. K. Udvardi, G. E. Oldroyd and J. D. Murray. "Rhizobial Infection Is Associated with the Development of Peripheral Vasculature in Nodules of *Medicago truncatula*." *Plant Physiol* 162, no. 1 (2013): 107-15.
- Gurich N, González JE. Role of Quorum Sensing in Sinorhizobium meliloti-Alfalfa Symbiosis . *Journal of Bacteriology*. (2009);191(13):4372-4382. doi:10.1128/JB.00376-09.
- Gutjahr, C., M. Banba, V. Croset, K. An, A. Miyao, G. An, H. Hirochika, H. Imaizumi-Anraku and U. Paszkowski. "Arbuscular Mycorrhiza-Specific Signaling in Rice Transcends the Common Symbiosis Signaling Pathway." *Plant Cell* 20, no. 11 (2008): 2989-3005.
- Gutjahr, C., D. Radovanovic, J. Geoffroy, Q. Zhang, H. Siegler, M. Chiapello, L. Casieri, K. An, G. An, E. Guiderdoni, C. S. Kumar, V. Sundaresan, M. J. Harrison and U. Paszkowski. "The Half-Size Abc Transporters Str1 and Str2 Are Indispensable for Mycorrhizal Arbuscule Formation in Rice." *Plant Journal* 69, no. 5 (2012): 906-920.
- Harrison, M. J., G. R. Dewbre and J. Liu. "A Phosphate Transporter from *Medicago truncatula* Involved in the Acquisition of Phosphate Released by Arbuscular Mycorrhizal Fungi." *Plant Cell* 14, no. 10 (2002): 2413-29.
- Hassan, S. and U. Mathesius. "The Role of Flavonoids in Root-Rhizosphere Signalling: Opportunities and Challenges for Improving Plant-Microbe Interactions." *J Exp Bot* 63, no. 9 (2012): 3429-44.
- Henricson, A., K. Forslund and E. L. Sonnhammer. "Orthology Confers Intron Position Conservation." *BMC Genomics* 11, (2010): 412.
- Hirsch, A. M., T. V. Bhuvaneshwari, J. G. Torrey and T. Bisseling. "Early Nodulin Genes Are Induced in Alfalfa Root Outgrowths Elicited by Auxin Transport Inhibitors." *Proc Natl Acad Sci U S A* 86, no. 4 (1989): 1244-8.
- Hirsch, S., J. Kim, A. Munoz, A. B. Heckmann, J. A. Downie and G. E. Oldroyd. "Gras Proteins Form a DNA Binding Complex to Induce Gene Expression During Nodulation Signaling in *Medicago truncatula*." *Plant Cell* 21, no. 2 (2009): 545-57.
- Hirsch, S. and G. E. Oldroyd. "Gras-Domain Transcription Factors That Regulate Plant Development." *Plant Signal Behav* 4, no. 8 (2009): 698-700.
- Hoffmann, Beate, Toan Hanh Trinh, Jeffrey Leung, Adam Kondorosi and Eva Kondorosi. "A New *Medicago truncatula* Line with Superior in Vitro Regeneration, Transformation, and Symbiotic Properties Isolated through Cell Culture Selection." *Molecular Plant-Microbe Interactions* 10, no. 3 (1997): 307-315.
- Horvath, B., L. H. Yeun, A. Domonkos, G. Halasz, E. Gobbato, F. Ayaydin, K. Miro, S. Hirsch, J. Sun, M. Tadege, P. Ratet, K. S. Mysore, J. M. Ane, G. E. Oldroyd and P. Kalo. "*Medicago truncatula* IPD3 Is a Member of the

- Common Symbiotic Signaling Pathway Required for Rhizobial and Mycorrhizal Symbioses." *Mol Plant Microbe Interact* 24, no. 11 (2011): 1345-58.
- Huo, X., E. Schnabel, K. Hughes and J. Frugoli. "RNAi Phenotypes and the Localization of a Protein::Gus Fusion Imply a Role for *Medicago truncatula* Pin Genes in Nodulation." *J Plant Growth Regul* 25, no. 2 (2006): 156-165.
- Jacobs, M. and P. H. Rubery. "Naturally Occurring Auxin Transport Regulators." *Science* 241, no. 4863 (1988): 346-9.
- Jasinski, M., E. Ducos, E. Martinoia and M. Boutry. "The ATP-Binding Cassette Transporters: Structure, Function, and Gene Family Comparison between Rice and *Arabidopsis*." *Plant Physiol* 131, no. 3 (2003): 1169-77.
- Jasinski, M., Y. Stukkens, H. Degand, B. Purnelle, J. Marchand-Brynaert and M. Boutry. "A Plant Plasma Membrane ATP Binding Cassette-Type Transporter Is Involved in Antifungal Terpenoid Secretion." *Plant Cell* 13, no. 5 (2001): 1095-107.
- Javot, H., R. V. Penmetsa, N. Terzaghi, D. R. Cook and M. J. Harrison. "A *Medicago truncatula* Phosphate Transporter Indispensable for the Arbuscular Mycorrhizal Symbiosis." *Proc Natl Acad Sci U S A* 104, no. 5 (2007): 1720-5.
- Jez, J. M., M. E. Bowman and J. P. Noel. "Role of Hydrogen Bonds in the Reaction Mechanism of Chalcone Isomerase." *Biochemistry* 41, no. 16 (2002): 5168-76.
- Jones, Angharad R., Eric M. Kramer, Kirsten Knox, Ranjan Swarup, Malcolm J. Bennett, Colin M. Lazarus, H. M. Ottoline Leyser and Claire S. Grierson. "Auxin Transport through Non-Hair Cells Sustains Root-Hair Development." *Nat Cell Biol* 11, no. 1 (2009): 78-84.
- Journet, E. P., N. El-Gachtouli, V. Vernoud, F. de Billy, M. Pichon, A. Dedieu, C. Arnould, D. Morandi, D. G. Barker and V. Gianinazzi-Pearson. "*Medicago truncatula* *ENOD11*: A Novel Rprp-Encoding Early Nodulin Gene Expressed During Mycorrhization in Arbuscule-Containing Cells." *Mol Plant Microbe Interact* 14, no. 6 (2001): 737-48.
- Kall, L., A. Krogh and E. L. Sonnhammer. "A Combined Transmembrane Topology and Signal Peptide Prediction Method." *J Mol Biol* 338, no. 5 (2004): 1027-36.
- Kamimoto, Y., K. Terasaka, M. Hamamoto, K. Takanashi, S. Fukuda, N. Shitan, A. Sugiyama, H. Suzuki, D. Shibata, B. Wang, S. Pollmann, M. Geisler and K. Yazaki. "*Arabidopsis* ABCB21 Is a Facultative Auxin Importer/Exporter Regulated by Cytoplasmic Auxin Concentration." *Plant Cell Physiol* 53, no. 12 (2012): 2090-100.
- Kaneda, M., M. Schuetz, B. S. Lin, C. Chanis, B. Hamberger, T. L. Western, J. Ehltling and A. L. Samuels. "Abc Transporters Coordinately Expressed During Lignification of *Arabidopsis* Stems Include a Set of ABCBs Associated with Auxin Transport." *J Exp Bot* 62, no. 6 (2011): 2063-77.

- Kang, J., J. U. Hwang, M. Lee, Y. Y. Kim, S. M. Assmann, E. Martinoia and Y. Lee. "PDR-Type Abc Transporter Mediates Cellular Uptake of the Phytohormone Abscisic Acid." *Proc Natl Acad Sci U S A* 107, no. 5 (2010): 2355-60.
- Kim, Y. K., S. Kim, J. H. Um, K. Kim, S. K. Choi, B. H. Um, S. W. Kang, J. W. Kim, S. Takaichi, S. B. Song, C. H. Lee, H. S. Kim, K. W. Kim, K. H. Nam, S. H. Lee, Y. H. Kim, H. M. Park, S. H. Ha, D. P. Verma and C. I. Cheon. "Functional Implication of Beta-Carotene Hydroxylases in Soybean Nodulation." *Plant Physiol* 162, no. 3 (2013): 1420-33.
- Klein, M., B. Burla and E. Martinoia. "The Multidrug Resistance-Associated Protein (MRP/ABCC) Subfamily of ATP-Binding Cassette Transporters in Plants." *FEBS Lett* 580, no. 4 (2006): 1112-22.
- Knox, K., C. S. Grierson and O. Leyser. "Axr3 and Shy2 Interact to Regulate Root Hair Development." *Development* 130, no. 23 (2003): 5769-77.
- Krattinger, S. G., E. S. Lagudah, W. Spielmeier, R. P. Singh, J. Huerta-Espino, H. McFadden, E. Bossolini, L. L. Selter and B. Keller. "A Putative Abc Transporter Confers Durable Resistance to Multiple Fungal Pathogens in Wheat." *Science* 323, no. 5919 (2009): 1360-3.
- Krattinger, S. G., E. S. Lagudah, T. Wicker, J. M. Risk, A. R. Ashton, L. L. Selter, T. Matsumoto and B. Keller. "Lr34 Multi-Pathogen Resistance Abc Transporter: Molecular Analysis of Homoeologous and Orthologous Genes in Hexaploid Wheat and Other Grass Species." *Plant J* 65, no. 3 (2011): 392-403.
- Kretschmar, T., W. Kohlen, J. Sasse, L. Borghi, M. Schlegel, J. B. Bachelier, D. Reinhardt, R. Bours, H. J. Bouwmeester and E. Martinoia. "A Petunia ABC Protein Controls Strigolactone-Dependent Symbiotic Signalling and Branching." *Nature* 483, no. 7389 (2012): 341-U135.
- Kuromori, Takashi, Takaaki Miyaji, Hikaru Yabuuchi, Hidetada Shimizu, Eriko Sugimoto, Asako Kamiya, Yoshinori Moriyama and Kazuo Shinozaki. "Abc Transporter AtABCG25 Is Involved in Abscisic Acid Transport and Responses." *Proceedings of the National Academy of Sciences* 107, no. 5 (2010): 2361-2366.
- Langowski, L., K. Ruzicka, S. Naramoto, J. Kleine-Vehn and J. Friml. "Trafficking to the Outer Polar Domain Defines the Root-Soil Interface." *Curr Biol* 20, no. 10 (2010): 904-8.
- Lankova, M., R. S. Smith, B. Pesek, M. Kubes, E. Zazimalova, J. Petrasek and K. Hoyerova. "Auxin Influx Inhibitors 1-NOA, 2-NOA, and CHPAA Interfere with Membrane Dynamics in Tobacco Cells." *J Exp Bot* 61, no. 13 (2010): 3589-98.
- Lee, M., Y. Choi, B. Burla, Y. Y. Kim, B. Jeon, M. Maeshima, J. Y. Yoo, E. Martinoia and Y. Lee. "The ABC Transporter AtABCB14 Is a Malate Importer and Modulates Stomatal Response to CO₂." *Nat Cell Biol* 10, no. 10 (2008): 1217-23.
- Li, H., Y. Cheng, A. Murphy, G. Hagen and T. J. Guilfoyle. "Constitutive Repression and Activation of Auxin Signaling in *Arabidopsis*." *Plant Physiol* 149, no. 3 (2009): 1277-88.

- Li, Z. S., M. Alfenito, P. A. Rea, V. Walbot and R. A. Dixon. "Vacuolar Uptake of the Phytoalexin Medicago by the Glutathione Conjugate Pump." *Phytochemistry* 45, no. 4 (1997): 689-93.
- Limpens, E., C. Franken, P. Smit, J. Willemsse, T. Bisseling and R. Geurts. "LysM Domain Receptor Kinases Regulating Rhizobial Nod Factor-Induced Infection." *Science* 302, no. 5645 (2003): 630-3.
- Liu, W., W. Kohlen, A. Lillo, R. Op den Camp, S. Ivanov, M. Hartog, E. Limpens, M. Jamil, C. Smaczniak, K. Kaufmann, W. C. Yang, G. J. Hooiveld, T. Charnikhova, H. J. Bouwmeester, T. Bisseling and R. Geurts. "Strigolactone Biosynthesis in *Medicago truncatula* and Rice Requires the Symbiotic Grass-Type Transcription Factors Nsp1 and Nsp2." *Plant Cell* 23, no. 10 (2011): 3853-65.
- Loyola-Vargas, V. M., C. D. Broeckling, D. Badri and J. M. Vivanco. "Effect of Transporters on the Secretion of Phytochemicals by the Roots of *Arabidopsis thaliana*." *Planta* 225, no. 2 (2007): 301-10.
- Madsen, E. B., L. H. Madsen, S. Radutoiu, M. Olbryt, M. Rakwalska, K. Szczyglowski, S. Sato, T. Kaneko, S. Tabata, N. Sandal and J. Stougaard. "A Receptor Kinase Gene of the LysM Type Is Involved in Legume Perception of Rhizobial Signals." *Nature* 425, no. 6958 (2003): 637-40.
- Maillet, F., V. Poinso, O. Andre, V. Puech-Pages, A. Haouy, M. Gueunier, L. Cromer, D. Giraudet, D. Formey, A. Niebel, E. A. Martinez, H. Driguez, G. Becard and J. Denarie. "Fungal Lipochitoooligosaccharide Symbiotic Signals in Arbuscular Mycorrhiza." *Nature* 469, no. 7328 (2011): 58-63.
- Marchant, A., R. Bhalerao, I. Casimiro, J. Eklof, P. J. Casero, M. Bennett and G. Sandberg. "*AUX1* Promotes Lateral Root Formation by Facilitating Indole-3-Acetic Acid Distribution between Sink and Source Tissues in the *Arabidopsis* Seedling." *Plant Cell* 14, no. 3 (2002): 589-97.
- Marsh, John F., Alexandra Rakocevic, Raka M. Mitra, Lysiane Brocard, Jongho Sun, Alexis Eschstruth, Sharon R. Long, Michael Schultze, Pascal Ratet and Giles E. D. Oldroyd. "*Medicago truncatula* Nin Is Essential for Rhizobial-Independent Nodule Organogenesis Induced by Autoactive Calcium/Calmodulin-Dependent Protein Kinase." *Plant Physiology* 144, no. 1 (2007): 324-335.
- Martinoia, E., M. Klein, M. Geisler, L. Bovet, C. Forestier, U. Kolukisaoglu, B. Muller-Rober and B. Schulz. "Multifunctionality of Plant ABC Transporters--More Than Just Detoxifiers." *Planta* 214, no. 3 (2002): 345-55.
- Mathesius, U. "Goldacre Paper: Auxin: At the Root of Nodule Development?" *Functional Plant Biology* 35, no. 8 (2008): 651-668.
- Mathesius, U., H. R. Schlaman, H. P. Spaink, C. Of Sautter, B. G. Rolfe and M. A. Djordjevic. "Auxin Transport Inhibition Precedes Root Nodule Formation in White Clover Roots and Is Regulated by Flavonoids and Derivatives of Chitin Oligosaccharides." *Plant J* 14, no. 1 (1998): 23-34.
- Maxwell, C. A., M. J. Harrison and R. A. Dixon. "Molecular Characterization and Expression of Alfalfa Isoliquiritigenin 2'-O-Methyltransferase, an Enzyme Specifically Involved in the Biosynthesis of an Inducer of *Rhizobium Meliloti* Nodulation Genes." *Plant J* 4, no. 6 (1993): 971-81.

- Maxwell, C. A., U. A. Hartwig, C. M. Joseph and D. A. Phillips. "A Chalcone and Two Related Flavonoids Released from Alfalfa Roots Induce Nod Genes of *Rhizobium Meliloti*." *Plant Physiol* 91, no. 3 (1989): 842-7.
- McFarlane, H. E., J. J. H. Shin, D. A. Bird and A. L. Samuels. "Arabidopsis ABCG Transporters, Which Are Required for Export of Diverse Cuticular Lipids, Dimerize in Different Combinations." *Plant Cell* 22, no. 9 (2010): 3066-3075.
- Mendoza-Cozatl, D. G., T. O. Jobe, F. Hauser and J. I. Schroeder. "Long-Distance Transport, Vacuolar Sequestration, Tolerance, and Transcriptional Responses Induced by Cadmium and Arsenic." *Curr Opin Plant Biol* 14, no. 5 (2011): 554-62.
- Miao, ZhenYan, DaoFeng Li, ZhenHai Zhang, JiangLi Dong, Zhen Su and Tao Wang. "*Medicago truncatula* Transporter Database: A Comprehensive Database Resource for *M. truncatula* Transporters." *BMC Genomics* 13, no. 60 (2012): (6 February 2012).
- Murray, J. D. "Invasion by Invitation: Rhizobial Infection in Legumes." *Mol Plant Microbe Interact* 24, no. 6 (2011): 631-9.
- Murray, J. D., D. R. Cousins, K. J. Jackson and C. Liu. "Signaling at the Root Surface: The Role of Cutin Monomers in Mycorrhization." *Mol Plant* 6, no. 5 (2013): 1381-3.
- Murray, J. D., R. R. Muni, I. Torres-Jerez, Y. Tang, S. Allen, M. Andriankaja, G. Li, A. Laxmi, X. Cheng, J. Wen, D. Vaughan, M. Schultze, J. Sun, M. Charpentier, G. Oldroyd, M. Tadege, P. Ratet, K. S. Mysore, R. Chen and M. K. Udvardi. "*Vapyrin*, a Gene Essential for Intracellular Progression of Arbuscular Mycorrhizal Symbiosis, Is Also Essential for Infection by Rhizobia in the Nodule Symbiosis of *Medicago truncatula*." *Plant J* 65, no. 2 (2011): 244-52.
- Nishimura, M. T. and J. L. Dangl. "*Arabidopsis* and the Plant Immune System." *Plant J* 61, no. 6 (2010): 1053-66.
- Noh, B., A. Bandyopadhyay, W. A. Peer, E. P. Spalding and A. S. Murphy. "Enhanced Gravi- and Phototropism in Plant MDR Mutants Mislocalizing the Auxin Efflux Protein PIN1." *Nature* 423, no. 6943 (2003): 999-1002.
- Noh, B., A. S. Murphy and E. P. Spalding. "Multidrug Resistance-Like Genes of *Arabidopsis* Required for Auxin Transport and Auxin-Mediated Development." *Plant Cell* 13, no. 11 (2001): 2441-54.
- Oba, Hirotsuke, Keitaro Tawaray and Tadao Wagatsuma. "Arbuscular Mycorrhizal Colonization in *Lupinus* and Related Genera." *Soil Science and Plant Nutrition* 47, no. 4 (2001): 685-694.
- Oldroyd, G. E. D. "Speak, Friend, and Enter: Signalling Systems That Promote Beneficial Symbiotic Associations in Plants." *Nature Reviews Microbiology* 11, no. 4 (2013): 252-263.
- Oldroyd, G. E. D. and S. R. Long. "Identification and Characterization of Nodulation-Signaling Pathway 2, a Gene of *Medicago truncatula* Involved in Nod Factor Signaling." *Plant Physiology* 131, no. 3 (2003): 1027-1032.

- Oldroyd, G. E., E. M. Engstrom and S. R. Long. "Ethylene Inhibits the Nod Factor Signal Transduction Pathway of *Medicago truncatula*." *Plant Cell* 13, no. 8 (2001): 1835-49.
- Oldroyd, G. E. and R. Geurts. "*Medicago truncatula*, Going Where No Plant Has Gone Before." *Trends Plant Sci* 6, no. 12 (2001): 552-4.
- Oliver, R. P. and S. V. Ipcho. "*Arabidopsis* Pathology Breathes New Life into the Necrotrophs-Vs.-Biotrophs Classification of Fungal Pathogens." *Mol Plant Pathol* 5, no. 4 (2004): 347-52.
- Ortu, G., R. Balestrini, P. A. Pereira, J. D. Becker, H. Kuster and P. Bonfante. "Plant Genes Related to Gibberellin Biosynthesis and Signaling Are Differentially Regulated During the Early Stages of AM Fungal Interactions." *Mol Plant* 5, no. 4 (2012): 951-4.
- Pacios-Bras, C., H. R. Schlaman, K. Boot, P. Admiraal, J. M. Langerak, J. Stougaard and H. P. Spaik. "Auxin Distribution in *Lotus Japonicus* During Root Nodule Development." *Plant Mol Biol* 52, no. 6 (2003): 1169-80.
- Pacios-Bras, C., Y. E. van der Burgt, A. M. Deelder, P. Vinuesa, D. Werner and H. P. Spaik. "Novel Lipochitin Oligosaccharide Structures Produced by *Rhizobium Etl* Kim5s." *Carbohydr Res* 337, no. 13 (2002): 1193-202.
- Pang, K. Y., Y. J. Li, M. H. Liu, Z. D. Meng and Y. L. Yu. "Inventory and General Analysis of the ATP-Binding Cassette (ABC) Gene Superfamily in Maize (*Zea Mays* L.)." *Gene* 526, no. 2 (2013): 411-428.
- Panikashvili, D., J. X. Shi, L. Schreiber and A. Aharoni. "The *Arabidopsis ABCG13* Transporter Is Required for Flower Cuticle Secretion and Patterning of the Petal Epidermis." *New Phytol* 190, no. 1 (2011): 113-24.
- Parniske, M. "Arbuscular Mycorrhiza: The Mother of Plant Root Endosymbioses." *Nat Rev Microbiol* 6, no. 10 (2008): 763-75.
- Parry, G., A. Delbarre, A. Marchant, R. Swarup, R. Napier, C. Perrot-Rechenmann and M. J. Bennett. "Novel Auxin Transport Inhibitors Phenocopy the Auxin Influx Carrier Mutation *AUX1*." *Plant J* 25, no. 4 (2001): 399-406.
- Peret, B., R. Swarup, L. Jansen, G. Devos, F. Auguy, M. Collin, C. Santi, V. Hocher, C. Franche, D. Bogusz, M. Bennett and L. Laplaze. "Auxin Influx Activity Is Associated with Frankia Infection During Actinorhizal Nodule Formation in *Casuarina Glauca*." *Plant Physiol* 144, no. 4 (2007): 1852-62.
- Perrine-Walker, F., P. Doumas, M. Lucas, V. Vaissayre, N. J. Beauchemin, L. R. Band, J. Chopard, A. Crabos, G. Conejero, B. Peret, J. R. King, J. L. Verdeil, V. Hocher, C. Franche, M. J. Bennett, L. S. Tisa and L. Laplaze. "Auxin Carriers Localization Drives Auxin Accumulation in Plant Cells Infected by *Frankia* in *Casuarina Glauca* Actinorhizal Nodules." *Plant Physiol* 154, no. 3 (2010): 1372-80.
- Pfeffer, Philip E, David D Douds, Guillaume Bécard and Yair Shachar-Hill. "Carbon Uptake and the Metabolism and Transport of Lipids in an Arbuscular Mycorrhiza." *Plant Physiology* 120, no. 2 (1999): 587-598.

- Pieterse, C. M., D. Van der Does, C. Zamioudis, A. Leon-Reyes and S. C. Van Wees. "Hormonal Modulation of Plant Immunity." *Annu Rev Cell Dev Biol* 28, (2012): 489-521.
- Pighin, J. A., H. Zheng, L. J. Balakshin, I. P. Goodman, T. L. Western, R. Jetter, L. Kunst and A. L. Samuels. "Plant Cuticular Lipid Export Requires an ABC Transporter." *Science* 306, no. 5696 (2004): 702-4.
- Pii, Y., M. Crimi, G. Cremonese, A. Spena and T. Pandolfini. "Auxin and Nitric Oxide Control Indeterminate Nodule Formation." *BMC Plant Biol* 7, (2007): 21.
- Pislariu, C. I., J. D. Murray, J. Wen, V. Cosson, R. R. Muni, M. Wang, V. A. Benedito, A. Andriankaja, X. Cheng, I. T. Jerez, S. Mondy, S. Zhang, M. E. Taylor, M. Tadege, P. Ratet, K. S. Mysore, R. Chen and M. K. Udvardi. "A *Medicago truncatula* Tobacco Retrotransposon Insertion Mutant Collection with Defects in Nodule Development and Symbiotic Nitrogen Fixation." *Plant Physiol* 159, no. 4 (2012): 1686-99.
- Poole, Philip and David Allaway. "Carbon and Nitrogen Metabolism in *Rhizobium*." *Advances in microbial physiology* 43, (2000): 117-163.
- Prayitno, J., B. G. Rolfe and U. Mathesius. "The Ethylene-Insensitive *sickle* Mutant of *Medicago truncatula* Shows Altered Auxin Transport Regulation During Nodulation." *Plant Physiol* 142, no. 1 (2006): 168-80.
- Prusty, R., P. Grisafi and G. R. Fink. "The Plant Hormone Indoleacetic Acid Induces Invasive Growth in *Saccharomyces Cerevisiae*." *Proc Natl Acad Sci U S A* 101, no. 12 (2004): 4153-7.
- Pumplin, N., S. J. Mondo, S. Topp, C. G. Starker, J. S. Gantt and M. J. Harrison. "*Medicago truncatula* VAPYRIN Is a Novel Protein Required for Arbuscular Mycorrhizal Symbiosis." *Plant J* 61, no. 3 (2010): 482-94.
- Pumplin, N., X. C. Zhang, R. D. Noar and M. J. Harrison. "Polar Localization of a Symbiosis-Specific Phosphate Transporter Is Mediated by a Transient Reorientation of Secretion." *Proceedings of the National Academy of Sciences of the United States of America* 109, no. 11 (2012): E665-E672.
- Radutoiu, S., L. H. Madsen, E. B. Madsen, H. H. Felle, Y. Umehara, M. Gronlund, S. Sato, Y. Nakamura, S. Tabata, N. Sandal and J. Stougaard. "Plant Recognition of Symbiotic Bacteria Requires Two LysM Receptor-Like Kinases." *Nature* 425, no. 6958 (2003): 585-92.
- Rahman, A., S. Hosokawa, Y. Oono, T. Amakawa, N. Goto and S. Tsurumi. "Auxin and Ethylene Response Interactions During *Arabidopsis* Root Hair Development Dissected by Auxin Influx Modulators." *Plant Physiol* 130, no. 4 (2002): 1908-17.
- Raichaudhuri, A., M. Peng, V. Naponelli, S. Chen, R. Sanchez-Fernandez, H. Gu, J. F. Gregory, 3rd, A. D. Hanson and P. A. Rea. "Plant Vacuolar ATP-Binding Cassette Transporters That Translocate Folates and Antifolates in Vitro and Contribute to Antifolate Tolerance in Vivo." *J Biol Chem* 284, no. 13 (2009): 8449-60.
- Ramlov, K. B., N. B. Laursen, J. Stougaard and K. A. Marcker. "Site-Directed Mutagenesis of the Organ-Specific Element in the Soybean Leghemoglobin LBC3 Gene Promoter." *Plant J* 4, no. 3 (1993): 577-80.

- Ramos, Javier and Ton Bisseling. "A Method for the Isolation of Root Hairs from the Model Legume *Medicago truncatula*." *Journal of Experimental Botany* 54, no. 391 (2003): 2245-2250.
- Rea, P. A. "Plant Atp-Binding Cassette Transporters." *Annu Rev Plant Biol* 58, (2007): 347-75.
- Rea, P. A., Z. S. Li, Y. P. Lu, Y. M. Drozdowicz and E. Martinoia. "From Vacuolar Gs-X Pumps to Multispecific ABC Transporters." *Annu Rev Plant Physiol Plant Mol Biol* 49, (1998): 727-760.
- Rees, D. C., E. Johnson and O. Lewinson. "ABC Transporters: The Power to Change." *Nat Rev Mol Cell Biol* 10, no. 3 (2009): 218-27.
- Riely, B. K., G. Lougnon, J. M. Ane and D. R. Cook. "The Symbiotic Ion Channel Homolog DMI1 Is Localized in the Nuclear Membrane of *Medicago truncatula* Roots." *Plant J* 49, no. 2 (2007): 208-16.
- Rightmyer, A. P. and S. R. Long. "Pseudonodule Formation by Wild-Type and Symbiotic Mutant *Medicago truncatula* in Response to Auxin Transport Inhibitors." *Mol Plant Microbe Interact* 24, no. 11 (2011): 1372-84.
- Sahasrabudhe, Madhuri M. "Screening of Rhizobia for Indole Acetic Acid Production." *Ann Biol Res* 2, no. 4 (2011): 460-468.
- Saier, M. H., Jr., V. S. Reddy, D. G. Tamang and A. Vastermark. "The Transporter Classification Database." *Nucleic Acids Res* 42, no. Database issue (2014): D251-8.
- Sanchez-Fernandez, R., T. G. Davies, J. O. Coleman and P. A. Rea. "The *Arabidopsis thaliana* ABC Protein Superfamily, a Complete Inventory." *J Biol Chem* 276, no. 32 (2001): 30231-44.
- Sánchez-Fernández, Rocío, T. G. Emyr Davies, Julian O. D. Coleman and Philip A. Rea. "The *Arabidopsis thaliana* ABC Protein Superfamily, a Complete Inventory." *Journal of Biological Chemistry* 276, no. 32 (2001): 30231-30244.
- Santelia, D., V. Vincenzetti, E. Azzarello, L. Bovet, Y. Fukao, P. Duchtig, S. Mancuso, E. Martinoia and M. Geisler. "MDR-Like Abc Transporter AtPGP4 Is Involved in Auxin-Mediated Lateral Root and Root Hair Development." *FEBS Lett* 579, no. 24 (2005): 5399-5406.
- Sasabe, M., K. Toyoda, T. Shiraishi, Y. Inagaki and Y. Ichinose. "Cdna Cloning and Characterization of Tobacco ABC Transporter: *NtPDR1* Is a Novel Elicitor-Responsive Gene." *FEBS Lett* 518, no. 1-3 (2002): 164-8.
- Schauser, L., A. Roussis, J. Stiller and J. Stougaard. "A Plant Regulator Controlling Development of Symbiotic Root Nodules." *Nature* 402, no. 6758 (1999): 191-5.
- Schnabel, E. L. and J. Frugoli. "The *PIN* and *LAX* Families of Auxin Transport Genes in *Medicago truncatula*." *Mol Genet Genomics* 272, no. 4 (2004): 420-32.
- Schroeder, J. I., E. Delhaize, W. B. Frommer, M. L. Guerinot, M. J. Harrison, L. Herrera-Estrella, T. Horie, L. V. Kochian, R. Munns, N. K. Nishizawa, Y. F. Tsay and D. Sanders. "Using Membrane Transporters to Improve Crops for Sustainable Food Production." *Nature* 497, no. 7447 (2013): 60-66.

- Shitan, N., I. Bazin, K. Dan, K. Obata, K. Kigawa, K. Ueda, F. Sato, C. Forestier and K. Yazaki. "Involvement of *CjMDR1*, a Plant Multidrug-Resistance-Type ATP-Binding Cassette Protein, in Alkaloid Transport in *Coptis Japonica*." *Proc Natl Acad Sci U S A* 100, no. 2 (2003): 751-6.
- Shitan, N., F. Dalmás, K. Dan, N. Kato, K. Ueda, F. Sato, C. Forestier and K. Yazaki. "Characterization of *Coptis Japonica CjABC2*, an Atp-Binding Cassette Protein Involved in Alkaloid Transport." *Phytochemistry* 91, (2013): 109-116.
- Singh, S., K. Katzer, J. Lambert, M. Cerri and M. Parniske. "CYCLOPS, a DNA-Binding Transcriptional Activator, Orchestrates Symbiotic Root Nodule Development." *Cell Host Microbe* 15, no. 2 (2014): 139-52.
- Smit, P., E. Limpens, R. Geurts, E. Fedorova, E. Dolgikh, C. Gough and T. Bisseling. "*Medicago LYK3*, an Entry Receptor in Rhizobial Nodulation Factor Signaling." *Plant Physiol* 145, no. 1 (2007): 183-91.
- Smit, P., J. Raedts, V. Portyanko, F. Debelle, C. Gough, T. Bisseling and R. Geurts. "NSP1 of the Gras Protein Family Is Essential for Rhizobial Nod Factor-Induced Transcription." *Science* 308, no. 5729 (2005): 1789-1791.
- Sprent, J. I. "Evolving Ideas of Legume Evolution and Diversity: A Taxonomic Perspective on the Occurrence of Nodulation." *New Phytol* 174, no. 1 (2007): 11-25.
- Stein, M., J. Dittgen, C. Sanchez-Rodriguez, B. H. Hou, A. Molina, P. Schulze-Lefert, V. Lipka and S. Somerville. "*Arabidopsis PEN3/PDR8*, an ATP Binding Cassette Transporter, Contributes to Nonhost Resistance to Inappropriate Pathogens That Enter by Direct Penetration." *Plant Cell* 18, no. 3 (2006): 731-46.
- Stougaard, Jens, Dorte Abildsten and Kjeld A. Marcker. "The *Agrobacterium Rhizogenes* P_{ri} TI-DNA Segment as a Gene Vector System for Transformation of Plants." *Molecular and General Genetics MGG* 207, no. 2-3 (1987): 251-255.
- Stukkens, Y., A. Bultreys, S. Grec, T. Trombik, D. Vanham and M. Boutry. "*NpPDR1*, a Pleiotropic Drug Resistance-Type ATP-Binding Cassette Transporter from *Nicotiana Plumbaginifolia*, Plays a Major Role in Plant Pathogen Defense." *Plant Physiol* 139, no. 1 (2005): 341-52.
- Sugiyama, A., N. Shitan, S. Sato, Y. Nakamura, S. Tabata and K. Yazaki. "Genome-Wide Analysis of ATP-Binding Cassette (ABC) Proteins in a Model Legume Plant, *Lotus Japonicus*: Comparison with *Arabidopsis* Abc Protein Family." *DNA Res* 13, no. 5 (2006): 205-28.
- Sugiyama, A., N. Shitan and K. Yazaki. "Involvement of a Soybean Atp-Binding Cassette-Type Transporter in the Secretion of Genistein, a Signal Flavonoid in Legume-Rhizobium Symbiosis." *Plant Physiol* 144, no. 4 (2007): 2000-8.
- Sun, J., H. Miwa, J. A. Downie and G. E. Oldroyd. "Mastoparan Activates Calcium Spiking Analogous to Nod Factor-Induced Responses in *Medicago truncatula* Root Hair Cells." *Plant Physiol* 144, no. 2 (2007): 695-702.
- Suzuki, T., K. Yano, M. Ito, Y. Umehara, N. Suganuma and M. Kawaguchi. "Positive and Negative Regulation of Cortical Cell Division During Root Nodule

Development in *Lotus Japonicus* Is Accompanied by Auxin Response." *Development* 139, no. 21 (2012): 3997-4006.

- Svistoonoff, S., F. M. Benabdoun, M. Nambiar-Veetil, L. Imanishi, V. Vaissayre, S. Cesari, N. Diagne, V. Hocher, F. de Billy, J. Bonneau, L. Wall, N. Ykhlef, C. Rosenberg, D. Bogusz, C. Franche and H. Gherbi. "The Independent Acquisition of Plant Root Nitrogen-Fixing Symbiosis in Fabids Recruited the Same Genetic Pathway for Nodule Organogenesis." *PLoS One* 8, no. 5 (2013): e64515.
- Svistoonoff, S., V. Hocher and H. Gherbi. "Actinorhizal Root Nodule Symbioses: What Is Signalling Telling on the Origins of Nodulation?" *Curr Opin Plant Biol* 20C, (2014): 11-18.
- Swarup, K., E. Benkova, R. Swarup, I. Casimiro, B. Peret, Y. Yang, G. Parry, E. Nielsen, I. De Smet, S. Vanneste, M. P. Levesque, D. Carrier, N. James, V. Calvo, K. Ljung, E. Kramer, R. Roberts, N. Graham, S. Marillonnet, K. Patel, J. D. Jones, C. G. Taylor, D. P. Schachtman, S. May, G. Sandberg, P. Benfey, J. Friml, I. Kerr, T. Beeckman, L. Laplaze and M. J. Bennett. "The Auxin Influx Carrier *LAX3* Promotes Lateral Root Emergence." *Nat Cell Biol* 10, no. 8 (2008): 946-54.
- Takanashi, K., A. Sugiyama, S. Sato, S. Tabata and K. Yazaki. "LjABCB1, an ATP-Binding Cassette Protein Specifically Induced in Uninfected Cells of *Lotus Japonicus* Nodules." *J Plant Physiol* 169, no. 3 (2012): 322-6.
- Takanashi, K., A. Sugiyama and K. Yazaki. "Auxin Distribution and Lenticel Formation in Determinate Nodule of *Lotus Japonicus*." *Plant Signal Behav* 6, no. 9 (2011): 1405-7.
- Takeda, N., T. Maekawa and M. Hayashi. "Nuclear-Localized and Deregulated Calcium- and Calmodulin-Dependent Protein Kinase Activates Rhizobial and Mycorrhizal Responses in *Lotus Japonicus*." *Plant Cell* 24, no. 2 (2012): 810-22.
- Tang, H., V. Krishnakumar, S. Bidwell, B. Rosen, A. Chan, S. Zhou, L. Gentzbittel, K. L. Childs, M. Yandell, H. Gundlach, K. F. Mayer, D. C. Schwartz and C. D. Town. "An Improved Genome Release (Version Mt4.0) for the Model Legume *Medicago truncatula*." *BMC Genomics* 15, (2014): 312.
- Teale, W. D., I. A. Paponov and K. Palme. "Auxin in Action: Signalling, Transport and the Control of Plant Growth and Development." *Nat Rev Mol Cell Biol* 7, no. 11 (2006): 847-59.
- Terasaka, K., J. J. Blakeslee, B. Titapiwatanakun, W. A. Peer, A. Bandyopadhyay, S. N. Makam, O. R. Lee, E. L. Richards, A. S. Murphy, F. Sato and K. Yazaki. "PGP4, an ATP Binding Cassette P-Glycoprotein, Catalyzes Auxin Transport in *Arabidopsis thaliana* Roots." *Plant Cell* 17, no. 11 (2005): 2922-39.
- Thimann, K. V. "On the Physiology of the Formation of Nodules on Legume Roots." *Proc Natl Acad Sci U S A* 22, no. 8 (1936): 511-4.
- Tiwari, S. B., G. Hagen and T. Guilfoyle. "The Roles of Auxin Response Factor Domains in Auxin-Responsive Transcription." *Plant Cell* 15, no. 2 (2003): 533-43.

- Turner, M., N. R. Nizampatnam, M. Baron, S. Coppin, S. Damodaran, S. Adhikari, S. P. Arunachalam, O. Yu and S. Subramanian. "Ectopic Expression of mir160 Results in Auxin Hypersensitivity, Cytokinin Hyposensitivity, and Inhibition of Symbiotic Nodule Development in Soybean." *Plant Physiol* 162, no. 4 (2013): 2042-55.
- Udvardi, M. and P. S. Poole. "Transport and Metabolism in Legume-Rhizobia Symbioses." *Annu Rev Plant Biol* 64, (2013): 781-805.
- Ulmasov, T., G. Hagen and T. J. Guilfoyle. "Dimerization and DNA Binding of Auxin Response Factors." *Plant J* 19, no. 3 (1999): 309-19.
- Underwood, W. and S. C. Somerville. "Perception of Conserved Pathogen Elicitors at the Plasma Membrane Leads to Relocalization of the *Arabidopsis* PEN3 Transporter." *Proc Natl Acad Sci U S A* 110, no. 30 (2013): 12492-7.
- van den Brule, S., A. Muller, A. J. Fleming and C. C. Smart. "The ABC Transporter *SpTUR2* Confers Resistance to the Antifungal Diterpene Sclareol." *Plant J* 30, no. 6 (2002): 649-62.
- van Noorden, G. E., J. J. Ross, J. B. Reid, B. G. Rolfe and U. Mathesius. "Defective Long-Distance Auxin Transport Regulation in the *Medicago truncatula* Super Numeric Nodules Mutant." *Plant Physiol* 140, no. 4 (2006): 1494-506.
- Veereshlingam, H., J. G. Haynes, R. V. Penmetsa, D. R. Cook, D. J. Sherrier and R. Dickstein. "*nip*, a Symbiotic *Medicago truncatula* Mutant That Forms Root Nodules with Aberrant Infection Threads and Plant Defense-Like Response." *Plant Physiol* 136, no. 3 (2004): 3692-702.
- Verrier, P. J., D. Bird, B. Burla, E. Dassa, C. Forestier, M. Geisler, M. Klein, U. Kolukisaoglu, Y. Lee, E. Martinoia, A. Murphy, P. A. Rea, L. Samuels, B. Schulz, E. J. Spalding, K. Yazaki and F. L. Theodoulou. "Plant ABC Proteins--a Unified Nomenclature and Updated Inventory." *Trends Plant Sci* 13, no. 4 (2008): 151-9.
- Wais, R. J., C. Galera, G. Oldroyd, R. Catoira, R. V. Penmetsa, D. Cook, C. Gough, J. Denarie and S. R. Long. "Genetic Analysis of Calcium Spiking Responses in Nodulation Mutants of *Medicago truncatula*." *Proceedings of the National Academy of Sciences of the United States of America* 97, no. 24 (2000): 13407-13412.
- Walker SA., Aspects of signaling and development during the Rhizobium-Legume symbiosis *Thesis* (2000)
- Walker, T. S., H. P. Bais, E. Grotewold and J. M. Vivanco. "Root Exudation and Rhizosphere Biology." *Plant Physiol* 132, no. 1 (2003): 44-51.
- Walter, M. H., D. S. Floss, J. Hans, T. Fester and D. Strack. "Apocarotenoid Biosynthesis in Arbuscular Mycorrhizal Roots: Contributions from Methylerythritol Phosphate Pathway Isogenes and Tools for Its Manipulation." *Phytochemistry* 68, no. 1 (2007): 130-8.
- Wang, E., S. Schornack, J. F. Marsh, E. Gobbato, B. Schwessinger, P. Eastmond, M. Schultze, S. Kamoun and G. E. Oldroyd. "A Common Signaling Process That Promotes Mycorrhizal and Oomycete Colonization of Plants." *Curr Biol* 22, no. 23 (2012): 2242-6.

- Wasson, A. P., F. I. Pellerone and U. Mathesius. "Silencing the Flavonoid Pathway in *Medicago truncatula* Inhibits Root Nodule Formation and Prevents Auxin Transport Regulation by Rhizobia." *Plant Cell* 18, no. 7 (2006): 1617-29.
- Waterhouse, P. M. and C. A. Helliwell. "Exploring Plant Genomes by Rna-Induced Gene Silencing." *Nat Rev Genet* 4, no. 1 (2003): 29-38.
- Xie, F., J. D. Murray, J. Kim, A. B. Heckmann, A. Edwards, G. E. Oldroyd and J. A. Downie. "Legume Pectate Lyase Required for Root Infection by Rhizobia." *Proc Natl Acad Sci U S A* 109, no. 2 (2012): 633-8.
- Yano, K., S. Yoshida, J. Muller, S. Singh, M. Banba, K. Vickers, K. Markmann, C. White, B. Schuller, S. Sato, E. Asamizu, S. Tabata, Y. Murooka, J. Perry, T. L. Wang, M. Kawaguchi, H. Imaizumi-Anraku, M. Hayashi and M. Parniske. "Cyclops, a Mediator of Symbiotic Intracellular Accommodation." *Proc Natl Acad Sci U S A* 105, no. 51 (2008): 20540-5.
- Young, N. D., F. DeBelle, G. E. Oldroyd, R. Geurts, S. B. Cannon, M. K. Udvardi, V. A. Benedito, K. F. Mayer, J. Gouzy, H. Schoof, Y. Van de Peer, S. Proost, D. R. Cook, B. C. Meyers, M. Spannagl, F. Cheung, S. De Mita, V. Krishnakumar, H. Gundlach, S. Zhou, J. Mudge, A. K. Bharti, J. D. Murray, M. A. Naoumkina, B. Rosen, K. A. Silverstein, H. Tang, S. Rombauts, P. X. Zhao, P. Zhou, V. Barbe, P. Bardou, M. Bechner, A. Bellec, A. Berger, H. Berges, S. Bidwell, T. Bisseling, N. Choisne, A. Couloux, R. Denny, S. Deshpande, X. Dai, J. J. Doyle, A. M. Dudez, A. D. Farmer, S. Fouteau, C. Franken, C. Gibelin, J. Gish, S. Goldstein, A. J. Gonzalez, P. J. Green, A. Hallab, M. Hartog, A. Hua, S. J. Humphray, D. H. Jeong, Y. Jing, A. Jocker, S. M. Kenton, D. J. Kim, K. Klee, H. Lai, C. Lang, S. Lin, S. L. Macmil, G. Magdelenat, L. Matthews, J. McCorrison, E. L. Monaghan, J. H. Mun, F. Z. Najar, C. Nicholson, C. Noirot, M. O'Bleness, C. R. Paule, J. Poulain, F. Prion, B. Qin, C. Qu, E. F. Retzel, C. Riddle, E. Sallet, S. Samain, N. Samson, I. Sanders, O. Saurat, C. Scarpelli, T. Schiex, B. Segurens, A. J. Severin, D. J. Sherrier, R. Shi, S. Sims, S. R. Singer, S. Sinharoy, L. Sterck, A. Viollet, B. B. Wang, K. Wang, M. Wang, X. Wang, J. Warfsmann, J. Weissenbach, D. D. White, J. D. White, G. B. Wiley, P. Wincker, Y. Xing, L. Yang, Z. Yao, F. Ying, J. Zhai, L. Zhou, A. Zuber, J. Denarie, R. A. Dixon, G. D. May, D. C. Schwartz, J. Rogers, F. Quetier, C. D. Town and B. A. Roe. "The *Medicago* Genome Provides Insight into the Evolution of Rhizobial Symbioses." *Nature* 480, no. 7378 (2011): 520-4.
- Yu, F. and V. De Luca. "ATP-Binding Cassette Transporter Controls Leaf Surface Secretion of Anticancer Drug Components in *Catharanthus Roseus*." *Proc Natl Acad Sci U S A* 110, no. 39 (2013): 15830-5.
- Zahir, Z. A., Shah, M. K., Naveed, M., & Akhter, M. J. (2010). Substrate-Dependent Auxin Production by *Rhizobium phaseoli* Improves the Growth and Yield of *Vigna radiata* L. Under Salt Stress Conditions. *Journal of Microbiology and Biotechnology*, 20(9), 1288-1294. doi: DOI 10.4014/jmb.1002.02010
- Zazimalova, E., A. S. Murphy, H. Yang, K. Hoyerova and P. Hosek. "Auxin Transporters--Why So Many?" *Cold Spring Harb Perspect Biol* 2, no. 3 (2010): a001552.
- Zhang, J., S. Subramanian, G. Stacey and O. Yu. "Flavones and Flavonols Play Distinct Critical Roles During Nodulation of *Medicago truncatula* by *Sinorhizobium Meliloti*." *Plant J* 57, no. 1 (2009): 171-83.

- Zhang, Q., L. A. Blaylock and M. J. Harrison. "Two *Medicago truncatula* Half-ABC Transporters Are Essential for Arbuscule Development in Arbuscular Mycorrhizal Symbiosis." *Plant Cell* 22, no. 5 (2010): 1483-97.
- Zhou, C., L. Han, C. Hou, A. Metelli, L. Qi, M. Tadege, K. S. Mysore and Z. Y. Wang. "Developmental Analysis of a *Medicago truncatula* *Smooth Leaf Margin1* Mutant Reveals Context-Dependent Effects on Compound Leaf Development." *Plant Cell* 23, no. 6 (2011): 2106-24.